University of Maryland

Minimum Crew Cabin Studies

ENAE484 X-Hab Final Report

May 31, 2020

Faculty Advisor: Dr. David L. Akin

Michael Baker	Bob Nobles	Lucia Stainer
Nicholas Behnke	Matt Ostrow	Shelly Szanto
Patrick Geleta	Hudson Paley	Einar Terrill
Eric Greenbaum	Zach Peters	Blaire Weinberg
Chirayu Gupta	Ramin Rafizadeh	Lauren Weist
Charlie Hanner	Tuvia Rappaport	Jeffrey Zhu
Zach Lachance	Brady Sack	

A. JAMES CLARK
SCHOOL OF ENGINEERING

Space
Systems
Laboratory

Contents

List of Figures

List of Tables

Definitions

- BKDF - Buckling Knockdown Factor
- BoM - Bill Of Materials
- CC - Carbon Composites
- CM - Conventional Metal
- COTS - Commercial Off The Shelf
- CTB - Cargo Transfer Bag
- DoF - Degree(s) of Freedom
- ECLSS - Environmental Control and Life Support System
- EDC - Electrochemical Depolarized Concentrator
- EMU - Extravehicular Mobility Unit
- EVA - Extra-Vehicular Activity
- FoS- Factor of Safety
- HID - High Intensity Discharge
- HUT - Hard Upper Torso
- ID - Inner Diameter
- IVA - Intra-Vehicular Activity
- LED - Light Emitting Diode
- LiOH - Lithium Hydroxide
- LV - Launch Vehicle
- METOX - Metal Oxide Absorption
- MoS - Margin of Safety
- MRE - Meals Ready to Eat
- MSG - Microgravity Science Glovebox
- OD - Outer Diameter
- PPE - Personal Protective Equipment
- SOV - Water Purification Facilities (Russian Translation)
- SPK-UM - System for Water Reclamation From Urine for ISS (Russian Translation, index “M” for Improved System)
- SRV-K2M - a System for Water Recovery from Humidity Condensate (Russian Translation)
- TLX - Task Load Index
- WRS-C - Water Recycling System - Condensate
- WRS-U - Water Recycling System - Urine
- 2BMS - 2 Bed Molecular Sieve
- 4BMS - 4 Bed Molecular Sieve

1 Overview

1.1 Research Motivation (Blaire Weinberg)

With renewed interest in human spaceflight, and the astronomically high cost to send things into space, NASA is looking into methods for minimizing all aspects of crewed flight. While maintaining a crew of at least two to four people, there are considerations into duration, habitat size, habitat orientation, and many other factors to try and get the most science, safely, for the least amount of money.

From these constraints, the class' project was organized. The topic of "Minimum Crew Cabin Sizing" was chosen, with a plan to do experimentation to verify or update some of the volumetric models for various activities. The actual crew cabin itself is something that can easily alter the mass, cost, and development time. In trying to quantify how small is too small – or what can be made smaller – programs can save money, time, and mass with an appropriately sized minimum volume habitat.

1.2 Requirements (Charlie Hanner, Blaire Weinberg)

In the decision to study minimum sizing of crew cabins, the project could not advance without a comprehensive set of defining requirements and a cumulative mission statement. The requirements can generally be perceived in one of two categories: 1) experimental conduct, and 2) hardware design and habitation parallels. ultimately, from these a guiding mission statement was found:

What is the minimum effective habitable volume for crew cabins?

For the requirements outlined in Tables 1, 2, and 3, the following identifiers were used for different types of requirements:

- M: Mission
- C: Crew
- H: Habitat
- T: Test

ID	Requirement	Source
M1	The project shall investigate the effect of cabin size on crew performance to identify minimum requirements for cabin sizing	MS
M2	The test protocol shall consider all applicable phases of human exploration beyond LEO	MS
M3	Test conditions shall reflect the achievable critical mission elements for exploration operations	MS
M4	Test operations shall adhere to all human testing and laboratory safety guidelines and protocols	MS

Table 1: Level 1 Requirements

ID	Requirement	Source
H1	The project shall build a reconfigurable habitat of varying volume capacities between 8 m^3 and 60 m^3	M1
H2	Underwater tests shall be conducted under lunar, Martian, and microgravity conditions	M2, M3
T1	Control testing shall be performed at 1g	M3
T2	Test subjects shall investigate interactions with the structure and equipment to study reach volumes, comfort, and safety	M2, M4
C1	The mock-up shall be capable of supporting multiple test subjects in the same experimentation period	M1, M2

Table 2: Level 2 Requirements

ID	Requirement	Source
T3	The project shall have structural considerations for entering and exiting water testing	H2
T4	The project shall incorporate medical operations that can properly ensure crew health	T2
T5	The project shall have considerations for viable repair of an ECLSS simulator	T2, C1
T6	The project shall consider volume requirements and interactions for food preparation and communal eating	T2, C1
C2	The habitat must support basic non-structural components such as handrails and footholds	T2

Table 3: Level 3 Requirements

1.3 Experiment Overview (Blaire Weinberg)

Originally, the research into minimum crewed habitats was going to be an in-person experiment. The goal of the experiment was to be able to better quantify the volume used doing different tasks (individual volumetric studies), and see how people interact doing those tasks together in a simulated environment (day-in-the-life testing). More specific details about both phases can be found in §2.1.

Both parts of the experiment would be conducted under varying levels of gravity, with the assistance of the Neutral Buoyancy Research Facility located within the Space Systems Laboratory at the University of Maryland. Four different gravity levels were considered for testing: Earth (baseline), Moon, Mars, and Microgravity. There was consideration for whether or not the Martian gravity would be more like Lunar or Earth, since it's between the two. Not only would it reduce the number of tests to do, it would also be an interesting conclusion.

For the day-in-the-life testing, there were three additional variables that were added to the scope of the experiment. The first of these were the volume of the habitat that the testing was being conducted in. Volumes between $7.8\,m^3$ at the smallest and $59.4\,m^3$ at the largest could be used to conduct tests in [1]. The second additional variable in the day-in-the-life testing was the crew size. Tests would be conducted with between two and four test subjects. Tests would be initially conducted with four test subjects, and would be reduced only if the space was too small for all subjects to complete all of their tasks reasonably. If four people could conduct their tasks successfully, there was little reason that fewer people would not be able to. The last variable that was added to the day-in-the-life testing was habitat orientation. Figures 4 and 5 show the difference between the two orientations. Both orientations would be tested to see if there is a discernable difference.

While working on the experiment, the class was organized into three different groups, shown in Table 4. The manufacturing team was responsible for designing the components required for the experiments, such as beds and stowage space. The habitat design team took the racks and components from the manufacturing

[1] Numbers pulled from Table 5

team and put them into theoretical space applications, such as ascent/descent vehicles or rovers. The experimental design team actually designed the tasks and data collection methods for the experiment itself.

Manufacturing	Habitat Design	Experimental Design
Patrick Geleta	Michael Baker	Charlie Hanner
Eric Greenbaum	Nicholas Behnke	Ramin Rafizadeh
Chirayu Gupta	Bob Nobles	Tuvia Rappaport
Zach Lachance	Hudson Paley	Brady Sack
Matt Ostrow	Einar Terrill	Shelly Szanto
Zach Peters		Blaire Weinberg
Lucy Stainer		Lauren Weist
Jeffrey Zhu		

Table 4: Experiment Design Groups

1.3.1 Rack Design Strategy (Charlie Hanner)

The first iteration of design aimed to create a variable OD mockup with an interior capable of variable configurations to simulate variance in total habitat volume. The selected mockups consisted of a pair of 80/20 sliding octagonal prism, each capable of encapsulating different volumes:

- 5-25 m^3
- 25-100 m^3

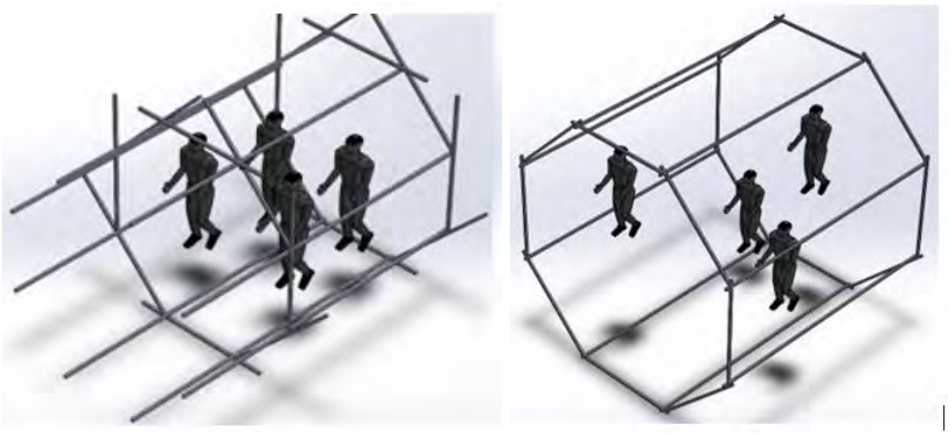

Figure 1: Preliminary Reconfigurable Cabin Concept

However concerns regarding interior outfitting, lab storage, and on-deck testing prevailed as dominating factors and the design was soon reconsidered. January 2020 led to a few design iterations ultimately settling on a modular rack-based design. A heavier focus regarding modeling IVA surfaces and usable volumes was applied, and as a result the following modular rack design became the primary test apparatus. A series of 12 racks, each a hollow 80/20 frame with dimension 20" x 40" x 80" (D x W x H), in various configurations can provide apt[2] interactive volume. Each experiment configuration then can utilize as many, or as few experiments and racks as the test conductor deems necessary with the total number of racks determining habitable volume.

[2]Apt here qualifies enough volume to house all intended experimental/test materials, in addition to volume for astronaut existence

Figure 2: Single Rack Assembly

Preliminary studies were performed assuming a circular assembly of racks, modeling a vertical habitat, to understand population requirements and estimated habitable volume.

Figure 3: Multirack Circular Assembly Example

Depending if the OD is measured from each rack's outer edge or tangent to its midpoint, estimated volumes range between $\approx 8m^3$ and $\approx 60m^3$ for a series of twelve racks.

Racks	V_{press} Min (m^3)	V_{press} Max (m^3)
4	7.8	10.0
5	11.5	13.8
6	15.7	18.1
7	20.6	23.1
8	26.2	28.8
9	32.5	35.2
10	39.6	42.5
11	47.6	50.5
12	56.4	59.4

Table 5: Rack Circular Configuration Volumes

An initial production of twelve racks were chosen for two reasons:

1. Covers a majority of originally interested volumes in minimization of habitat volumes
2. Purchase of all required materials summed to just under the state maximum purchasing limit

Racks can be assembled into differing configurations beyond variance in rack population such as modeling vertical and horizontally aligned habitats.

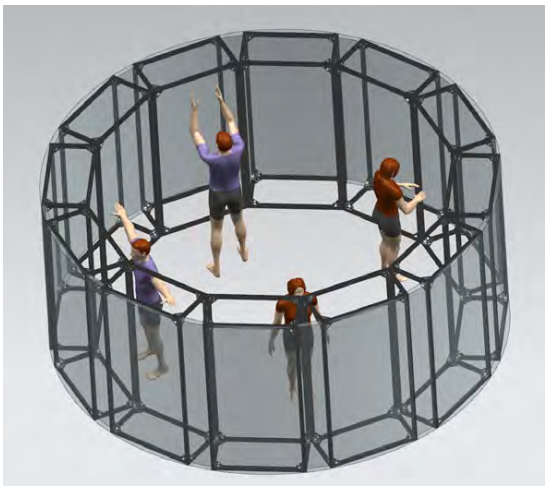

Figure 4: Circular/Vertical Rack Configuration

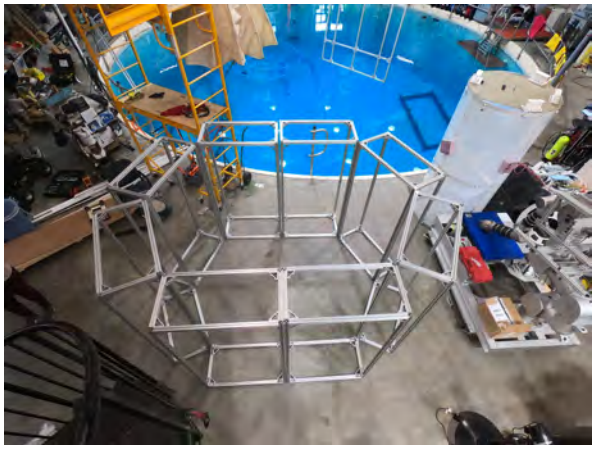

Figure 5: Rectangular/Horizontal Rack Configuration

An additional consideration for the rack assembly design was for data collection and motion tracking systems, requiring a clear line of sight to each target for both Qualisys and April Tag use. This hollow rack design allows for subjects inside of the habitat to be majorly unobstructed beyond the thin reflective pillars and the experimental materials chosen to outfit the racks.

1.4 Remote Work Overview (Blaire Weinberg)

As spring break approached in mid-March, the class was forced to reconsider what it was really trying to accomplish as the class became distanced, online learning. Initially, there was still some hope that research labs could be kept open, and experiment progress could still continue, although at a slower, and more careful pace. However, the University implemented severe research restrictions before spring break was over, and the experiment officially had to end in the planning stages.

In the remote learning for the last month or so of the school year, the class decided to consider the whole habitable volume instead of just what an astronaut test subject may be interacting with. Instead of designing an experiment, the class transitioned to a more trade-study based approach of looking into what sort of things would be needed in a habitat, similar to the experiment, though including things like actual life support systems, hygiene, gloveboxes, and other individual facilities instead of stand-ins. The design space was narrowed to only looking at "surface" and "microgravity" missions, as opposed to the wider variety of specific gravity levels being looked at with the experiment. The findings of these trade studies would then be integrated into six habitats, three surface and three microgravity, of different sizes. Ideally, we would still be able to draw some conclusions about the original trade space without gathering actual experimental data.

For this portion of our class, we organized ourselves in the more traditional groups for a capstone project, shown in Table 6. The systems integration team was responsible for integrating the components into most of the habitats, and interfacing between the groups to make sure everyone was on the same page as much as possible. The mission planning group determined the new reference mission to design around. The power thermal group conducted trades to determine things like solar panels, radiators, and heat exchangers for the habitats. Crew systems coordinated the trade studies and CAD effort for all of the interior components of the habitats. The loads and structures team determined the orientation and dimensions of the habitats that were used for analysis.

Systems Integration	Mission Planning	Power, Thermal	Crew Systems	Loads, Structures
Blaire Weinberg	Tuvia Rappaport	Michael Baker	Nicholas Behnke	Eric Greenbaum
	Brady Sack	Hudson Paley	Patrick Geleta	Chirayu Gupta
		Ramin Rafizadeh	Charlie Hanner	Bob Nobles
		Shelly Szanto	Zach Lachance	Matt Ostrow
			Lucy Stainer	Zach Peters
			Lauren Weist	Einar Terrill
				Jeffrey Zhu

Table 6: Remote Work Groups

2 Experimental Design

2.1 Experiment Overview and Phases (Brady Sack)

The experiments were separated into two phases, (1) individual volumetric studies and (2) simultaneous tasks studies. In the first phase, we planned to test certain individual tasks, indicated in table 7 below, in order to determine the required workspace volume for each task and measure the effect of gravity level on workspace required.

Due to constraints on time and number of eligible divers, we were forced to reduce the test matrix to a subset of tasks. We decided to test every task in Earth gravity because these tests could be conducted outside of the tank without the need for trained subjects. The volume required would be recorded using AprilTags fiducial markers, described later in the Data Collection Methods section. As for tests We chose the suitport task at the specific request of a member on the NASA Langley Team, who wanted to verify workspace estimates for suitports made in previous studies, which is discussed later in this report.

We were particularly interested in determining whether or not there was a substantial difference between the affects of Earth and Martian gravity because, if tests did not reveal a significant difference, we could significantly reduce the test matrix of the second phase.

Category	Task	Earth	Mars	Lunar	Micro
Medical	First Aid	x			
	Monitoring	x			
Workstation	General	x	x	x	x
Life Support	Meal Prep	x			
	Maintenance	x	x	x	x
	Personal Care	x			
Airlock	Repair	x			
	Suitport	x	x	x	x
	Main Entrance	x			

Table 7: Individual Task (Phase I) Testing Matrix
'x' indicates a test that will be conducted

- Experiments will be split into two phases
- In the first phase, individual components will be tested to determine:
    1. Effect of gravity level on the volume required to complete a task
    2. Volume required for each task
- Data collected with motion tracking systems discussed in next section

- In the second phase, we'll have subjects complete tasks simultaneously in order to study the effect of rack arrangement on ability to complete tasks
  - Identify best practices for arranging racks and problematic configurations
- Data collected with motion tracking systems along with qualitative methods discussed in next section

2.2 IRB (Shelly Szanto)

Due to our research seeking data from human test subjects, approval from the Institutional Review Board (IRB) was required. The initial application included all necessary components including the subject selection, eligibility, and rationale. The procedure section of the application included a detailed description and plan for the initial land (1g) testing and what the test subjects will be required to do for each test. It concluded with a description of the iteration over different gravity levels and how the researchers will explain the test scenarios and conduct the data collection. The most important part of the application was to describe the possible risks and mitigation and contingency plans for those risks. It was concluded that there are no known risks for the 1g testing, but the underwater tests would observe typical dive safety and precautions when completing test procedures.

The consent form explains the confidentiality protection for all test subjects and allows test subjects to provide their signature with consent to participate in the research. All experiment procedure protocols, survey documents, and advertisement for test subjects were attached in the cumulative application. Approval form the Review Board was received on March 18th.

2.3 Tasks

The following sections are dedicated to describing the experimental tasks for testing, each of which belong to one of four categories:

1. Medical
2. Workstation
3. Life Support
4. Airlock

2.3.1 Medical - First Aid (Lauren Weist)

One set of activities that was identified as being particularly volume intensive is first aid and related medical tasks, which we broke into two separate categories. The first group of activities is first aid, which encompasses all reactive medical activities.

This test is to be conducted in all four gravity levels (micro, Mars, Moon, and Earth) and at all interested habitat sizes.

The participants in this experiment are:

- Test Subject 1 - Rescuer
- Test Subject 2 - Injured
- Test Subject 3 - Rescuer Assistant (optional)
- 2-3 Safety Divers

The data collection methods utilized to get useful data are:

- Qualsys

- April Tags
- Post-Experiment Survey
- Experiment Timer

The procedure for this experiment goes as follows:

- Setup
    1. Put the CTB containing the first aid supplies in one of the racks
    2. TS1 and TS2 enter the habitat through the airlock
- Testing
    1. TS2 requires first aid
    2. TS1 retrieves first aid kit from CTB A
    3. TS1 performs preliminary check on TS2
    4. TS2 requires a bandage and stitches on their arm and leg
    5. TS1 stitches TS2
    6. TS1 bandages TS2
    7. TS2 at risk of head-neck-spinal injury
    8. TS1 backboards TS2 on the ground
    9. TS1 safely stores medical waste and tools
    10. Test subjects first aid is visually inspected
    11. Test subjects perform post test evaluation
- Evaluation
    1. Time how long each step takes
    2. Extraneous movement
    3. TLX
    4. Qualitative Survey
    5. Amount of space each step requires
    6. Inspection of First Aid Treatment

The following scenario script is provided to give context to the test subjects so that they have an understanding of the experiment:

- Test subjects are back inside the habitat after TS 2 was injured while on EVA. The un-injured test subjects must perform first aid on TS 2.

A scenario drawing provides a visual layout of the habitat and experiment so that both test subjects and test conductors have a good understanding on what is being done at all times.

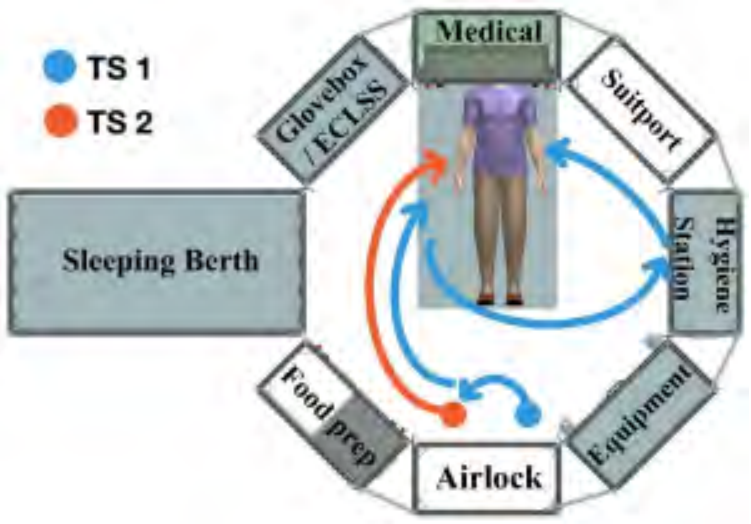

Figure 6: First Aid Scenario Drawing by Ramin Rafizadeh

2.3.2 Medical - Monitoring (Brady Sack)

This task is meant to simulate nominal medical monitoring, including collecting data on subject blood pressure, heart rate, blood sugar levels, mass etc. Such data may be useful for researchers interested in studying the effects of Martian gravity and radiation on human bodies.

This test is to be conducted in all four gravity levels (micro, Mars, Moon, and Earth) and at all interested habitat sizes.

The participants in this experiment are:

- Test Subject 1 - Patient
- Test Subject 2 - Medical Monitor
- 2-3 Safety Divers

The data collection methods utilized to get useful data are:

- Qualsys
- April Tags
- Post-Experiment Survey
- Experiment Timer

The procedure for this experiment goes as follows:

- Setup
    1. Set up the rack with the table
    2. TS1 and TS2 begin in habitat
- Testing
    1. TS1 pulls down table from rack
    2. TS2 sits on table
    3. TS1 sets up medical equipment

4. TS 1 takes and records TS2's blood pressure, heart rate, oxygen saturation, and temperature
5. TS 1 sets up IV on TS 2 (tape tube to arm, hang bag)
6. TS 1 draws blood samples and stores them
7. TS 1 sets up EKG on TS 2
8. TS 1 removes EKG and cleans-up

- Evaluation

1. Time how long each step takes
2. Extraneous movement
3. TLX
4. Qualitative Survey
5. Amount of space each step requires

A scenario drawing provides a visual layout of the habitat and experiment so that both test subjects and test conductors have a good understanding on what is being done at all times.

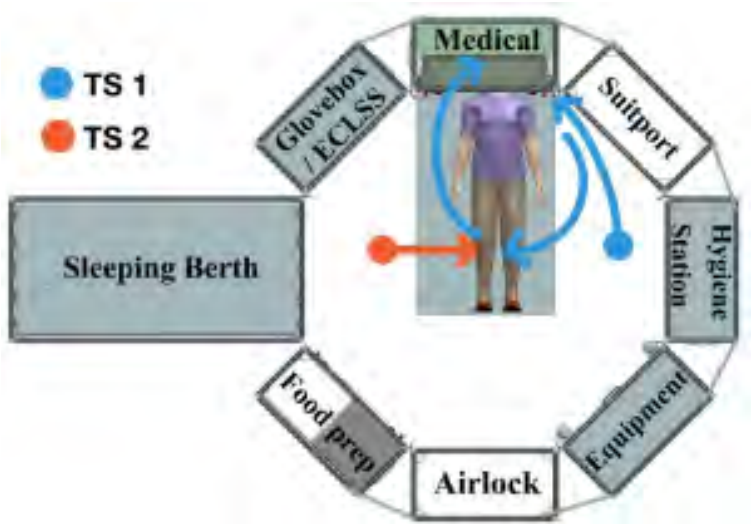

Figure 7: Workstation Scenario Drawing by Ramin Rafizadeh

2.3.3 Workstation - General (Ramin Rafizadeh)

An important task which needed to be studied was the interaction of the test subjects with the glovebox, robot control station, and tools stored in equipment rack.
This test is to be conducted in all four gravity levels (micro, Mars, Moon, and Earth) and at all interested habitat sizes, and will only require one test subject and the required safety divers.

The data collection methods utilized to get useful data are:

- Qualsys
- April Tags
- Post-Experiment Survey
- Experiment Timer
- Control Panel Data Collection

The procedure for this experiment goes as follows:

- Setup
    1. place the tools and supplies in the appropriate CTBs in the equipment rack
    2. Glovebox is setup with proper equipment inside
- Testing
    1. TS1 retrieves supplies and tools from CTB H
    2. TS1 pulls 50 feet of wire out of a box
    3. TS1 spools wire
    4. TS1 retrieves sample from CTB K
    5. TS1 places sample inside glove box
    6. TS1 places hands in glovebox and places shaped pegs into holes
    7. TS1 removes sample from glovebox
    8. TS1 places samples in a CTB K and returns to a rack
    9. TS1 sets up robot control station
    10. TS1 pokes buttons with the robot
    11. TS1 performs post test evaluation
- Evaluation
    1. Time how long each step takes
    2. Extraneous movement
    3. TLX
    4. Qualitative Survey
    5. Amount of space each step requires
    6. Inspection of First Aid Treatment

The following scenario script is provided to give context to the test subjects so that they have an understanding of the experiment:

- Test subject is inside the habitat and needs to perform a test on a sample inside the glovebox. The test requires to gather the appropriate tools and supplies from the equipment rack in the process of performing the test.

A scenario drawing provides a visual layout of the habitat and experiment so that both test subjects and test conductors have a good understanding on what is being done at all times.

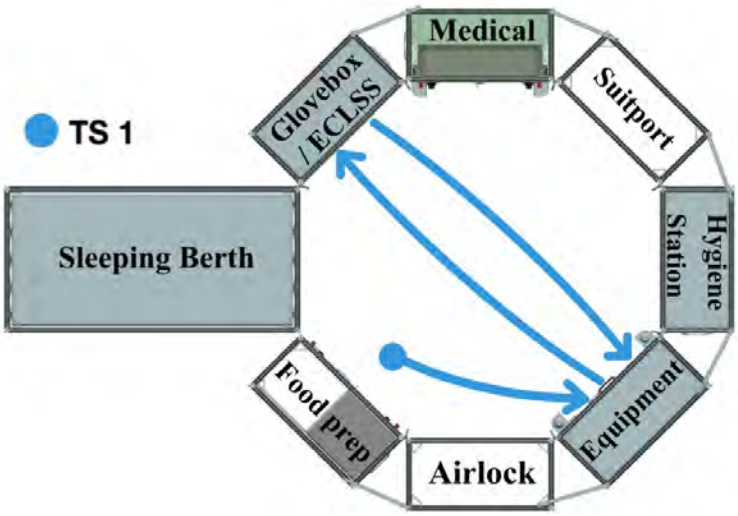

Figure 8: Workstation Scenario Drawing by Ramin Rafizadeh

2.3.4 Life Support - Meal Prep (Lauren Weist)

One activity that is going to occur frequently is meal preparation, and so it was high on the list of nominal task experiments.
This test is to be conducted in all four gravity levels (micro, Mars, Moon, and Earth) and at all interested habitat sizes, and will only require one test subject and the required safety divers.

The data collection methods utilized to get useful data are:

- Qualsys
- April Tags
- Post-Experiment Survey
- Experiment Timer

The procedure for this experiment goes as follows:

- Setup
    1. Food stand-in is placed in a CTB
    2. TS1 enters the habitat through the airlock
- Testing
    1. TS sets up food table
    2. TS retrieves food pouch and utensils from CTB M and CTB L
    3. TS opens microwave and places food pouch inside
    4. TS waits 30 seconds for food to cook
    5. TS opens microwave and removes food pouch
    6. TS takes food pouch to hydration station
    7. TS inserts hydration tube into pouch and waits 5 seconds
    8. TS removes pouch and moves to the communal eating area
    9. TS sits at meal table and eats food for 2 minutes

10. TS cleans up food prep area and disinfect the table
11. TS returns materials to appropriate CTB M and CTB L
12. Test subjects perform post test evaluation

- Evaluation

1. Time how long each step takes
2. Extraneous movement
3. TLX
4. Qualitative Survey
5. Amount of space each step requires

The following scenario script is provided to give context to the test subjects so that they have an understanding of the experiment:

- Test subject shall prepare, eat and clean up after a meal.

The scenario drawing is also shown below.

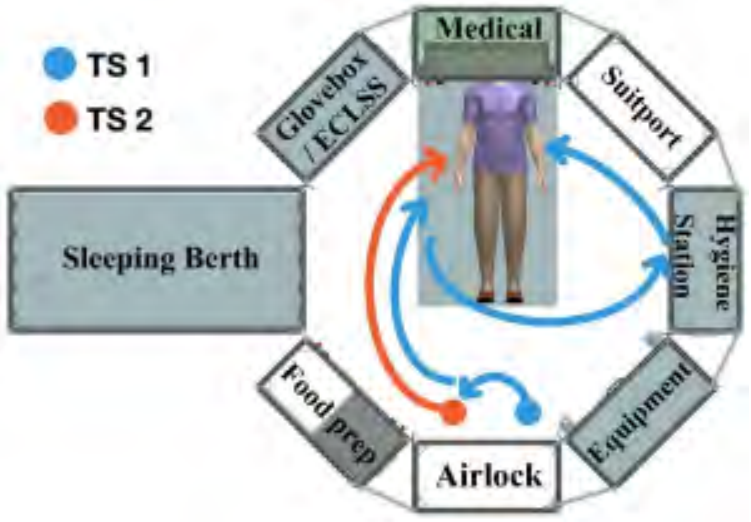

Figure 9: Meal Preparation Scenario Drawing by Ramin Rafizadeh

2.3.5 Life Support - Maintenance (Shelly Szanto)

The purpose of this experiment is to simulate an repair of any life support system such as a CO2 scrubber, temperature control unit, or anything else that needs to be repaired. Maintenance is a task that occurs often and can require tools that require volume and storage space. This task will mostly be understanding the volume that these tools take up and if that could potentially interfere with another test subject's daily tasks. There is one test subject that will be completing this task.

The follow scenario script will be read to tst subjects before the experiment begins to provide context to the test subjects: "The following is a repair of the ECLSS life support system. It is up to you (the test subject) must gather all necessary tools and then use them to repair a broken system."
The summarized procedure is as follows:

1. Remove the malfunctioning items indicated in the ECLSS rack
2. Gather tools from equipment rack

3. Complete maintenance repair on the electronics in the ECLSS rack
4. Replace the fixed component
5. Find and plug a leak
6. Go to the equipment rack to get more tools to replace a filter
7. Anchor tools down if in a micro-gravity experiment
8. Replace air filter
9. After repair finishes, put all tools away in the equipment rack

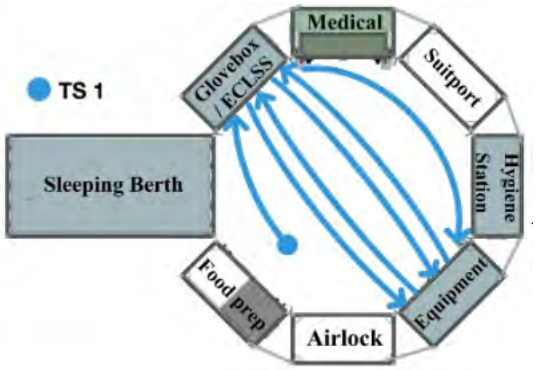

Figure 10: Life support maintenance workflow - Credit: Ramin R.

Data collected during this task include:

1. Time for task
2. Movement from motion capture
3. TLX scores
4. Qualitative Survey

With this data, we will be able to understand the volume required for a simulated life support system maintenance.

2.3.6 Life Support - Personal Care (Shelly Szanto)

The purpose of this experiment is to complete the necessary and salient task of personal care and hygiene. Using exercise equipment, changing clothes, completing hygiene, and sleeping are all simulated during this experiment. There is only one test subject involved with this experiment and equipment required is stored in CTB R, CTB T, the treadmill, resistive bands, pretend clothes, and the sleeping berth.

The following scenario script will be read to test subjects before the experiment begins to provide context to the test subject: "Participants will begin in the sleeping quarters. You will move to the treadmill where you will run for a determined period of time. Then, proceed to the exercise equipment area and use resistive exercise bands for determined period of time. All the resistive bands will then be placed in the exercise equipment shelf. You will then move to the hygiene station change into and out of clothes and discard old clothes into designated container. Then, move to sleeping berth and climb in to the sleeping berth for a determined period of time and then climb out of bed. The experiment will conclude with the storing the sleeping bed."

The summarized procedure is as follows:

1. Exit sleeping quarters rack and move to exercise rack
2. Run on treadmill
3. Retrieve CTB R
4. Use resistive bands
5. Store exercise equipment in CTB R
6. Move to hygiene station
7. Put on a new pair of close and discard old clothes into CTB T
8. Set up sleeping berth
9. Climb into sleeping berth and go to sleep
10. Wake up and climb out of bed
11. Store sleeping berth

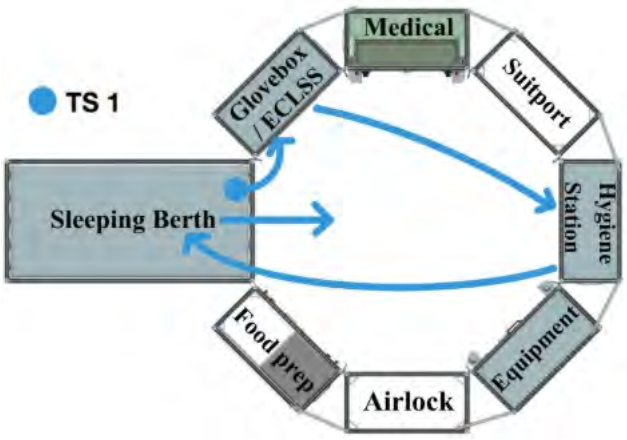

Figure 11: Self-care workflow - Credit: Ramin R.

Data collected during this task include:

1. Time for task
2. Movement from motion capture
3. TLX scores
4. Qualitative Survey

With this data, we will be be able to determine how much volume is required to complete hygiene such as showering, brushing teeth, sleeping, and exercising.

2.3.7 Airlock - Repair (Ramin Rafizadeh)

An important task which needed to be studied was the interaction of the test subjects with the tasks required to repair the airlock.
This test is to be conducted in all four gravity levels (micro, Mars, Moon, and Earth) and at all interested habitat sizes, and will require three test subjects and the required safety divers.

The data collection methods utilized to get useful data are:

- Qualsys
- April Tags
- Post-Experiment Survey
- Experiment Timer
- Control Panel Data Collection

The procedure for this experiment goes as follows:

- Setup
    1. All TS are performing previous nominal tasks
    2. Alarm goes off indicating the airlock requires emergeancy repair
- Testing
    1. All task subjects drop their previous tasks
    2. All task subjects put on emergency life support suits
    3. TS1 retrives necessary tools from tool CTB W and CTB P
    4. TS2 and 3 clear work area near airlock
    5. TS1 leads airlock repair, all other TS assist as needed
    6. TS2 and 3 tape over airlock
    7. TS1 adjusts dials of control panel
    8. Test subjects complete repair of airlock, alarms are deactivated
    9. Test subjects move to workstation and complete post-test evaluation
- Evaluation
    1. Time how long each step takes
    2. Extraneous movement
    3. TLX
    4. Qualitative Survey
    5. Amount of space each step requires
    6. Inspection of First Aid Treatment

The following scenario script is provided to give context to the test subjects so that they have an understanding of the experiment:

- The airlock will be mounted in a rack and an emergency repair operation will be performed by all test subjects. When the airlock experiences a critical failure an alarm will go off and remain on until the airlock is repaired. The purpose of this is to heighten the mental load on the test subjects. To repair the airlock the test subjects must coordinate to both tape over the breach and successfully complete the control panel challenge.

A scenario drawing provides a visual layout of the habitat and experiment so that both test subjects and test conductors have a good understanding on what is being done at all times.

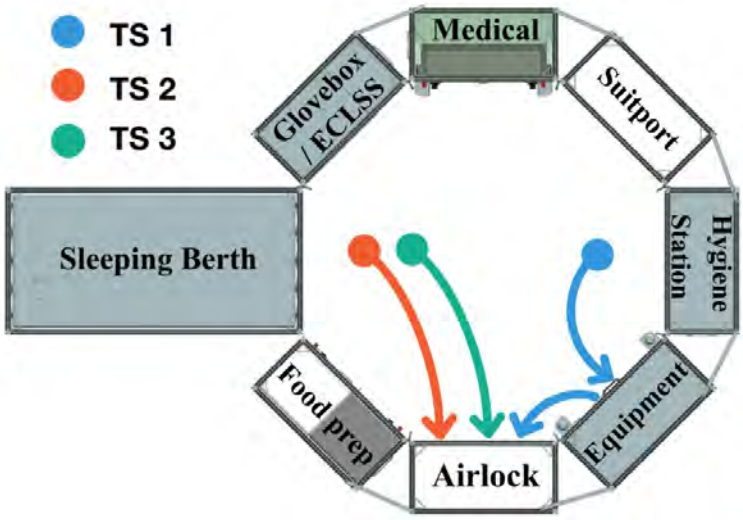

Figure 12: Airlock Repair Scenario Drawing by Ramin Rafizadeh

2.3.8 Airlock - Suitport (Charlie Hanner)

One area of pointed focus was chosen to be the donning and doffing required volume of a rear-entry spacesuit in the habitat volume due to a specific request from a NASA Langley team member. The suitport studies were planned to verify NextSTEP Attachment H Appendix F Dimensions as they were created theoretically and had never been documented or tested in a controlled and motion-tracked environment.

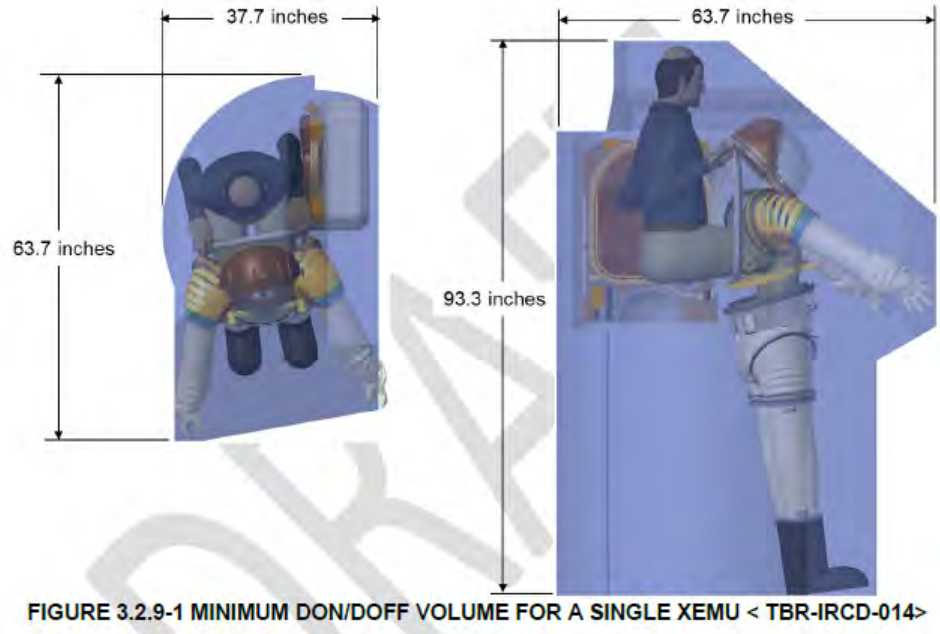

Figure 13: NASA NextSTEP Attachment H Appendix F - Suitport Donning/Doffing Requirements

The suitport experiment would consist of two test subjects, the primary and the assistant, and a simple four step procedure:

1. Test subject primary dons spacesuit through rear-entry hatch

2. Primary subject rests
3. Primary subject doffs spacesuit
4. Repeat process as test dictates

The role of the assistant unfolds into both aiding the subject as needed and being a first point of response for the test subject's safety, a point of utmost concern especially underwater.

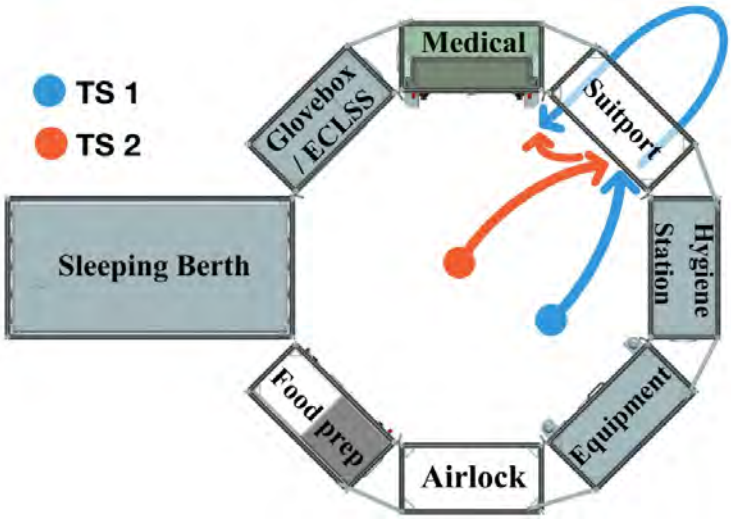

Figure 14: Suitport Experiment Workflow - Credit: Ramin Rafizadeh

To gather useful data to draw comparisons from each donning/doffing cycle of the test will conclude with a TLX recording, and at the end of each experiment (i.e. after the suitport test has been completed x number of times), the test subjects will be asked to evaluate:

- TLX
- Modified Cooper-Harper Rating
- Qualitative survery

Finally, quantitative data will be collected throughout the duration of the testing in two ways:

1. Time each procedural step requires
2. Volume of the subject's movements in each step

These both will be collected either from April Tag or Qualisys data depending on the location (land or underwater) of the testing during the post processing segment. Each recording can be broken into each procedural step for comparison and statistical analysis, however it is expected that Qualisys data provide a higher fidelity during this experiment due its ability to track multiple parts of the body with smaller markers when compared to the relatively large size of the April Tags. An additional strategy to acquire more data in the on-land scenarios would be the use of cameras from the same perspective as Figure 13, and scale markers both throughout the frame as well as on the test subject's joints and all measurements between the joint markers.

2.3.9 Airlock - Main Entrance (Ramin Rafizadeh)

An important task which needed to be studied was the interaction of the test subjects with the going through the main entrance airlock.
This test is to be conducted in all four gravity levels (micro, Mars, Moon, and Earth) and at all interested habitat sizes, and will only require one test subject and the required safety divers.

The data collection methods utilized to get useful data are:

- Qualsys
- April Tags
- Post-Experiment Survey
- Survey
- TLX

The procedure for this experiment goes as follows:

- Setup
    1. Set up equipment to be moved in and outside the habitat
    2. TS begin by workstation
- Testing
    1. TS 1 and TS 2 exit habitat through airlock
    2. TS 1 and TS 2 move equipment from outside airlock to inside airlock
    3. TS 1 and TS 2 place cargo inside habitat
- Evaluation
    1. Time how long each step takes
    2. Extraneous movement
    3. TLX
    4. Qualitative Survey
    5. Amount of space each step requires

The following scenario script is provided to give context to the test subjects so that they have an understanding of the experiment:

- There is cargo that needs to be moved across the airlock. Test subjects will exit through the airlock and bring in supplies and organize them. Depending on the habitat size there will be different optimal ways for them to move the supplies.

A scenario drawing provides a visual layout of the habitat and experiment so that both test subjects and test conductors have a good understanding on what is being done at all times.

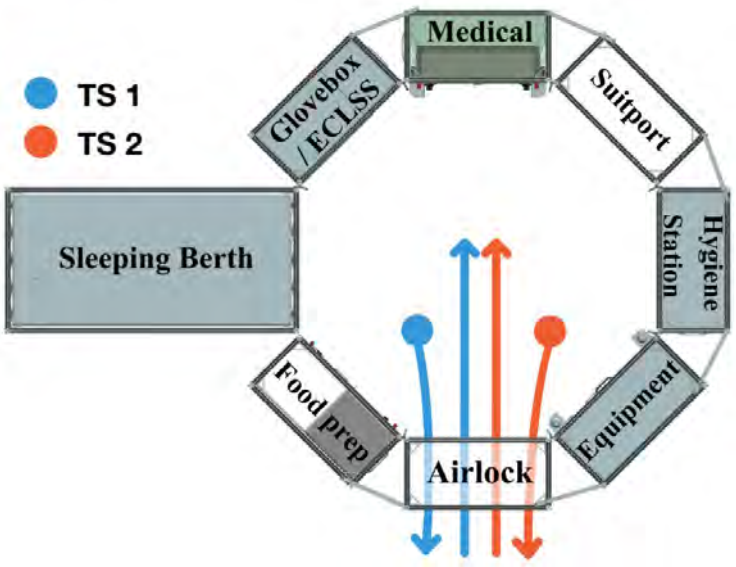

Figure 15: Airlock Main Entrance Scenario Drawing by Ramin Rafizadeh

2.4 Materials (Blaire Weinberg)

For each of the tasks in §2.3, a list of required materials was put together. These lists were meant for things that we would use in the experiment, and not necessarily as a comprehensive list of everything that would actually be needed for the task in real life. Tables 8 - 14 show the materials needed for each task, and the sized CTB associated with it. For the experiment, the standard used was a half sized CTB. While most things are used in single on the ISS, half sizes allowed for ample extra storage for what we were going to be storing in each container. Each task and the associated materials were then organized into CTB bags for similar contents. They were all alphabetically labeled for ease of storage and identification.

CTB A - Single	CTB C - Half	Behind Rack
First Aid Kit	Suture Kit	Backboard

Table 8: First Aid Materials List

CTB D - Single	CTB E - Half	CTB F - Half	CTB G - Half
Patient Monitor	IV Bags	Empty for used vials	Vials for blood draw
Blood pressure wrap			
O2 Mask			

Table 9: Medical Monitoring Materials List

CTB H - Single	CT K - Single
Spools for 3D printer	Wrenches
	Bolt Taskboard

Table 10: Workstation Materials List

CTB L - Half	CTB M - Half	CTB N - Half
Utensils	Food Pouches	Cleaning cloths

Table 11: Meal Prep Materials List

CTB P - Half	CTB Q - Half	Drawer A
Duct Tape	Replacement Filters	Hex Keys
		Scissors

Table 12: Maintenance Materials List

CTB R - Half	CTB S - Half	CTB T - Single	CTB U - Double	CTB V - Half
Exercise Bands	Washcloths	Change of clothes	Empty for trash	Water Bottles
	Toothbrush			
	Toothpaste			

Table 13: Personal Care Materials List

CTB W - Half
Extra Fabric

Table 14: Repair Materials List

At PDR, there was a comment that we weren't going to be repairing an airlock with spare fabric and duct tape. While this is true, we didn't have enough time before switching to remote learning to actually rectify the situation. That is still left in, knowing it's unrealistic, since it's still how the experiment was set up.

Once all of the materials were identified, the next step was to determine where in the experiment to put them. The actual organization was only done for the four, six, and eight rack setup. A ten or twelve rack setup would just contain empty racks as additional storage. The racks were organized into specialized sections, so similar materials could be closer together. Figures 16, 17, and 18 show the 4, 6, and 8 rack configurations, respectively. For these images, a bold black line is where there would be a shelf, described later in §3.11.

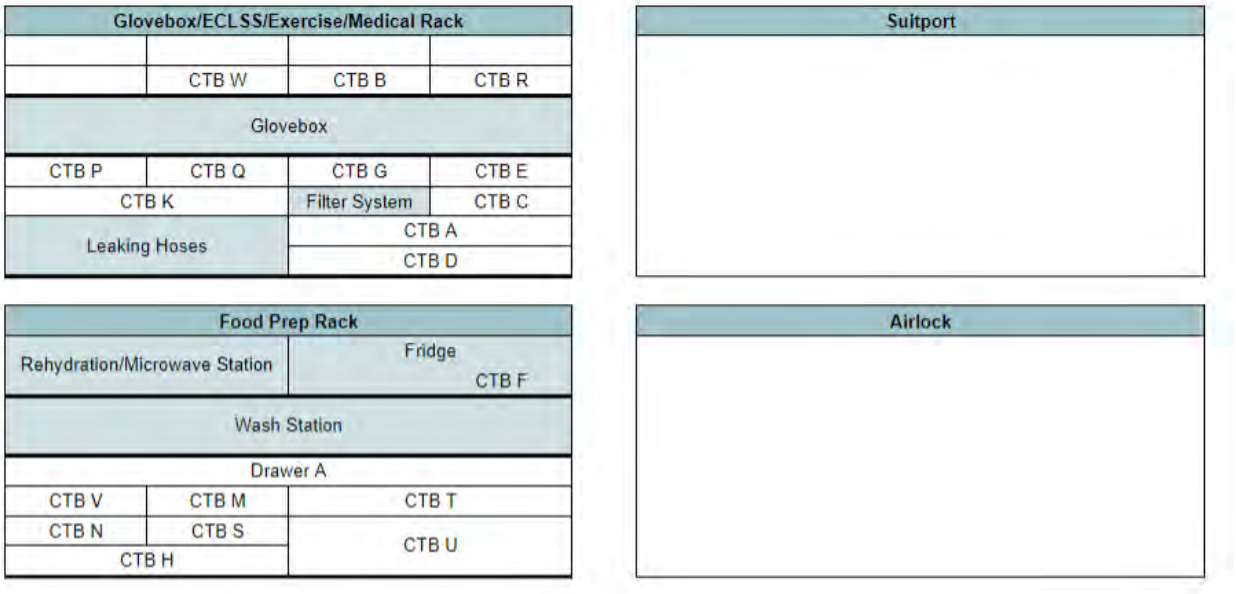

Figure 16: 4 Rack Configuration

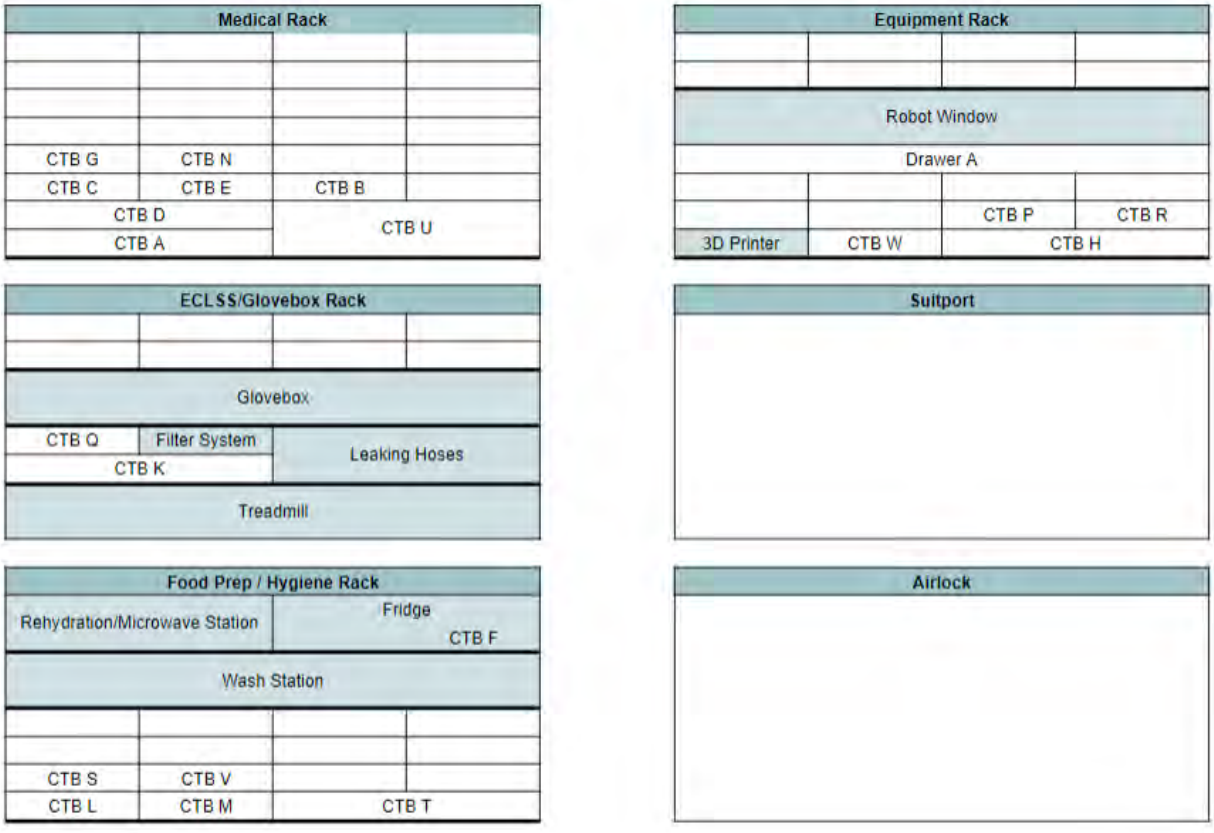

Figure 17: 6 Rack Configuration

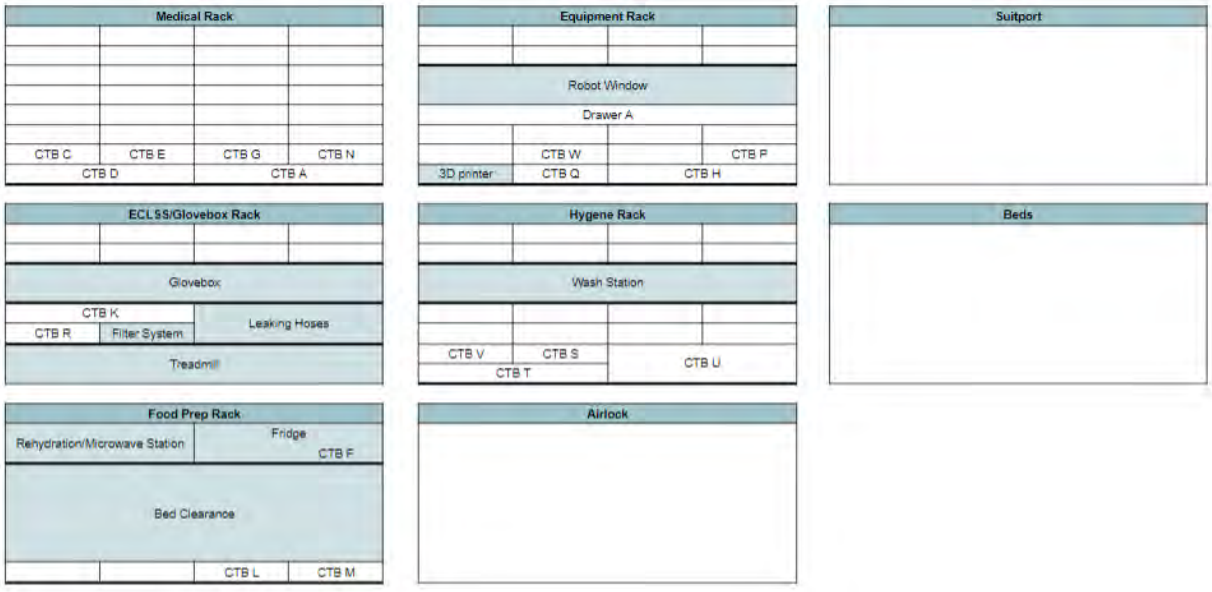

Figure 18: 8 Rack Configuration

2.5 Test Subject Itinerary (Tuvia Rappaport)

The core of phase II is the test subject itinerary, a representative full crew workflow to test the habitat volume holistically.

The itinerary is designed for four test subjects. Test subjects 1 and 2 are designated as primary, and test subjects 3 and 4 are secondary. This way habitats can easily be retested with smaller crew sizes using the same itinerary. Test subjects 3 and 4 only perform individual tasks or act as optional assistants to the primary test subjects, the experiment can continue without them.

After every task the test subjects complete the TLX survey, and when specified they also complete the qualitative survey. This compromise was made to ensure timely completion of the overall experiment given the constraint of limited available dive time. By focusing the in-depth qualitative surveys on the collaborative tasks and on test subjects 1 and 2 we can get a sufficient data set. The data collected will be associated with an identifier to the associated itinerary and test subject identifier. This enables us to easily analyze the data in the context of the experiment.

In order to limit the scope of the project we set out to to design a single complex itinerary that could serve as a universal test regimen across all habitat configurations. The limitation of this is some habitat sizes may necessitate a layout that this itinerary is sub-optimal for.

Each task has a storyboard associated with it and the itinerary has an overall story for the entire experiment. The key points of the itinerary is an initial full crew transit through the airlock, general tasks, a suit-port EVA, an emergency repair of the airlock, followed by a medical emergency and first aid. A viable habitat must be able to successfully complete this testing battery, the objective is to illustrate whether a habitat can remain functional during emergency situations in addition to normal operations.

Test Title	Experiment 1
Test Date	2020-2-20
Duration Goal	55
Participants	4
Habitat Size	10
Number of Tasks	8

Storyboard

Full day of tasks for a four test subject habitat. Test subject 1 and 2 are the primary test subjects, 3 and 4 primarily perform individual tasks or are assitants. Experiment starts with moving cargo through the main airlock and organizing, then test subjects perform individual tasks. The next group activity is medical monitoring to record vitals. After more individual tasks, test subject 1 performs an EVA through the suitport. After the EVA there is an emergeancy repair needed on the airlock. Test subjects 1-3 work on the repair after it it is complete Test subject 1 gets injured and the test subjects 2 and 3 bring them back inside and begin first aid. After first aid the experiment is complete.

Task	Test Subject 1	1001	Task	Test Subject 2	1002	Task	Test Subject 3	1003	Task	Test Subject 4	1004
1	Task Title	Airlock - Main Entrance	1	Task Title	Airlock - Main Entrance	1	Task Title	Airlock - Main Entrance	1	Task Title	Airlock - Main Entrance
	Role	Test Subject 1 - Primary		Role	Test Subject 2 - Secondary		Role	Test Subject 2 - Secondary		Role	Test Subject 2 - Secondary
	Estimated Time	5		Estimated Time	5		Estimated Time	5		Estimated Time	5
	TLX and Survey			TLX and Survey			TLX and Survey			TLX and Survey	
2	Task Title	Workstation - General	2	Task Title	Life Support - Meal Prep	2	Task Title	Workstation - General	2	Task Title	Life Support - Personal Care
	Role	Test Subject 1 - Primary		Role	Individual		Role	Test Subject 2 - Secondary		Role	Individual
	Estimated Time	5		Estimated Time	5		Estimated Time	5		Estimated Time	5
	TLX			TLX			TLX			TLX	
3	Task Title	Medical - Monitoring	3	Task Title	Medical - Monitoring	3	Task Title	Medical - Monitoring	3	Task Title	Life Support - Meal Prep
	Role	Test Subject 1 - Primary		Role	Test Subject 2 - Secondary		Role	Test Subject 2 - Secondary		Role	Individual
	Estimated Time	5		Estimated Time	5		Estimated Time	5		Estimated Time	5
	TLX and Survey			TLX and Survey			TLX and Survey			TLX	
4	Task Title	Life Support - Maintenance	4	Task Title	Life Support - Personal Care	4	Task Title	Life Support - Meal Prep	4	Task Title	Workstation - General
	Role	Individual		Role	Individual		Role	Individual		Role	Individual
	Estimated Time	5		Estimated Time	5		Estimated Time	5		Estimated Time	5
	TLX			TLX			TLX			TLX	
5	Task Title	Airlock - Suitport	5	Task Title	Airlock - Suitport	5	Task Title	Life Support - Personal Care	5	Task Title	Life Support - Maintenance
	Role	Test Subject 1 - Primary		Role	Test Subject 2 - Secondary		Role	Individual		Role	Individual
	Estimated Time	10		Estimated Time	10		Estimated Time	10		Estimated Time	10
	TLX and Survey			TLX and Survey			TLX			TLX	
6	Task Title	Airlock - Repair	6	Task Title	Airlock - Repair	6	Task Title	Airlock - Repair	6	Task Title	Workstation - General
	Role	Test Subject 2 - Secondary		Role	Test Subject 1 - Primary		Role	Test Subject 2 - Secondary		Role	Individual
	Estimated Time	5		Estimated Time	5		Estimated Time	5		Estimated Time	5
	TLX and Survey			TLX and Survey			TLX and Survey			TLX	
7	Task Title	Airlock - Injury	7	Task Title	Airlock - Injury	7	Task Title	Airlock - Injury	7	Task Title	Life Support - Maintenance
	Role	Test Subject 1 - Injured		Role	Test Subject 2 - Primary Rescuer		Role	Test Subject 3 - Secondary Rescuer		Role	Individual
	Estimated Time	5		Estimated Time	5		Estimated Time	5		Estimated Time	5
	TLX and Survey			TLX and Survey			TLX			TLX	
8	Task Title	Medical - First Aid	8	Task Title	Medical - First Aid	8	Task Title	Medical - First Aid	8	Task Title	Medical - First Aid
	Role	Test Subject 1 - Injured		Role	Test Subject 2 - Primary Rescuer		Role	Test Subject 3 - Secondary Rescuer		Role	Test Subject 4 - Secondary Rescuer
	Estimated Time	5		Estimated Time	5		Estimated Time	5		Estimated Time	5
	TLX and Survey			TLX and Survey			TLX and Survey			TLX and Survey	

Figure 19: Full Test Subject Itinerary

2.6 Data Collection Methods

Motion capture systems will be used to track the motion of humans and other objects in the test environment.

2.6.1 Qualisys (Tuvia Rappaport)

Qualisys is a high fidelity motion capture system that uses numerous dedicated motion capture cameras to track reflective markers. Because of the small size of the markers, Qualisys is capable of tracking full body kinematics. In addition it is capable of handling hundreds of markers simultaneously. We are operating a mixed system that consists of Qualisys 7+ Underwater cameras in addition to a mix of older cameras. The cameras have a range of up to 30 meters and are position around the Neutral Buoyancy tank allowing full tracking of the testing area. There are many integrations available, notably there are integrations for ROS and Unity. The system returns each markers position in the world space, by attaching multiple markers to an object the position and orientation can be determined. There are some limitations to the system. The system at the Space Systems Laboratory as configured can only be used for underwater testing. In addition in the underwater environment the system can be prone to errors, for example it can confuse the reflective bubbles from the divers with the Qualisys markers. In addition in order to make effective use of the system, the setup is relatively complex. Markers must be grouped and tagged appropriately in advance in order to ensure effective analysis later.

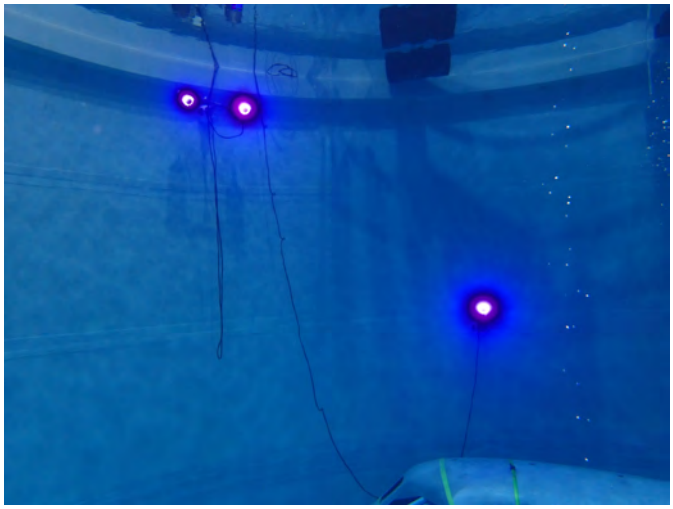

Figure 20: Three Qualisys Cameras in the NBRF Recording

For this experiment Qualisys will only be used for the underwater testing.

2.6.2 AprilTags (Brady Sack)

When compared to Qualisys, AprilTags is a lower fidelity motion capture system that uses normal cameras to track fiducial markers. The software was developed by AprilLabs at the University of Michigan, and is now open-source. Several ROS wrappers have been developed, making it relatively simple to set-up. The software can identify several unique targets and at once and return data on their cartesian position in the form of a vector and quaternion relative to the camera's coordinate frame.

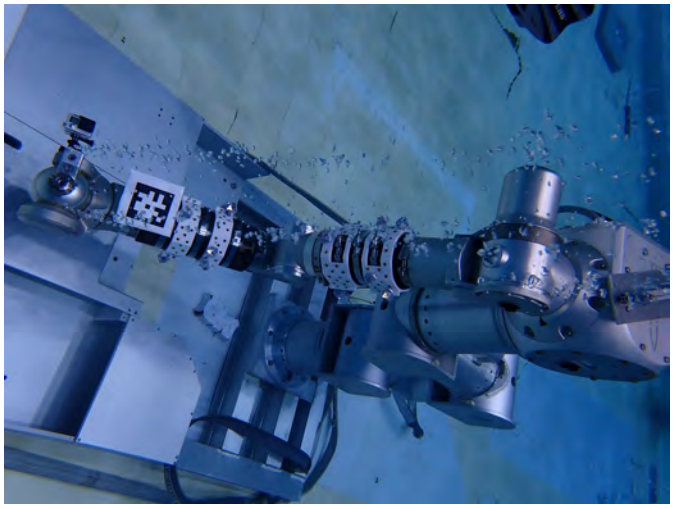

Figure 21: April tag and Qualisys markers on the Ranger arm

2.6.3 NASA Task Load (Shelly Szanto)

The NASA Task Load Index (TLX) is a standard quantitative survey that asks subjects about the workload with respect to comfort inside different habitat volumes. Test subjects would be asked 6 questions assessing their mental, physical, and temporal demand, performance, effort, and frustration while completing tasks in each habitat configuration. Answering "0" is low demand and "10" is high demand. From this we would

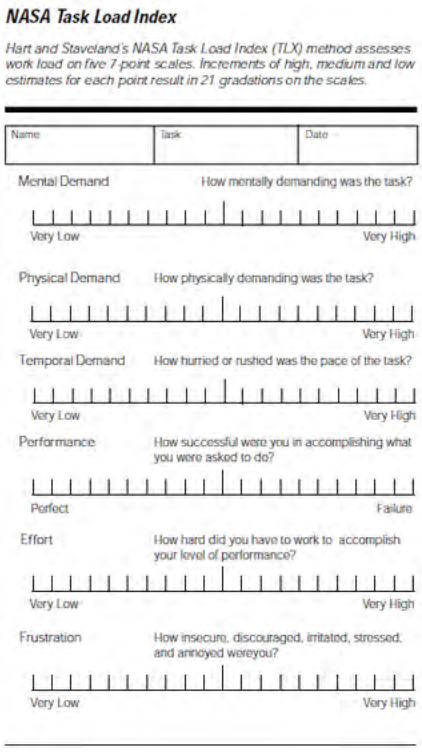

NASA Task Load Index

Hart and Staveland's NASA Task Load Index (TLX) method assesses work load on five 7-point scales. Increments of high, medium and low estimates for each point result in 21 gradations on the scales.

Name	Task	Date

Mental Demand — How mentally demanding was the task?
Very Low — Very High

Physical Demand — How physically demanding was the task?
Very Low — Very High

Temporal Demand — How hurried or rushed was the pace of the task?
Very Low — Very High

Performance — How successful were you in accomplishing what you were asked to do?
Perfect — Failure

Effort — How hard did you have to work to accomplish your level of performance?
Very Low — Very High

Frustration — How insecure, discouraged, irritated, stressed, and annoyed wereyou?
Very Low — Very High

Figure 22: NASA Task Load [25]

understand how having more test subjects inside the habitat, smaller habitat volume, or different habitat configurations put more demand or stress on test subjects.

Test subjects will be asked to complete the survey for each habitat configuration and not after each task in order to reduce the amount of data and analysis complexity. For example, once the test subject has run through the all of the tasks for a specific habitat volume and configuration, their TLX assessment would be completed. For test subjects completing the survey underwater, the paper survey would be made laminated so that divers would be able to circle the number while staying underwater.

2.6.4 Qualitative Survey Questions (Shelly Szanto)

Due to the fact that the TLX is a subjective questionnaire, a follow up survey was used to assess the test subject's feelings about the working and livable volume that an individual had in relation to the other test subject's completing tasks simultaneously. Land test subjects can complete a google form with their sentence responses and underwater subjects can write out their responses on an laminated blank paper with the questions written on it. The following are the survey questions:

1. Did you bump into anybody while completing your tasks?
2. Did you bump into anything while completing the task?
3. Did you have any issues getting to/from the task?
4. Are there tasks that would need less or more volume?

The survey responses would be analyzed in the form of pie charts to categorize the different types of responses received. From the responses, the internal layout design can be modified to reduce the interference between subjects completing tasks or move task areas to be in a better placement.

2.7 Data Analysis (Tuvia Rappaport)

The motion capture data, TLX survey data, and qualitative survey data will be used to determine if a habitat configuration is viable. By analyzing both quantitative motion capture data and qualitative survey data we can build a model for habitat performance. The data analysis will enable us to do the following:

- Determine the effectiveness of a habitats layout
- Determine the effectiveness of a test subject itinerary
- Determine the overall performance of a habitat

In order to conclude if a habitat volume is viable it is necessary to first optimize the habitats layout and test subject itinerary. Consequently, analysis will need to be performed throughout the experiment in order to produce a data-driven habitat configuration. As the effectiveness of the layout and itinerary improve, the overall performance should improve until it either reaches an acceptable threshold or the volume is considered non-viable.

2.7.1 TLX and Survey Analysis (Tuvia Rappaport)

Effective data analysis requires a metric for habitat performance. The metric needs a defined threshold for acceptable, a total failure of any one task in the itinerary must be reflected accordingly in the metric. The TLX survey data can be used to create a rudimentary metric for performance. Combining the TLX survey data with the qualitative survey data will provide added detail and validation that will enable us to ensure a failure is reflected in the metric and to understand why a particular configuration scored as it did. Because of the transition to remote work the survey design was put on hold.

2.7.2 Motion Capture Analysis (Tuvia Rappaport)

Motion capture data can be messy if a sufficient data analysis plan is put in place prior to collection. For this experiment we will have two sources of motion capture data, the Qualisys system and the AprilTags. The data will be analyzed for movement taken for each task and compared to the ideal movement required. From this we can derive the extraneous movement taken for a task. This for example, could be due to the necessity to move out of the way of another test subject. We hypothesize that extraneous movement will be a predictor for habitat performance. The motion capture systems also enable us to easily track the elapsed time to perform a task. We hypothesize that the elapsed time will also be a predictor for habitat performance. A more difficult but still achievable metric to track is the number of collisions between test subjects. This can be tracked in Qualisys by defining a bounding volume around each crew member and checking for overlaps. We can validate whether collisions occurred using the qualitative survey, but motion capture will allow us to quantitatively analyze how close crew members were forced together. Collisions are a result of a combination of poor habitat layout, poor itinerary design, and insufficient habitat volume. We hypothesize collisions will be a predictor for habitat layout. Finally the motion capture data can be used to map unused space in the habitat. By looking at the percent of space utilized we can reconfigure the habitat to take advantage of the underutilized areas. We hypothesize that the percent of space underutilized will be a predictor of a poorly configured habitat.

Another use of the motion capture systems will be to investigate the required task area and volume for particular tasks. This will be done both in conjunction with the itinerary analysis as part of phase II but also during the task analysis during phase I. We are particularly interested in investigating the required task area and volume for suit-ports. Motion capture data is useful here because we can generate point clouds of the work space boundaries. This information can then be overlaid with the associated work area (e.g. the suit-port or glove-box) and inform future habitat reconfirmations. A habitat design that incorporates these work space boundaries should reduce collisions and improve the effectiveness of a habitats layout.

In summary, the motion capture data will be analyzed for:

- Movement Taken

- Extraneous Movement
- Elapsed Time
- Number of Collisions
- Required Task Area and Volume
- Unused space

2.7.3 Data Visualization (Tuvia Rappaport)

In addition to the quantitative analysis we intend to do for the motion capture data we also plan to provide interactive data visualizations in Unity. Qualisys developed a plug-in for Unity to support real-time data streaming as well as data recording playback. We will use this functionality to

This can easily be configured to work with virtual reality and enable the user to fly through the habitat and playback the motion of the test subjects throughout the experiment.

In order to do this prior planning is necessary. Qualisys markers must be placed on all objects intended to be tracked. This includes all of the racks in the habitat, all tools of interest, and full body rigs for the test subjects. If configured properly 3D models can be associated with all the tracked components and brought into Unity with their position based on the Qualisys markers.

Motion capture data will be visualized using:

- Heat maps
- Interactive playback in Unity

2.8 Integration and Test Configurations (Michael Baker, Jeffrey Zhu)

2.8.1 Rack Configurations (Michael Baker)

Once all components and racks were designed, we needed to assemble the racks into testing configurations. This was a collaborative effort between the members working in the experimental design group, and those working in the manufacturing group. The goal was that, over the course of the semester of testing, we could create a list of all configurations we tested, and use that list to draw more general conclusions regarding the layout of the internal components and the volumes they require. Having in-depth CAD models of the testing configurations also allows for the optimization of internal component placement as testing iterates for each individual orientation and volume. We were able to create one testing configuration prior to the transition to remote work that consisted of eight racks, and followed the component requirements from the experimental design team given in Figure 18.

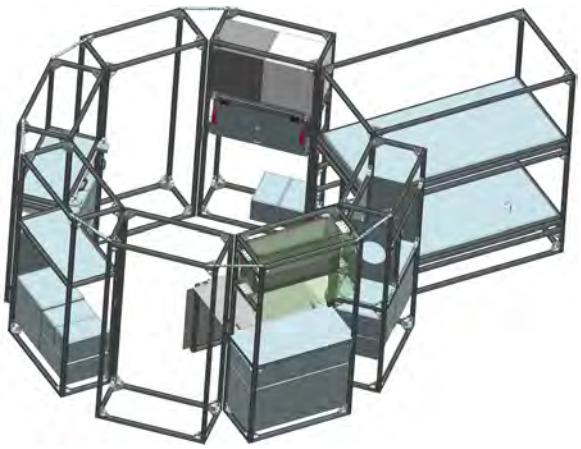

Figure 23: Isometric view one of test configuration one

Figure 24: Isometric view two of test configuration one

This configuration was designed with some attention given to the placement of racks, but no rigorous optimization. For example, the crew berths were placed directly opposite of the hygiene station to limit cross contamination from the crew bathing or using the bathroom. Additionally, the medical table was placed directly across from the airlock so, in the case of an emergency, the remaining crew could evacuate without hindrance from the extended medical table. There were, however, some potential issues with the design which could negatively impact the crew's performance of tasks like the tools being far away from the glovebox, and the suitport being separated from the airlock. Future testing would show if these rack placements are the most efficient, and subsequently inform rack placement for further designs.

2.8.2 Rack Configurability (Michael Baker)

Once rack configurations are determined, we must find a simple and efficient way to configure the racks and decrease down time between tests. This was a particularly important challenge to solve under water, as accurately positioning the angles between the racks would be significantly more difficult when diving. We determined that the best way to solve this issue would be to pair a hinge and an angle locking bar with predrilled guide holes for configurations from 6 to 12 racks.

Figure 25: Angle locking bar connecting the outer corners of the racks

The angle locking bar would only require two bolts to be screwed in for each rack to lock it in place, and the hinge on the internal circumference of the racks would be entirely toolless. The addition of these components means that assembling a test configuration would only require one individual given that the number of racks in the configuration is known.

2.8.3 Rack Assembly (Jeffrey Zhu)

While the angle locking bar fixes racks at predetermined angles, pinned constraints along the inner diameter of a rack configuration allows racks to be easily shifted from one angle to another while underwater. These pinned constraints should be easily removable by divers underwater while not impeding on the experiments being conducted. The two aluminum hinges supporting the pins are mounted on the vertical 80/20 supports along the mating side, leaving the side open to habitable volume free of any features so maximize area for mounting of experiments. Pins are made with aluminium rods and 3D printed two part handles for locking and unlocking the hinges of adjacent racks together.

Figure 26: Tool-less Assembly Pin

Figure 27: Locked Pin in Hinge

These hinges and pins allow racks to be individually loaded into the tank and assembled by shifting the racks to align the hinge axis. Velcro strapping and also be used to assist in aligning the hinges by tightening the supports together and holding them in place while inserting and locking the pins. Then, the shape of the rack configuration can be adjusted and locked in place using the angle locking bars.

2.9 Conclusion (Charlie Hanner)

In conclusion, globally effective experiment design in this study is crucial in the analysis of both crew habitability and task volume estimation within each habitat mockup. During the project identification phase, previous projects were analyzed for their failings, and many of these issues were identified as having resulted from poor experimental design. Effective crew itineraries, habitat layouts, and analysis metrics were identified as ways to prevent this, and to prevent the likelihood of viable volumes being deemed nonviable. In working around this issue, test subject itineraries and workflows were generated in advance of testing to ensure consistent subject workload under different habitat layouts for consistent data analytics. Additionally, each testing configuration can be mocked up and saved in Siemens NX for both procedural documentation, and the possibility of virtual reality revisits or 3D task-related volume mapping. However, due to a lack of testing opportunities arising from a quick transition to severe research restrictions, the task hardware mockups, testing, and large amounts of the planned data collection were left uncompleted, Instead, they all are documented as a viable footprint for future research endeavors in minimum crew cabin volume sizing.

3 Manufacturing

3.1 Rack Production (Charlie Hanner)

In the first round of purchasing, a total of 1,057 items were sourced from Rankin Automation to assemble the dozen 80/20 structures, in addition to 48 threaded casters sourced elsewhere. All 80/20 purchased was 1515-Lite series to conserve cost and weight while maintaining strength.

Quantity	Item
48	1515-Lite x 80”
48	1515-Lite x 37””
48	1515-Lite x 17”
288	Corner Gusset
625	T-Nut/Bolt Combo
48	5/16”- 18 x 1” Threaded Casters

Table 15: 12 Rack Bill of Materials

Figure 28: Twelve Racks Produced

After the assembly process was completed rack internal designs began to take shape following requirements and planned experiments including:

- Glovebox
- Suitport
- Life support systems (ECLSS Servicing)
- CTB Storage
- Meal prep areas
- Medical station racks
- Folding communal table designs
- Tool storage
- Workstation and robot control

3.2 Suitport Rack (Charlie Hanner)

In designing suitable experimental hardware for the study of spacesuit ingress and egress a minimum of three base requirements needed to be satisfied:

1. The rack must be portable both underwater and on-land to support positioning both in the main habitat area and integrated into the hab structure
2. The hardware must support a human's required actions in full fidelity
    - This requires for the inclusion of torso, arms, and legs in limiting movement in a realistic manner
3. Safety must be held to the highest priority, and rescue options must be easily accessible

To satisfy all of these requirements an existing spacesuit simulator in the Space Systems Laboratory, MX-2, would be adapted into a standard rack. MX-2 was originally designed to be a fully functional underwater pressure suit to simulate astronaut EVA operations, but was decommissioned within the last decade and remained as a static display. As the study only required for ingress and egress of a depressurized suit the adaptation possibility was clear.

Figure 29: MX-2 Suit Simulator - Credit: Dr. David L. Akin/SSL

The rack the suit is currently suspended from (shown in Figure 29) sits at just over the 40" width of a standard rack, and it was ultimately decided that this was acceptable for preliminary test if this slight amount of extra volume (when integrated in to the hab structure) was accounted for in the testing plan. Additionally during the decommissioning process parts of the suit arms were preserved for future use, and the remaining arm segments consisted of mostly loose fabrics and very little structure. To work around this lack of realistic structure, hard-structured spacesuit arms taken from a previous single person spacecraft

(SCOUT - Figure 30) were planned on being adapted to the suit's HUT. A simple adapter plate was going to be used to adapt the new arm configurations to the original structure, however the transition to remote work interrupted this planned schedule.

Figure 30: Hard Suit Arms Demonstration - SCOUT - Credit: SSL Photo Archive

Additional modification possibilities included leg assemblies and the helmet. The legs of the spacesuit were deemed to have enough structure and realism when compared to fully-functional spacesuit. MX-2 was designed to be a realistic simulator, and the decommissioning process left the leg portions unmodified. However, the bubble-style helmet posed a potential safety concern underwater as it was designed for the subject to be wearing only a Snoopy Cap type garment, and not a full-face SCUBA mask that has the potential to get caught unexpectedly. To remedy this it was deemed necessary to remove and preserve the half-dome bubble, a simple operation requiring an marman-style clamp adjustment, with the added bonus of removing any possibility of trapping the test subject's expelled air while SCUBA diving.

3.2.1 MX-2 Modifications (Brady)

Several groups have already conducted feasibility studies on suitport ingress and egress procedures. A group at Johnson Space Center working with a Z-1 spacesuit prototype had 8 tests subjects perform donning, undocking, docking, and doffing procedures with two rear-entry suitport concepts: the marman clamp system, and the pneumatic flipper design. While the tests' primary focus was on the suitport type, after the first round of testing 6 of the 8 subjects tested reported a need for some type of foot restraint for donning procedures in order to straighten the legs. Additionally, all the test subjects reported the need for an overhead pull-up bar and dipping bars for the doffing procedure. After incorporating both of these ideas, the same 6 respondents' modified Cooper Harper scores decreased (indicating increased acceptability). Notably, the other two subjects had great difficulty with and without the aids, but actually reported more difficulty when using the aids.

Given these findings, our team decided to modify the current MX-2 suit rack to include a foot restraint. Since the MX-2 boots were designed to interface the NBL Portable Foot Restraint (PFR), we mounted a 3D printed (with ABS material) model of the PFR to a piece of 80-20, which allowed us to adjust the foot restraint for the subject's comfort. These modifications were made just prior to the transition from in-person to online training, and so we were unable to add the pull-up and dip bars for the doffing. Before future

testing begins, these changes should be made immediately.

These modifications will allow us to verify the results found in prior studies. We'll also be able to extend the results of that study, by testing the donning/doffing procedures in varying levels of gravity and studying how those changes change required volume and aid requirements.

3.3 Glovebox Rack (Lucia Stainer)

As mentioned earlier, one of our planned experiments centers around workstation activities that would commonly be performed in a microgravity or surface gravity habitat. We had decided to accomplish this by building a glovebox analog that could replace a real glovebox for the purpose of the testing. This section of the report will establish the requirements for this analog in order to accurately be used instead of a functional glovebox during testing, as well as the design of the glovebox rack that we had planned to use during the experimental phase of this project.

All of the requirements for the glovebox analog were devised in order to make sure that it was feasible to build the glovebox within the allotted time, budget, and building capabilities and to ensure that the glovebox, for the purpose of the experiment, is used in functionally the same way as a standard glovebox. The first requirement was that the glovebox analog fits within the standard 20" x 40" x 80" rack frame that we were already in the process of building. This requirement was created in order to make the glovebox easier to build and fit together with the other components. The other requirements were that the glovebox analog should have a place where samples can be placed inside of and removed from the glovebox, should allow the testers to manipulate the samples contained within the glovebox, and should have adequate space within the glovebox to conduct geological experiments. It should also be an accurate representation of the volume requirement of a standard-sized glovebox.

In the process of designing how the glovebox analog should be assembled, two different designs were created. The initial design, as shown in Figure 31, fits within the 20" x 40" x 80" rack frame and contains both a side access port and two front-facing holes on the hab-side of the box in order to allow testers to place, manipulate, and remove samples from the glovebox. These front-facing holes were placed approximately 43 inches (3.6 ft) above the ground so that they would be at a height that an average-sized person could comfortably place their arms in. The frame was made out of 80/20, while all other surfaces were made using acrylic sheets, with the front sheet being transparent in order to allow testers to see within the glovebox.

One of the requirements was that there had to be an adequate amount of space within the glovebox work volume to be able to conduct geological experiments. This was accomplished by modeling the glovebox internal dimensions after a glovebox that is currently being used on the International Space Station, the Microgravity Science Glovebox. NASA's Marshall Space Flight Center lists the work volume of a Microgravity Science Glovebox as being 19.69" x 35.67" x 25.08", and so we used these dimensions to dictate the dimensions of the glovebox analog [102]. The dimensions for this first design were 20" x 25" x 25", which still fit within the 20" x 40" x 80" rack frame. While both the depth and the height of the glovebox are comparable to that of the Microgravity Science Glovebox, its width is almost 11" shorter. This was done to provide enough room to be able to comfortably transfer the sample to and from the glovebox via the side compartment, while still keeping the glovebox within the rack frame. Something else to note about this design is that the glovebox rack has no top or back faces. Since this design was only an analog for a glovebox, it did not need to be airtight, and so any faces that were not being interacted with were considered to be extraneous and were therefore not included. Additionally, since only the work volume of the glovebox was going to be used during testing, it had been determined that there was no reason to construct an analog for the glovebox's filtration, airlock system, etc. Therefore, this design does not include any of these extraneous features.

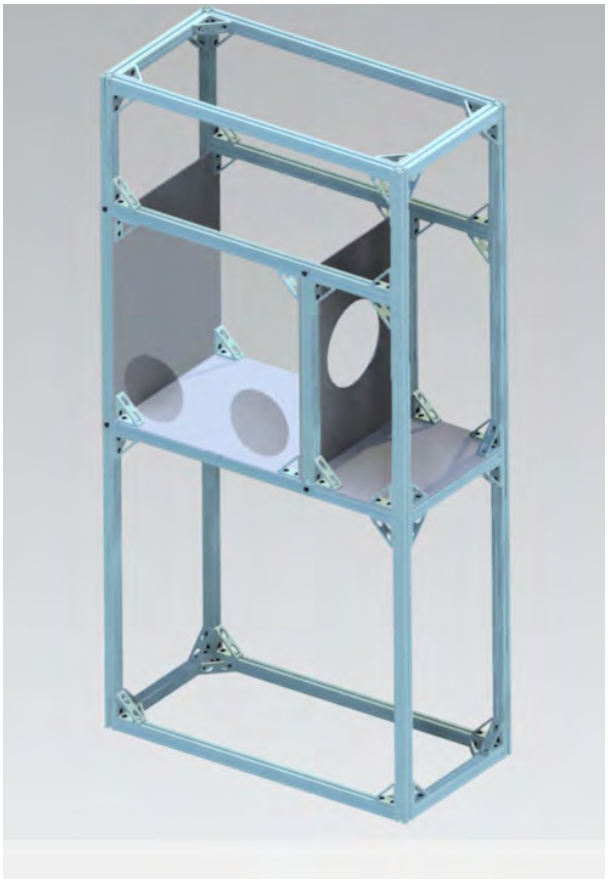

Figure 31: Glovebox Testing Unit, Design 1

The second design, shown in Figure 32, is similar to the previous design, but some revisions were made after receiving to the feedback from the Preliminary Design Review. The primary difference between the two designs is that the work volume portion of the glovebox in this second design extends out into the habitat in order to more accurately represent the Microgravity Science Glovebox, which the design was based off of. The experimental portion of this project was focused on determining whether the volume within a habitat falls within the realm of livable, and as a result, it is important that any analogs for systems used in the habitat take up a comparable volume to their real counterparts. While the total volume of this rack was not compared to the total volume of the MSG due to the limitations of the standard rack size, the work volume was designed to be very similar. This design has the total dimensions 40.25" x 40" x 80", work volume dimensions of 20" x 40" x 26.5", and just like the first design, has two glove access ports. Unlike the first design, this design has two side access ports on either side, which also matches more closely with the MSG. This glovebox rack was also planned to be made of the standard 80/20 rack frame and acrylic sheets. Had we continued with the project on campus, this is the version of the glovebox rack that we would have most likely built and tested with.

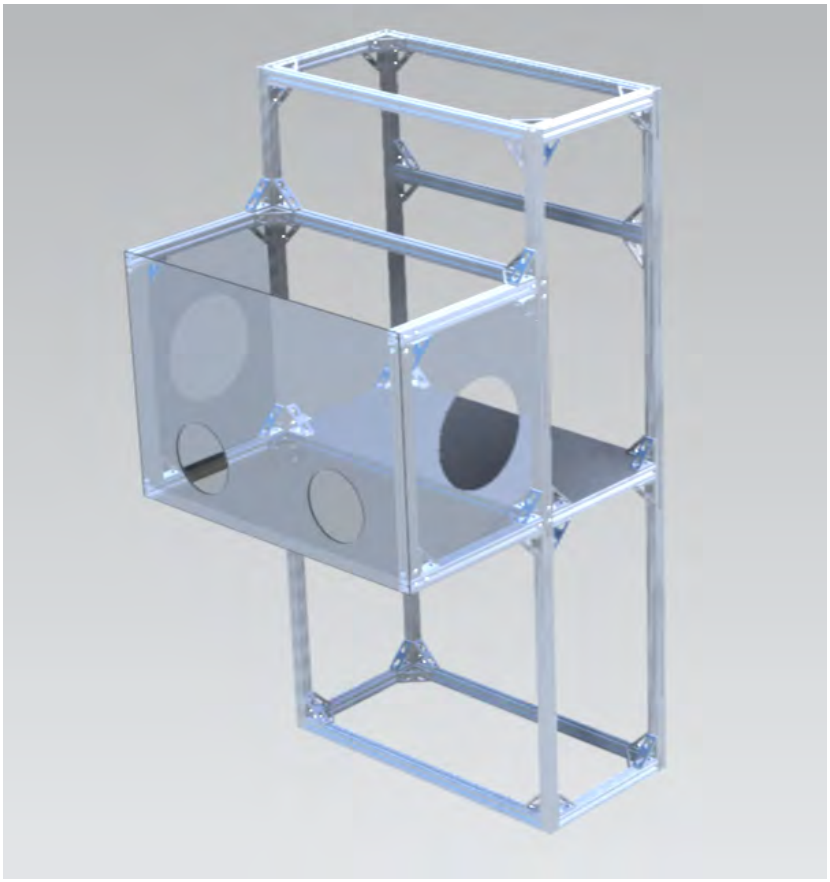

Figure 32: Glovebox Testing Unit, Design 2

3.4 Tool Storage (Zach Peters)

Most of the work done in space habitats are maintenance and repair tasks. This means that substantial portions of the pressurized habitat volume must be allocated for storage of tools and other utilities needed to perform these tasks. On the ISS, tools are stored in drawers like the one shown in Figure 33 [89]. Tools are constrained within their respective drawers via custom foam inserts with cutouts for each individual tool type and size. This method of tool storage was to be simulated in the habitat rack mockup via custom drawers built to interface directly with the 80/20 racks. The initial design for these drawers is shown in Figure 34. This design was to be constructed out of custom cut 80/20 extrusions and plastic panels in order to fit perfectly in the racks with plastic handles mounted to the front of each drawer. The drawer's motion was facilitated by steel linear guides which connected the drawer to additional 80/20 structure that was mounted within the racks. Due to the numerous custom sized parts that were required, this design proved to be unnecessarily expensive. Additionally, in order to assure effective and repeated use in testing in the lab's neutral buoyancy facility, other materials for the linear guides were considered in a second design iteration.

Figure 33: ISS Tool Storage Module [89]

Figure 34: Initial Tool Storage Drawer Design

The second design made use of off-the-shelf plastic storage bins which were modified to operate as a drawer. These bins were approximately 35-5/8" x 18-1/4" x 6-1/4". The modifications included mounting the plastic handles from the initial design to the front of each bin, as well as 3D printing linear guide rails. These guide rails are shown in orange and yellow in the figures below. The orange c-channel pieces were mounted directly to the 80/20 drawer support structure in each rack while the yellow pieces mounted to the bins slid in and out. Counterbored holes were used in each case to assure proper movement of the drawers. In the future, a locking mechanism should be added to prevent the drawer from opening prematurely and to prevent the drawer from sliding completely off the rack. The drawers can be placed in a stacked configuration as shown in Figure 36, or they can be placed individually throughout the habitat mockup depending on the experiment design and amount of storage needed. For the intended experiments in this paper, materials were purchased for the assembly of five drawers. The tools can be stored within the drawers by various means such as Velcro restraints, foam inserts, or simply loose storage depending on the experiment design and gravity level. For testing in neutral buoyancy to simulate microgravity, holes should be drilled in the bottom of each drawer to allow water to pass through when placed in, or removed from, the water.

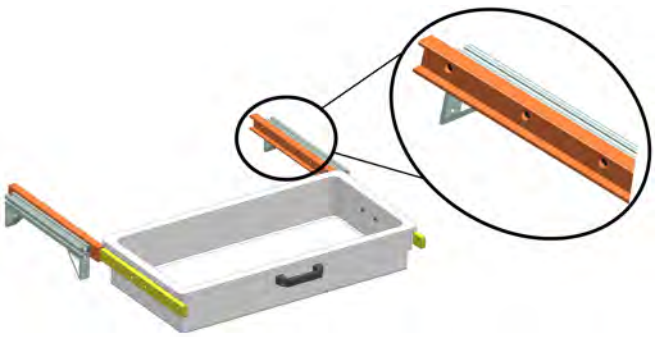

Figure 35: Plastic Tool Drawer Design

Figure 36: Tool Storage Rack Assembly

3.5 Overhead Storage (Matthew Ostrow)

3.5.1 Purpose

The Overhead Storage Module (OSM) provides a method of storing test supplies in a container at heights not normally reachable via the slide-out drawer system used for Tool Storage in section 3.4. A specific purpose the OSM served was to act as an analog to the ISS's Food Rehydration Module, seen below:

Figure 37: ISS Food Rehydration Module [107]

The ISS Food Rehydration Station features a port on its front face where dehydrated food pouches are inserted for rehydration. The OSM's front panel features a circular cutout to act as an analog for the rehydration port, seen below:

Figure 38: OSM Front Panel View

Apple sauce packets were planned to be used as analogs for the dehydrated food pouches. Although the ISS food rehydration station does not store the food pouches in the module, the OSM was designed to have internal storage to serve multiple purposes within the test habitat. In a full-sized habitat, it is very likely that some form of overhead storage modules would be needed, so these overhead storage modules could be used for other tests involving removal of supplies and tools from different parts of the habitat.

3.5.2 Design Overview

The contents of the OSM need to be easily accessible, and so the front panel was designed with a torsion spring and hinges to open the panel once the deadbolt was unlocked. The torsion spring holds the panel open while the test subjects have full access to the inside and can safely remove contents without concern of having to hold the panel open.

The mass of the OSM is **58 lbm**. This should be lifted by two people during installation.

The torsion spring is in its uncompressed state when the panel is open, and thus is preloaded and held closed when a test subject rotates the panel down and engages the spring-loaded deadbolt. The deadbolt was chosen to be spring loaded so that any random jostling of the racks would not accidentally disengage the deadbolt.

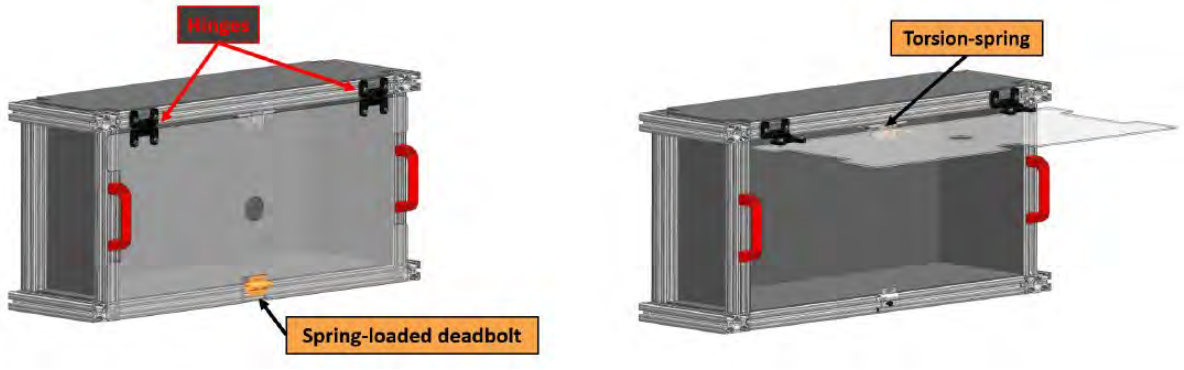

Figure 39: OSM Latch, Spring, and Hinges

The internal dimensions of the storage volume are such that two Half sized CTB's or one Single sized CTB could fit within the OSM. Dimension comparisons are shown below:

OSM Internal Volume Dimensions:	33.5"x17.0"x10.0"
Half CTB Stand-in Dimensions:	12"x16"x8"
Single CTB Stand-in Dimensions:	19.7"x14.2"x19.7"

Table 16: OSM Internal Dimensions & CTB Stand-in Dimensions

3.5.3 Installation

The OSM can be installed at any height within a test rack. Four slide bearing subassemblies receive the slide rails of the OSM to hold the OSM at the installed height. There are hard stops on the slide bearings to control the depth at the which the OSM is installed. The installation hardware matches the hardware used in test rack assembly as to minimize unique part count and ensure compatibility.

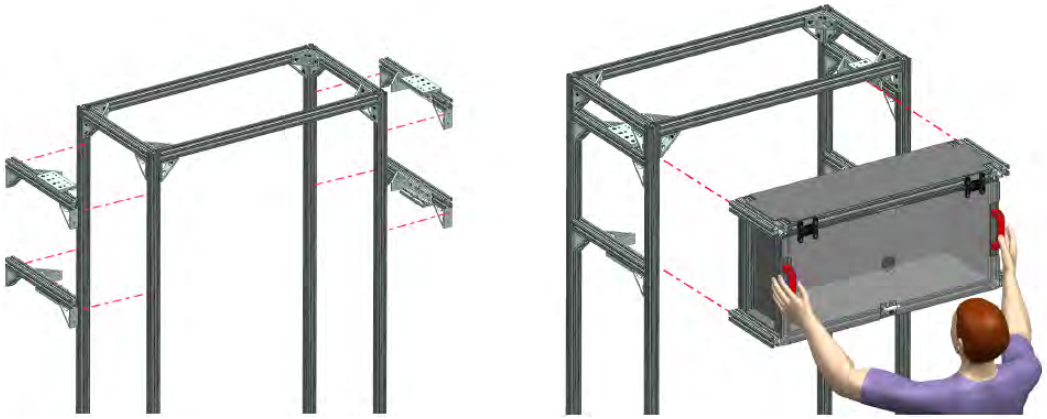

Figure 40: Slide Bearing Rail Install (left) & OSM Slide Rail Insertion (right)

The installation procedure is as follows:

1. Assemble OSM and four slide bearing subassemblies separately
2. One person holds the OSM at the desired height in test rack assembly
3. Another person matches the slide bearings and tightens T-nut bolts at locations where OSM slide rail extrusions fit onto slide bearings

Installing the slide bearings while the OSM is held in place ensures that a match fit between the OSM's slide rails and the slide bearings, similar to a match drilling procedure. This is beneficial because it allows for larger manufacturing and assembly tolerances, as the slide bearing can always be installed at a height that allows the slide bearings and slide rails to interface.

3.6 Medical/Food Prep Rack (Patrick Geleta, Chirayu Gupta, and Zach Lachance)

3.6.1 Food Preparation and Medical Rack Combination (Zach Lachance)

Due to the similarity in requirements and intended design for the food preparation rack and the medical rack, consisting of the overhead module (described in Section 3.5) and the table (described in the following sections), it was determined that both of these requirements could be served by a single rack. This is because, for almost the entire anticipated testing program, both racks would not be needed at the same time since no operations involving both would be happening concurrently. This reduces the construction time by only having to build one rack instead of two highly similar or identical racks. Additionally, the cost is reduced by only needing to buy one set of parts instead of two, thereby halving the cost that would be needed to construct them separately. This also allows for reduced rack switching during the testing program, as both functionalities could be accomplished out of the same rack. As such, for a test using a rack configuration that does not include all of the constructed racks, both of these experimental task sets can be conducted without the need to change the rack configuration. This concern is especially useful for underwater testing, as while it is relatively easy to switch racks in surface testing, it is a much more difficult task underwater, as it could involve tools and/or the crane and also requires a significant number of man-hours between the divers and supporting personnel. Finally, for larger rack configuration habitats, this increases the line-of-sight capabilities of the data tracking systems. This is because, instead of having two full racks to impede line-of-sight, it would instead be one full rack and one empty rack, the latter of which is much better for the vision system tracking.

However, this combination of the racks poses a few drawbacks, and as such mitigation strategies were developed for the largest issues. These are summarized in Table 17.

Drawback	**Mitigation Strategy**
Having meal preparation and medical operations in the same space within a habitat is not sanitary.	This is not important due to the testing nature of the project. An actual functioning habitat would have separate spaces for these two activities or appropriate procedures for cleaning and sterilization.
Cannot test food preparation and medical activities at the same time.	This only impacts a few desired tests, and a CTB rack will be constructed such that it can be converted into a temporary alternate food preparation rack (details in Section 3.6.7).

Table 17: Medical and food preparation rack drawbacks and mitigation strategies

3.6.2 Table Requirements and Specifications (Patrick Geleta)

In this study, multiple testing conditions (meal prep, and medical operations) depended on a dedicated table. As mentioned above, the table will only be used in one configuration for any given testing scenario. This table was designed to meet the following series of requirements for testing.

The proposed Multi-Function Table must:

- reconfigure into an extended medical table, capable of supporting an individual's weight
- reconfigure into a meal-prep table
- stow away into its dedicated rack
- be able to be adjusted into different layouts by 1 test subject

3.6.3 Original design attempts (Patrick Geleta)

Originally, there were several potential designs considered. At first we planned on having a single panel folding table fixed to a linear rail. This would allow it to be raised to variable heights, and allow access to space both above and below the table, but the additional mechanism of the linear rail presented unnecessary complexity and difficulty in operation.

The desire to have simple mechanisms for configuring the table, as well as enabling access to storage space throughout the unused portions of the rack contributed to the final design conditions outlines in the next section.

3.6.4 Design 2.0 (Patrick Geleta and Chirayu Gupta)

The final design iteration featured a 3-segment table constructed at a height of 35 inches above the ground. The first segment was simply a rectangular plate fixed at 35 inches via the same corner brackets used to hold the racks together. The plate was designed to be an acrylic sheet fixed to 80/20 beams running the perimeter of the rack. The second and third table segments were 35 X 37 in acrylic panels supported by a series of 80/20 beams arranged in a rectangular fashion beneath the panels.
The three panels were connected together by 80/20 model 4488 zinc hinges. 2 of these hinges were placed at the intersections of the 1st and 2^{nd} panels, and the 2^{nd} and 3^{rd} panels. It was necessary to use 2 hinges at each intersection in order to ensure the table's strength and stability for supporting subjects. These hinges have attached levers that can be twisted by hand to an open or closed position, allowing for or locking rotation respectively. These hinges are capable of rotating through 180 degrees, and by proper placement, allowed for all intended orientations.

1. **Orientation 1 (stowed upwards)**: 3^{rd} panel is folded flush against the 2^{nd} panel. The 2^{nd} panel is then folded so that it is oriented upwards, flush against the front face of the rack. This enables access to storage below the table while it is stored away.
2. **Orientation 2 (stowed downwards)**: is similar to orientation 1, only the second panel is folded downward and flush against the front of the rack, rather than upwards. This allows access to the upper storage areas of the rack.
3. **Orientation 3 (medical table)**: both panels 2 and three are folded so that they are parallel to the floor, forming a table. When in this position, the legs are then inserted beneath panel 3, supporting it in the configuration.
4. **Orientation 4 (meal prep table)**: panel 2 is extended parallel to the floor, while panel 3 hangs below it, perpendicular to the floor. The legs are then inserted beneath panel 2, supporting it as a smaller table than the medical alternative.

3.6.5 80/20 and Table Surface Bill of Materials (Chirayu Gupta)

Table 18 encloses the final BoM of Design 2.0. BoM includes the 80/20 components and building materials that would have been purchased and assembled in the NBRF alongside other 80/20 rack components.

Part	Dimension	Drill Info	Quantity	Price
Acrylic Table Sheets	30”x37”x1/4”	F - .257	2	
1515 Lite Vertical 80/20	27”	-	4	In Stock In NBRF
1515 Lite Horizontal Beams	31”	-	2	In Stock In NBRF
4488 Locking Hinge	-	-	4	
3114- Button Head Socket Cap Screw (BHSCS)	5/16-18 x .750”	-	8	
3203-Standard Slide-In T-Nut	5/16-18	-	8	
3330 Flanged Button Head Socket Cap Screw (FBHSCS)	5/16-18 x .687”	-	16	In Stock In NBRF
3278 Slide-in Economy T-Nut - Offset Thread	5/16-18	-	16	In Stock NBRF

Table 18: Design 2.0 BoM

3.6.6 Design 2.0 CAD Visualization (Patrick Geleta and Chirayu Gupta)

Figure 41: Medical/Meal Prep Table Orientation 1

Figure 42: Medical/Meal Prep Table Orientation 3

Figure 43: Medical/Meal Prep Table Orientation 4

Figure 44: Close-Up of Medical/Meal Prep Table Locking Hinge System

3.6.7 Alternate Food Preparation Rack (Zach Lachance)

As described in Section 3.6.1, the mitigation strategy for any potential tests which require both food preparation and medical operations is an alternate food preparation rack. For this rack, a CTB rack was designed with additional side rails to allow for the mounting of the overhead module and a small table similar in design to the horizontal rack divider (but removable). Thus, these two components can be slid in and removed to convert between a food preparation configuration and a CTB configuration. A CAD design for the alternate food preparation rack is shown in Figures 45 and 46.

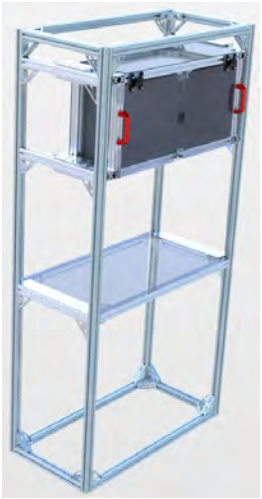

Figure 45: Food prep configuration

Figure 46: CTB configuration with components

The overhead module is slid into this rack in the same method as for the main food and medical rack, as the mounting hardware is identical (see Section 3.5 for more details), and the temporary table is held in place by horizontal constraining plates and a locking pin. The table can thus be slid in between the constraining plates, which hold it stable in the vertical direction, while the pin passes through both the constraining

plates and the table itself to keep the table from moving or sliding back out. A backstop is also located at the end to preventing the table from being slid in too far and to help ensure easy alignment of the pin holes. This allows for both components to be easily moved between racks, if needed. This constraining system can be seen in Figure 47.

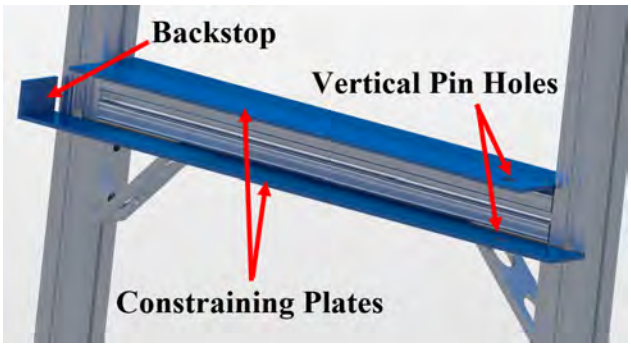

Figure 47: Right-side table attachment mechanism (mirrored on other side of the rack)

3.7 Life Support Maintenance Simulation Rack (Zach Lachance)

One of the most common activities on the ISS is life support maintenance. These common repairs and key life support systems include:

- The ECLSS system
  - Water recovery
  - oxygen generation
  - Atmospheric filters
- Electronics
  - Computers
  - Printers
  - Sensors
  - Cables
- Waste management systems
- Hygiene systems

The above list is generated based on data from the ISS daily status report logs [60].

With these components and the associated maintenance tasks, the life support rack was designed to provide analog repair tasks without the need for advanced components. Thus, two main test categories were envisioned: a large-scale repair involving the removal and replacement of a high-volume component and small-scale dexterity-based repairs.

For the large-scale repair task, the original idea was to utilize either 80/20 beams or PVC piping to make a box structure that occupies the upper quarter of a rack. As such, this box would measure 40x20x20. This could then have weights added to achieve desired weights for both surface and underwater testing. However, a different SSL team was working on a similar simulation, thus it was determined that we would try and utilize that system if they finished by the time we were ready to test (this design is similar to the original 80/20 box design, but has better optimization capabilities for weighting). A previous ECLSS testing analog used by the University of Maryland Neutral Buoyancy Research Facility can be seen in Figure 48.

Figure 48: Previous neutrally-weighted ECLSS underwater simulator

For the smaller-scale dexterity tasks, additional components would be placed throughout this rack and, if possible, in other racks to allow for a wide variety of tests. Such components would include:

- Hoses
- Valves
- Wires/Cables
- Small filter analogs
- Electronic task board

Utilizing these components, various different interaction types could be performed and analyzed. While some would be placed such that they are easy to access, simulating common/anticipated repairs, others would also be positioned in hard-to-reach or otherwise obscure areas of the racks to simulate rare/unforeseen/difficult repairs. Going into detail for the utilization of specific components, the hoses and cables can be used to simulate both replacement of these components or finding and repairing if one became dislodged. The small filter analogs (small rectangular sheets) can be used to test small-scale replacement of components. The small nature of these filter analogs also allows for them to be placed in obscure orientations for simulating the rare/unforeseen/difficult repair tasks since the large-scale analog can only be placed in one position due to the size.

While the valves only serve one purpose, to test dexterity in actuation interactions in different areas/environments, they can be used for more advanced simulations. In these simulations, a test administrator could have participants conduct a troubleshooting or malfunction isolation task where various valves are actuated and the administrator verbally tells the results in the goal of the subject locating, isolating, and resolving a simulated issue. As an example, this simulation could be regarding a hypothetical air leak. Thus, the participants would actuate valves one at a time, with the administrator relaying the "impact" that the actuation had. The participants would then use this information to narrow in on the leak, locate it, and isolate it. From here, the test could simply end or participants could then be expected to replace a hose component, simulating repairing of the leak. Thus, an entire life support air system repair, from detection to isolation to solution, could be simulated by just these components.

The last included component is an electronics task board. This component serves to simulate computer and/or printer repairs, especially software repairs, as these are frequently required on the ISS as shown by the ISS daily task logs [60]. Further details on the task board are explained in Section 3.8.

3.8 Task Board (Blaire Weinberg)

One of the things that we wanted to include in some of the tests was a way to mimic debugging. This debugging could be electronics, fiddling with sensors or filters, or any other general sort of messing around task. Our solution to this problem was a task board: a bunch of switches that, when all turned to the correct position, would turn off a blinking LED. Due to the transition to remote work, this board was designed, but did not go through manufacturing, assembly, or testing.

The board schematic is shown in Figure 49. The brains behind the board were an Arduino Micro, the smallest Arduino that had enough pins to route all of the switches to. The only requirement that we had for this board came from Dr. Akin, and that was to include both toggle and rotary switches, of which the board contains five of each. Everything is powered off of a 9V battery, which has a holder on the board.

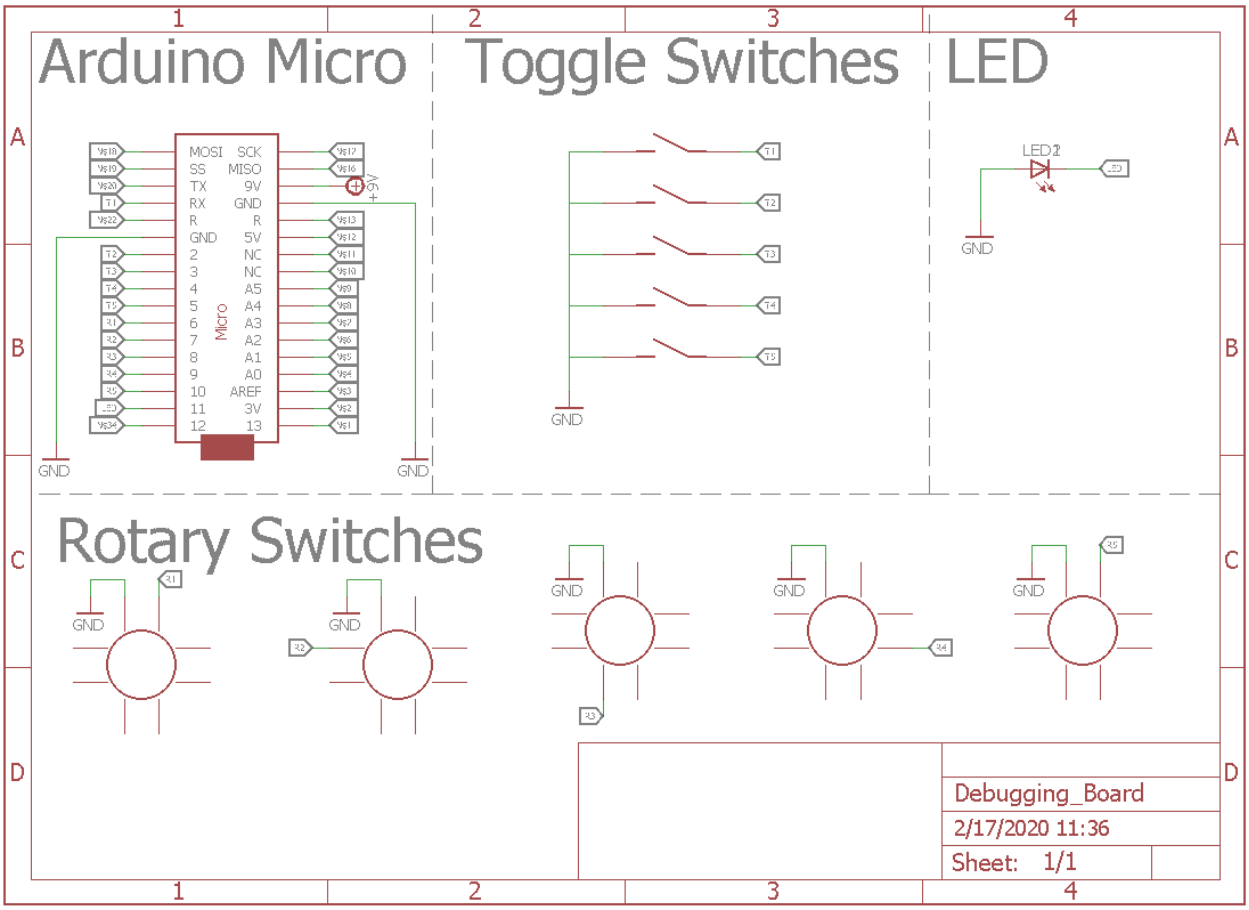

Figure 49: Task Board Schematic

Figure 50 shows the actual board layout for the task board. The board is an eight inch square, with mounting holes for 5/16" bolts for bolting into the 80/20 racks. The silkscreen of the board contains the instructions for which position to turn the switches to. The top left has the battery holder, which securely holds the 9V battery with four 2-56 flat screws. Each switch is labeled with a letter, and each position a number for the rotary switches.

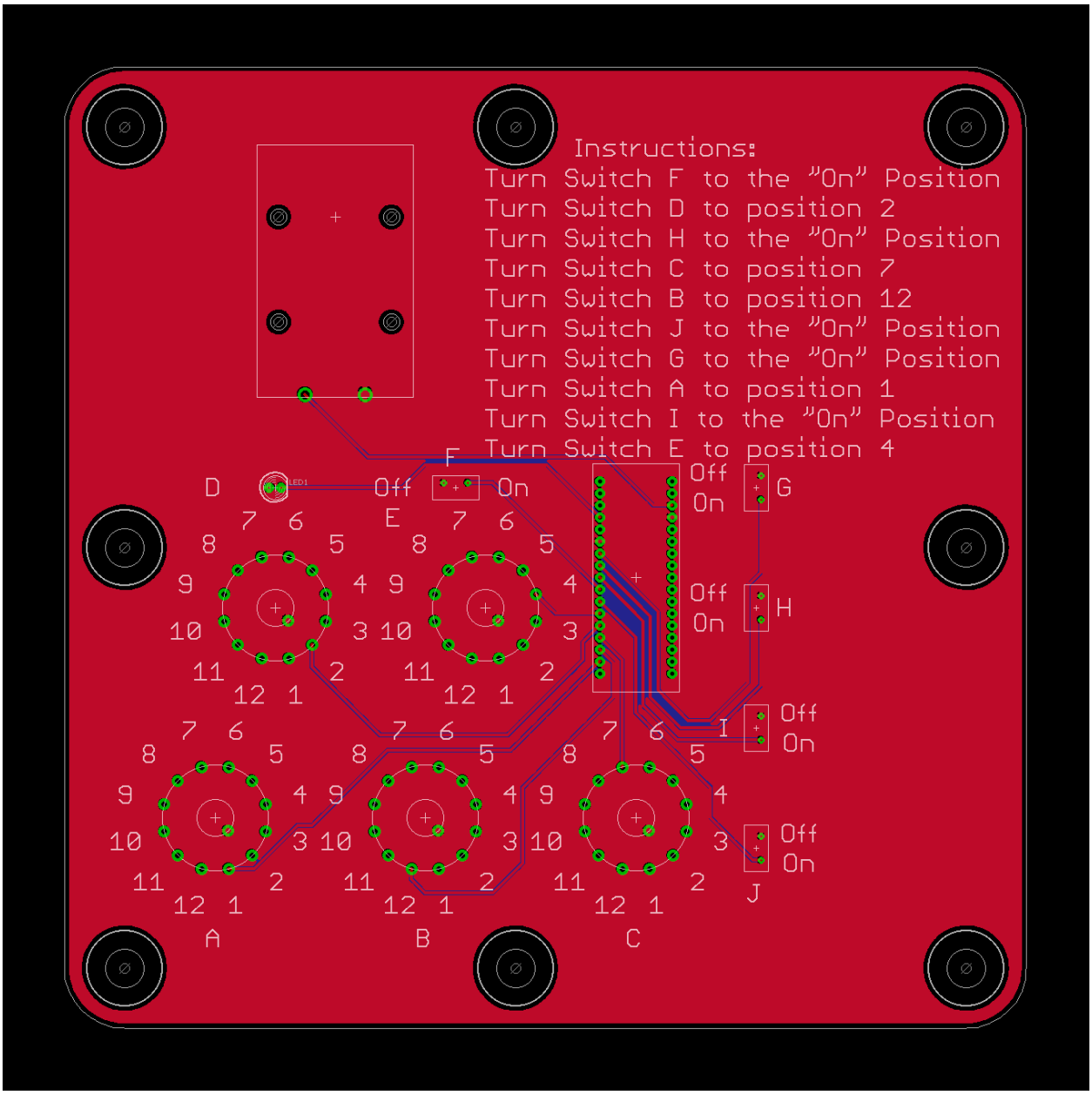

Figure 50: Task Board Board Layout

Table 19 contains the BoM for the task board, with part numbers for the manufacturer. The electronics were all sourced from Digikey, and the screws from McMaster-Carr. The only thing excluded from Table 19 is the 9V battery, since that can be sourced from just about anywhere.

Description	Quantity	Part Source	Part Number
Battery Holder	1	Digikey	36-1291-ND
Toggle Switch	5	Digikey	CW202-ND
Rotary Switch	5	Digikey	CKN10200-ND
LED	1	Digikey	C503B-RAN-CZ0C0AA1-ND
Switch Knob	5	Digikey	GH7657-ND
Arduino Micro	1	Digikey	1050-1066-ND
Battery Holder Screws	4	McMaster-Carr	94414A313
Locknuts for Battery	4	McMaster-Carr	91831A002
Sleeve Washer for Battery	4	McMaster-Carr	91145A110

Table 19: Task Board BoM

Since nothing was ever sourced, there is no code currently written for the Arduino Micro. The only things that would need to be in there are code for checking whether or not the switches all form complete circuits, and then the logic for whether or not to blink the LED.

For assembly, all of the individual parts would be soldered onto the board. This would include the switches, LED, Arduino Micro, and the two power leads to the battery holder. For the battery holder, the screws would bolt in from the underside, and then attach to the collar before going through the board. The larger part of the collar should face the screw head, since the smaller part is for going through the holes on the board. This allows for enough offset from the soldered components. The locknuts would then hold the assembly together on the top.

3.9 Crew Berths (Eric Greenbaum)

For experiments involving personal care or hygiene, simulation of sleeping quarters would have been required. To accomplish this, an expanded 80/20 rack was designed to emulate crew berths for test subjects to simulate climbing into, climbing out of, and resting within their personal, private areas. The initial design for this crew berth rack incorporated stowable beds, which were hinged on one end and folded up when not in use. Figure 51 showcases this original design. As seen in the figure, chains would have supported the weight of the bed platform, and the weight of a test subject had they simulated laying down in their personal quarters. After discussions with the Manufacturing team, this design was determined to be overly complex and possibly dangerous. If the crew berth rack tipped over, or if the supporting chains or hinges failed, a test subject could be seriously injured.

Figure 51: Initial Stowable Crew Berth Design

Figure 52 displays the modified, second design for the crew berth rack. This design included two fixed bed platforms instead of folding, suspended platforms used in the original design. Additionally, the second design included ladders which would assist the test subjects in entering and exiting the simulated beds, whereas the original design did not have any steps or ladders included. The outer dimensions of this expanded rack measure 80 inches x 80 inches x 40 inches, whereas a typical rack used to simulate other areas of the habitat typically fit within a volume of 20 inches x 40 inches x 80 inches. Although it is much larger in size, this large crew berth rack was designed with modularity in mind, with design features that would have allowed it to be used for a variety of testing purposes and habitat configurations.

Figure 52: Modified Fixed Crew Berth Design

The new berth rack design incorporates dual, fixed ladders. There is a ladder on an end of the rack which is 40 inches across, and there is a ladder on a side which measures 80 inches long. These fixed ladders would allow for the rack to be easily utilized in both rear-entry and side-entry applications, without the need for additional tools or time to remove and replace a ladder between the two sides. If the 40 inch length of the crew berth rack was located "internal" to the simulated habitat, subjects would test the crew berth rack in the rear entry configuration. If the 80 inch length of the rack was oriented so it faced "internal" to the simulated habitat, the test subjects would experiment with a side entry berth. Figures 53 and 54 demonstrate the two possible configuration for the crew berth rack in different simulated habitats.

Figure 53: Side Entry Berth Configuration

Figure 54: Rear Entry Berth Configuration

This design also was designed for testing in both gravity and micro-gravity environments. When testing occurred outside of the NBRF, to simulate Earth gravity, foam mattresses would be placed on top of acrylic panels on the "bed" portion of the crew berth racks. This will ensure the safety and comfort of test subjects. However, when testing would investigate the effects of micro-gravity on habitat processes, the foam mattresses would be removed and the acrylic panels alone would be used to simulate the bed areas, so the foam mattresses would not become submerged in the water.

Structural analysis was started for the crew berth rack prior to the course moving to an online environment. The ladders were the first portion of the rack investigated for structural integrity. The loading condition that was considered was the weight of a test subject (weighing 200 lbf) standing on the center of a ladder rung. Numerous failure modes were considered throughout analysis including shear failure in the screws holding the ladder rung in place, bending stresses (normal and transverse shear) developed in the horizontal rung, and buckling of the vertical posts of the ladder. Results of this analysis are demonstrated in Table 20.

Failure Mode	**Factor of Safety**	**Margin of Safety**
Bolt Shear	3	30.14
Rung Normal Stress	3	12.48
Rung Transverse Shear Stress	3	28.37
Post Buckling	3	4849

Table 20: Berth Ladder Structural Analysis

The margins of safety that resulted from this analysis show that the ladder was over designed. Further work was required to modify the design to decrease the margins of safety, or analysis for additional or harsher loading conditions was needed. However, due to the shift in the team's efforts from experimental rack design to full scale habitat design after the course was shifted to an online environment, further analysis of the ladder and a complete analysis of the rack was not completed.

3.10 CTB Standin (Blaire Weinberg)

As mentioned in §2.4, all of the components for our experiment were going to be stored into CTB-like boxes. The goal was to find something suitable that was close enough to the correct sizes to be useful, but with enough margin that we could buy them COTS instead of having to make our own. We ended up going with three different types of fabric storage containers, seen in Figure 55, with handles so that way they could be easily submerged, and taken in/out of racks.

Figure 55: Comparison between Actual CTB (Left) and Stand-in (Right)

While the half and double sized CTB Stand-ins are currently still being sold on Amazon, the Single ones are not. For future reference though, the single stand-ins were the "Qozary 3 Pack 53L Storage Bags for Comfortors, Blankets, Clothes, Quilts, and Towels, Betterand Sturdy Under Bed Organizer Bag, Large Storage Bags Great for Closets, Bedrooms (53L)". The ASIN was "B07TH2HVPY". Table 43 shows the dimensions of all of the stand ins, with links to the two still sold on Amazon.

CTB Size	Actual LxWxH (in)	Stand-in LxWxH (in)	Percent Volume Difference
Half	9.75x16.75x9.25	12x16x8	1.68%
Single	19.75x16.75x9.75	22.8x15.7x9	-0.12%
Double	18.75x16.75x19.75	19.7x14.2x19.7	-11.15%

Table 21: Comparison between Actual and Stand-in CTBs

3.11 Shelving (Jeffrey Zhu)

Shelving has multiple purposes to support experiments in racks assemblies. The primary purpose of shelves is to separate racks into smaller units to support smaller volume constrained equipment and experiments. They can also be used as storage space as they are designed to support the full weight of two maximum loaded double size CTBs. Shelves are designed to be easily reconfigured along the vertical axis of a rack. each shelf uses the same 80/20 extrusions used on the top and bottom of the frame. A 1/4 inch acrylic panel sits within the inner groove of the 80/20 frame, which can be cut and drilled for mounting of equipment and test stands above or below the shelf. Under maximum loading of two 120 lb CTBs, finite element analysis results show a maximum von-mises stress of 1437 psi, giving a margin of safety of 5.2.

Figure 56: Single Shelving Unit

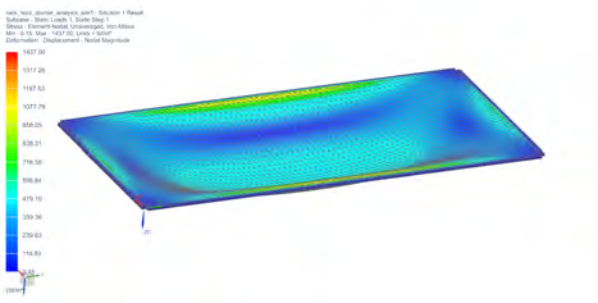

Figure 57: FEA Under Maximum Loading

Shelves can also be used as part of human interaction experiments. One example is simulating a robot control workstation. The purpose of the shelf is to vary the height and mounting positions for hand controllers and displays within a rack. Hand controllers are simulated with 3D printed replicas that can be attached at various angles and positions on a shelf. The display can be adjusted along the vertical axis, as well as tilting up and down via a VESA mount to 80/20 adapter. A flat panel can be used as a display simulator for micro gravity testing.

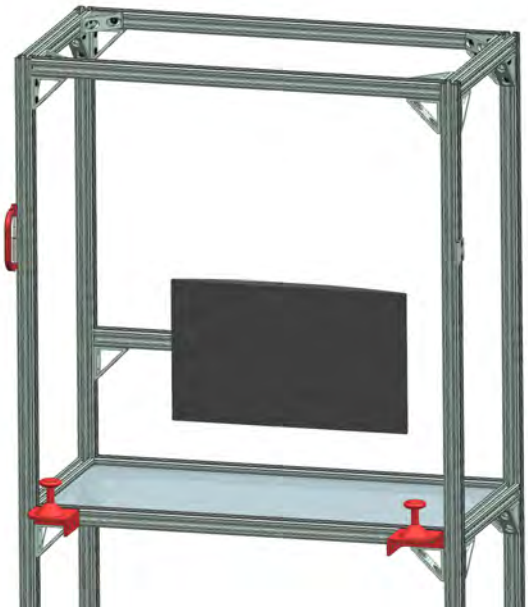

Figure 58: Robot Control Workstation

4 Big Picture

4.1 Big Picture Overview (Nicholas Behnke, Hudson Paley)

In designing the team layout at the beginning of the project, we believed it was pertinent to create a cyclical system of design and testing; design iterations based on the testing team's feedback would efficiently lead us to idealized habitats. Along this line of thinking, the Big Picture Group was established. The role of the big picture group was to research and formulate ideas of potential designs for minimum sized habitats, and provide these designs to the group as potential pre-rendered test areas that could be recreated using the 80/20 racks that the team constructed. After testing our our mock-ups with 80/20 racks, the subsequent

data taken and analyzed by the experimental design team would inform changes to the respective habitat designs.

With this goal in mind, the Big Picture Group set out to create this variety of potential habitat volumes for both surface and micro-gravity purposes. After deliberation within the group, it was decided we would produce individual habitats of both vertical and horizontal layouts, encompassing the habitat types of a stationary surface habitat, a micro-gravity habitat, an ascent/descent vehicle, and a rover habitat. These habitat designs represent volumes that would have seen further intense redesign after the analysis of testing results from the 80/20 areas. Each habitat design is provided along with an 80/20 rack layout that would have been used during the testing phase of the habitat. This section will detail these preliminary designs and how testing areas were planned to be customized for each type. These designs represent early work done that would eventually help in the transition into full habitat design that was done by the whole team later in the semester.

4.2 Micro-Gravity Habitat (Bob Nobles)

Before the team transitioned to working from home due to the COVID-19 pandemic, the focus of the Big Picture Team was designing CAD mockups for various gravity levels. The micro-gravity habitat mockup was made to be a cylindrical structure with hemispherical endcaps. The difficult part was getting the structure to an appropriate volume, particularly the endcaps. This issue would later be resolved by the LSM team by using elliptical endcaps instead of hemispherical ones.

Figure 59: Micro-Gravity Habitat Design Pre-Transition

Being this is a micro-gravity habitat, there was no need for leg supports. The habitat would simply be in its orbit for a maximum period of 30 days. The interior had two walls; the outer wall is purely cylindrical for structural reasons. The inner all was made to accommodate racks and other items that would not fit well to a curved surface.

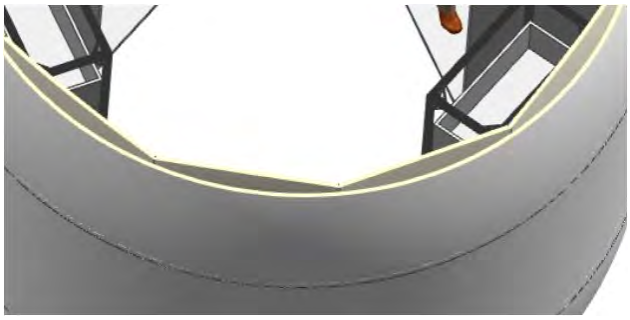

Figure 60: Micro-Gravity Pre-Transition: Inner Walls of micro-gravity habitat

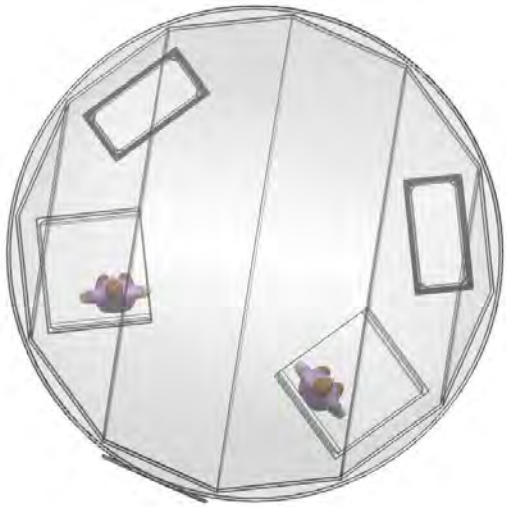

Figure 61: Micro-Gravity Pre-Transition: Rack layout

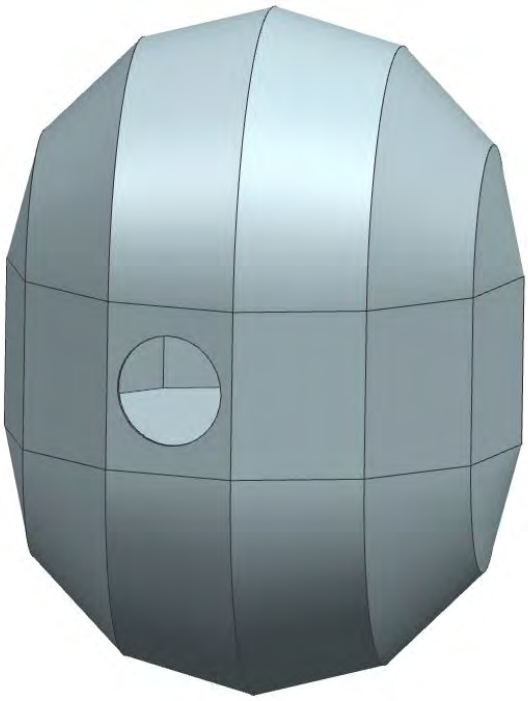

Figure 62: Micro-Gravity Pre-Transition: Interior Shell of Habitat

The habitat interior was to have spaces for storage of food and equipment, as well as sleeping quarters. A single window was also put in for viewing the outside.

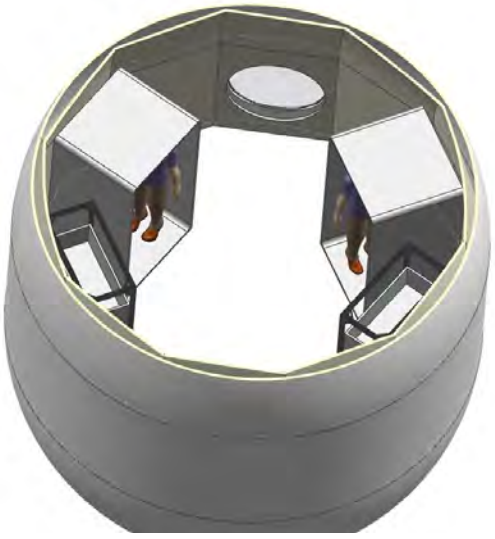

Figure 63: Micro-Gravity Pre-Transition: Interior of Habitat

More components were to be put in this habitat once the endcap problem was figured out. Unfortunately, after PDR the team began reorganizing and the work on this was halted. Later when everyone transitioned to working from home, more complete CAD mock-ups were developed for a better big picture of the habitat.

4.3 Preliminary Surface Habitat Design (Hudson Paley)

When compared to the microgravity environments, surface habitats have a different set of problems and objectives. Part of what makes visiting other planetary and lunar bodies compelling, besides accomplishing survival for extended periods of time, is the exploration and retrieval of natural resources for usage and study. Therefore, efficiency and ease-of-use were major considerations for scenarios where crew members would be having repeat EVAs. Additionally, exterior habitat repair and disposal of waste would only add to each crew member's EVA duties. For this reason, for a crew of two, a single suitport and airlock were determined to be optimal for the preliminary overall design. Suitports would cut down on space and time dedicated to EVA preparation, yielding more time spent exploring and repairing as well as more internal habitat volume dedicated to racks and utility. Since suitports require internal human assistance, one crew member would stay inside the habitat while the other is on EVA. The suitport displayed in the habitat is based on NASA's current xEMU spacesuit project, which incorporates a sealable backplate for rear donning and doffing[18]. To accomplish proper retrieval of samples and resources, an airlock is necessary, in which samples could be brought into the pressurized habitat separate from the crew members. Additionally, in the event of a necessary evacuation, the airlock could be used for docking with another craft so that both crew members could safely escape, which required a larger airlock volume compared to a simple sample airlock. The airlock's orthogrid and door were designed with respect to the Kibo module's airlock [17]. Its utility for experiments could prove useful when visiting our moon or Mars.

The above considerations were incorporated into the habitat model below, which features an 8-rack design, with two allocated for the airlock, one for the suitport, two for the berths and three for the equipment. Both the equipment inside the racks and the orientation would have changed based on findings from the experimental group's testing if access to the lab wasn't cutoff. Despite the lack of testing, there are a couple of major flaws found in the design. The airlock was determined to be unusable for evacuation since it couldn't accommodate astronauts standing erect-forcing them to crawl through the chamber. Additionally, the length of the chamber was unnecessarily long for tasks that don't necessitate experiments executed in the airlock, especially if its primary use was for bringing in samples from the lunar or martian surface. Furthermore, the oblong portion, designed with comparatively thicker walls to reduce the amount of radiation on crew members during rest, was determined to be impractical due to shear points along the connection to the primary walls of the habitat. In lieu of the oblong portion, it was later determined that a separate berth module would better accommodate this radiation condition along with mitigating manufacturing difficulty. However, later, a thinner plate of radiation shielding in the shell of each berth replaced both of these designs to coincide with the goal of minimum habitat sizing.

If the Neutral Buoyancy lab wasn't closed due to the pandemic, the following model, which features $10m^3$ of usable internal volume and an 8-rack configuration, could have been scaled according to the experimental group's conclusions.

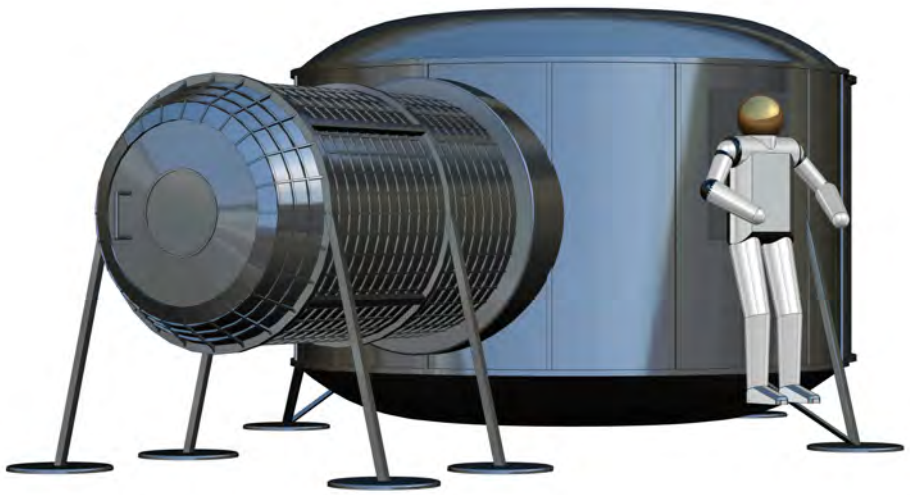

Figure 64: Preliminary Surface Habitat Exterior

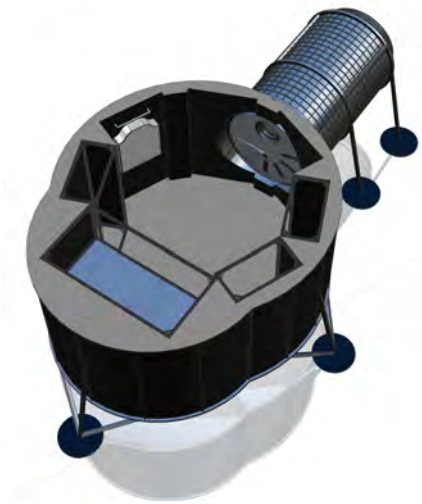

Figure 65: Preliminary Surface Habitat Internals

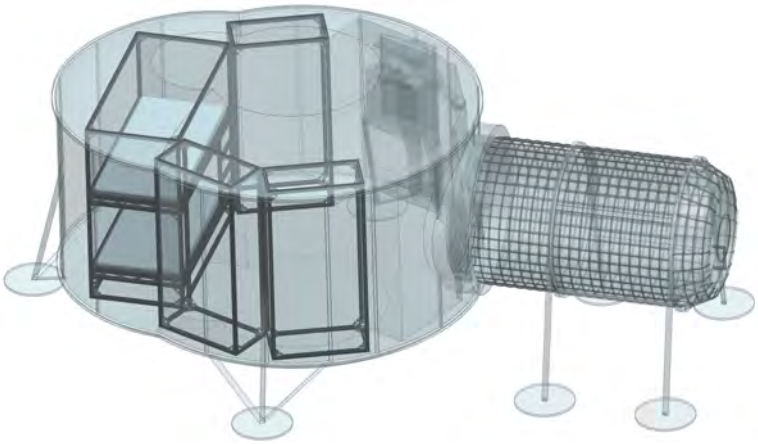

Figure 66: Preliminary Surface Habitat Racks

4.4 Ascent/Descent Vehicle Design (Einar Terrill)

Prior to the transition to remote learning, our large team of twenty was broken down into four sub-teams; of the four teams, the one I was involved in was the Big Picture Sub-team that focused on taking the habitat requirements and applying them to the macro-level. A planetary habitat, micro-gravity habitat, planetary rover, and ascent/descent vehicle were designed in NX1872 to get a better idea of the capabilities of different volume constraints. Much of the challenge centered around fitting our habitats designs to fit an 80-40-20 rack configuration; a pentagonal prism shape was chosen utilizing ten racks as shown below:

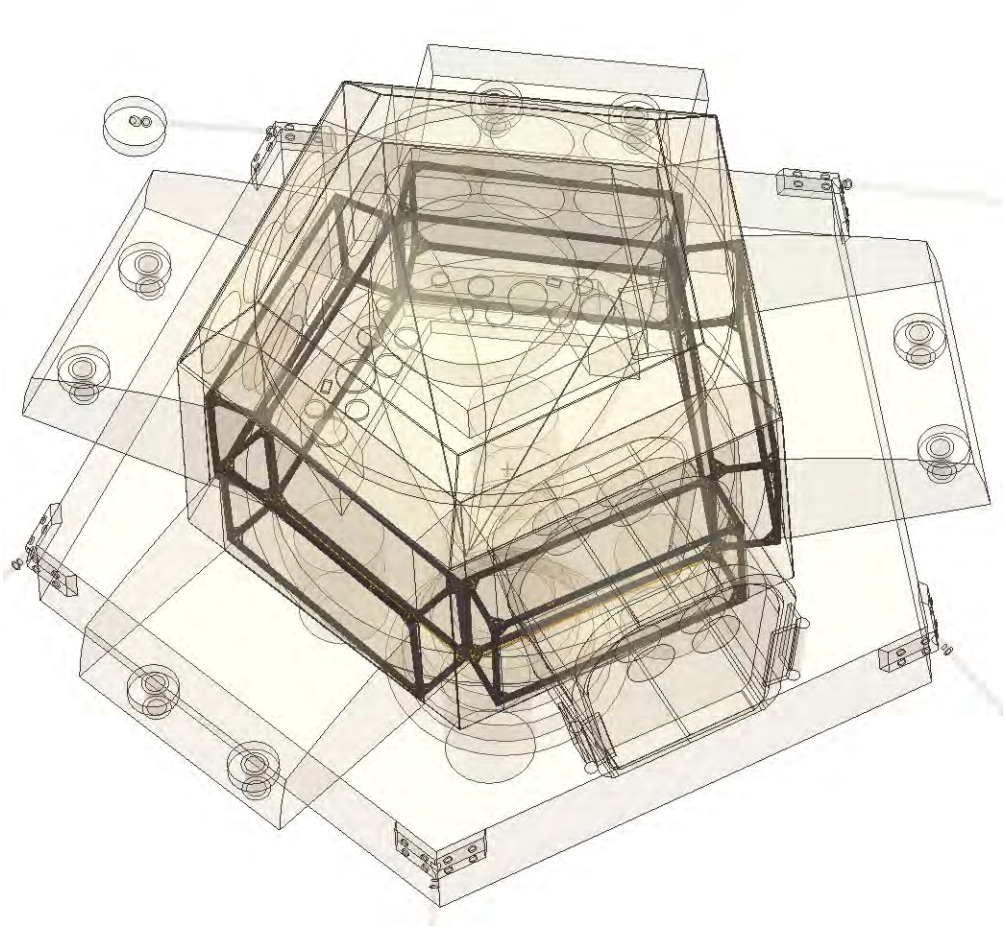

Figure 67: Preliminary Ascent Vehicle Rack Layout

This structure is designed to be launched from and landed onto any planetary surface as would any ascent/descent vehicle; thus this structure is equipped with a main propulsion system on the bottom as well as four additional boosters along the outside. The mission duration was set to 30 days and with a crew size of two to four people. With a ten-rack configuration to form a pentagonal prism, we're able to use some geometric relationships to determine the available space within the configuration; the resultant shape has a side length and height of eighty inches. Equations 1 and 2 shown below can be used to determine the volume:

$$Area_{polygon} = \frac{ns^2}{4tan(\frac{\pi}{n})} \tag{1}$$

n: Number of sides s: Side length

$$Volume_{PolygonalPrism} = Area_{Polygon} * height \tag{2}$$

The volume of this ascent and descent vehicle computes to 14.4351 cubic meters.

The internals of the habitat were much more difficult to project without proper trade studies having been done prior. However, basic necessities such as: sleeping, navigation, avionics, first-aid, and flight control were taken into account initially. Preparing for these requirements netted these required additions:

- Lofted sleeping hammocks
- First Aid kits

- Pilot/Copilot seating
- Avionics Equipment
- Control Station
- Observation window

The resulting external design is shown below:

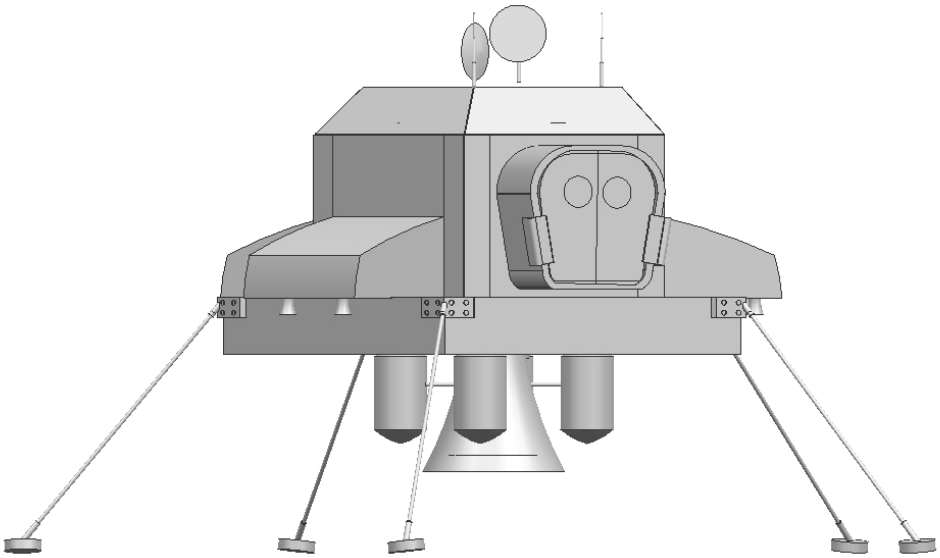

Figure 68: Preliminary Ascent Vehicle External

A top-down view of the ascent vehicle's internals are shown below:

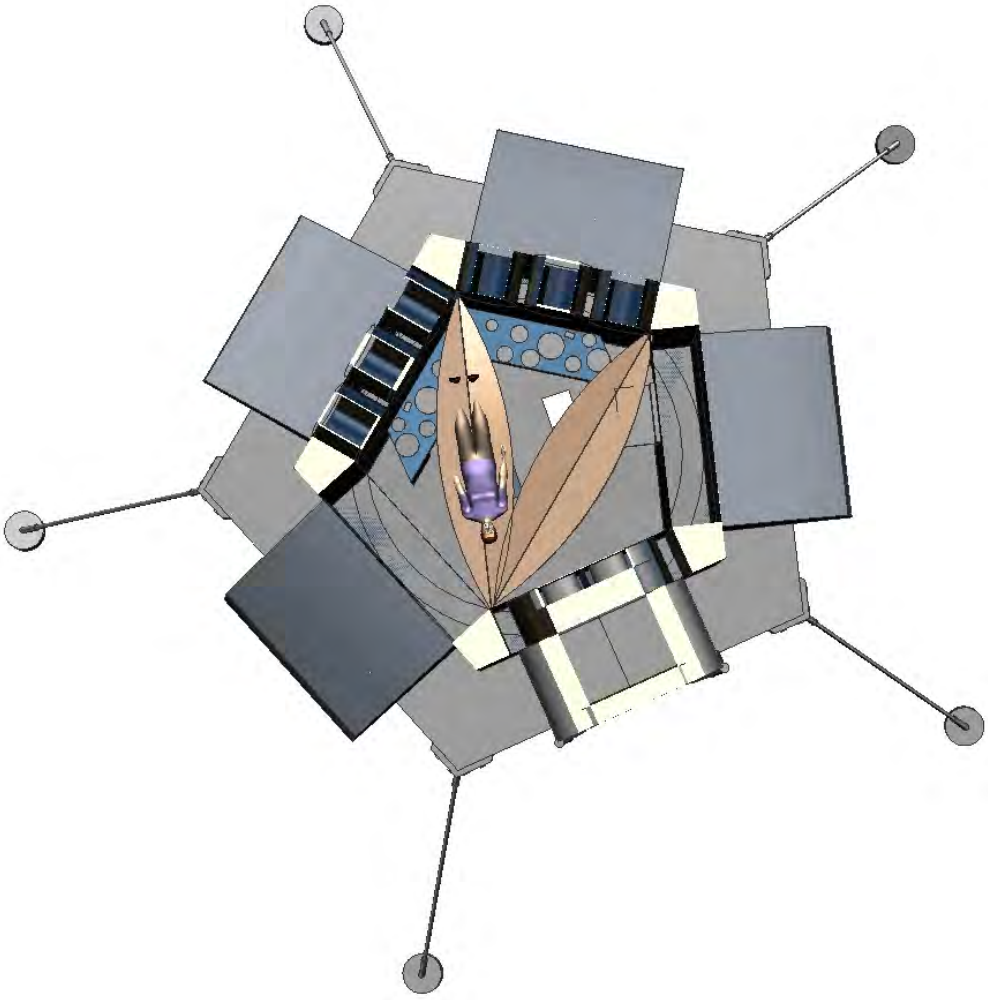

Figure 69: Preliminary Ascent Vehicle Internal

4.5 Rover Habitat (Nicholas Behnke)

The rover habitat detailed in this section represents preliminary work that was intentioned to see iterations made as testing was conducted. Following the transition of the workflow of the project, work was focused away from this design to more fleshed out versions of the micro-gravity and surface habitats. Despite these changes, research conducted and some parts made for this design were put to use in the creation of of the new designs, post-transition.

The following images 64 and 71 represent the early attempt at a surface rover habitat. The design takes basic inspiration from designs currently being tested by NASA for mobile habitats in desert environments. The internal space of this habitat represents 20 m^3 of habitable space, with a diameter of 2.64 m. The initial intention of this specific design was a habitat of two individual crew members. The number of crew berths and the number of suit-ports would be adjusted according to the crew size. As can be seen from designs presented from the latter half of the project, a substantial number of systems were not included in these preliminary designs. In a redesign of this habitat, not only would these systems need to be taken into consideration, their volume requirements alongside those needed to allow the system to fully function as a rover would also need to be included. Significant increases to the volume would need to be seen, especially in the case of a larger number of crew members being considered. A higher fidelity version of this habitat

would look similar to the 20 m^3 surface habitat designed during the latter portion of the semester.

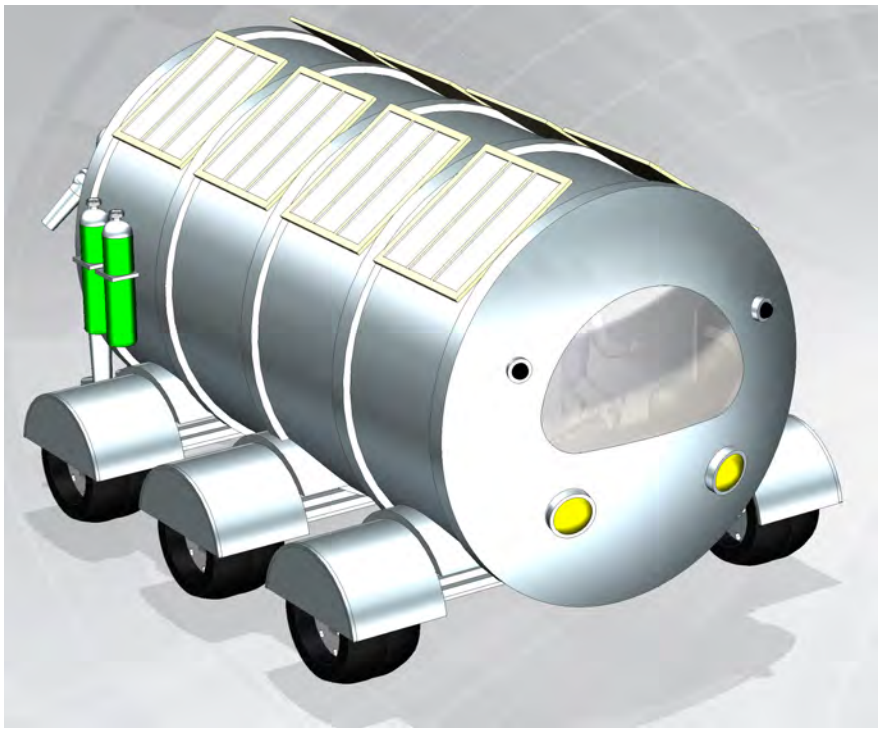

Figure 70: Preliminary Rover Habitat Exterior

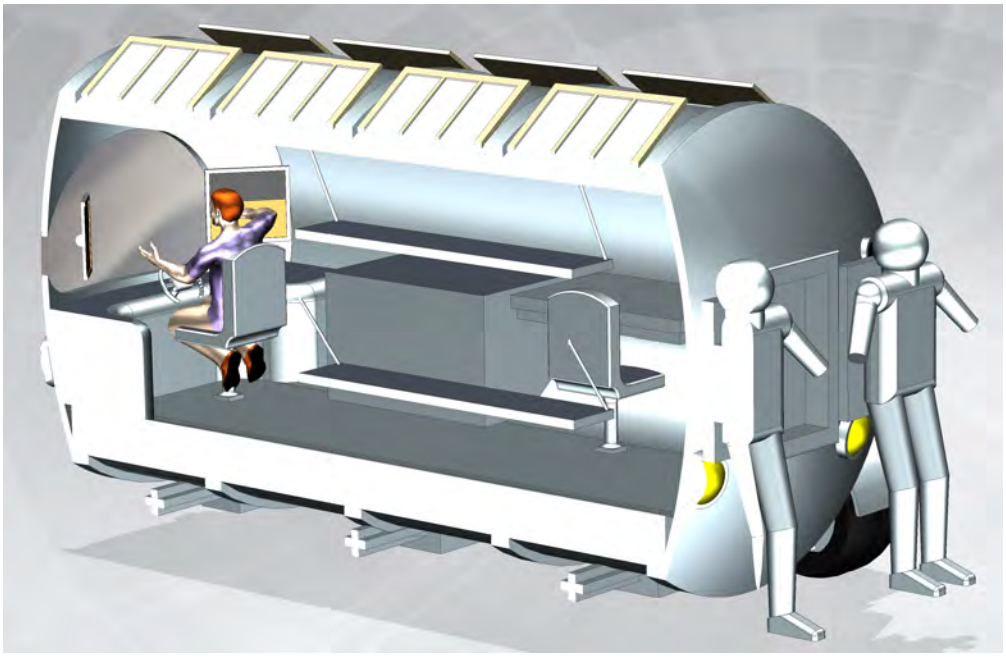

Figure 71: Preliminary Rover Habitat Interior

The following depiction represents the aforementioned use of the 80/20 racks constructed by the team to lay out a potential testing zone as shown in Figure 72. This design is a twelve rack horizontal layout.

Here the racks are overlaid on the transparent rover. Should testing have continued as planned, not only would the rover have seen major redesigns, but the implementation of the relative rack designs created by the manufacturing team would have occurred.

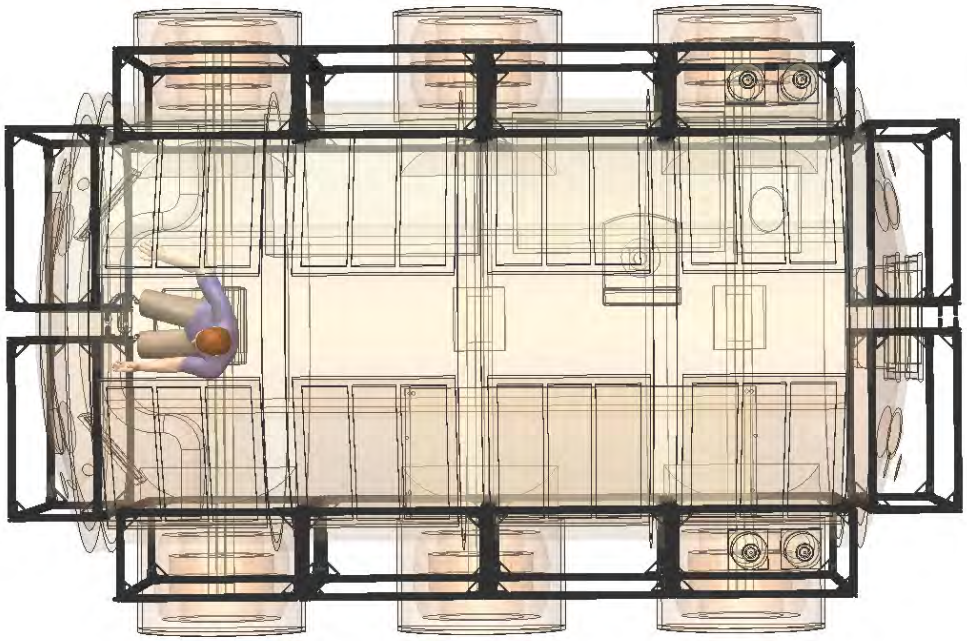

Figure 72: Rover Habitat with 80/20 Rack Overlay

Transition to Remote Work

5 Mission Planning

5.1 Transition to Remote Work (Tuvia Rappaport)

The mission planning and analysis team focused on driving requirements for the science objectives and the habitat's functionality. The design and analysis of these vehicles focused on the internal layouts. Instead of experimentally testing minimum volume habitat designs the team transitioned to designing a series of small habitats to analyze the trade-offs and accommodations that must be made in smaller habitat designs. The volume requirements of these habitats is driven by the mission requirements.

5.2 Mission Planning Requirements (Tuvia Rappaport)

ID	Requirement	Source
MPA1	The mission shall investigate the habitat layouts across multiple volumes to identify miniumum requirements for cabin sizing.	MS
MPA2	The habitats shall support a crew of four for a duration of 30 days	MS
MPA3	The mission shall investigate habitats for both micro-gravity and surface operations	MS
MPA4	The mission shall the complete the science objectives	MS
MPA5	The mission shall be able to perform under emergency situations	MS

Table 22: Mission Requirements

5.3 Mission Overview (Tuvia Rappaport)

The minimum viable habitat volume depends on the mission profile. There are two mission profiles explored in this analysis, a micro-gravity habitat and a surface habitat located on either the Moon or Mars. Both the surface and micro-gravity missions share many commonalities in this analysis, these are:

- Crew Size: 4
- Duration: 30 days
- Habitable Volume: 20,40,80 m^3
- Mass: 11,700 - 16,800 kg

The crew will be composed of a mission commander, a medical doctor, a planetary scientist, and a technical specialist. These specialties ensure that both teams performing EVA's to complete the science objectives will be effective, as well as handling the technical and medical challenges. Extensive cross-training will be required to ensure safety and the effective use of the short mission duration.

5.4 Micro-Gravity Habitats (Tuvia Rappaport)

The team will examine three sizes of micro-gravity habitats. These habitats are designed as short term transit vehicles or stations.

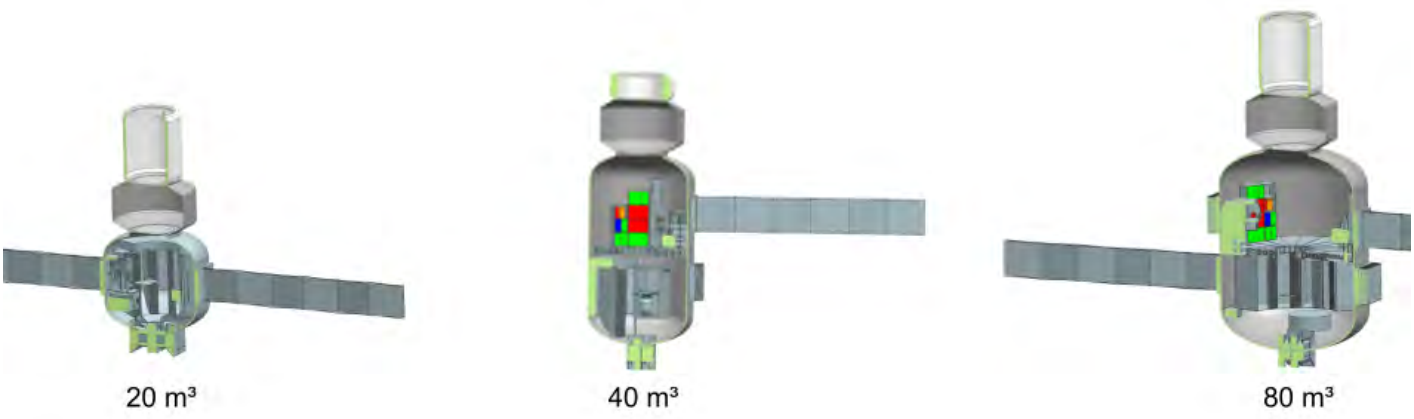

Figure 73: Microgravity Habitats

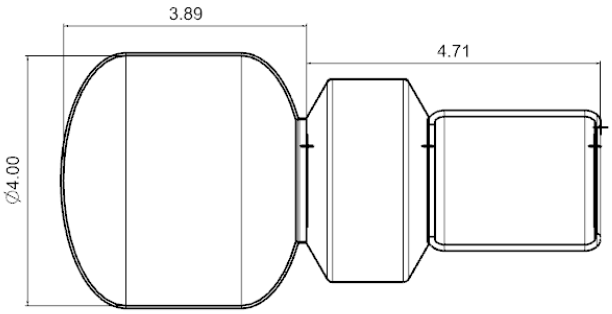

Figure 74: Micro-gravity 20 m^3 Dimensioned External Drawing, units in meters

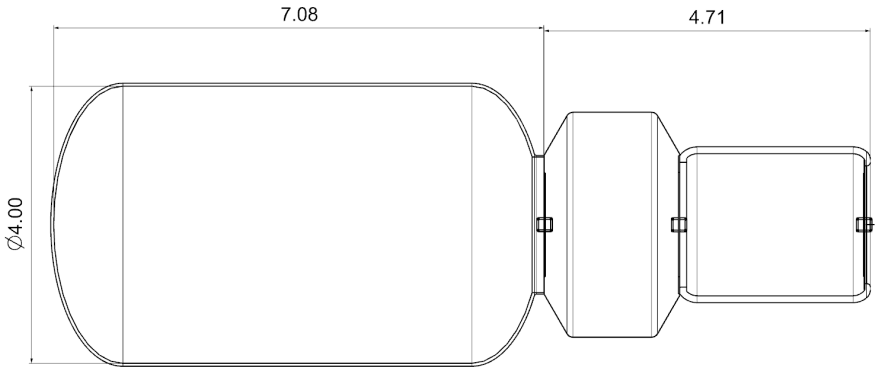

Figure 75: Micro-gravity 40 m^3 Dimensioned External Drawing, units in meters

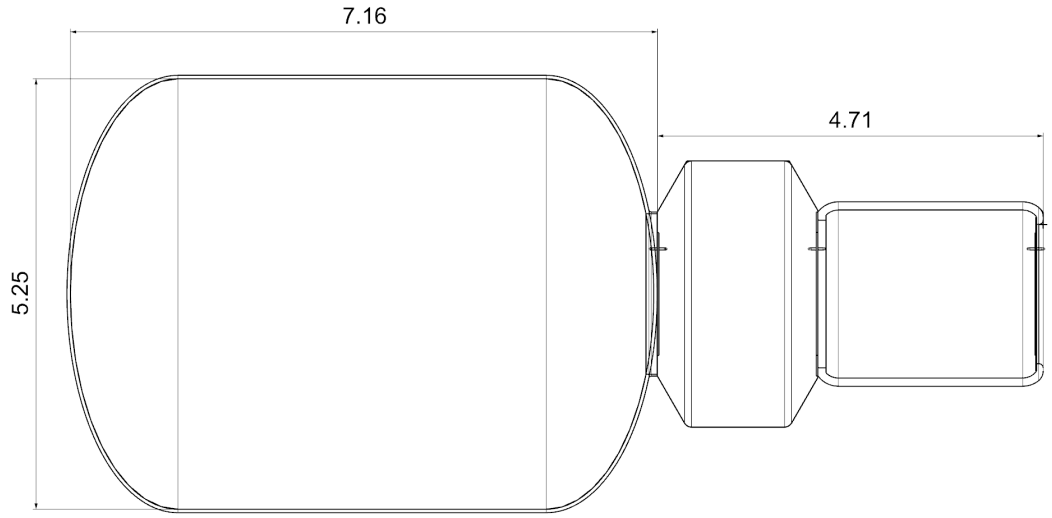

Figure 76: Micro-gravity 80 m^3 Dimensioned External Drawing, units in meters

5.5 Surface Habitats (Tuvia Rappaport)

The team will examine three sizes of surface habitats. Because of the emphasis on the internal layout these habitats are viable for both Mars and the Moon.

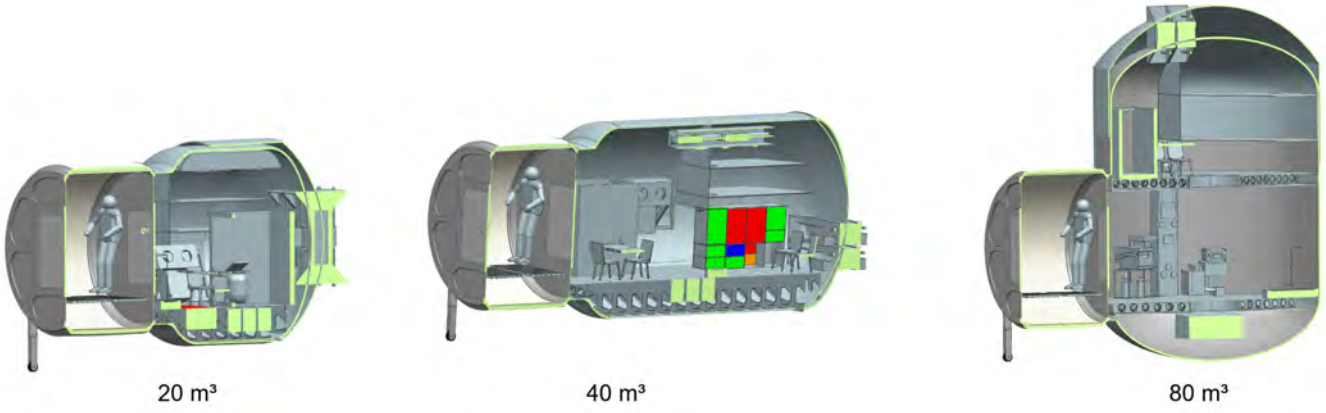

Figure 77: Surface Habitats

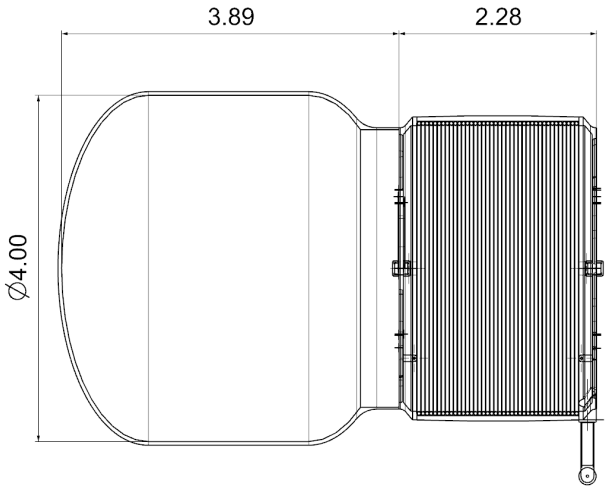

Figure 78: Surface 20 m^3 Dimensioned External Drawing, units in meters

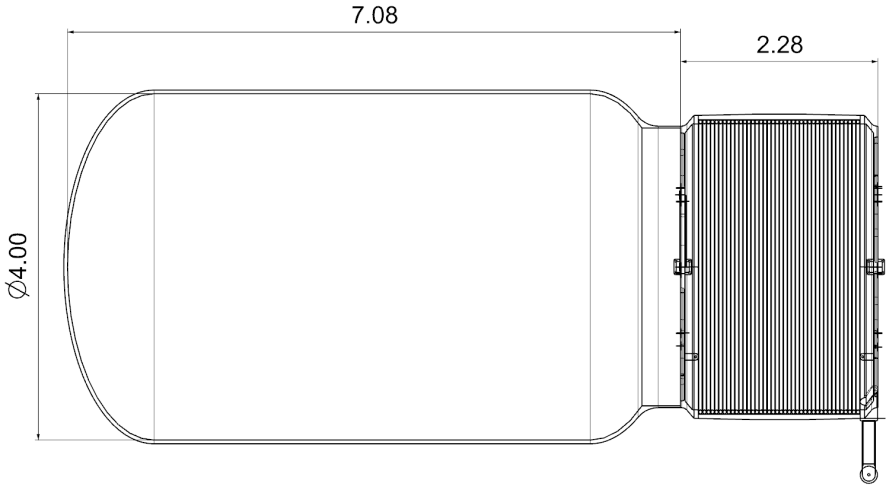

Figure 79: Surface 40 m^3 Dimensioned External Drawing, units in meters

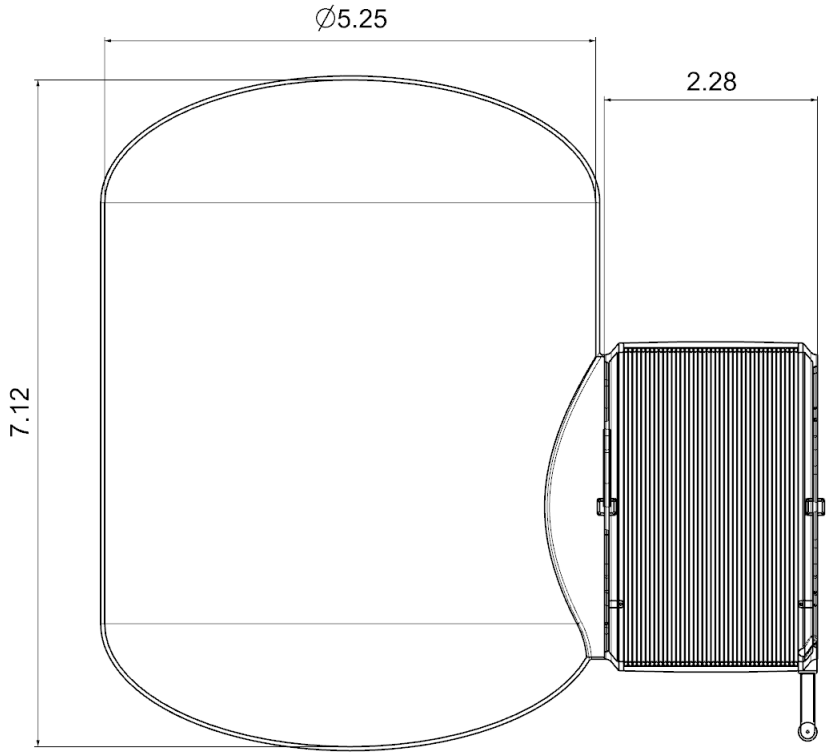

Figure 80: Surface 80 m^3 Dimensioned External Drawing, units in meters

5.5.1 Landing Sites (Tuvia Rappaport)

Landing sites were selected for both the Moon and Mars in order to incorporate the power and thermal impacts on the internal volume. The sites were chosen in order to satisfy current NASA science objectives while providing manageable power and thermal constraints. The sites selected are Chasma Boreale on Mars and Shackleton Crater on the Moon.

Chasma Boreale (82.6N 47.3W) was selected as the Mars landing site because it is considered a strong candidate for both ancient and extant life and it may contain large quantities of frozen water and carbon dioxide.

Shackleton Crater (89.9N, 0.0E) was selected as the Moon landing site because it receives near continual sunlight on the peaks along the crater's rim and within the crater's interior are permanently shadowed regions.

5.6 Notional Schedule (Tuvia Rappaport)

In the experimental phase of this project the team created a schedule for each member of the crew during a challenging day, the itinerary. For this phase the team instead focused on the crew's 30 day mission schedule.

Two emergencies have been designed into the notional schedule to drive requirements for performing repairs in a minimal volume habitat. For both the surface and micro-g missions an airlock failure occurs on day 18 and a medical emergency on day 26. These events are driven by the research performed in the experimental phase of the project for repair and medical requirements. In order for a minimum habitat design to be viable it must be able to perform in these emergency situations.

5.6.1 Surface Mission Schedule (Tuvia Rappaport)

The short 30-day duration of the mission necessitates frequent EVA's in order to complete the science objectives. The mission is designed around alternating teams of 2 performing EVA's. This provides the astronauts time to recover before their next EVA and has the added benefit of freeing up space in the minimal volume habitat.

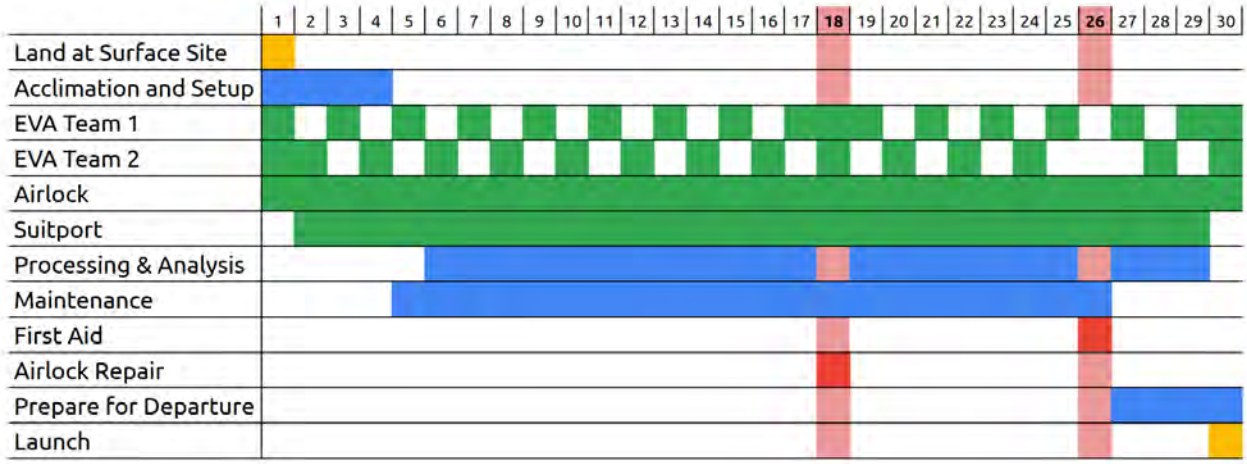

Figure 81: Surface Mission Schedule

5.6.2 Micro-gravity Mission Schedule (Tuvia Rappaport)

For the micro-gravity mission, regular EVA's are not required to meet the science objectives. The primary objective of the crew will be maintenance and to respond to the two scheduled emergencies. This vehicle could be serving as a short term station or transit vehicle.

Figure 82: Micro-g Mission Schedule

5.7 Science Objectives (Brady Sack)

Since missions are driven primarily by their science objectives, they have a crucial impact on the mass and volume of any habitat. For this analysis, we'll assume the micro-gravity habitat acts as a transport vehicle, and thus carries the same scientific equipment that the surface habitats have. The science objectives for our

Martian surface mission, based on the Mars Reference Design Architecture (MDRA) for human exploration [50] and overall NASA Mars Exploration Program objectives [82] and split into three categories, are detailed in Table 23.

While one might argue that science equipment is not necessary for crew survial, it could be strategically removed to reduce volume. However, according to the Human Exploration of Mars Science Analysis Group(HEM-SAG), a well-equipped laboratory will significantly reduce the mass of sample material that must be returned [50]. Thus, while removing science equipment may reduce volume, it may actually increase mass on return.

Geology	**Atmospheric Sciences**	**Astrobiology**
Study structure and composition of martian interior	Study water and carbon dioxide cycles	Determine whether life on Mars every existed
Study chemical and mineral composition of martian surface	Characterize surface radiations	Verify and catalogue the presence of organic compounds detected by earlier robotic missions.
Identify and collect rock samples to return home	Collect data on surface conditions (temperature, sunlight, humidity, etc.)	Determine whether organic compounds have biotic or abiotic origins

Table 23: Science Objectives

5.7.1 Geology (Brady Sack)

To investigate subsurface geological features, several reports recommend the use of ground penetrating radar and reflection seismology [96] [5]. In the case of reflection seismology, one group successfully used a linear array of 24 geophones spaced 4m apart to detect subsurface water beneath the Mars Arctic Research Station (MARS). They were able to generate good results using a sledgehammer to generate mini-quakes and a seismograph to collect and read data[90]. In pressurized suits, the use of sledgehammers may be difficult, so alternative equipment may need to be developed.

For studying the mineralogical composition of surface and near-surface materials, astronauts need magnetometers and infrared mineralogical analyzers. Mining companies use portable infrared mineralogical analyzers (PIMA) to quickly analyze minerals in the field. For astronauts, quick decisions in the field would dramatically reduce the amount of samples they need to return to the habitat science lab for further analysis [5]. Finally, MDRA recommends astronauts photographically document cliff faces, grabens, and other geological features to study the tectonic history of Mars [5].

5.7.2 Atmoshpheric Sciences (Brady Sack)

The atmospheric science goals can be accomplished through careful and continuous environmental monitoring. Fortunately, several pieces of technology that are applicable to this have already been flown and proved on rover missions, including Curiosity's Rover Environmental Monitoring Station (REMS) and the Radiation Assessment Detector (RAD). These technologies are lightweight and not large, and capable of taking measurements on temperature, pressure, humidity, CO2 levels, and sunlight [44] [43].

5.7.3 Astrobiology (Brady Sack)

Organic matter was first discovered on Mars by the Viking landers through the use of gas chromatography mass spectrometers. At the time of discovery, however, it was assumed its presence was due to terrestrial contamination prior to launch, and so the discovery was discarded. It was not until 2015, when the Curiosity rover rediscovered the presence of organic compounds, specifically chlorobenzene, that the matter was taken more seriously [52]. Later in 2018, Eigenbrode et al. used evolved gas analysis (EGA) and pyrolysis-based techniques to find aromatic and thiophene compounds at Gale Crater [52]. These pyrolysis-based techniques, however, are destructive to certain organic compounds, and it is believed that alternative mass spectrometry

techniques could lead to the discovery of additional organic matter. For this reason, to complete the first two astrobiology science objectives, the surface habitat requires a laser-desorption mass spectrometer (LD-MS) and a gas-chromatograph mass spectrometer (LD-MS), similar to the ones found on the Rosalind Franklin Rover, now scheduled to launch in 2022 [41]. Laser-based spectrometry is recommended by the authors as a non-destructive technique for discovering the presence of organic matter. [52] This same laser-spectrometer could also be used by the astronauts to conduct isotopic analysis of surface material to determine whether or not the thiophenes have biotic or abiotic origin[95] [52]. In addition to in-situ analysis of samples, it will be necessary for astronauts to return samples to Earth for further analysis by more specialized researchers.

5.7.4 Science Equipment Summary (Brady Sack)

The mass and volume requirements for all of the equipment discussed is summarized in the table below:

Tool	**Category**	**Field or Lab**	**Mass Estimate** (kg)	**Volume Estimate** (m^3)
PIMA [66]	Geology	Field	2.5	.01
Camera [88]	Geology	Field	.25	.00025
Glovebox [45]	Geology	Lab	–	1.8
Geophones (x24) [56]	Geology	Field	4.8	.002
Seismograph [51]	Geology	Lab	18	.03
Magnetometer [51]	Geology	Lab	34.5	0.15
Ground Penetrating Radar [51]	Geology	Lab	15	.09
RAD [44]	Atmospheric	Both	2	0.004
REMS [43]	Atmospheric	Both	2	0.003
GC-MS [42]	Astrobiology	Lab	11.5	.15
LD-MS∗	Astrobiology	Lab	–	–
Drill [50] ∗∗	All	Field	<100	–
Total			**191**	**2.25**

Table 24: Science Equipment Mass and Volume Requirements

The mass and volume estimates for the LD-MS mass spectrometer are included in the GC-MS estimates. These estimates were taken from Rosalind Franklin Rover's ExoMars MOMA instrument mass and volume [42]. Since the drill technology described in the Mars Desigin Reference Architecture 5.0 (MDRA) has not been developed yet, accurate estimates for its volume were not obtained. The MDRA estimated that a drill capable of reaching a depth of 10m would have a mass of around or under 100 kg [50]. It is likely that the drill would be large and stored outside of the habitat, thus having no impact on the internal volume.

5.8 Impact on Habitable Volume (Tuvia Rappaport, Brady Sack)

The crew schedule impacts the habitable volume requirements. In smaller habitats, working space is at a premium. By scheduling alternating daily EVA's for half the crew, the habitat becomes less cramped. This means two full workstations is adequate for smaller habitat volumes. A goal of the experimental phase of this course was to analyze the impact of the crew's schedule on the required habitable volume. The main takeaway from that research that can be applied here is that planning the crews schedule in conjunction with data driven component placement will enable smaller habitat designs to be viable.

Because of the necessity for frequent EVA's the habitat pressure also has a significant impact on required habitable volume. The habitat pressure impacts the time required to prepare for EVA's. Furthermore in smaller habitat designs the airlock begins to take up a larger percent of the total volume. In these habitats mixed use of the airlock should be considered to maximize usable volume.

The science objectives also directly impact the habitable volume requirements. Since none of the science objectives are necessary for crew survival, the science equipment can be removed or added with no impact on the success of other systems. Of the science equipment, the component with the largest volume requirement will likely be the glovebox. The micro-gravity science glovebox currently installed on the ISS requires a

volume of 1.8 m^3. Certainly a smaller glovebox could be designed; however, for it to be usable, it must be significantly larger than the other science equipment. The glovebox is discussed in greater detail later in the report. While the glovebox can be removed without harm to the crew, it is critical for the completion of the geological and astrobiological science objectives.

The mission objectives drive the volume requirements, for this analysis we fixed the crew size, duration, and location in order to compare what trade-offs need to be made at smaller habitat volumes. By establishing the science requirements for the mission, we defined the need to allocate portions of the habitat for scientific instruments and work areas.

6 Crew Systems

6.1 Airlock Design (Zach Lachance)

There are several different methods for implementing airlocks for EVA purposes, all of which have benefits and drawbacks depending on the mission profile for which they will be subjected. The six most commonly used and/or cited designs are:

- Vent cabin
- Single-chamber airlock
- Dual-chamber airlock
- Suitport
- Rear-entry airlock
- Airlock-suitport hybrid

Each of these designs will be briefly explained, followed by their specific benefits and drawbacks in order to explain the conducted trade study and the conclusions drawn from it. The analysis focuses on the following categories, as these are the most commonly discussed factors found in various NASA documents [57, 58, 69, 83]:

- Mass/Volume impacts
- System complexity
- Contingency/Safety
- Dust mitigation and planetary protection
- EVA quantity/access
- Consumable loss and depressurization/repressurization system mass/volume

A table summarizing all of the findings can be found in Section 6.1.7.

6.1.1 Venting the Cabin

The preference of the US during the Mercury to Apollo Era, venting the cabin is the utilization of the entire pressurized spacecraft volume as the airlock.

The benefits of this design are mainly in the form of the simplicity of its implementation and that it requires almost no additional mass or volume devoted solely to an airlock. The only additional mass and volume required are those of the depressurization/repressurization system, which scale with the size of the spacecraft. The use of the habitable volume as the airlock also poses no issue to suit maintenance, although it does not have any strong benefits besides this lack of impedance. Finally, this system is TRL 9 due to its

use in the Mercury, Gemini, and Apollo missions.

However, the drawbacks are rather significant, as there is no safety or contingency built in for a failure, such as the hatch not closing. Furthermore, such a failure would result in the failure of the entire mission and likely loss of the crew, as it would render the entire spacecraft inhabitable. This design also has no capacity for dust mitigation and planetary protection, as the suits are exposed at all times to the main habitable volume. While not a major concern for micro-gravity habitats, this would pose a difficulty for surface missions due to the dust, as experienced in the Apollo missions with the electrostatically-charged lunar dust getting into the equipment, being inhaled by the crew, and sticking to clothing. This would also pose significant issues for planetary protection, as the exterior of the suit is exposed to both the entire spacecraft atmosphere (and any microorganisms therein) and the surface of the planetary body. Additionally, the previously mentioned scaling of the depressurization/repressurization system with habitable volume can be a drawback for larger habitat volumes, although this is less of a concern for smaller volumes. There is also a high consumables loss, scaling with internal volume, due to the large volume that is being depressurized and repressurized. Finally, this system of depressurizing and repressurizing the spacecraft is highly time-consuming and requires all persons to be in EVA suits, even if they are not exiting the habitable volume, thus it significantly limits EVA quantity and access.

6.1.2 Single-Chamber Airlocks

Single-chamber airlocks are another system that have seen frequent use by several different space agencies and consists of a single separate pressure volume and separated from the spacecraft volume and external environment by independent, airtight hatches.

The main benefits of this system are the improvements over venting the cabin without significant increases to the system complexity. By sacrificing some mass/volume and simplicity, significant consumables and depressurization/repressurization system mass/volume savings can be achieved, especially for larger volume habitats. The airlock allows for the habitable volume to be scaled with almost no impact on the airlock system mass and consumables usage, as these are controlled by the airlock volume instead. Additionally, this design adds redundancy to the system by having two independent hatches to access the main habitable volume, thus allowing for the habitable volume to be vented and then repressurized in an emergency without a guaranteed failure of the mission or risk to the crew (assuming ample consumables are available for this contingency scenario). It also adds an entire separate volume between the main habitable volume and the dust from a planetary surface or the microorganisms within the habitable volume itself. This is true during suit maintenance as well, as this can be done either in the airlock or the main volume, thus allowing for a greater degree of control and maintenance than venting the cabin. EVA quantity and access are also benefited by the ability to reduce the pressure and change the atmospheric composition in the airlock to save time during pre-breathing without the need to reduce the entire habitable volume. Finally, this method is TRL 9 due to its utilization on various missions, such as Skylab, MIR, and the Space Shuttle.

The main drawbacks of this design, however, are the limitations of its performance in these categories. As described above, the addition of an airlock to a design increases the mass and volume of the system due to the need for this dedicated space that is not useful for other operations. There is also an increase in system complexity that results from having two separate pressure-sealing hatches that need to work, as opposed to the single one for venting the cabin. While this allows for a greater degree of maintenance, safety/contingency, dust mitigation, and planetary protection compared to venting the cabin, it is still a limited benefit. The contingency scenario is relatively risky and requires a very large loss of consumables compared to other options, and it also requires all crew members to be in EVA suits. The crew are also still directly exposed to dust and the suits to microorganisms during suit donning and doffing, thus while the airlock reduces the amount entering the main habitat it still poses an issue to the crew and planetary protection. The area within the airlock for suit maintenance and donning/doffing is also limited by the desire to reduce consumables usage and depressurization/repressurization system mass/volume, thus both of these considerations are non-optimal. EVA access and quantity are also harmed by the donning and doffing time, especially considering that this is likely to be occurring in the minimal volume possible for consumables

optimization.

6.1.3 Dual-Chamber Airlocks

By comparison to the Single-Chamber Airlock described above, the Dual-Chamber airlock has two consecutive, independent airlock chambers that the astronauts pass through between the main habitable volume and the exterior of the spacecraft. Thus, there are two airlock volumes which are separated by a third pressure-sealing hatch in addition to the hatch between the main volume and the airlock and the hatch leading outside of the spacecraft. This is the design of the main airlock on the ISS, which is shown in Figure 83. On the ISS, the airlock sections are called the Equipment Lock, referring to the first/inner section (relative to the habitable volume), and the Crew Lock, referring to the second/outer section (E/L and C/L in the figure, respectively).

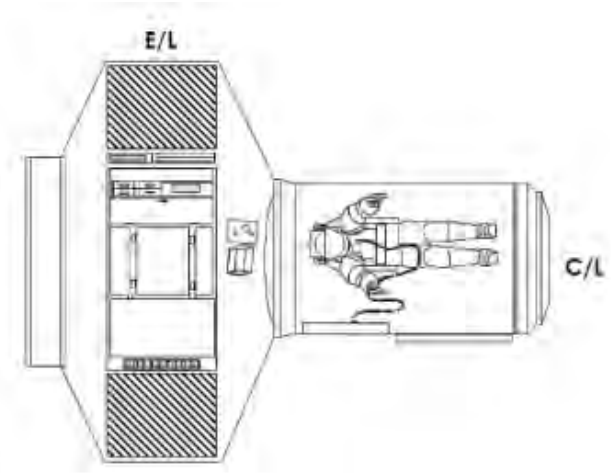

Figure 83: ISS Quest Joint Airlock [69]

The main benefit of the Dual-Chamber Airlock is in the increased contingency/safety, with some additional minor benefits to dust mitigation, EVA access, suit maintenance, consumables loss, and depressurization/repressurization system mass/volume. For this type of airlock, a single failure in a hatch still allows for the airlock to be used as a Single-Chamber Airlock, allowing for a much better contingency plan compared to the Single-Chamber Airlock. Additionally, the use of two chambers means that there are two volume regions before entering the main volume and one chamber before the donning/doffing volume for dust to collect, thus moderately reducing the crew's exposure. However, this does not offer any benefit to planetary protection as the same contact with the suit occurs compared to the Single-Chamber Airlock. This design also allows for the reduction of the outer airlock portion to reduce consumables usage/loss and reduce the mass and volume of the depressurization/repressurization system since this portion of the airlock can be sized to be just large enough to fit the crew without the need to worry about donning/doffing or suit maintenance, as this occurs in the larger inner chamber. Therefore, this also allows for an increase in the volume available for suit maintenance and for the donning/doffing volume, increasing EVA access. As with the previous design, this allows for atmospheric adjustments within the airlock to reduce pre-breathe times, but it also allows for the two chambers to be pressurized independently, allowing for greater operational flexibility during the pre-breathe. For example, once the crew moves into the outer chamber, the inner chamber could be repressurized to allow for suit maintenance or other operations within the airlock by other crew members. The increase in flexibility from an operational standpoint makes EVAs slightly easier, thus demonstrating a slight improvement over the single-chamber design. Finally, the system is TRL 9 due to its utilization on the ISS.

The drawbacks for this design are in the increased mass/volume of the airlock itself and in the system complexity. The mass and volume of the design are marked increases compared to a single-chamber design,

as now two full airlock chambers are required. These increases are likely to be less than double the single-chamber design volume since the outer chamber can have a significantly lower volume than a single-chamber design, thus forming an upper bound to the relative sizing. Additionally, the inner chamber will require at least the volume of a Single-Chamber Airlock by itself since it must achieve all of the same minimal goals (don/doff volume, maintenance space, etc). This implies that the inner airlock will have a lower constraint of the single-chamber volume, and indeed it will likely be larger to aid in donning/doffing and maintenance. Thus, for most designs, the volume of this airlock will be somewhere between 1-2 times that of a comparable single-chamber design. However, any higher accuracy regarding this numerical conclusion is not practical nor meaningful due to the wide impact of the mission profile on airlock design and volume, which is described in more detail in Section 6.1.8. The volume conclusions also hold for mass by the same reasoning. However, the depressurization/repressurization system can be reduced in mass and volume due to only needing to fully cycle the outer chamber, which is smaller than the single-chamber design, but this is highly dependent on the mission profile with regard to the utilization of the innermost chamber and the volume of the two airlocks. Additionally, while this system is TRL 9, it does require additional complexity due to the need for three separate hatches to function properly. However, some complexity is reduced in the depressurization/repressurization system due to the reduced capability requirements.

6.1.4 Suitports

A suitport is a design concept that became popular as NASA began to look towards surface mission designs, especially pressurized rovers. The design calls for a small port that the suit attaches to while remaining completely external to the habitable volume. The port is then used to ingress/egress the suit, the bulkhead door is closed, and the suit detaches from the vessel. Figures 84 and 85 show a suitport concept drawing and concept CAD design, respectively.

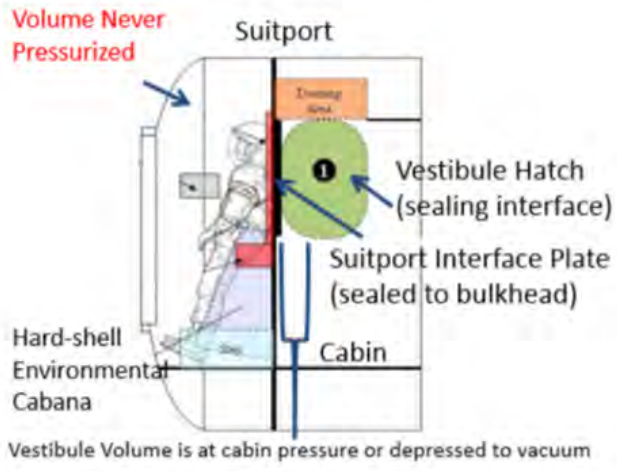

Figure 84: Suitport Diagram [69]

Figure 85: Suitport Concept Image for the Lunar Electric Rover [84]

Suitports have large benefits over traditional airlocks with regard to mass/volume, dust mitigation, planetary protection, EVA access, consumables loss, and depressurization/repressurization system requirements. The utilization of suitports allows for a high degree of mass and volume reduction, as there is no need for the large airlock volume and mass. Instead, all that is required is enough wall space for the ports and sufficient space behind and above for donning/doffing, but this volume easily be used for other purposes by the crew when donning/doffing are not occurring. Current NASA estimates call for 0.3 m above the ports and 3.1 m^3 behind for donning/doffing, but these values are highly preliminary as the testing that has been conducted on suitport designs is very limited. However, these values are substantially lower than the requirements for an airlock, which are approximately 7 m^3 for simultaneous 2-crew donning/doffing [69]. With regard to mass, there is only the additional mass of the ports, as the only other component to the design are the suits themselves. Thus, suitports have significantly lower additional mass and volume requirements compared to all of the other designs. Additionally, suitports offer near-complete dust mitigation and planetary protection, as the only external portion of the suit that is exposed to the internal habitat is the small portion that opens with the port bulkhead. This exposure can be further mitigated through the design of the bulkhead hatch, such as by designing it to open with the suit such that it always remain sealed over this portion of the suit. EVA access is also higher for suitport designs since the donning/doffing time appears to be lower compared to traditional airlock designs, although these results too are subject to further testing to determine higher fidelity results. Furthermore, for an 8.2 psi, 34% O_2 atmosphere, the time for donning and suit checkout is approximately the same as the pre-breathe time, meaning that it is highly likely that no additional, idle pre-breathe time would be required [78] (see Sections 6.2 and 6.3 for additional details on the atmosphere pressure and oxygen percentage selection impacts). Due to the small port and suit size compared to an airlock, as well as the fact that there is no airlock volume that is required to cycle between cabin pressure and vacuum, the consumables loss is solely from suit leakage, which occurs at a low rate when stored at a lower pressure (such as 0.9 psi, which is the minimal required to ensure that the suit repressurizes properly [69]). Also, the depressurization and repressurization system requirements are minimal due to only needing to control the suit pressures, and this could potentially even be accomplished solely by the suit life support systems in future suits.

However, suitports also have significant drawbacks. Unlike all other designs, there is no capacity for maintenance of the suits, as they are always external to the habitable volume. Since the suits are constantly exposed to the environment, they are also at increased risk of environmental damage. This is especially noteworthy given the aforementioned lack of maintenance capability. There is also very limited contingency for suitports, as the only available options are to either use one suitport for two suits or by using a docking hatch, if one is available, and venting the entire habitable volume. The former contingency process will be

further explained in the "Risk Mitigation and Contingency Analysis" section (Section 6.1.11). Suitports also significantly constrain the cabin pressure, as the pressure differential across the suits cannot be greater than 8.3 psi for current suit designs [78]. Thus, during all donning/doffing, the cabin pressure must be low enough to ensure this. Finally, the system complexity is high for this concept, as it requires the sealing of several ports. While the exact number depends on the mission, as it is likely there will either be one per crew member or one per person anticipated to go on EVA at any single time. Additionally, the suits act as the pressure hull of the spacecraft when the port is open, which greatly increases the complexity of the suits themselves and means that the entire habitat is dependent on the suits for remaining pressurized. Finally, the entire concept is highly preliminary. While the Z-2 suit design was supposed to be compatible with suitports and be delivered with a TRL of 7, this was never accomplished in full and, as such, significant research and design work would be required to implement a suitport.

6.1.5 Rear-Entry Airlocks

Rear-Entry Airlocks are similar to suitports, but feature an outer vestibule which encases the suits. This vestibule can be pressurized to cabin pressure for donning/doffing and then depressurized to allow for EVA operations. This vestibule can also have an access hatch to the main habitable volume to enable crew access for maintenance. Figures 86 and 87 show a concept drawing and test design, respectively.

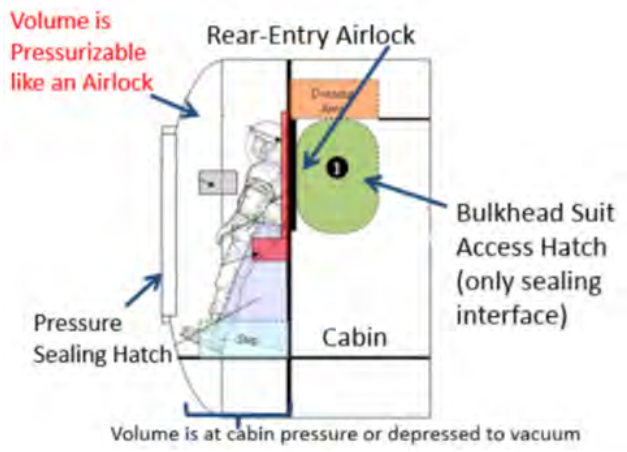

Figure 86: Rear-Entry Airlock Diagram [69]

Figure 87: Rear-Entry Airlock on the Multi-Mission Space Exploration Vehicle [35]

The main benefit of this design compared to just suitports is the ability to conduct maintenance on

the suits through the use of the access hatch. Thus, the suit can be maintained on the suitport or in the spacecraft itself. This is the major way, based on the aforementioned criterion, where this design is superior. However, since the lack of maintenance with a suitport is a major design flaw for some mission profiles, this can be used to mitigate this effect without the need for a much larger hybrid design, as described in Section 6.1.6. In addition to the maintenance benefits, the vestibule also offers a small amount of contingency in the event of a suitport failure by being able to act as an impromptu airlock. While it is not designed for this and, as such, this would likely pose some issues (such as donning and doffing of suits), it is a potential option in an emergency situation that suitports lack. This design also has a benefit to EVA access, as the limit imposed by the suitport on cabin atmosphere is not necessarily true for this design due to the pressurizable vestibule. This also means that the suits are not required to act as the main pressure wall between the habitat and the external environment. However, both of these factors depend on how the vestibule is used, as it could be pressurized during donning/doffing or not based on operational considerations at the time of the EVA. For example, it may be desired to use it as a suitport instead of pressurizing the vestibule so as to not require repressurization in-between two consecutive EVAs. In this case, these two requirements would be the same as in the suitport case. Finally, the vestibule protects the suits from environmental damage compared to the suitport design (when not on EVA).

Compared to the suitport, this design has an increase in mass and volume resulting from the vestibule mass and volume. Additionally, if the vestibule is pressurized and then depressurized, the losses in this process will affect the consumables loss. The need for this pressurization cycle also necessitates the reintroduction of a depressurization/repressurization system for the habitat. While this system is likely smaller than that of a Single-Chamber Airlock due to the reduced donning/doffing volume, it depends on the desired vestibule size which is, in part, a function of the mission profile (such as how many times and what maintenance operations need to be conducted, which would vary with mission duration). However, it is unlikely that this is smaller than the optimized smaller chamber of a Dual-Chamber Airlock due to the need for maintenance volume. Thus, the mass, volume, and depressurization/repressurization system requirements will likely be constrained between the single- and dual- chamber airlock designs. During maintenance, the crew would also be exposed to dust and the suits to microorganisms, thus degrading the dust mitigation and planetary protection. However, this is only for maintenance unlike the single- and dual- chamber airlocks, and during these operations the crew can don PPE before entry into the vestibule to help mitigate these drawbacks. Thus, while this poses a slight efficiency loss from suitports, it is still a very large improvement over the more traditional airlock designs. The system poses an increase in system complexity as well, as it adds the operation of the vestibule exterior and interior hatches to the suitport designs and the depressurization/repressurization system. Finally, this system shares the issues regarding low TRL and the unproven nature of the suitport system.

6.1.6 Airlock-Suitport Hybrids

Airlock-Suitport Hybrids (also called Suitport-Airlock Hybrids or Hybrid Airlocks) are similar to a single-chamber airlock, but feature the addition of internal suitports between the main volume and the airlock volume. This allows for the utilization of the space as both a traditional airlock and as a suitport to get the benefits that accompany both of the designs. Figures 88, 89, and 90 show a concept drawing and concept CAD designs, respectively.

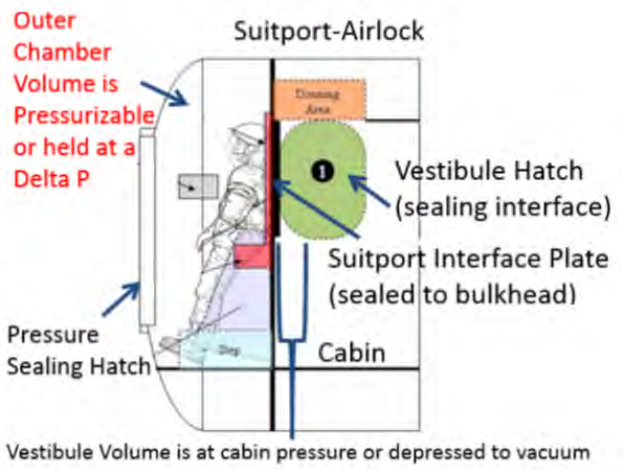

Figure 88: Airlock-Suitport Diagram [69] [35]

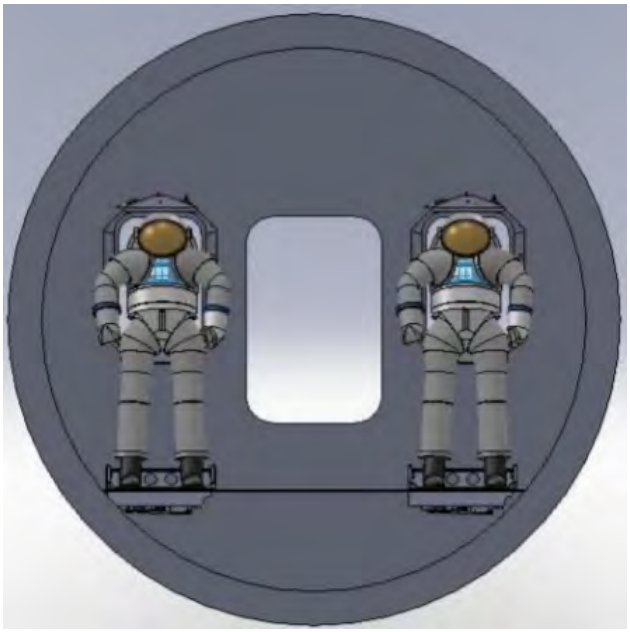

Figure 89: Airlock-Suitport CAD Concept Image[69]

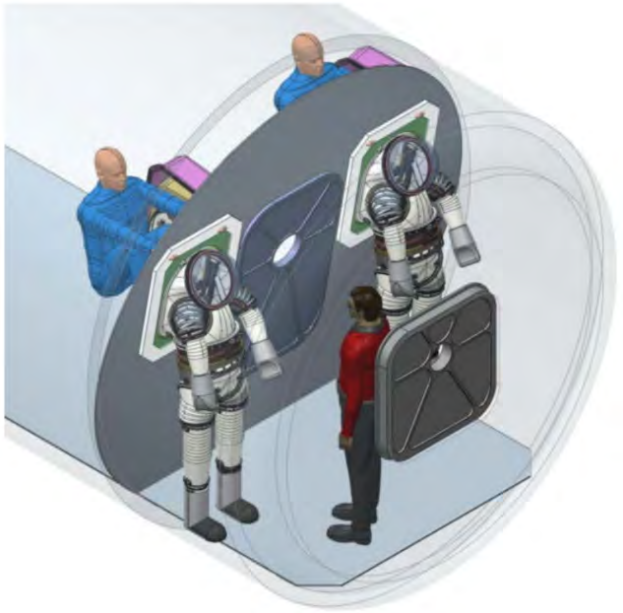

Figure 90: Airlock-Suitport CAD Concept Image [69]

The main benefit of a hybrid design compared to a rear-entry airlock is that it is intended to be able to be used as an airlock, meaning that the contingency capability of using the airlock system is always present. Thus, the contingency capabilities of this design are higher than both of the other two suitport designs. Indeed, the hybrid system has higher safety the Single-Chamber Airlock as well due to the capability to use the suitports as a contingency for certain failure scenarios. As such, the only design that offers a higher level of contingency is the Dual-Chamber Airlock, since the hybrid design still has single-failure conditions/scenarios where the only option is to vent the habitat unlike the Dual-Chamber Airlock (see Section 6.1.11 for a full hybrid airlock contingency analysis). Additionally, while there is higher complexity compared to a traditional airlock as a result of the suitports, the benefit is that the hybrid design is not solely dependent on them like in the rear-entry design. Thus, while the suitport elements are still a low-TRL, the airlock partially compensates by being TRL 9. EVA access is also similar to the rear-entry airlock design, but it allows for a slight improvement due to the flexibility between suitport and airlock use. Thus, even if only two suitports are included for a four crew mission, all crew members could still use the airlock portion for a full-crew EVA unlike in a suitport or rear-entry design where this option would not be present (with the same number of ports). Finally, the hybrid design also allows for suit maintenance, dust mitigation, and planetary protection in the same manner as the Rear-Entry Airlock.

The main drawbacks to this design are in the mass, volume, and complexity. The mass and volume are slightly higher than a Single-Chamber Airlock due to the additional suitport requirements, although this is not significant enough to make it definitively larger than the Dual-Chamber Airlock, but it could be depending on the implementation and mission profile (especially regarding the number of suitports, as a 4 suitport design would very likely be higher in total volume). Regarding the complexity, it has at a minimum the complexity of the Rear-Entry Airlock in addition to the complexity of an airlock. While the airlock elements are TRL 9, the low-TRL of the suitports and the overall complexity of the system as a whole are significant detriments.

The consumables loss and depressurization/repressurization system mass/volume, however, are variable. Since the hybrid design can serve both as a suitport and as a Single-Chamber Airlock, the effects on these factors will be somewhere within the range of these two systems depending on how the airlock is used on any given EVA. For the purposes of the ranking in Section 6.1.7, the optimal case was considered (the design acting like a suitport), as this is the likeliest method of operation for most EVAs if this design is utilized due to the planetary protection, dust mitigation, and EVA access benefits.

6.1.7 Trade Study Summary

The following table is a summary of the results from the previous sections:

	Vent Cabin	Single-Chamber Airlock	Dual-Chamber Airlock	Suitport	Rear-Entry Airlock	Airlock-Suitport Hybrid
Mass/Volume	- No additional airlock mass/volume	- Additional mass/volume of one airlock	- Additional mass/volume of two airlocks - Outer airlock can be smaller than a standard airlock (does not need to support don/doff)	- Low additional mass/volume requirements	- Additional mass/volume requirements of vestibule and suitports	- Additional mass of suitports and single airlock - Volume slightly larger than single airlock
System Complexity	- TRL 9 - Complexity of depress/repress system - Depress/repress system depends on total s/c volume	- TRL 9 - Complexity of depress/repress system and single airlock	- TRL 9 - Complexity of depress/repress system and two airlocks	- Low TRL - Unproven system - Complexity of suit interface including sealing of 4 suitports and hatches - Suits act as s/c hull	- Low TRL - Unproven system - Complexity of suit interface - Does not require suit sealing but requires vestibule and 4 suitport hatch sealing	- Low TRL for suitports, TRL 9 for airlock - Unproven system - Complexity of both suitports and airlock
EVA Contingency/ Safety	- None	- Vent s/c	- Use of either chamber	- If docking port is present, vent s/c, otherwise none	- Use vestibule as airlock	- Use as suitport or airlock - Vent s/c
Suit Maintenance	Suits can be maintained in s/c	Suits can be maintained in s/c or airlock	Suits can be maintained in s/c or airlock	None	Suits can be maintained in s/c or on suitport	Suits can be maintained in s/c, in airlock, or on suitport
Dust Mitigation/ Planetary Protection	- None	- Single chamber between dust and s/c - Crew directly exposed during don/doff	- Two chambers between dust and s/c - Crew directly exposed during don/doff	- Nearly complete dust protection (only exposure from suitport opening, which can be further mitigated through suitport design)	- Same as suitport for don/doff - PPE can be utilized for maintenance - Suits can be cleaned and then moved inside s/c for maintenance	- Same as suitport or single airlock for don/doff (depending on utilization) - Same as rear-entry airlock for maintenance
EVA Quantity/ Access	- Difficult and infrequent EVAs - Requires venting cabin atmosphere - All crew must be in suits - Pre-breathe depends on cabin atmosphere	- Infrequent EVA - Pre-breathe depends on cabin atmosphere but can be reduced by the airlock pressure	- Infrequent EVA - Pre-breathe depends on cabin atmosphere but can be reduced by the two airlock pressures	- Frequent EVA - Short pre-breathe (due to low cabin pressure)	- Frequent EVA - Pre-breathe depends on cabin atmosphere	- Frequent EVA - Pre-breathe depends on cabin atmosphere but can be reduced by airlock pressure
Consumable Loss and Depress/ Repress System Mass/Volume	All consumables lost or significant depressurization systems requirements	Less requirements than venting s/c, but cannot be optimized for consumables loss since crew don/doff volume must be ensured	Consumable loss can be minimized in the "outer" ("crew lock" for ISS) section while don/doff occurs in the "inner" ("equipment lock" for ISS) section	No loss due to airlock, some loss due to suit leakage	Loss in the vestibule volume, which is likely less than that of a single airlock but greater than the smaller chamber of the dual chamber	Variable (range from suitport to single-chamber airlock, depending on utilization)

Table 25: Summary of Airlock results

Based on the results of the trade study, the rankings in Table 26 were constructed. Due to the highly variable nature of many of these variables with respect to the mission profile, the table presents an unweighted

ranking. While a comprehensive list of the impacts of mission profile on potential weighting is not feasible due to the number of considerations, some examples are listed below.

- Dust mitigation is highly dependent on mission location, as it would be weighted close to zero for a non-surface habitat due to there not being significant amounts of dust in space, but would clearly be weighted with at least some importance for a surface mission such as on Mars or the Moon.
- Maintenance requirements would be highly dependent on mission duration, as a one week mission would have much lower maintenance needs than a one year one. Thus the mission duration would impact the suit maintenance weighting. However, this would also impact the overall airlock mass and volume, as a larger volume may be needed to accommodate and facilitate maintenance needs. For example, while a one month mission might only be expected to do minor repairs and therefore be suited to a lower required maintenance volume, a one year mission may need to be able to conduct large-scale overhauls and thus would need more space to accommodate for this.
- The number of crew members expected to go on an EVA would result in drastically different values of system mass and volume, as the size or suitport number for having 4 crew members on EVA would be approximately double that of purely 2 crew EVAs. However, it cannot be assumed that the relationship between number of crew on EVA and system mass/volume is purely linear either, as volumes may be able to overlap if the mission profile allows. For example, overlapping suitport donning/doffing volume might be possible by staggering of the crew donning/doffing by a few minutes, thus resulting in diminishing volume and mass requirements on a per-port basis as the number of ports is increased. However, this would need to be verified as feasible from a mission planning and operations standpoint beforehand based on the mission EVA requirements. As such, neither general numerical results nor numerical results on a per-crew member basis can be guaranteed to hold.

As is demonstrated in the examples above, the overall weights of the analysis categories change with mission profile, numerical values for quantities such as mass, volume, consumables usage, etc. of each system are dependent on the mission profile, and individual relative weights within a category can also be affected due to varying numerical values. As a result, in-depth numerical analysis and creation of a weighted table is not possible without a highly defined mission profile, which is contrary to the X-Hab goal of drawing generalized conclusions. Thus, in an effort to keep the conclusions relevant to all potential system designs, an unweighted table is presented. The conclusions that can be drawn from this analysis, in accordance with the X-Hab goals, are described in more detail in the conclusions section (Section 6.1.8).

	Vent Cabin	Single-Chamber Airlock	Dual-Chamber Airlock	Suitport	Rear-Entry Airlock	Airlock-Suitport Hybrid
Mass/Volume	1	4	6	2	3	5
System Complexity	1	2	3	4	5	6
EVA Contingency/ Safety	6*	3	1	5**	4	2
Suit Maintenance	5	3 (tie)	3 (tie)	6*	1 (tie)	1 (tie)
Dust Mitigation/ Planetary Protection	6*	5	4	1	2 (tie)	2 (tie)
EVA Quantity/Access	6	5	4	1	3	2
Consumable Loss and Depress/Repress System Mass/Volume	6	5	3	1	4	2

*no capability **potentially no capability

Table 26: Unweighted system ranking

6.1.8 Conclusions

As introduced previously, airlock configuration remains highly mission dependent.

- A long-term, non-surface mission does not require dust mitigation or planetary protection, nor does it require frequent EVAs, thus the categories in which designs containing suitports trade best are weighted very low. However, the long-term nature requires better consumable usage than venting the habitat. Thus, such a mission would likely find a single- or dual- chamber airlock most practical, depending on the contingency requirements and the risk assessment concerning failure of the airlock hatch.
- Short term, small volume, non-surface mission with infrequent EVAs (Mercury, Gemini, etc) would likely find venting the spacecraft the best option, as the significant reductions in mass and volume are likely the constraining factors for this type of mission, thus elevating the weight of this category significantly compared to the airlock designs (the suitport designs are not useful for the same reasons as in the first example).
- A Lunar/Martian rover would likely find suitports or a rear-entry airlock best suited, depending on the risk assessment and maintenance requirements. This is because the mass/volume for these missions would be paramount, thus elevating these designs. However, the need for efficient consumables usage, as these systems are likely to be desired to last over the course of several missions given the implementation costs, necessitate a better solution than venting the cabin.
- A Lunar/Martian habitat with frequent EVAs would likely find an Airlock-Suitport Hybrid or Rear-Entry Airlock best suited, depending on the mission size and a risk assessment. A larger mission would favor the hybrid, whereas a smaller mission would potentially necessitate a Rear-Entry Airlock. This is due to the strong need for maintenance (eliminating suitports) and preference for dust mitigation, planetary protection, and EVA quantity, elevating these two designs over the single- and dual- chamber airlocks.
- A Lunar/Martian habitat which also has a rover, however, could instead have a single- or dual- chamber airlock on the habitat which is supplemented by the rover suitports, which are used to compensate for the lower habitat EVA quantity.

The final example in this list is especially noteworthy, as it demonstrates that even when the factors of location, size, and mission duration are known, various different features of the mission profile still prevent general conclusions from being made in these cases. However, despite the strong mission dependence, there are still some conclusions that can be made to scale down the number of choices in certain cases.

- Suitports are likely not useful for non-surface missions (no need for dust mitigation, planetary protection, or frequent EVAs), thus the best solutions are likely to be venting the cabin or to use one of the two airlock designs.
- Rovers and small surface missions need to optimize mass/volume savings, thus they are best suited by venting the cabin, suitports, or rear-entry airlocks.
- Long-term surface missions necessitate maintenance of EVA suits and consumable optimization and thus are best suited by an airlock, rear-entry airlock, or airlock-suitport hybrid.

However, despite that numerical analysis and conclusions would be highly desired, such analysis is not feasible based on currently available data. The extreme implications of mission profile, duration, crew size, and mission-specific risk analysis on the design selection for airlock systems and sizes makes any in-depth numerical analysis largely meaningless and misleading from a generalized sense (the reasoning behind this can be found in Section 6.1.7). As such, the two mission profiles of a 30 day micro-gravity mission and a 30 day Lunar/Martian surface mission were used to demonstrate example mission-specific in-depth analysis for the configurations that are most likely to be implemented in the "near" future.

6.1.9 30 Day Micro-Gravity Mission

Narrowing in on the 30 day micro-gravity mission that the team chose to focus on for more in-depth analysis, several assumptions still had to be made about the mission profile to allow for the analysis. In order to analyze the worst-case scenario, it was assumed for this purpose that a return to Earth would be difficult or impossible in an emergency, as would be the case for a mission far from Earth (like a Mars-orbiting station), thus increasing the importance of EVA contingency and safety. Additionally, it was assumed that novel EVA technologies were not being tested, thus eliminating the only reason for a suitport-based design in a non-surface habitat. Thus, the result was that a Dual-Chamber Airlock was selected, as it traded best due to its high contingency capabilities. Venting the cabin was seen as not viable due to the loss of consumables and the potential for crew members to remain in the habitable volume while others are on EVA, as would likely occur for a 4-person crew.

This airlock was based off of the ISS Quest Airlock, which is shown in Figure 83 (Section 6.1.3), but reduced in size since the ISS equipment lock would be oversized for a 30 day mission. While there is not a significant amount of data regarding minimum airlock volumes, the best estimates by NASA are that two astronauts need at least 7 m^3 for simultaneous donning and doffing of the EVA suits in a standard airlock. Support hardware takes up an additional 1.1 m^3, and logistical hardware and tools another 2.3 m^3, approximately [69]. Thus, the inner airlock portion was designed to meet these total volume requirements. The outer airlock portion (crew lock on the ISS) was designed to similar specifications to the ISS airlock, since this portion is just big enough to fit the crew members in both designs. Additional details on the airlock design, including structural design/analysis and CAD designs, are found in Section 7.8.3.

6.1.10 30 Day Surface Mission

Narrowing in instead on the 30 day surface mission, this too required some assumptions to be made about the mission profile for the analysis. For this design, it was assumed that the surface would be dusty (Moon/-Mars), that the habitat would be independent of other systems (i.e. no rover or other such additional feature), and that return to Earth was not feasible in an emergency (as in the previous design) to analyze the worst-case scenario. As in the micro-gravity design, venting the cabin can be eliminated, and the surface nature of the mission implies a suitport-based design in accordance with the previously-stated conclusions regarding dust mitigation, planetary protection, and EVA access. Due to the isolated nature of the mission, suit maintenance will be important, thus eliminating suitports. As a result, due to the contingency benefits, the Airlock-Suitport Hybrid design was selected as the best trade. This design was also selected in part due to there being more interesting analysis that could be conducted, such as the risk mitigation strategies that could potentially be used that are presented in Section 6.1.11.

The airlock portion of this design was based off of the same numbers as described in the micro-gravity case for the inner chamber portion of the airlock. For the suitports, the values presented in Section 6.1.4 were also utilized, combined with the additional maintenance volume metric of 1.22 m^3 being required in front of the suit (inside of the airlock) [69]. Additional details on the airlock design, including structural design/analysis and CAD designs, are found in Section 7.8.5.

6.1.11 Risk Mitigation and Contingency Analysis

Suitports

For the suitport design, ingress in the event of one suitport failure (assuming there is more than one suitport on the craft) could be accomplished by having one astronaut use the suitport, then having the second remove the first suit (either mounting it on the malfunctioning suitport for storage to mitigate dust or leaving it on the ground) and use the suitport. For egress, this process would be reversed, with the first person using the suitport and then mounting the second suit (from the malfunctioning suitport) for the second person to use. While this would be an incredibly difficult and time-consuming operation, it could be done in an emergency situation to ensure crew survival.

Airlock-Suitport Hybrid

For the hybrid design, analyses were conducted as to possible contingency scenarios for failure of any one component. These were all conducted under the assumption of a 4 crew mission, and are broken down by both the number of suitports within the airlock (2 or 4) and whether the ingress/egress is a normal EVA ingress/egress or an injury scenario (resulting in 4 studies). The failures analyzed are:

- Outer hatch closing failure
- Inner hatch closing failure
- Failure of the seal between the suit and the suitport
- Failure of the seal of the suitport bulkhead

Additionally, the normal EVA scenarios are:

- 2 crew outside attempting ingress with 2 crew inside
- 2 crew outside and 2 crew inside attempting egress
- 4 crew outside with 2 attempting ingress
- 4 crew inside with 2 attempting egress
- 4 crew outside all attempting ingress
- 4 crew inside all attempting egress

The scenarios for medical operations are:

- 2 crew outside attempting ingress with 2 crew inside who are injured
- 2 crew outside, with either one or both being injured, and 2 crew inside attempting egress for rescue
- 4 crew outside with 1 injured attempting ingress
- 4 crew inside with 1 injured attempting egress (such as an evacuation)

For the normal EVA scenarios, this is the full range of combinations that are possible assuming that all EVAs are conducted with either 2 or 4 people, as a one person EVA is highly unlikely given the risks and the conditions for a three person EVA can be easily interpolated from the others. For the medical scenarios, these selections were chosen to represent the range of most likely cases, as there are too many combinations to summarize effectively otherwise. The first scenario would occur if there was an issue with the habitat air supply, for example. The second scenario would occur if there was an issue on a 2 person EVA that affected both astronauts, such as an issue with the EVA suit air resupply system on the habitat (this is motivated by such a scenario trained for in diving). In this case, the astronauts who are inside would need to egress to rescue the other astronauts, and then it is the same as a 4 crew ingress. The third would occur if someone on EVA tripped and injured their leg. Finally, the fourth would occur in the event of a medical issue requiring evacuation of the habitat. These are just examples of how these events may occur, and while some are more feasible than others, they provide an effective range of scenarios for the purposes of the analysis.

The results of these analyses are summarized in the tables below.

Complete redundancy	Risk can be eliminated operationally	Potential critical failure	Critical failure

Table 27: EVA risk mitigation and contingency analysis color key

	2 crew outside, 2 inside, 2 ingress	2 crew outside, 2 inside, 2 egress	4 crew outside, 2 ingress	4 crew inside, 2 egress	4 crew outside, 4 ingress	4 crew inside, 4 egress
Normal ingress/ egress	Suitports	Airlock	Suitports	Suitports	Airlock	Airlock
Outer hatch failure (airlock at ambient pressure)	Use suitports	Outer crew attach suits 3 and 4 to suitports, 3 and 4 use suitports	Use suitports	Use suitports	1) 1 and 2 use suitports 2) 3 and 4 remove suits and use suitports	1) 1 and 2 use suitports 2) 1 and 2 mount 3 and 4 suits 3) 3 and 4 use suitports
Inner hatch failure (airlock at cabin pressure)	- Can be mitigated operationally by not represurizing airlock during EVA - Vent cabin	- Postpone EVA until fixed - Vent cabin	Can be eliminated operationally by not repressurizing airlock during EVA	- Postpone EVA until fixed - Vent cabin	Can be eliminated operationally by not represurizing airlock during EVA	- Postpone EVA until fixed - Vent cabin
Suitport-suit seal failure	Use airlock	n/a - suitports not used	Use airlock	Use airlock	n/a - suitports not used	n/a - suitports not used
Suitport-bulkhead reseal failure	Can be eliminated operationally by not opening suitport during EVA	n/a - suitports not used	Can be eliminated operationally by not opening suitport during EVA	- Postpone EVA until fixed - Vent cabin	n/a - suitports not used	n/a - suitports not used

Table 28: 4 Crew, 2 Suitport Single-Airlock Hybrid Standard Risk Analysis

	2 outside, 2 inside (injury), 2 ingress	2 outside (injury), 2 inside, 2 egress to assist	4 outside (1 injury), 4 ingress	4 inside (1 injury), 4 egress (evacuation)
Outer hatch failure (airlock at ambient pressure)	Use suitports	- if 1 injury, similar to regular ingress - if 2 injury, vent cabin	1) 1 uses suitport 2) 2 and 3 help injured 4 onto suitport and remove 1 suit 3) 2 uses suitport and 1 and 2 help 4 4) 3 removes 2 suit and use suitport	1) 1 uses suitport 2) 1 mounts 4 suit 3) 2 and 3 help injured 4 into suitport 4) 2 uses suitport 5) 1 and 2 mount 3 suit and remove 4 6) 3 uses suitport
Inner hatch failure (airlock at cabin pressure)	- Can be mitigated operationally by not represurizing airlock during EVA - Vent cabin	Vent cabin	Can be eliminated operationally by not represurizing airlock during EVA	Vent cabin
Suitport-suit seal failure	Use airlock			
Suitport-bulkhead reseal failure	Can be eliminated operationally by using airlock for all medical ops except for airlock failure			

Table 29: 4 Crew, 2 Suitport Single-Airlock Hybrid Medical Risk Analysis

	2 crew outside, 2 inside, 2 ingress	2 crew outside, 2 inside, 2 egress	4 crew outside, 2 ingress	4 crew inside, 2 egress	4 crew outside, 4 ingress	4 crew inside, 4 egress
Outer hatch failure (airlock at ambient pressure)	Use suitports	**Use suitports**	Use suitports	Use suitports	**Use suitports**	**Use suitports**
Inner hatch failure (airlock at cabin pressure)	- Can be mitigated operationally by not represurizing airlock during EVA - Vent cabin	- Postpone EVA until fixed - Vent cabin	Can be eliminated operationally by not repressurizing airlock during EVA	- Postpone EVA until fixed - Vent cabin	Can be eliminated operationally by not represurizing airlock during EVA	- Postpone EVA until fixed - Vent cabin
Suitport-suit seal failure	Use airlock	Use airlock	Use airlock	Use airlock	Use airlock	Use airlock
Suitport-bulkhead reseal failure	Can be eliminated operationally by not opening suitport during EVA	**- Postpone EVA until fixed - Vent cabin**	Can be eliminated operationally by not opening suitport during EVA	- Postpone EVA until fixed - Vent cabin	**Can be eliminated operationally by not opening suitport during EVA**	**- Postpone EVA until fixed - Vent cabin**

Table 30: 4 Crew, 4 Suitport Single-Airlock Hybrid Standard Risk Analysis

Note: Bold text indicates significant change from 2 suitport design

	2 outside, 2 inside (injury), 2 ingress	2 outside (injury), 2 inside, 2 egress to assist	4 outside (1 injury), 4 ingress	4 inside (1 injury), 4 egress (evacuation)
Outer hatch failure (airlock at ambient pressure)	Use suitports	**Use suitports**	**Use suitports**	**Use suitports**
Inner hatch failure (airlock at cabin pressure)	- Can be mitigated operationally by not represurizing airlock during EVA - Vent cabin	Vent cabin	Can be eliminated operationally by not represurizing airlock during EVA	Vent cabin
Suitport-suit seal failure	Use airlock			
Suitport-bulkhead reseal failure	Can be eliminated operationally by using airlock for all medical ops except for airlock failure			

Table 31: 4 Crew, 4 Suitport Single-Airlock Hybrid Medical Risk Analysis

Note: Bold text indicates significant change from 2 suitport design

The main conclusion from these tables is that there are several scenarios for which the use of a hybrid design can be creatively used to mitigate potential failure scenarios that would result from Suitports or a Single-Chamber Airlock by themselves. Additionally, it is interesting to note that there are no critical failure scenarios for normal 2 suitport EVA operations (where venting is necessary) that are resolved from the additional suitports in a 4 suitport design. The only benefits occur in scenarios that are resolvable in the 2 suitport configuration. While the additional suitports would allow for much faster and better solutions in these cases, there is not a benefit in the most critical failures. Indeed, due to the fact that the additional ports are going to be used, it even adds some critical failure scenarios that would require postponing the EVA or venting the cabin to resolve. This is because, if the suitports exist for all 4 people, then they will be used as the default for all EVA types, which results in issues for certain crew configurations under a bulkhead failure, as shown in the tables. The conditions that can cause this would not have been possible in the 2 suitport configuration, however, thus posing certain increased risks in the utilization of additional suitports. As such, from a purely contingency analysis standpoint, there is no major benefit to the 2 additional suitports and there are some increased risks, making additional suitports potentially more dangerous with regards to the available contingencies for all failure types.

6.2 Atmosphere Selection (Zach Lachance)

With regards to the atmospheric selection, the largest implication is that lower pressures and nitrogen percentages reduce the amount of pre-breathe time. As such, reduction of pressure and nitrogen percentage is a key goal for high EVA access. However, lower oxygen percentages are ideal for fire risk mitigation. Finally, the oxygen percentage is constrained by the habitability range of hypoxia on the low end and toxicity on the high end. The range of values where crew performance is unimpaired is shown in Figure 91. Additionally, as seen in the figure, there are only two flight certified, TRL 9 atmospheres for long-term space habitation (long-term being greater than 1 week for these purposes for terminology consistency with relevant NASA documents). These are ISS with 14.7 psi and 21% O_2 and Skylab with 5 psi and 70% O_2.

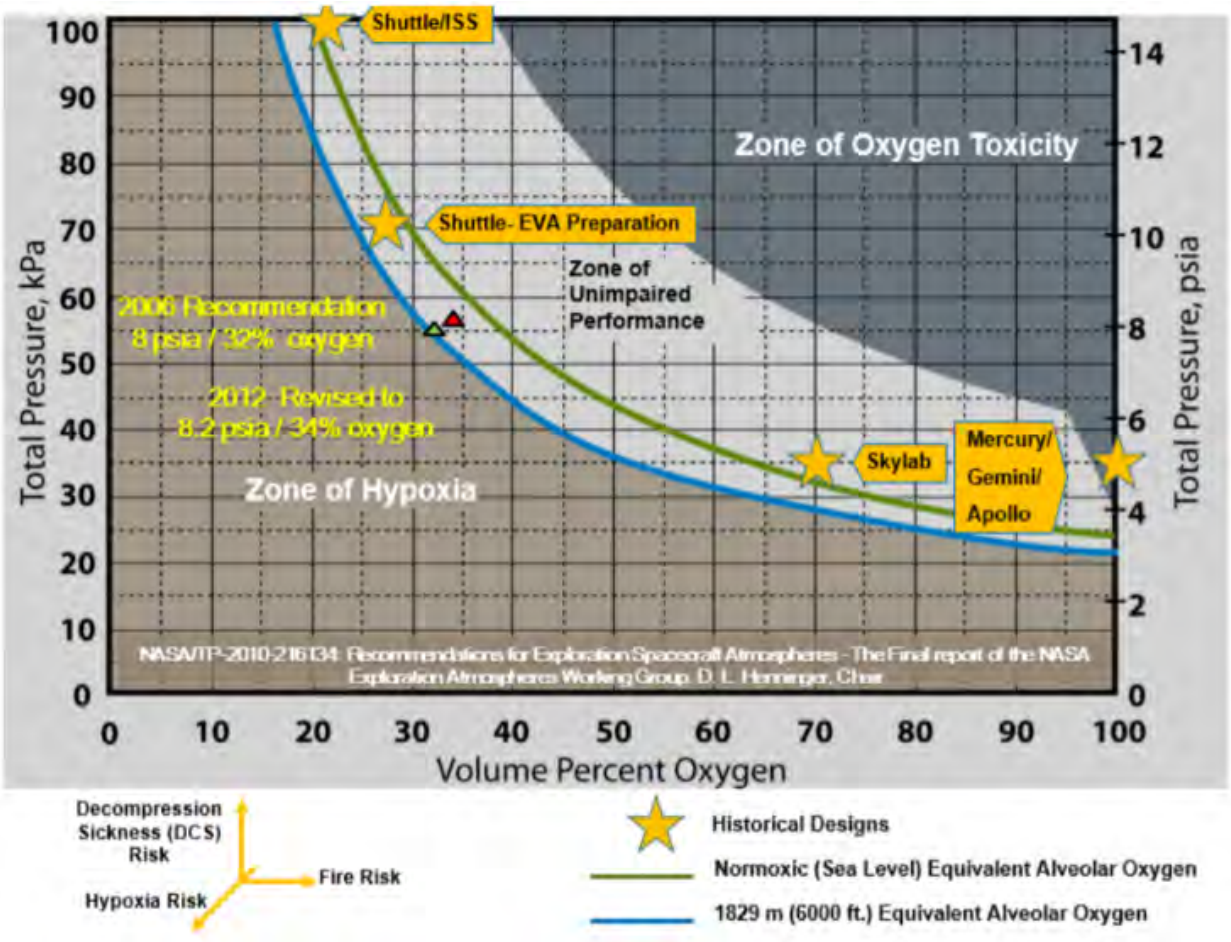

Figure 91: Range of atmospheric oxygen percentages [69]

While other studies have been conducted to find the "optimal" atmosphere for balancing these risks, they all note that there is no available evidence for the medical risks of any conditions other than the two flight-rated atmospheres due to the lack of experimental verification. While such pressure and oxygen percentages proposed do not pose a medical risk on Earth, the implications of these atmospheres on human physiology in the lower gravity, higher CO_2, and higher radiation spaceflight environments is unknown for any long periods of time. These concerns include: vision changes, sleep quality degradation, fatigue, sensorimotor and immune dysfunction, and other medical risks. Thus, this lack of experimental verification and the risks involved for long-term missions has resulted in the NASA Human Research Program office declaring that such atmospheres cannot be approved for missions longer than one week in duration at this time. Additionally, the atmosphere of Skylab is deemed unacceptable for missions that occur further from Earth due to the increased fire risk and the difficulty with evacuation compared to a near-earth station. As such, the

only currently approved long-term habitat atmosphere is 14.7 psi, 21% O_2 [69]. Thus, this atmosphere is taken as the worst-case scenario for the analyses conducted in the event that, for medical reasons, no other atmospheres can be approved by NASA for such missions.

However, since it is also unlikely that this lack of research would remain the case for a true mission, as NASA would likely either prioritize such research or certify more atmospheres beforehand due to the immense pre-breathe times, an atmosphere more suited to ideal pre-breathe times was also selected for elements of the analysis. For this atmosphere, the conclusions of 8.2 psi, 34% O_2 found by NASA's Exploration Atmosphere Working Group were chosen due to the achieved balance of hypoxia risk, flammability, and decompression sickness [83]. These results are also similar to the 8.0 psi, 32% O_2 found in "Recommendations for Exploration Spacecraft Internal Atmospheres: The Final Report of the NASA Exploration Atmospheres Working Group," [57], thereby supporting the conclusions. The former however are slightly more recent and trade better, as described in the paper itself (as it compares their findings to the latter paper directly). These results were also selected because, being the most recent atmospheric conclusions made by NASA that could be found, this is likely the atmosphere NASA would attempt to certify first. As such, 8.2 psi, 34% O_2 were selected for analysis in anticipation that NASA would take steps to certify this or a similar atmosphere before such a mission. Finally, an intermediate atmosphere that is also commonly proposed of 10.2 psi, 26.5% O_2 was also included in elements of the analysis as an alternative in the event that, for medical reasons, the optimal value is not permissible.

6.3 Atmospheric Consumables (Charlie Hanner)

In determining the required mass of gaseous O2 and N2 for the mission duration, each calculation assumed a continuous intra-habiat load of 4 crew members for 30 day continuous duration, and an assumption of 1 kg of O2 consumption per crew member per day. Additionally, an overestimated 30 total main-airlock cycles were accounted for with a 90% scavenging rate. Additionally a global temperature of 23°C was assumed and the Ideal Gas Law was assumed. Tables 32 and shows the required consumables for each habitat and atmosphere considered.

Pressure/%O2	8.2psi/34	10.2psi/26.5	14.7psi/21
$20m^3$ O2 req.	140	139	140
$20m^3$ N2 req.	46	50	99
$40m^3$ O2 req.	145	144	148
$40m^3$ N2 req.	55	62	118
$80m^3$ O2 req.	154	152	158
$80m^3$ N2 req.	73	86	155

Table 32: Atmospheric Consumables - Surface

Pressure/%O2	8.2psi/34	10.2psi/26.5	14.7psi/21
$20m^3$ O2 req.	138	137	140
$20m^3$ N2 req.	42	57	89
$40m^3$ O2 req.	142	141	145
$40m^3$ N2 req.	50	69	107
$80m^3$ O2 req.	154	152	155
$80m^3$ N2 req.	68	94	145
Pre-breathe time	30 mins	40 mins	140 mins

Table 33: Atmospheric consumables - microgravity and estimated prebreathe times

The only variance between the surface and microgravity calculations lies in the airlock configurations, and both scenarios show the maximum reduction in consumable mass occurring within the 8.2psi/34% O2 condition. For each atmosphere, the estimated pre-breathe times were calculated assuming the crew was moving directly to the 4.3 psi pressure of an EMU suit, and the 30 and 40 minute durations can be considered an acceptable zero pre-breathe condition.

6.4 Life Support Selection (Charlie Hanner)

6.4.1 Life Support Trade Study (Charlie Hanner)

In studying air revitalization, eight systems were considered covering both heavilty consumable based and steady-state technologies. The interest in utilization of a consumable based system such as Lithium Hydroxide (LiOH) or Metal Oxide Absorption (METOX) is a shared commonality in technology with EVA operations, especially with the reusable capabilities of some systems. The following systems were considered in the trade study:

- 2BMS - 2 Bed Molecular Sieve
- 4BMS - 4 Bed Molecular Sieve
- LiOH - Lithium Hydroxide
- METOX - Metal Oxide Absorption
- EDC - Electrochemical Depolarized Concentrator
- Mini-Sabatier add on
- Bosch

Each system was studied under the same assumptions as the atmospheric consumables, with the added requirement in consuming <1KW of total power. The trade study revealed the following estimations for each system:

	2BMS	4BMS	LiOH	METOX	EDC	Sabatier*	Bosch
Mass (kg)	64	120	210	193	44	–	2800
Volume (m^3)	0.36	0.44	0.18	0.49	0.08	0.014	15.6
Power (W)	310	680	<100	1000	240	–	6600

Table 34: Life Support System Comparison

Four systems were then ultimately chosen for further in-depth study: 2BMS, 4BMS, EDC, and mini-Sabatier.

6.4.2 2 Bed Molecular Sieve (2BMS)

The 2 Bed Molecular Sieve uses a combination of coolers with a pair of carbon molecular sieves for CO_2 removal from the atmosphere as shown in Figure 92. Alternating adsorbing and desorbing cycles ensure continual up time. A TRL level of 3[21] shows little advancement and flight readiness, however it does provide the advantages of being the second lightest overall system, while consuming the least power.

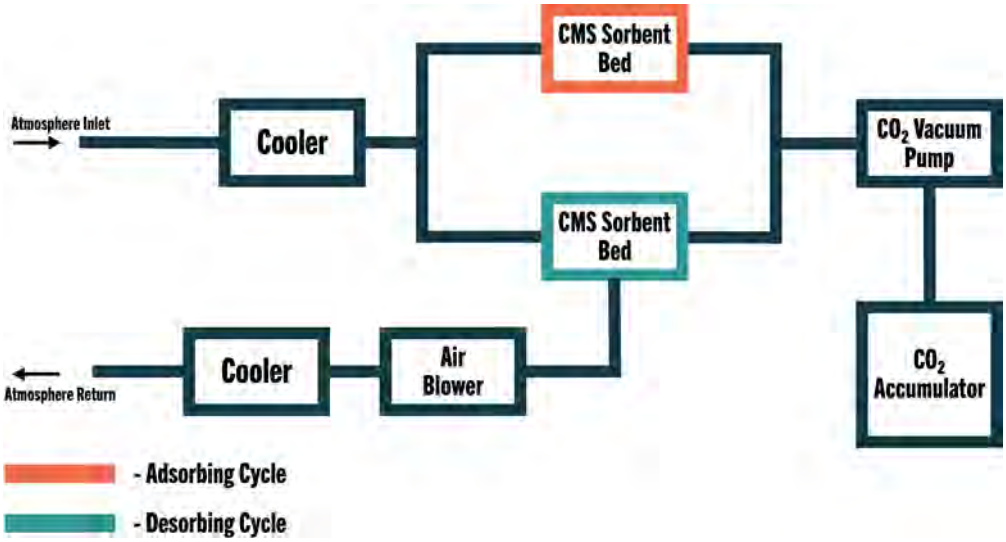

Figure 92: 2 Bed Molecular Sieve Diagram - Charlie Hanner

6.4.3 4 Bed Molecular Sieve (2BMS)

The 4 Bed Molecular Sieve follows the 2BMS's technology in alternating sorbent beds, with the addition of a pair of alternating desiccant beds for better moisture recovery as the expense of a mass increase and a volume increase of 0.08 m^3 over the 2BMS. However, a TRL 9[21] makes this system a higher reliability option.

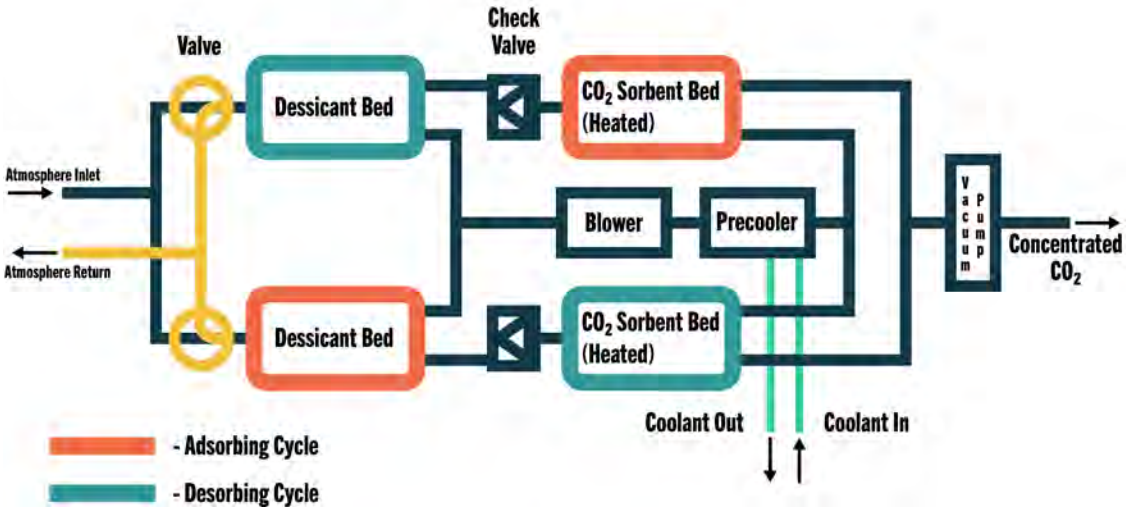

Figure 93: 4 Bed Molecular Sieve Diagram - Charlie Hanner

6.4.4 Electrochemical Depolarized Concentrator

For the EDC systems estimates, the 44 kg mass does not include necessary anode expendables, and further research into the anode technologies was required. Life Systems, Inc. studies recommend the progression of EDC systems only for extremely short duration missions that require very few expendables. However, as total duration increases towards the 240+ hour systems "expendables cause the ZHG/EDC subsystem equivalent launch mass to rapidly increase as the total EVA time increases". The main technologies developed for the EDC filters are Zinc based, and noted to have potential health hazards associated. They also conclude that

the "Zn/EDC concept has not been experimentally proven feasible as a CO_2 scrubber", and "no additional development effort should be directed towards the improvement of the ZHG/EDC or Zn/EDC CO_2 removal concepts" [92] [91]. Additionally, H2 management systems are cautioned for EDC systems, and a secondary system is recommended, and a final TRL level of 6 means a lower technology readiness than the 4BMS.

In summary, the 4BMS is the most ready technology to be put forth into a habitat, and was ultimately chosen for this mission due to its proven reliability, high TRL (9), and moisture recovery. If the mission permitting, and research was funded into the further progression of the 2BMS, a pursued interest in its utilization may be brought to light due to it's advantages in volume and mass. A preliminary combination of a pair of 2BMS's could also provide a greater level of reliability (reliability calculation not performed due to little data in applicational system reliability) while having 8 kgs more mass, 0.28 m^3 smaller, and consume 64 W fewer than the 4BMS. Little data on the reliability of each system contributes to this cautionary approach, and a possible inclusion of a mini-Sabatier add on system can be considered depending on mission and habitation requirements.

6.4.5 Sabatier System (Nicholas Behnke)

A to be included alongside the currently proposed 4BMS could be a Sabatier system. The Sabatier system is a life support supplementary system that, through the process of a chemical reaction, recycles carbon-dioxide and hydrogen into water and methane. The Sabatier system potentially has a TRL level of 9 should a similar system be used to the one in place on the ISS. Both carbon-dioxide and hydrogen are outputs of a traditional life support system as carbon-dioxide is naturally produced by crew members and hydrogen is a byproduct of electrolysis in turning water into oxygen [103]. The Sabatier reaction is an exothermic reaction that performs at maximum efficiency between 250 and 400°C [34]. Exposing the reactants to one another in these high temperatures in the presence of a catalyst initiates the reaction. The following equation displays the reaction.

$$CO_2 + 4H_2 => CH_4 + 2H_2O - 165kJ/mol$$

The benefit of including this system is that the Sabatier reaction lowers the need to jettison carbon-dioxide and hydrogen. Prior to the installation of a Sabatier system on the ISS in 2010, excess carbon-dioxide and hydrogen were vented as to avoid unnecessary build up. UTC Aerospace Systems, the company responsible for the reactor in place on the ISS, claims that the reactor outputs three liters of drinking water per day [109]. Intense ISS resupply of water was common. After its installation, the Sabatier system was able to supplement some of this water and lower the amount needed during resupply §94. In the case of any habitat with a life support system, it is important to make use of every available resource. By avoiding unnecessary venting of materials, a habitat is brought closer to being a closed loop system [70]. It has also been proposed that the methane produced in the process of the Sabatier reaction could be recycled for use elsewhere, potentially as fuel, instead of venting. In our habitat, despite the fact that the mission duration is only 30 days, it is still important to consider resupply. A Sabatier system would decrease the water mass needed to deliver on resupply.

There have also been proposals made for miniature Sabatier reactors. The Microlith Catalytic Reactor is just one of these proposed systems. With a reactor sized at approximately 103 cm^3, one study found success in catalyzing the reaction at a rate similar to the carbon-dioxide output rate of 3-4 crew members [34]. Should a Sabatier reactor the size of the one placed on the ISS be placed in our habitat it would consume the volume of approximately 0.09 m^3 and add a mass of 250 kg [94]. However, the reactor in place on the ISS services a volume far larger than our habitat designs. Pursuing the results of reactors like the Microlith Catalytic Reactor would be exceedingly preferred in our goal to minimize required volume while creating a more self sufficient environment.

Figure 94: NASA Photo of Sabatier Reactor prior to installation [94]

6.5 Water Processing (Lauren Weist)

6.5.1 Water Considerations

When considering potable water for the habitat, there were two main considerations made: to bring all the necessary water with the crew, or to utilize a water recycling system to decrease the potable water amount, but increase the mechanical weight of the habitat. In order to decide between these options, a trade study was conducted to compare different water processing system masses with the total possible mass of potable water. For this study, flight verified processing systems were analyzed, as there are more efficient experimental systems, but none of them have a high enough flight readiness level to be considered for a mission at this time. The systems focused on in the trade study are the Russian Zvezda Service Module life support systems on the ISS, the Mir Space Station life support system, and the American Life Support Module on the ISS.

As a baseline, the water provided for consumption and food use for American astronauts is 2.84 kilograms per person per day [2]. If you populate this out for the designed habitat crew (4) and duration (30). This leads to a baseline of 340.8 kgs of water needed for the whole mission. Note that the Russian astronauts are actually provided 4 kg/person-day of water, but in order to make the trade study equivalent for comparisons sake, the calculations were done as if each provided water amount were equivalent, as the system information is provided in kg/person-day possible to be produced, and can therefore be calculated for this mission regardless of water requirements of the astronauts.

The following table gives the numbers used in the calculations for each subsystem:

	No Reclamation	Zvezda	MIR	ISS LSM
Water Needs (kg/person-day)	2.84	2.84	11.36 (kg/day)	2.84
Water Needs Total (kg)	340.8	340.8	340.8	340.8
WRS-U (kg/person-day)	-	0.86	5 (kg/day)	0.3
WRS-C (kg/person-day)	-	1.8	1.8 (kg/day)	1.8
Supply Water (kg/person-day)	2.84	0.18	4.56 (kg/day)	0.74
Total Supply Water (kg)	340.8	21.6	136.8	88.8
Total Water to Bring	340.8	32.24	143.6	96

Table 35: Water Processing System Comparisons [80] [63]

All modules have both urine and condensate processing systems, with different productions. Additionally, looking at the two most efficient systems, the Zvezda system and the LSM system, we can further decide between the two by looking at system masses. The LSM system has a mass of 1,383 grams, while the Zvezda system has a mass of 215 grams [63] [11]. Since the Zvezda water processing system is lower in mass and processes more water, it was selected for use in the habitat.

6.5.2 Zvezda System Details

The water processing system aboard the Zvezda Module of the ISS consists of three different systems: the SRV-K2M for processing condensate, and both the SPK-UM and SOV for urine processing.

System	SRV-K2M	SPK-UM	SOV
Purpose	Condesate	Urine	Urine Purification
Take-off Mass	115 kg	75 kg	25 kg
Specific Mass Consumption	0.08 kg/kg H20	0.07 kg/kg H20	0.025 kg/kg H20
Specific Energy Consumption	2 W-hr/kg	20 W-hr/kg	0.3 W-hr/kg
Continuous Power Required	0.29 W	6.0 W	0.09 W
Process Details	Sorption/catalytic and ionic exchange and Capillary Porous Membrane	Pretreat with sulphuric acid with chromium dioxide, rotary separator	Sorption and ionic exchange

Table 36: Water Processor Breakdown [63]

The SRV-K2M works by first separating the humidity from the air using an air/water filter made of a porous hydrophilic channel wall which uses capillary action to separate and move the water, passing the dry air on to the CO2 scrubbing system and the water on to the sorption/catalytic (s/c) system. The s/c system utilizes specific materials and resins that have chemical compositions that break down dangerous perchlorates into nontoxic chlorine and water [61]. Image 95 shows how this process operates to neutralize this compound. Additionally, this system can operate in both micro-gravity and gravity environments, making it ideal for habitats that could require either.

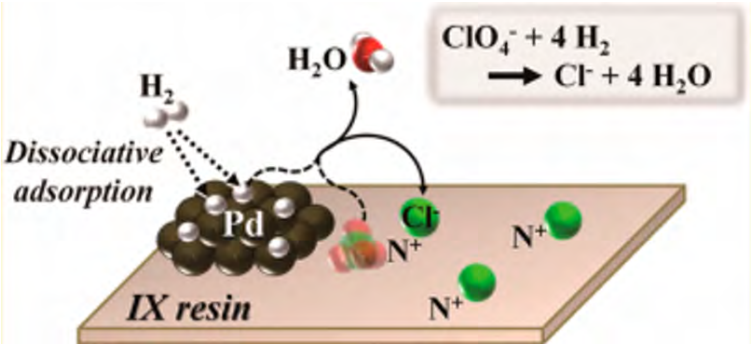

Figure 95: S/C and Ionic Exchange Process by Y. Kim [61]

The SPK-UM and SOV systems work together to first pre-treat the urine, and then also use a sorption and ionic exchange. The SPK-UM system first takes the urine and pre-treats it with sulphuric acid and chromium dioxide, then sends the urine to a rotary separator that takes the urine and uses a rotary evaporator-separator and thermoelectric heat pump which rotate in alternating chambers. This works to create condensate from the liquid and then pump it out of the system. This can work under gravity situations, or under a vacuum for micro-gravity situations. This condensate is then moved through to the SOV system, which works the same way as the SRV-K2M module[63].

This leads to a total mechanical weight of 215 kgs of processing, and 908 kg of potable water. The potable water is broken down into 2.84 kg/person-day of food and drinking water, and 7.3 kg/person-day of hygiene water [23]. Additionally, the combined systems pull 6.38 Watts continuous and takes up a total of 1.27 m^3, with urine processing taking up 0.656 m^3 and condensate processing taking up 0.614 m^3.

6.5.3 Water Processor Mock-Up for Habitat

Analogs to these systems were created in NX with an emphasis on preserving volume and major characteristics without over-complication. Pictured below are the systems and NX analogs.

Figure 96: SRV-K2M System [87], CAD by Lauren Weist

Figure 97: SPK-UM and SOV Systems [87], CAD by Lauren Weist

6.5.4 Water Tank Design

Because of the changeable nature of water tanks, the tanks were the last thing to design for the habitats. The three surface habitats have the same tanks located under the floor of the habitat, for ease of access. The need for three tanks stems from the support structure of the floors, as it limits the available width of the tanks. The three combined tanks hold a total of 0.908 m^3 of water, which is what is needed for the total duration of the mission.

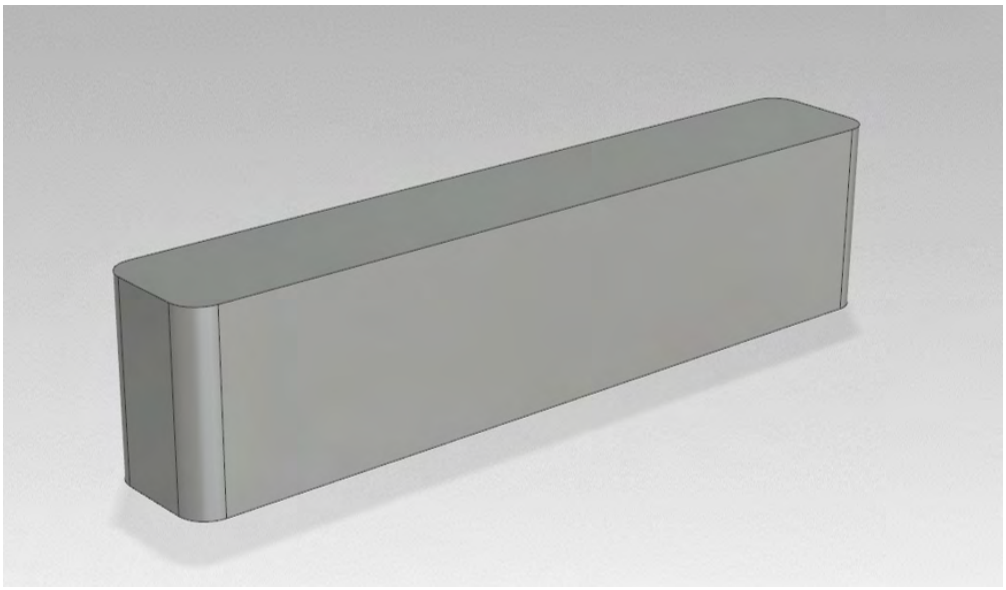

Figure 98: Surface Habitat Water Tank

The micro-gravity habitat water tank has a more complicated design, as there is not a floor to hide the tanks under. Instead, these tanks are designed to be placed atop the crew beds. In addition to taking up a previous unused space, there's a chance that if there is a radiation event, it could provide additional protection.

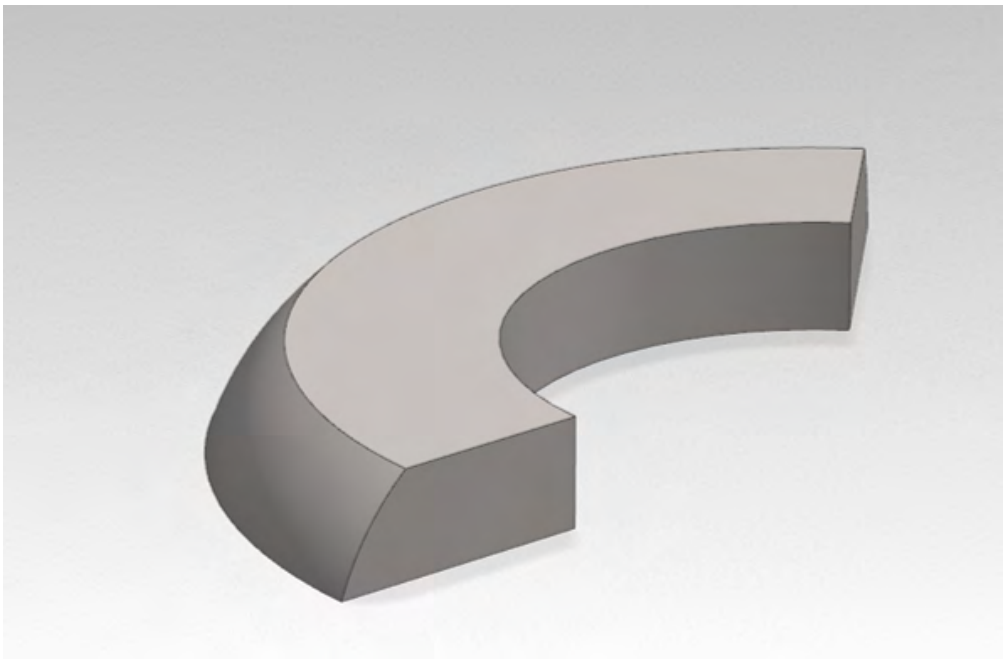

Figure 99: Micro-gravity Habitat Water Tank

6.6 Clothing Selection (Lauren Weist)

Clothing considerations were made in order to both consider necessary storage volume as well as to reduce water mass. On the ISS, they have water allocated for clothing and dish washing, but this mass or volume requirement would be quite large for this habitat. In order to try and reduce this requirement, a comparison was done to see if bringing all necessary clothes for the mission with the crew would be less massive than bringing washing water.

The table below itemizes the NASA standard for clothing, as well as the acceptable use duration and mass per item. This, populated out for a 30 day mission for four days, gives us a mass requirement of 48.7 kg of clothing [110].

	Duration of Use (days)	# for 30 days	Mass Per Item (kg)	Total for Mission (kg)
Exercise Short and Shirt	3	10	0.45	4.5
Work Short and Pant	10	3	1.2	3.6
Undershirt	10	3	0.25	0.75
Underwear	2	15	0.1	1.5
Sweater (2)	30	1	0.55	0.55
Oversocks	30	1	0.08	0.08
Socks	2	15	0.08	1.2
Total Per Person	-	-	-	12.18

Table 37: Clothing Masses and Use Duration [110]

This mass can be compared to the wash water standard from NASA, which is 17.9 kg/person-day, for a total of 2148 kg of wash water. As this is larger than the 48.7 kgs of clothes, the decision was made to not allot for wash water, and instead bring all clothing with the crew.

The volume of clothing was calculated using cotton, as it is a common fabric used in the astronaut shirt-clothes uniform, and is in the middle of the range of densities for clothing. Cotton has a density of 1.55

g/cm^3, which leads to the estimated volume of stowed clothing being 0.0314 m^3.

6.7 First Aid Considerations (Lauren Weist)

Due to the distance and duration of the mission, NASA has standards in place for first aid and medical requirements. In order to meet these requirements, the habitat must support either a Level of Care 4, for habitats near Earth such as microgravity and on the Moon, or a Level of Care 5, for habitats on Mars. These levels have been developed with the intention of being able to take care of an injured astronaut since returning to Earth for care would take a long time [9]. As these standards are already in place, the habitat can meet these standards by carrying the Advanced Life Support Pack and Ambulatory Medical Pack, which contains the first aid equipment required and takes up a CTB each [6].

ALSP and AMP used on the ISS [36]

6.8 Exercise Equipment (Lauren Weist and Patrick Geleta)

6.8.1 Resistance Exercise

In order to maintain muscle mass, inhabitants must have some form of resistive exercise. Resistance bands work in micro-gravity, take up only .12 of a CTB, and weigh only 1 kg for an average weight range from 5 to 30 kgs. This is an alternative to resistive weight machines utilized on the ISS which are, while more advanced and easier to use, take up much more volume, and were therefore not chosen.

6.8.2 TVIS Treadmill

Cardio exercises are also important for maintaining the health of astronauts. One method already utilized in the ISS is a dedicated treadmill. These treadmills must have built in vibration isolation for microg habitats, as they would otherwise damage and disrupt other systems within the habitat. They function by constraining the astronaut with bungee cables and a harness - the harder the astronaut steps, the greater the force they'll be pulled back to the treadmill surface with. Current models have a track size of 33cm X 112cm. Due to its inherently bulky design to mitigate vibrations, this treadmill is only feasible for the 80m habitat designs.

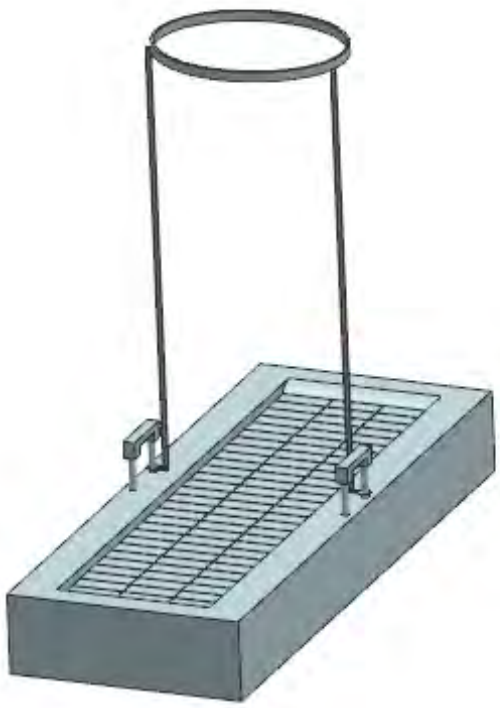

Figure 100: TVIS treadmill CAD model

6.9 Radiation Shielding (Patrick Geleta)

One of the greatest concerns facing astronauts is the impending and constant threat of radiation exposure. With a host of possible lethal afflictions, both immediate and long term, serious consideration must be taken in reducing its effects.

In space, there are three primary forms of radiation to be accounted for; GCRs (Galactic Cosmic Rays) SPEs (Solar Particle Events), and Van Allen Belt radiation. Van Allen belt radiation is however due to the radiation trapped by the earths magnetic field, and is therefore not a concern for habitats out in open space and lunar environments. GCRs are particles that occur randomly throughout the open expanse of space. While they occur in lower quantities than other particles, they have a much wider range in particle energy. The important takeaway from this is that GCRs pose the threat of high kinetic energy particles that occur rather infrequently. Due to their high energy, GCRs are both hard to stop, and able to excite more low energy particles as they pass through a thick material. This reduces the effectiveness of shielding with lower density materials. SPEs on the other hand, occur with solar flares, and when the sun rapidly offloads a high

density series of medium intensity protons.

These two different types of radiation also pose different threats to astronauts. GCRs are known to incite the long term effects of cancers that manifest years after the mission. Because of the rapid exposure induced by SPEs, without proper shielding they can cause a series of immediate effects, with lower exposures causing nausea, while greater exposures can result in death over a span of days or weeks. SPEs can also last for any period from hours to days, wherein astronauts will have to retreat to an area of greater shielding.

6.9.1 Reinforced Berths

Solving the problem of radiation shielding in space follows to an ultimate dilemma: the only realistic way of dealing with radiation is through the use of additional shielding material, while one of the greatest prerogatives for space missions is a reduction in mass. It is not realistic to reinforce the entire habitat due to practical mass limitations, An acceptable solution is found in reinforcing the crew berths instead. Astronauts already find themselves occupying these spaces for a large portion of time (as they sleep in them), and can confine themselves to these areas in case of an SPE taking place.

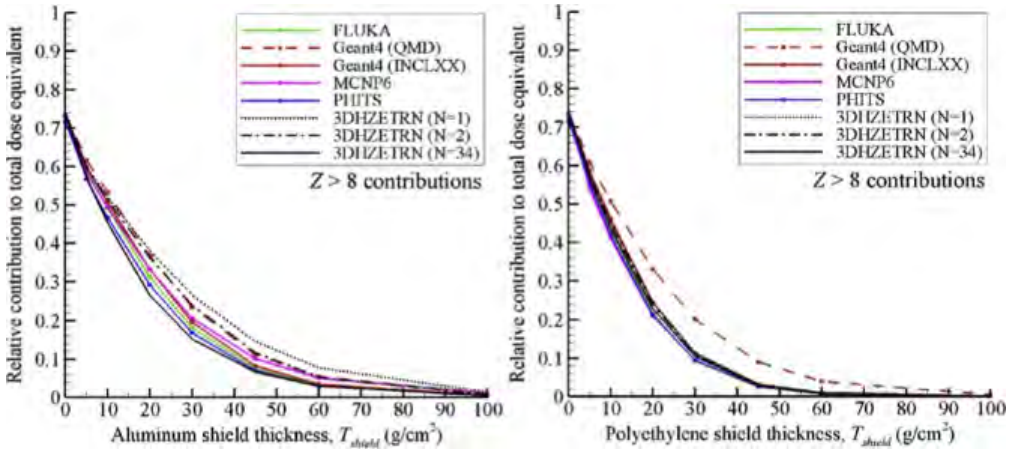

Figure 101: Effectiveness of various shielding materials [98]

Rather than using more layers of aluminum for radiation shielding, it was important to consider an array of other potential materials. Polyethylene arose as a stronger alternative. It can be acquired in sufficient amounts to line the berths, its already been approved for use on the ISS, and it does a better job at reducing the radiation dose to astronauts for a given thickness. Reinforced parts of the ISS have effective shielding on the order of 20g/cm2 of aluminum. This can be reduced to below 15g/cm2 (as indicated by the above chart) for equivalent shielding with polyethylene.

6.9.2 CAD Models of Integrated Berths

For the final integrated environments, a redesign of the berths was necessary to fit these models properly. These berths had to deal with the obvious concerns above of meeting passive radiation shielding requirements, while also conforming to the environment in a way that prioritized space, and being usable to the resident astronauts. It was therefore necessary to construct unique models for micro gravity and surface habitats at each radius.

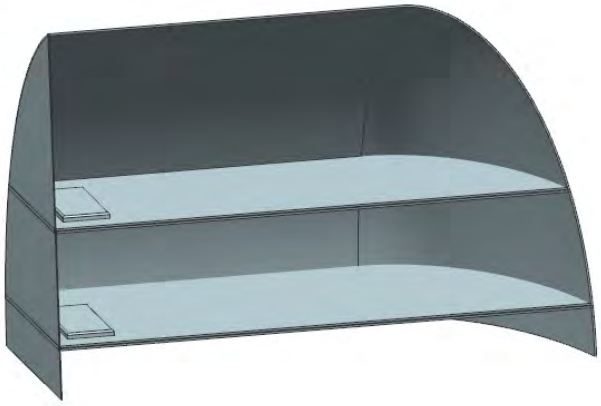

Figure 102: Berth for $20/40m^3$ surface habitat

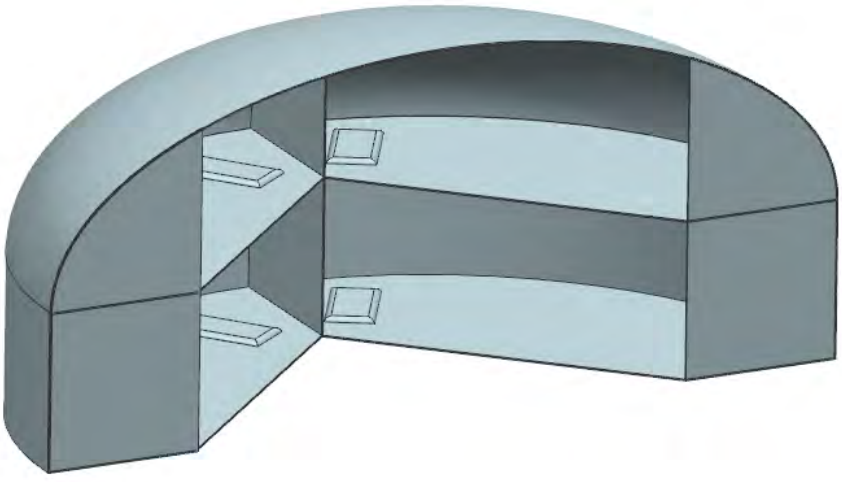

Figure 103: Berth for 80 m^3 surface habitat

For the above surface berths, They were designed to fit flush against the top of the habitat, as they can be climbed into, saving use able space below. The walls of the berths serve to reinforce their occupants against incoming radiation in accordance with the observations above.It is noted that due the limited size

of the 20m and 40m habitats, their berths are smaller in use able volume than the 80m habitat alternative. The smaller design offers individuals 1.96 cubic meters of space, while the larger berth offers individuals 3.1 cubic meters.

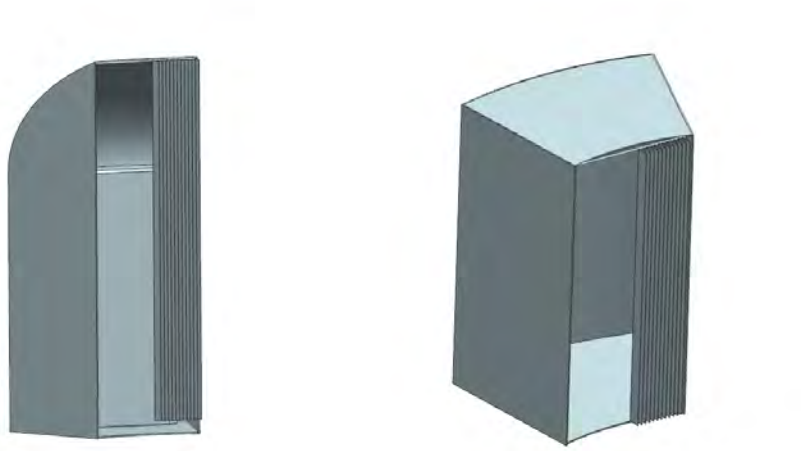

Figure 104: Berths for the 20m/40 m^3 (left) and 80 m^3 (right) micro gravity habitats

The micro gravity berths have fewer spatial limitations than the surface berth due to the lack of mandate for dedicated bottom. The smaller design gives each individual 2.04 cubic meters of usable volume, while the large gives each individual 2.12 cubic meters. These berths contain sleeping bags to restrain astronauts into their desired orientation as they sleep. These berths are similar in design to those seen on the ISS, and could potentially be fitted with personal computer systems, and with quick storage along the door like seen on the ISS.

6.9.3 Wearable Radiation Shielding

In addition to the reinforced panels mentioned above, another viable way of supplementing further radiation protection is in the form of wearable radiation shielding equipment. Hydrogen rich compounds tend to be best at absorbing radiation, so these vests are often proposed to either be filled with water, or manufactured with hydrogen polymer blends.

Already such prototypes have been sent to space. The Italian Space Agency launched tests for PERSEO (Personal Radiation Shielding for Space Exploration) in 2017, where they had an astronaut aboard the ISS wear water filled vest to test for feasibility in application. The vest featured 4 compartments covering the torso's front and back, which were filled with 22 litres of drinking water. This system was capable of being filled within the 30 minute required window for responding to SPEs and offered 7cm of protection. The astronaut reported that the vest did not seriously inhibit his range of motion, and ability to complete tasks.

Further developments in the field of personal radiation protection have been recently developed, and are already slated to be tested for their viability in space. One of the most promising such projects is the development of Astrorad vests by Lockheed Martin. These vests contain hydrogen rich composites, and are layered to be different thicknesses over different portions of the body. Older less feasible approaches tried

to layer the body with as much material as possible - this approach instead acts to reinforce more essential and vulnerable organ systems, while areas of the body with lower risks for radiation damage, and greater levels of tissue are left with less shielding. A particular focus is placed on blood forming organs (BFOs), bone marrow, lungs, colon, and the stomach.

These Astrorad vests will be sent along the Artemis-1 program, where they will be attached to "phantoms" - mannequins designed to mimic the composition of human tissue and body systems. These phantoms are laced with an internal set of sensors designed to register the radiation imparted to the phantoms throughout the duration of the mission. By sending a "control" phantom without the vest, and one with, a more complete knowledge of personal radiation protection in space will be developed. There are also plans for astronauts to test wearing these vests over the summer, so they can report on their comfort and ease of use.

6.10 Fire Safety (Lucia Stainer)

Due to the habitat's relatively high oxygen concentration (up to 34% oxygen, compared to 21% on Earth), small volume, and confined crew, a fire aboard could easily be catastrophic, or at the very least, mission-ending. This is why it is so important to adopt proper fire safety practices on these types of missions. Fire safety is broken up into the following four fields: [49]

1. Fire Prevention
2. Fire Detection
3. Fire Suppression
4. Cleanup

While it is still crucial to prevent habitat fires by using less flammable materials and minimizing available ignition sources, the two components of fire safety that have the greatest impact on the total mass, volume, and power of the habitat are fire detection and fire suppression. As a result of this, those subjects will be the primary focus of this section.

6.10.1 Fire Detection (Lucia Stainer)

Fires act much differently in microgravity than they do in partial or Earth gravity levels. For example, ignition is more likely to occur in microgravity due to the reduction of natural convection and the presence of flammable aerosols lingering in the air [48]. Additionally, if there is no airflow, then the rate at which flames spread is greatly reduced. However, if there is airflow, then the flames will spread much faster in the direction of the oxygen source [48].

The most important fact about the behavior of fire in microgravity is the size of soot particles that are created and dispersed by the fire. Soot particles in microgravity tend to be larger and have a further range than they are in Earth gravity [48]. This fact is important because it directly dictates which type of fire detector would work the best, since different types of fire detectors can detect different sized particles of soot. Therefore, the best type of fire detector to use in a microgravity habitat is one that is capable of detecting larger soot particles, such as a photoelectric detector. Photoelectric detectors, such as the ones on the International Space Station, can detect particles that are greater than 1 μm in length [108]. These detectors are 1.5 kilograms each and use 1.48 watts of power [48]. Due to a lack of available information on the volume of these detectors, we are estimating the volume of each detector to be approximately .0025 m^3.

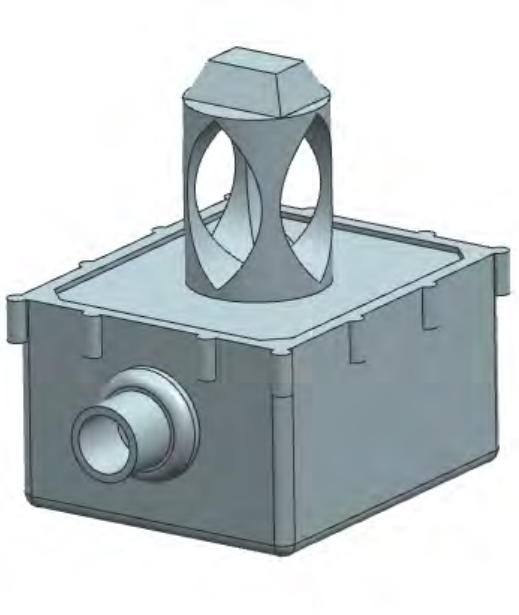

Figure 105: 3D Model of Photoelectric Fire Detector

In Earth gravity, soot particles tend to be smaller than they are in microgravity. The best type of fire detectors for these smaller particles are ionization detectors, which can detect smoke particles that are between .4 and .7 μm [108]. These types of detectors are also 1.5 kilograms and have a power requirement of 9 watts [48]. Due to a similar lack of information as the photoelectric detector, the volume requirement had to be estimated to approximately .0015 m^3 each.

The behavior of fire in partial gravity is a little less known due to a limited amount of testing on the matter. The flammability behavior and flame-spread rate are at a maximum at .15 g to .4 g, since the buoyant flow velocities are optimal in this range [48]. However, we were unable to find the size of the soot particles produced by fires in partial gravity. In order to cover a wider range of soot particle sizes, we are going to include both a photoelectric detector and an ionization detector in the partial gravity habitats. Assuming that there is only one of each type of detector in each habitat, the total mass is 3 kilograms, the total power usage is 10.48 watts, and the total volume is approximately .004 m^3.

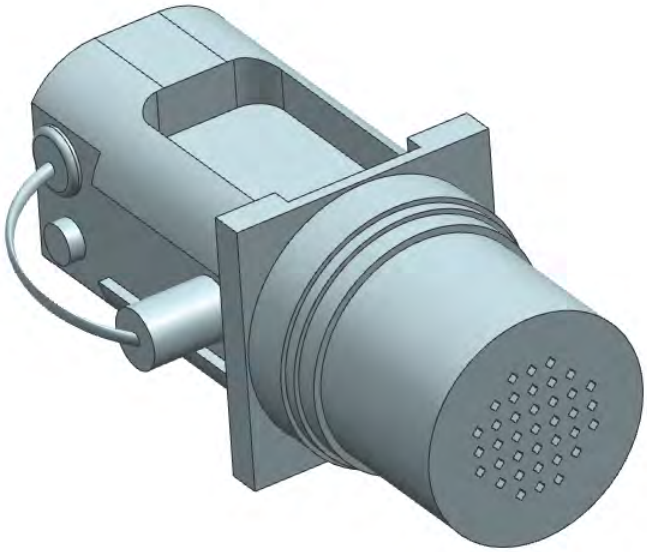

Figure 106: 3D Model of Ionization Fire Detector

Now that we know which detectors to use within each habitat, we need to know where these detectors should be located within the habitat. It was mentioned earlier that flames tend to spread toward sources of oxygen, so detectors should be placed near these oxygen sources. This matches the Human Integration Design Handbook, which states that fire detectors should be placed in cabins, equipment bays, and all ventilation supply and return ducts [85]. As of right now, there is only one photoelectric detector placed in each of the microgravity habitat models and one of each detector type placed in the partial gravity habitat models. Realistically, there should be many more detectors included within each habitat, but for the sake of simplicity, we only included the minimum amount.

6.10.2 Fire Suppression (Lucia Stainer)

Once a fire has been detected, there must be the means aboard the habitat to suppress it. We will be looking at the pros and cons of four different fire extinguishers in order to determine which type of fire suppressant would be the best to use on each habitat. The fire extinguishers we researched for the project were Halon 1301 extinguishers, CO_2 extinguishers, nitrogen extinguishers, and aqueous foam extinguishers.

The first suppressant we will discuss is Halon 1301, or bromotrifluoromethane, which is what was used on the Space Shuttle. Even though Halon 1301 is a thermally stable and very effective fire suppressant, there are some major problems with using it. One of the biggest issues with using it is that it decomposes into toxic gaseous byproducts when exposed to sufficiently high temperatures (about 480 °C) [68]. These hydrogen halide reaction products are both toxic and corrosive, and are not easily removable by the habitat's ECLSS [47]. Due to these factors, this suppressant should definitely not be used.

Next, we will be looking at CO_2 as a fire suppressant. Carbon dioxide extinguishers, which are the type of extinguishers that are used on the U.S. modules of the International Space Station, are less efficient than Halon 1301, but are more efficient than nitrogen due to having a higher mass specific heat at high temperatures [68]. Carbon dioxide is also very easy to clean up once the fire has been put out. However, there are also some downsides to using carbon dioxide as a suppressant. The biggest negative to using carbon dioxide is that local concentrations of CO_2 in a fire zone can be 20 mole %, which is enough to be toxic. Additionally, there is a low concentration of carbon monoxide that might also be produced [47]. Finally, carbon dioxide is not a very effective suppressant when the fire is fueled by its own source of oxygen [85]. The combi-

nation of these factors makes it a bad idea to use carbon dioxide as a suppressant in a small, occupied habitat.

Another option is to use N_2 as a fire suppressant. Nitrogen gas extinguishers, as mentioned earlier, are less efficient than carbon dioxide extinguishers, and also pose a threat of asphyxiation [68]. Like CO_2, it is not very efficient at putting out fires that are continuously fueled by their own sources of oxygen. The benefit of using nitrogen is that it does not pose the same threat of a toxic concentration being in the habitat that carbon dioxide does [47], plus any excess nitrogen can be easily removed from the habitat by ECLSS once the fire has been put out.

The last fire suppressant option that we will be examining is aqueous foam, which is what is used on the Russian modules of the International Space Station, as well as Skylab. One benefit of using aqueous foam as a suppressant are that it does not become toxic at high temperatures or concentrations. It is also particularly useful in putting out fires that are fueled by a continuous source of oxygen, unlike nitrogen and carbon dioxide [85]. One of the issues with aqueous foam extinguishers is that they can be difficult to use in lower gravity levels [46]. Additionally, these types of extinguishers tend to be harder to clean up after, since the suppressant is not in a gaseous form that can be vented out of the habitat.

After having examined these fire suppression methods, we determined that it would be best to provide both a nitrogen extinguisher and an aqueous foam extinguisher on all habitats. Nitrogen gas was chosen to be used because it is non-toxic, inert, and relatively easy to clean up, while aqueous foam was chosen because it is good at putting out oxygen-fueled fires. The reason that two different types of extinguishers were chosen is that different types of suppressants are better at putting out different types of fires [32]. Therefore, including multiple types of extinguishers within the habitat is the safest possible option.

For the nitrogen extinguisher, the total mass is 6.6 kg and the total volume is .0067 m^3 [8]. These values were obtained by looking at the mass and dimensions of a nitrogen extinguisher that is used on Earth. For the aqueous foam extinguisher, the total mass is 3.629 kg (8 pounds) [68] and the total volume is .0136 m^3 [1]. These values were obtained by looking at the mass and dimensions of the aqueous fire extinguisher from Skylab. We can then use these values to help determine the required mass and volume that the habitats must accommodate. Each habitat will contain at least one nitrogen extinguisher and one aqueous foam extinguisher. Therefore, the total mass and volume between these two extinguishers are 10.23 kg and .21 m^3.

Figure 107: 3D Model of Nitrogen Detector

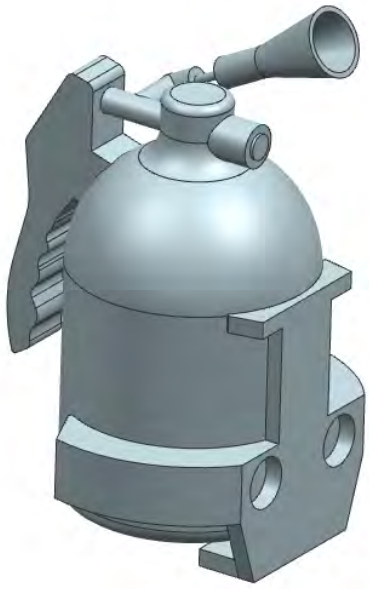

Figure 108: 3D Model of Aqueous Foam Detector

6.11 Workstation Activities (Lucia Stainer)

6.11.1 Glovebox (Lucia Stainer)

When it comes to the workstation activities for the habitat, a large focus was on the inclusion of a glovebox. A glovebox should be included in each habitat if possible, since it will provide a closed environment for any geological experiments that occur during the mission. This section will explore the differences between gloveboxes in micro-gravity and surface gravity and how the choice in glovebox affects the overall habitat design.

The glovebox that we decided to use for geological experiments in the micro-gravity habitat is NASA's Microgravity Science Glovebox, which is currently the glovebox in use on the International Space Station. This decision was made because, as the name suggests, the Microgravity Science Glovebox was built for the specific purpose of being used in microgravity. This glovebox has a work volume of 255 liters and total dimensions of .85 m x 1.046 m x 2.014 m (D x W x H) [45]. Therefore, the total external volume requirement for this glovebox is 1.791 m^3. These were the dimensions that were used when modeling this glovebox, in addition to a curved back that was added to fit the curvature of each habitat. When it comes to the glovebox's power requirements, it consumes no power when not in use, but can consume up to 1000 watts of allocated power when it is in use [59]. Due to a lack of available information on the topic, the mass of the glovebox was roughly estimated to be about 400 kilograms, given its known volume. Using these volume, power, and mass requirements, we can determine whether the micro-gravity habitats that we designed can feasibly include a Microgravity Science Glovebox.

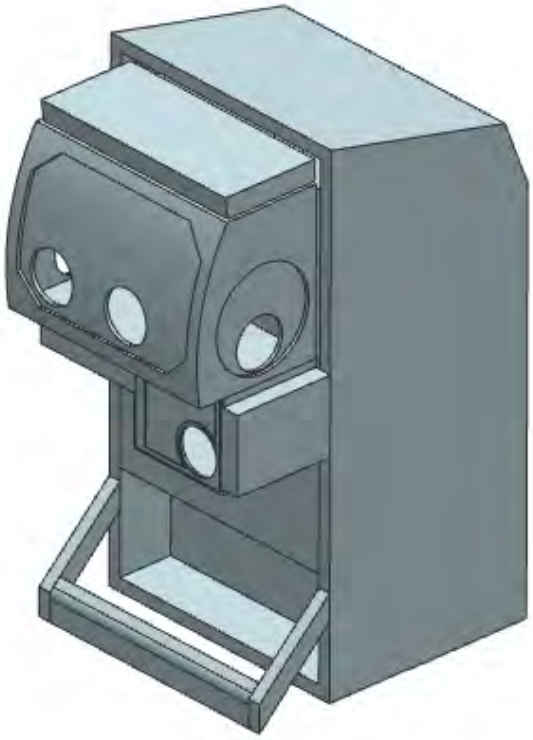

Figure 109: 3D Model of Microgravity Science Glovebox

The glovebox that was chosen to be used in partial gravity was the GeoLab glovebox. This glovebox was built by NASA's Johnson Space Center to be used for geological experiments on planetary surface missions and currently resides in NASA's Deep Space Habitat [31]. Unlike the Microgravity Science Glovebox, the GeoLab glovebox is wall-mounted and contains three vacuum antechambers that lead outside of the habitat. This glovebox was chosen because it was specifically designed to be used for geological experiments in partial gravity, which is exactly what we want for a glovebox within the partial gravity habitat. The dimensions for the 3D model, and subsequently, the volume requirement, were estimated given images of the GeoLab glovebox and the fact that the glove access holes are 10 inches in diameter [64]. The external dimensions were estimated to be approximately .8 m x 1.96 m x 1.15 m (D x W x H), which makes its volume about 1.8 m^3. Due to a lack of available information, the mass was also estimated to be approximately 400 kilograms. This value was obtained by using the volume of the 3D model from Figure §110 and the densities of stainless steel and poly-carbonate, the materials that the GeoLab glovebox is made of. Just like the Microgravity Science Glovebox, we can use these requirements to determine if this glovebox will fit within the planetary surface habitats that we designed in this project.

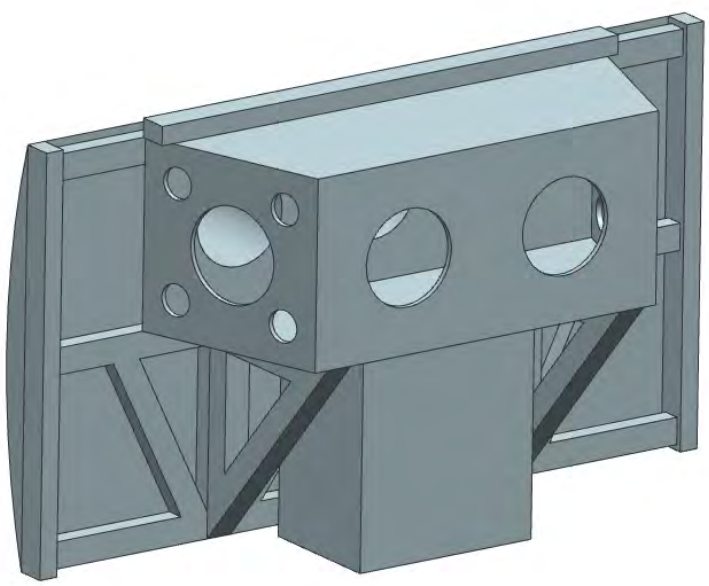

Figure 110: 3D Model of Geolab, Front

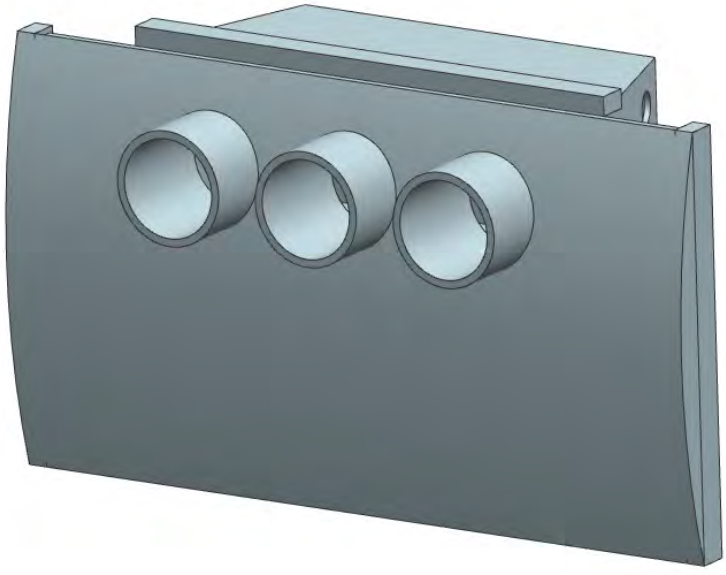

Figure 111: 3D Model of Geolab, Back

6.11.2 3D Printer (Lucia Stainer)

Another important workstation activity that should be included within each habitat is a 3D printer. The inclusion of a 3D printer will be useful for the crew members on the habitat, since they might need to print a tool or part that would not have been previously available to them. The model of 3D printer that we used for this project is Made In Space Inc.'s Additive Manufacturing Facility, which is currently the printer used aboard the International Space Station. The benefit to using this type of printer is that it is gravity independent [65], and can therefore be used in both the micro-gravity and partial gravity habitats. It has

a mass of 45 kg and a volume of .0713 m^3. When in use, it requires 600 watts of power [65]. We can use these mass, volume, and power requirements to determine whether each habitat can accommodate this 3D printer.

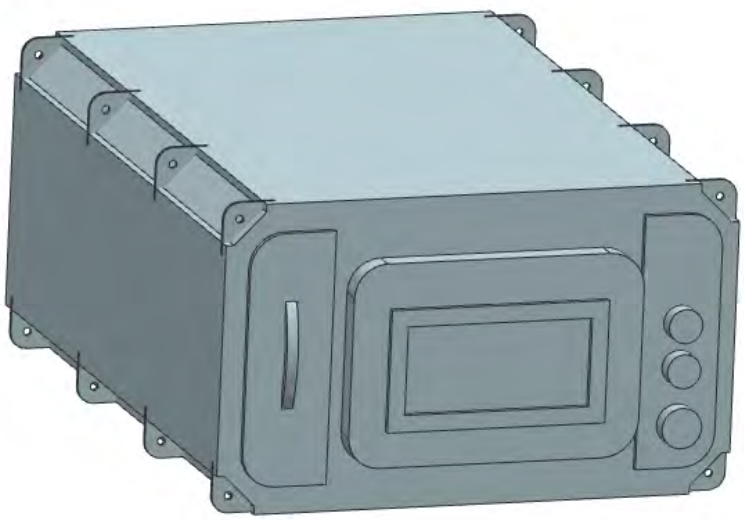

Figure 112: 3D Model of Additive Manufacturing Facility

6.11.3 Galley Table and Seating (Nicholas Behnke)

Further working surfaces would be essential to allowing a high density crew to work at maximum efficiency. Not only that, but eating surfaces are to be included in both a surface habitat and micro-gravity habitat. It is essential when considering these aspects that the functionality is found with as minuscule of an impact to the overall volume of the habitat as possible, whilst still accomplishing the goal of providing for the crew. This section will detail our habitats approach to this issue.

The following figures 114 and 113 represent the galley table currently implemented into our CAD designs of the overall habitat layouts. Due to the necessity for work and dining space in both micro-gravity and surface habitats, along side the set number of four crew members, this table appears in both types of habitats. The design of this table draws inspiration from both the medical table that had been designed earlier in the semester for use in connection with the 80/20 racks, as well as from the Hunch Galley Table currently in place on the ISS. In concept, the table would be a modular system, allowing it to be attached to or removed from a designated position in the habitat by the crew based on their current needs. In the current habitat configurations the table is attached to the sanitation station and positioned in a way that it would be accessible for crew use. The table features an extension that can allow for a larger workable area when necessary. Also notable are the handles, which are specifically useful in micro-gravity for crew stabilization and orientation. The table represents a stowed volume requirement of approximately 0.034 m^3. The working surface area is approximately 3560 cm^2 and 5420 cm^2 when the table extension is in use. Assuming an aluminum structure, the mass of the table was estimated at a maximum of 75 kg, however this is likely a gross overestimate as the entire structure would not be solid aluminum for the purposes of mass reduction.

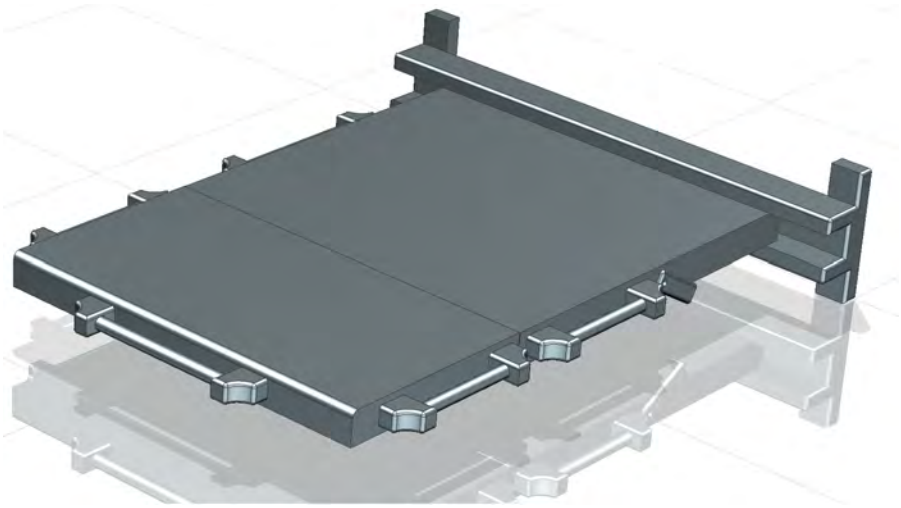

Figure 113: Extended Galley Table

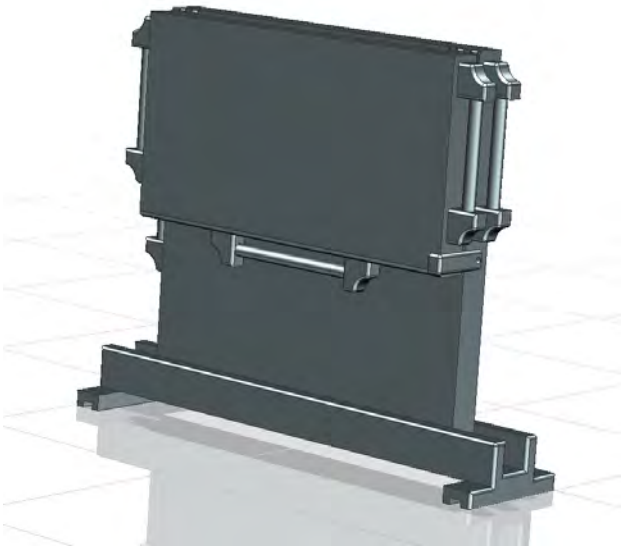

Figure 114: Collapsed and Stowed Galley Table

In considering both the surface and micro-gravity habitats, it was also deemed necessary to have seating arrangements for the crew in the surface habitats. The following figures depict the seats currently displayed in each of the surface habitats §115. Like with the table, it was important that volume be minimized whilst still meeting the needs of the crew. While stowed, the chairs have a volume of 0.02 m^3 and stowed dimensions 115 x 450 x 380 mm^3 §116. Therefore habitats stowing enough seating for four crew members must allocate approximately 0.08 m^3 of stowage. Assuming an aluminum structure for the seating, the mass is estimated at 13.3 kg. For a habitat with four stowed chairs, seating represents a mass of 53.2 kg.

Figure 115: Surface Habitat Seating

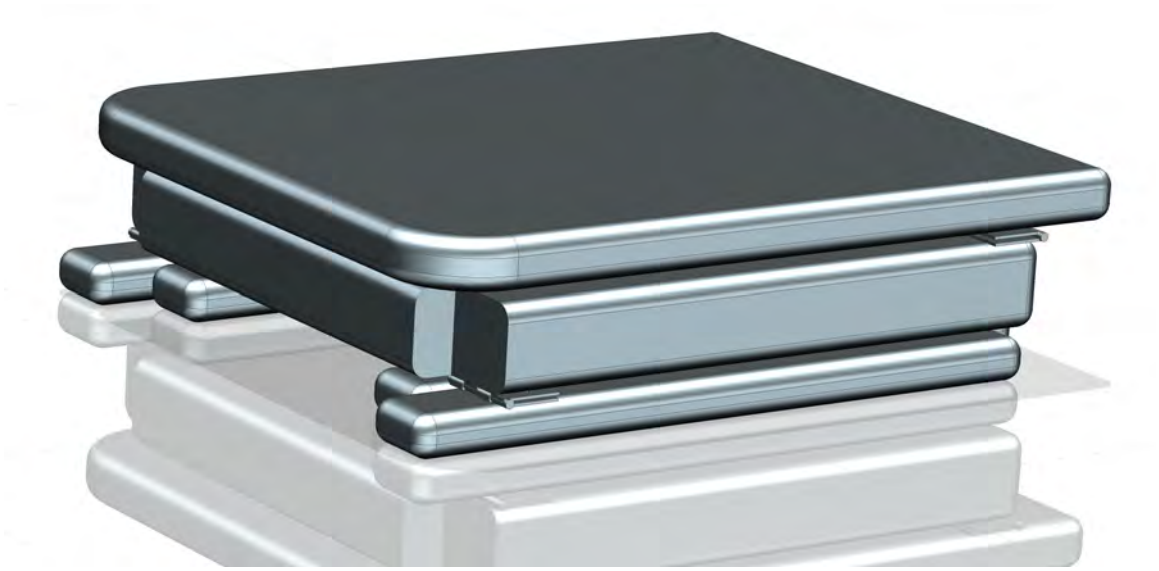

Figure 116: Collapsed and Stowed Seating

6.12 Lighting (Nicholas Behnke)

The following section will detail the choices made in configuring the lighting systems for the habitats. Lighting type, coloration, and power requirements will all be discussed here.

6.12.1 Lighting Type (Nicholas Behnke)

Determining the lighting system for the habitat and crew is an essential part of defining the total power requirements of the whole system. Firstly, however, the lighting system must be properly defined in order to determine power draw. A study was conducted to determine Which lighting type would be best suited for our habitats. In the Lighting Analysis §38 table below, a variety of bulbs and lighting fixtures were analyzed as to determine which would best suit our mission requirements. While for a long duration, fluorescent

lights were the preferred method of spacecraft lighting, it has been found that solid state lighting fixture like LEDs are not only more efficient in terms of their luminescence per unit of power, they have also be found to last significantly longer than most other lighting methods. Analyzing each lighting type, incandescent and fluorescent lighting rank much worse than either HID or LED lighting. Between HID and LED lighting, though their values are close, LED lighting has benefits that HID does not. HID lights work based on chemical reactions and are less reliable than solid state LEDs. HIDs also run at a much higher operating temperature [85]. Meanwhile, LED lights operate in a larger lighting frequency. Specifically they possess the ability to better simulate natural lighting [105]. With these considerations in mind, LED lighting appears to be the most ideal choice for our habitat. Following this study into lighting fixtures, it becomes clear why the ISS also chose to transition its lighting fixtures from fluorescent to LED over the last few years.

	Lifespan (hrs)	**Efficiency**
Incandescent	<1000	17-20 lm/W
Fluorescent	7500-20000	45-75 lm/W
High-intensity Discharge	18000-24000	95 lm/W
Solid State/LED	30000-50000	80-100 lm/W

Table 38: Lighting Analysis [85]

6.12.2 Power Requirements (Nicholas Behnke)

The power requirements of a lighting system as inherently based on the luminescence that system will require. In the case of our project, the system is any surface within the habitat that the crew members might need to interact with. Luminescence, or brightness, is the number of lumens a surface needs. In terms of lighting, an individual lumen is approximately the same amount of light as that produced by an individual candle. Lumens are determined by the area of the room, and by the necessary lux (lm/m^2) for actions that are expected to be taken in that room. The levels of well lit rooms typically fall on the range of 100 lm/m^2 to 1000 lm/m^2.

In the case of our system, approximately 1000 lux are being considered as the requirement due to the quantity of work and amount of precision that would be expected in the habitable space of the habitats. Within our habitats, lighting would be completely crew adjustable. However, for the sake of worst case power requirements, it is assumed that the lighting system is on at full working capacity for all 30 days of the mission. This quantity of lighting being required is in no way anticipated, however this value should stand as an absolute maximum for the lighting power draw.

Each designed habitat has its surface area that must be lit. By using that area along with the assumption that the cabin will be held at approximately 1000 lux the power draw of the whole lighting system can be found. The following table is used to identify the necessary power requirements for each habitat volume, using the assumption that the selected LED lighting system produces 80 lm/watt, a typical value that could be expected whilst deciding between LEDs [85]. Based on the final estimations, The worst case power requirement for the lighting system is 804 W §39. The conclusions that can be drawn from the lighting system, in terms of volume and the purpose of the project, are as follows. The needs of the lighting system are directly proportional to the surface area that needs to be lit. As the volume of the habitat increases, greater resources will need to be allocated to lighting the volume. As a direct consequence of this, a larger strain is place on the power supply, potentially requiring a larger allocation of resources and volume in power systems as well.

Habitable Volume	Total Surface Area (m^2)	# of floors	Lumens Required	Worst Case LED Power (W)
20 m^3	57	1	27600	345
40 m^3	97	2	46970	587
80 m^3	133	2	64398	804

Table 39: Habitat Lighting Power

6.12.3 Lighting Coloration (Nicholas Behnke)

While considering any sized habitat, it is import to consider crew health and mentality. Especially in our case considering the fact that a minimum sized volume habitation will already be taxing on those individuals who are crew members. One way to help address the question of crew mental health is to implement a system within the lighting that simulates the natural lighting found on Earth. It is unnatural and unhealthy to to experience cyclical artificial white light [33]. Effecting the circadian rhythm of an individual can cause major physical and psychological tolls on the human body. For individuals already placed in a mentally taxing situation, it is the job of those designing the habitat to cause the least physical and mental strain on the crew whilst still meeting our minimum volume goal.It has been proven that exposure to certain lights, such as intense blue lighting typically produced by fluorescent lights, at the wrong point of an individuals circadian cycle can begin to lead to high levels of stress and potentially insomnia. Figure 117 gives an indication of the desired habitat lighting versus what was, at one point, the lighting of the ISS. Implementation of an altering lighting color temperature, however, would be relatively simple. LEDs are able to function well in the expected color temperature range that natural daylight transitions through [33]. Crew members would have full control of the lighting systems based on their needs. Based on crew sleep cycles, color temperature transitions would be adjusted.

Figure 117: Lighting Color Temperature Ranges [33]

6.12.4 Windows (Nicholas Behnke)

Another consideration that should be addressed for the habitat is the inclusion of windows. It is universally agreed that windows should be included on any habitat, whether it be on a surface or in micro-gravity. Windows serve a variety of important rolls for a crew, from taking measurements to making observations to simply allowing for a place of crew relaxation. Windows in place must also adequately allow for the completion of any tasks or observations they may be required for. According to the NASA, all human spacecraft and habitats must have at least two windows other than those found on a hatch [85]. It is also noted by NASA that at least one of these windows must be of a minimum viewing aperture of 40 cm [85]. This is for the purpose of crew safety, situational awareness, and the ability to properly address any problems that may occur outside of the internal livable space. Allowing natural light to enter the cabin is also beneficial for the sake of crew health, as natural light is a direct source of vitamin D.

Despite being vital to any mission, windows were not implemented into the current habitat design. Despite this, in a later, more refined version, each of the habitats would see the inclusion of windows into their design. The rationale for the absence of windows at this stage is that they are not inherently intrusive to the volume of the habitat, nor do they draw power from the habitat. For the purposes of our project in volume minimization, further discussion of habitat windows was discontinued.

6.13 Food and Food Storage (Nicholas Behnke)

6.13.1 Food Volume Estimation

This section will discuss the analysis and considerations that have gone into food selection and storage for the mission duration in each of the habitats. As the major focus of this project is volume minimization, it is imperative to know the total amount of storage required for a mission of our proposed duration. Food storage and the required containers for food storage have been calculated here for the thirty day mission duration of four crew members.

A variety of food storage methods have been utilized in space travel. In the notable case of the ISS, specially designed food storage containers are used to package food. NASA's Human Integration Design Handbook identifies MRE's as another method of food transportation in a space habitat. No matter the method, humans require the consumption of 0.62 kg of solid food per day [22]. With this requirement, a crew of 4 living in a habitat for a 30 day mission duration would require, at minimum, 74.4 kg of food stowed. Allowing for a food surplus of 1.5 times that amount arrives at a food mass requirement of 111.6 kg of stowed food. This mass does not account for the containers used in stowage, solely the food and food packaging.[22][85]

The following table §40 recognizes standard MRE packages along with their corresponding volumes and masses. Also included in this table is the volume of an ISS container, which is used in a separate volume approximation.

Food Packaging	Dimensions (cm)	Volume (cm^3)	Mass (g)
Thermostabilized Food	20.62 x 12.06 x 2.3	572	87-236
Irradiated Food	20.62 x 12.06 x 2	497.4	86-197
Rehydratable Food	15.49 x 14.22 x 3.65	804	25-96.6
Natural-Form Food	18.54 x 14.22 x 3.65	601.6	21-69
ISS Food Container	38.1 x 30.48 x 12.32	14307	1701

Table 40: Food Container Volumes[22][85]

These MRE volumes were used to simplify the process of identifying volumes to corresponding mass requirements of food. The use of these volumes allows for the extrapolation of the data to find the approximated volume for the mission duration. In the following graph, the volume and mass of the Thermostabalized food MRE is used to identify the required volume of food to be stowed for a given duration and crew size.

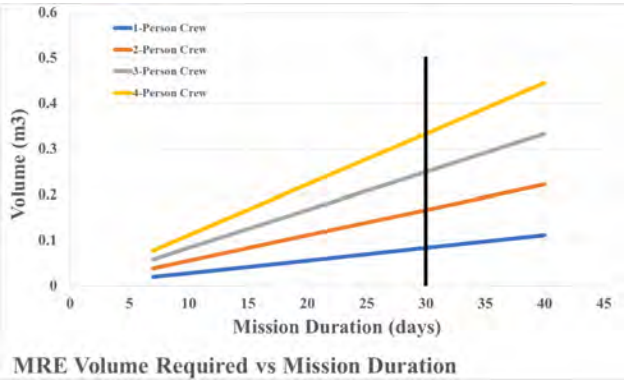

Figure 118: Food Volume Estimation

According to the values calculated using the food estimation graph §118, for our purposes of a 30 day duration for four crew members, approximately 0.334 m^3 of food storage is required.

	Empty Mass (kg)	Full Mass (kg)	Mass of Stored Food (kg)	Volume Per Container (m^3)
ISS Container	1.7	6.49	4.79	0.0143

Table 41: ISS Container Food Storage Values[22]

Another method of confirming food requirements is to compare the average mass of the ISS food storage container mentioned earlier, when it is full versus when empty §41. From this can be found the mass of food typically stored on one of these containers. Using these values, the average mass and volume of the ISS container, and the amount of food necessary per person per day, it is then possible to find the number of ISS food containers. With these values, a new volume and mass estimation can be found. As seen in the following table §42, this estimation places the anticipated volume of food and containers at approximately 0.343 m^3 and the anticipated mass at 155.8 kg in storage.

Number of Crew	30 Day Mass of Dry Food (kg)	30 Day Volume of MRE (m^3)	ISS Containers Required	30 Day Volume Using ISS Containers (m^3)	Mass of Full ISS Containers (kg)
1	27.9	0.083	6	0.086	38.9
2	55.8	0.17	12	0.172	77.9
3	83.7	0.25	18	0.257	116.8
4	111.6	0.334	24	0.343	155.8

Table 42: Volume/Mass Estimates[85]

Following these estimations, it can be seen that using both methods of estimation, the anticipated volume of food storage was relatively similar, 0.334 m^3 compared to 0.343 m^3. Using the estimates, the approximate number of CTBs was found for the required volume. Specifically for the required volume of food in CTB storage, two triple CTBs and a portion of a half CTB are estimated to be required. These volumes are accounted for in the full CAD representations of each habitat. As can be seen in figure §43, where food storage CTBs are marked in red. Food storage is a constant as habitat volume increases, and solely depends on mission duration, the purpose of the mission, and the number of crew on the mission.

6.13.2 Further Food Considerations

During research into food requirements for any habitat, further considerations were found that would impact food systems in our mission. A major consideration that must be made is with regards to the shelf life of stowed food. In cases of near Earth habitats, such as those orbiting the Earth, or placed on the moon, these considerations are less relevant. However, for habitats planned for distances like Mars, the need for shelf life considerations increases. In these cases, standards dictate that shelf life of the transported material be at least 5 years [77].

In this case, none of the food packaging methods are of appropriate shelf life, with the longest shelf life of the MREs being two years. In order to increase shelf life to the desired standard, more intense and volume inefficient packaging measures would be necessary. The use of canned foods has been proposed, however the dramatic increase in both volume and mass that would accompany this decision is counter productive to the goal our project is trying to pursue. It is for these reasons that the food volumes estimates found in this section have the limitation of not being applicable to a Mars habitat, until advancements are made in food science and storage shelf life.

6.14 Storage (Tuvia Rappaport)

All of the storage discussed in the previous sections were allocated to the appropriately sized CTB's. The CTB's were then placed on a rack together to make first pass estimations of acceptable habitat size easier. If this rack as is can fit, then habitat should have no storage issues. We then broke up the rack into smaller racks for the smaller habitat sizes. Some components, like food are not typically stored in CTB's, but by combining all storage into CTB's for this analysis we were able to easily allocate storage space in the six different habitat sizes.

Minimum viable habitat designs will need to make clever storage space placement to ensure it is both accessible, but not interfering. Note the color coding of the table corresponds to the CTB in the rack.

Component	**Volume (m^3)**	**Mass (kg)**
Food	0.34	111.3
Geology Equipment	0.19	60
Atmospheric Science Equipment	0.1	20
Astrobiology equipment	0.15	12
Clothes	0.03	49
Resistance Bands	0.003	1
Totals	**0.85**	**252**

Table 43: Volume and Mass Breakdown for Mission storage requirements

An additional 0.15 m^3 and 148 kg were added to account for the rack and the contexts of an extra whose space was allocated for.

This brings the storage totals to 1 m^3 and 400 kg.

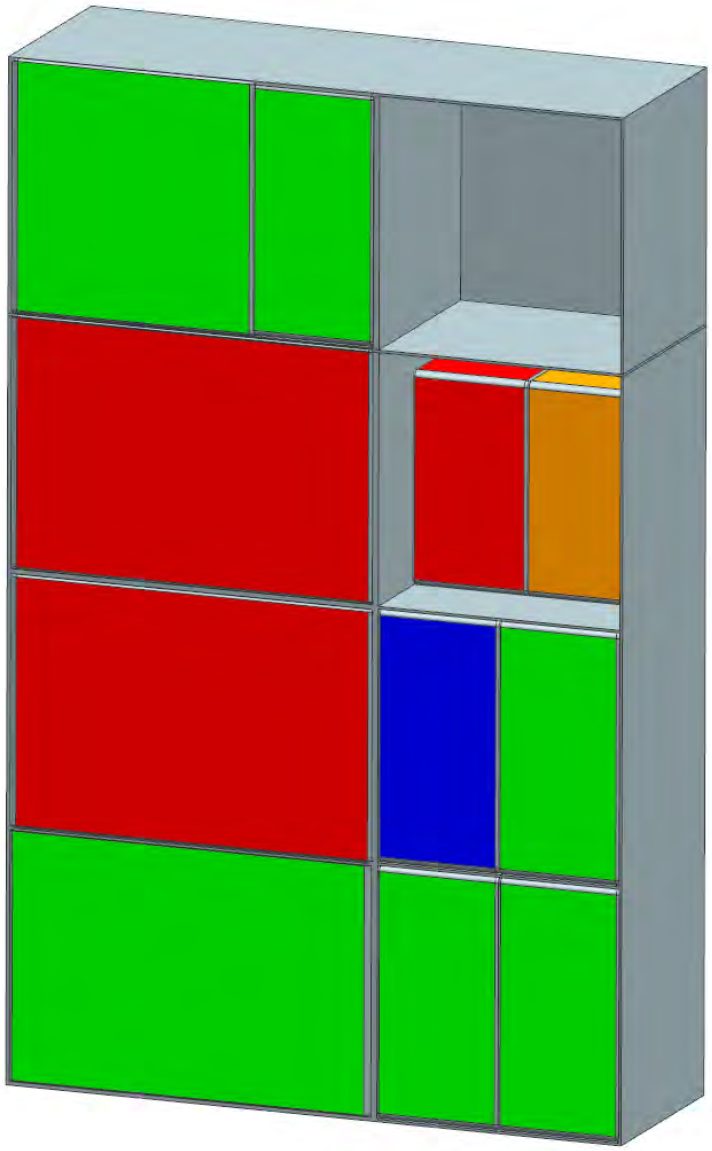

Figure 119: Storage Rack

7 Loads, Structures, and Mechanisms

7.1 Habitat Dimensions and Orientation Trade Studies (Jeffrey Zhu)

7.1.1 General Constraints, Variables, and Metrics

Structures of micro-gravity and surface habitats must be mass efficient to extend launch, entry, and deploy options. Habitat design starts with the pressure vessel, which is the primary structure that internal and external components will all mount to and support.

A main variable of habitat structures is the diameter constraint of payload packaging. Not only does this variable depend on other structures outside a habitat, but also of any inter-stage that might be needed

for reentry or deployment of the habitat. Two gravity dependant variables that can be defined are floor thickness and ceiling height. These variables primarily rely on the gravity level of the habitat environment to be defined. For example, an environment with a small gravity load such as the Moon requires less floor thickness to support the weight of the crew and systems, but more ceiling height for crew movement. Ceiling height is also a derivative of the instruments and activities of the crew. Finally, a variable that defined the area used by a ladder or stair that is subtracted from the total area of floor available with each additional floor should be defined. Choosing a ladder or stair depends on missions goals. A ladder is optimal because it takes up the least amount of area per floor, but some missions require heavy loads to be moved from one floor to another, which can impact the choice between a ladder and stair.

Habitable volumes of pressure vessels account for about 50% of the total pressure vessel volumes based off of historical crewed system data. The other 50% is taken up by habitat structures, systems, un-maintained consumables storage, and wiring. Within a habitable volume, there are several metrics that can be used to analyze the effectiveness and optimal shape of the volume. Derived from ceiling height, the walk-able floor area can be defined as the area of available floor that has at least the minimum ceiling height of free space above it. The walk-able perimeter can then be defined as the length that encompasses the walk-able floor area. This is important in minimum habitat studies as the walk-able perimeter defines the amount of area that can be directly accessed from a walk-able floor area, meaning the crew will have to walk to the perimeter to interact with an object, tool, or system. Thus, the total habitable area does not need to be constrained to just the walk-able area, but can also include areas where the ceiling is lower. These volumes can be used for activities other than walking such as sleeping, sitting, and exercising.

7.1.2 Habitat Shape and Mass

The pressure vessel of the habitat will be constructed using a cylindrical body and ellipsoidal end-caps for ease of manufacturing. The cylindrical body allows the aspect ratio to be varied without affecting the geometry of end-caps, which allows designs to be scaled easily within diameter constrained packaging. Varying the volumes slightly will be beneficial for mass and area optimizations. The aspect ratio of the pressure vessel is defined by the diameter over the total height, including the height of the end-caps.

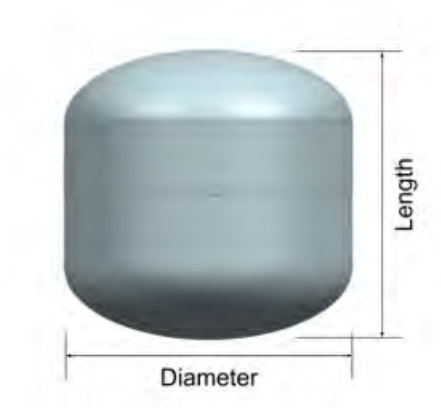

Figure 120: Aspect Ratio Definition

The end-caps of the pressure vessel are ellipsoidal for ease of manufacturing and verification with a constant thickness skin. Semi-circular end-caps have less stress concentration with constant thickness shells under pressure, which are not mass efficient. Finite element analysis of semi-circular end-caps and ellipsoidal end-caps with a 2:1 radius to height ratio show more constant distributed loading and thus more mass efficient end-caps using ellipsoidal designs. The ratios of ellipsoidal end-caps can be adjusted to accommodate for airlock integration or mounting to payload adaptor rings.

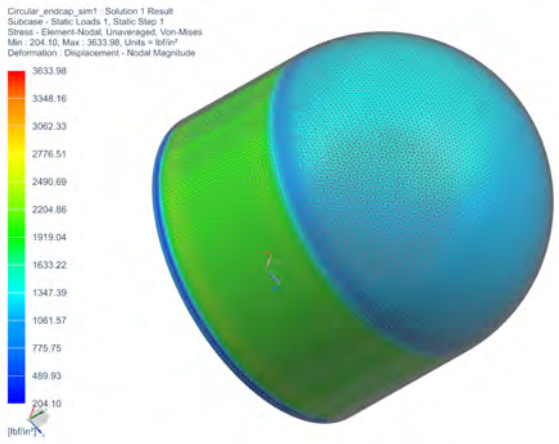

Figure 121: Stress on Circular Endcap

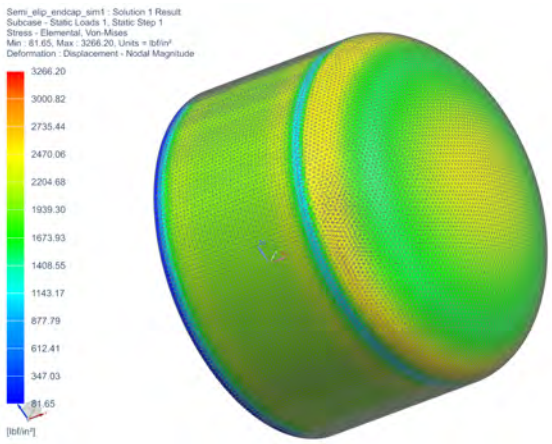

Figure 122: Stress on 2:1 Ellipsoidal Endcap

By keeping the radius to height ratio of ellipsoidal end-caps constant at 2, an optimal aspect ratio for the entire habitat can be calculated to maximize volume and minimize mass. This shape of a habitat with an aspect ratio of 0.8815 is persistent through all volumes. However, payload constraints can limit the diameter of aspect ratios for each of the three examined habit volumes, so a mass trade-off can be calculated from the new geometry at each volume. By examining the mass trade-off at higher aspect ratios for larger habitats, one can determine when it would be beneficial to move to a larger launch vehicle option. In this study, habitat volumes at $20m^3$ and $40m^3$ were selected to launch in the 4m diameter of falcon Heavy, and $80m^3$ volume was moved to the 5.25m diameter faring of New Glenn. The mass differences are shown in the figures below:

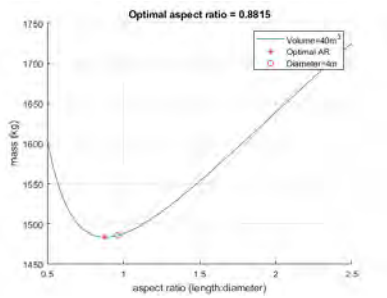

Figure 123: $20m^3$ in Falcon Heavy, 2.1kg difference*

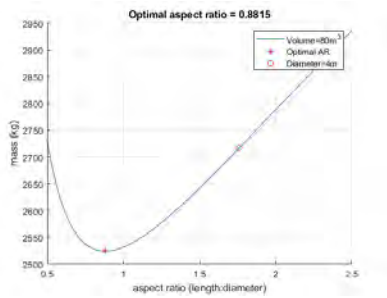

Figure 124: $40m^3$ in Falcon Heavy, 192.5kg difference*

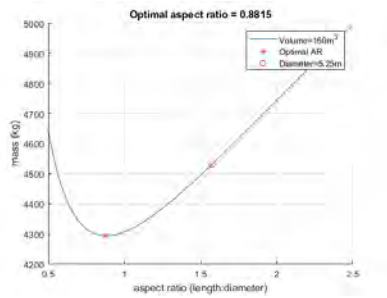

Figure 125: $80m^3$ in New Glenn, 236.9kg difference*

*Mass calculated using JSC-26096: $M(kg) = 13.94(A_{surface}(m^2))^{1.15}$

7.1.3 Habitat Orientation Study

On gravity loaded environments, orientation of the pressure vessel changes many features internal and external of the habitat. An optimal orientation maximizes habitable volume within a habitat by calculating the optimal locations of floors given floor thickness and ceiling height. For this study, floors are set to 0.254m or 10 inches of thickness to support stowage of CTBs. Ceiling height is set at 2.5m as a general metric of lunar and martian gravity levels. By varying floor locations, the maximum walk-able areas and perimeters can be calculated for each volume. For each additional floor, the ladder/stair area is subtracted from the floor area. The walk-able floor areas multiplied by the ceiling heights can represent a general habitable volume, but it is important to note that many systems can take up space within the walk-able area. Also, floor areas not within the walk-able perimeter can also be considered habitable areas. The figure below shows how the walk-able floor area differs from the total available floor area.

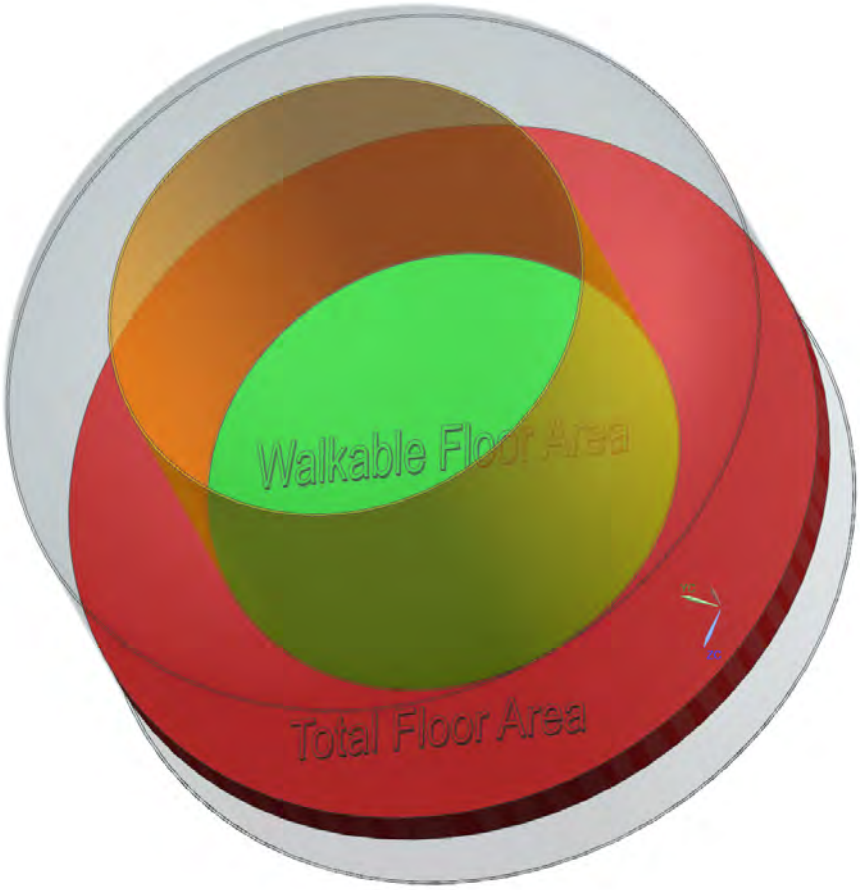

Figure 126: Walk-able Floor Area

When choosing an orientation based off of maximum walk-able floor area, it is important to remember that roughly 50% of the pressure vessel volume will be habitable. If the walk-able floor volume is much greater than 50% of the total pressure vessel volume, adding multiple floors to achieve such a high amount of walk-able area is not mass efficient. Thus, by choosing the walk-able areas that best match the 50% volume constraint is the most mass efficient method to pick an orientation. Volumes ranging from $40m^3$ to $100m^3$ are studied at a 4m diameter constraint. Volumes ranging from $80m^3$ to $160m^3$ are studied at a diameter constraint of 5.25m.

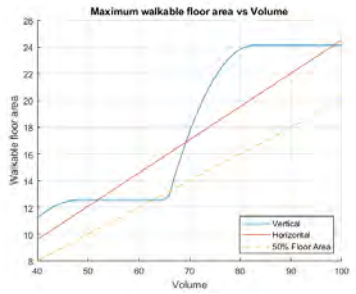

Figure 127: $40m^3$ - $100m^3$ Walk-able Area

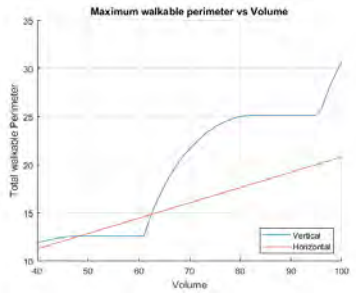

Figure 128: $40m^3$ - $100m^3$ Walk-able Perimeter

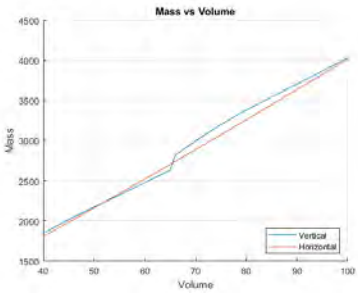

Figure 129: $40m^3$ - $100m^3$ Total Mass

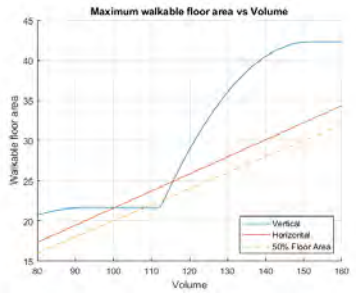

Figure 130: $80m^3$ - $160m^3$ Walk-able Area

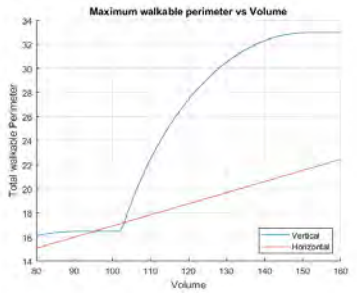

Figure 131: $80m^3$ - $160m^3$ Walk-able Perimeter

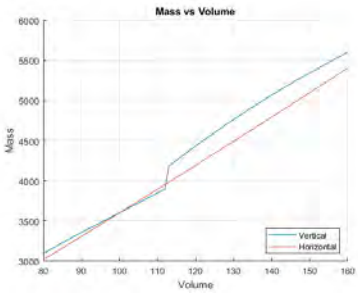

Figure 132: $80m^3$ - $160m^3$ Total Mass

The functions used to generate these plots can be found in the matlab portion of the appendix.

From these plots, optimal orientations can be picked for pressure vessel volumes of $40m^3$, $80m^3$, and $160m^3$. For the 4m diameter constrained volumes, the horizontal orientation's walk-able area best matches the total habitable volume constraint. At the 5.25m diameter volumes, the walk-able areas and perimeters in the vertical orientation becomes much higher than that of the horizontal orientation. At the volume of $160m^3$, vertical perimeters are nearly 50% greater than that of horizontal perimeters. Most of these perimeters are located near the inner pressure vessel shell. Thus, the vertical orientation is chosen for maximum perimeters without much mass penalty, and the 50% habitable volume constraint can be satisfied by mounting systems and equipment to the vertical walls of the habitat.

7.1.4 Reconfigurable Designs

One option in creating a more optimized layout of spaces within pressure vessels is the use of re-configurable spaces. Sliding or folding panels allow habitable spaces to be reconfigured to the user's tasks when only one task can be completed in the selected space.

Re-configurable Space

- Sleeping
- Food prep
- Exercising
- Storage

Permanent Space

- Airlock access
- Life support systems
- Work / sample examination
- Communications
- Waste Management

Sliding panels need more constraints in the form of rails and wire routing. This makes the initial mass to support sliding panels more than folding panels, which only requires a single axis of movement. However, adding more sliding panels along the same axis is more volume efficient, as each panel can support full volume access on the sides. Folding panels need to be thin enough to support full volume access, thus cannot be tiled as sliding racks can. Folding panels may be better suited for vertical oriented habitats as volume dividers. horizontally sliding panels may be better suited for horizontally oriented habitats where more panels can be fit onto a rail system on one side of the habitat outside the walk-able area.

7.2 Fairing Packaging (Zach Peters)

Part of the consideration for habitat size and orientation involved optimizing habitat radius and length to best make use of the usable fairing volume. Since the three habitat volumes being explored are fixed at 20 m^3, 40 m^3, and 80 m^3, a change in diameter or length will result in an inverse change in the other respective variable. After attempting to optimize the diameter and length of each habitat in order to minimize mass, the dimensions were then altered to best package the habitat within the smallest possible fairing. It is ideal to attempt to make as many of the habitats as possible fit within a standard 5 m fairing such as SpaceX's Falcon fairing. To minimize cost and complications of on-orbit assembly, it is also ideal to launch each habitat assembly in one launch. The figures below depict each habitat in its fairing to scale. The models for the fairings were created based on dimensions given in the user guides for each launch vehicle [29][100].

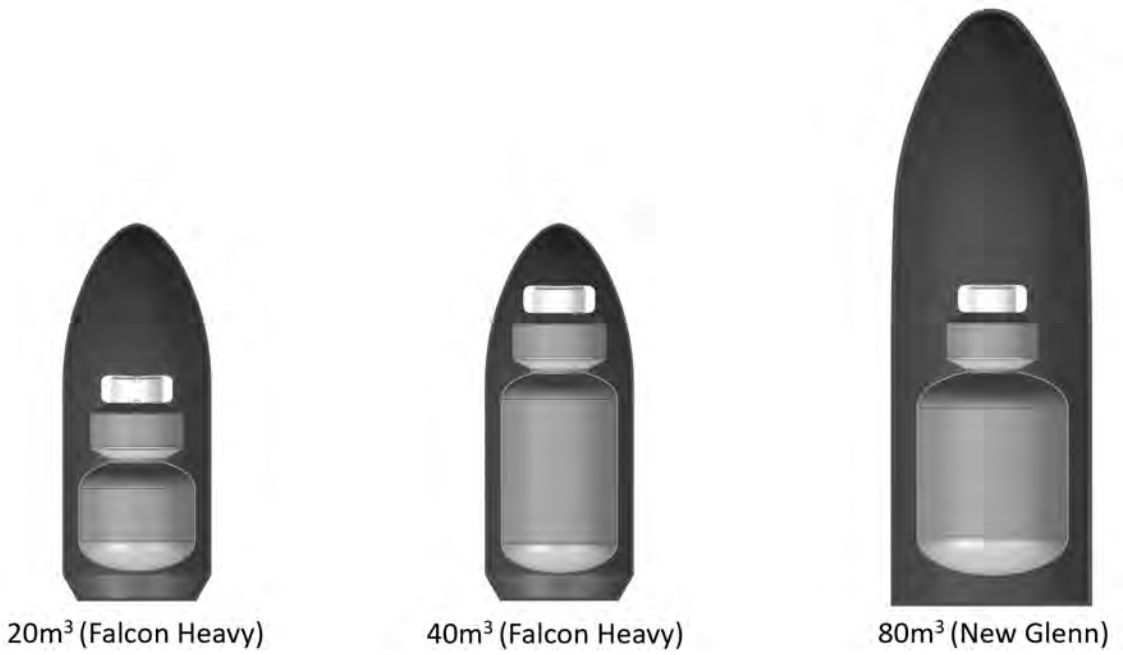

Figure 133: Microgravity Habitats in Fairings

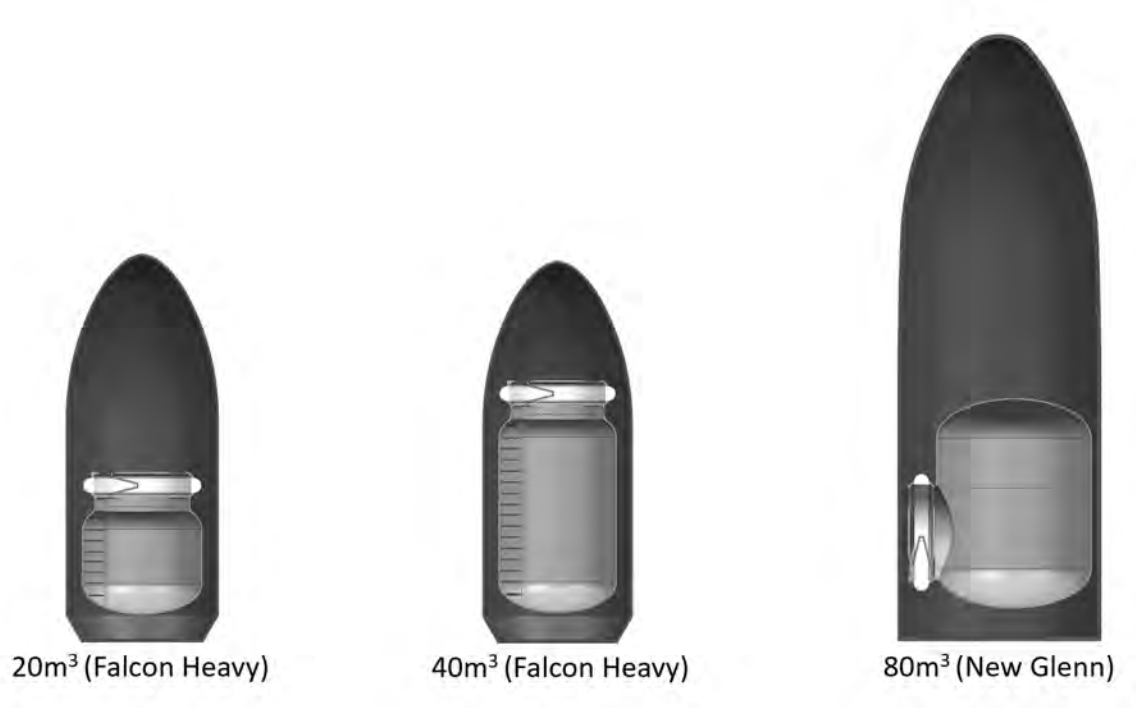

Figure 134: Surface Habitats in Fairings

With a diameter of 4 m, the two smaller habitats (20 m^3 and 40 m^3) are able to effectively fit inside the 5 m fairing for both the micro-gravity and surface configurations.

Fairing packaging also impacted decisions such as orientation for the surface habitats as well as airlock designs for both the micro-gravity and surface habitats. By choosing a horizontal orientation for the 20 m^3 and 40 m^3 surface habitats, the airlock is able to be moved to the endcap of the habitat. This thereby allows for the diameter of 4m to be used as extra space is no longer needed in the fairing to the side of the habitats. Since the diameter is effectively maximized at 4 m, the 20 m^3 and 40 m^3 habitats are shorter in length and able to fit comfortably in the Falcon Heavy fairing. The size constraint of the fairings also created a need to design the airlocks to be inflatable. In the figures above, the airlocks are shown in their unpressurized, collapsed state.

When it came to the 80 m^3 habitats, the diameter was chosen to be 5.25 m. This diameter is too large to fit in the Falcon Heavy and other smaller launch vehicles. Reducing the diameter of the 80m^3 habitat to that similar to the 20 m^3 and 40 m^3 habitats presents a challenge in terms of the length of the habitat. Since the volume is held constant, the 80m^3 habitat becomes too long at smaller diameters to fit in the Falcon Heavy. At this point, the decision was made to launch the 80 m^3 habitat on a 7 m diameter fairing such as New Glenn shown above. An added benefit to launching this habitat in a larger fairing is that it allows for the possibility of both a horizontal and vertical orientation. As seen above, the 80 m^3 surface habitat was chosen to be vertical and the collapsed, unpressurized airlock is able to package within the fairing as a part of the full habitat assembly.

Secondary launch structure would be necessary in order to properly interface between the habitat assembly and the payload attach fitting, as well as distribute loads to the payload from the launch vehicle. This structure would occupy portions of the remaining usable volume within the fairing. An exact design for this structure was not pursued as it was determined to be out of the scope of the X-Hab project description to study various minimum habitat volume requirements and designs.

7.3 Primary Structures Material Selection (Eric Greenbaum)

Aluminum 7075-T6 was chosen as the primary material for the stiffened pressure vessel of each habitat. A trade study was performed to assist in this decision, where various aerospace-grade aluminums were considered. The table below showcases the materials that were considered and their corresponding material properties. [75] [76] [74] [73] [72]

	6061-T6	**7075-T6**	**2219-T6**	**2024-T6**	**8090-T651**
Density (kg/m^3)	2700	2810	2840	2780	2540
Ult. Strength (MPa)	310	572	414	427	515
Yield Strength (MPa)	276	503	290	345	450
Shear Strength (MPa)	207	331	255	283	300
Elastic Modulus (GPa)	68.9	71.7	73.1	72.4	77
Ult. Strength-to-Weight	1.15E+05	2.04E+05	1.46E+05	1.54E+05	2.03E+05

Table 44: Aluminum Trade Study

Aluminum 7075-T6 was chosen as the primary structural material, as it demonstrated the highest strength-to-weight ratio out of all of the metals considered. This decision was made with the intention of designing the most mass efficient pressure vessel as possible. Additionally, although the Elastic Modulus of Aluminum 7075-T6 is not the largest of the materials considered, it is still on the same order of magnitude as the other metals' moduli. This is important as the material will demonstrate similar resistance to buckling as the other metals.

7.4 Launch Loads (Chirayu Gupta)

7.4.1 Trade Study Rationale

In order to create a baseline for structural stiffening analysis in the LSM sub team, a data-driven trade study was conducted to better understand launch environments of a select number of currently operational and close to fabrication LV Systems. In order to narrow the list of Launch Vehicle targets in this study only heavy and super-heavy lift LVs were chosen and researched upon. Following are the 6 LVs that were studied upon.

- Space Exploration Technologies Corporation's Falcon Heavy
- Space Exploration Technologies Corporation's Starship
- National Aeronautics and Space Administration's SLS Block 1B Cargo
- United Launch Alliance's Delta IV Heavy
- Blue Origins' New Glenn
- European Space Agency-ArianeGroup's Ariane 6

7.4.2 Trade Study Findings

Research that was encapsulated within this trade study was primarily found from the official mission planner's guides and user manuals for each respective LV system. Following is a brief list of the launch environment load variables that were found pertinent to the motive of this trade study:

1. Acoustic Environments (dB)

2. Lateral and Axial Accelerations (G)

3. Lateral and Axial Sinusoidal/Random Vibrations (G)

In order to create single-value trade variables, only the maximum values of these following launch loads were noted down as to set allowable stress thresholds for later structural analysis. The following table lists all of the said launch environment maximum caseloads for each LV system. Specific LV maximum launch load values are payload mass-dependent as certain aerospace manufacturers like SpaceX categorize payloads as either " 'standard' mass (over 4,000 lb)"[100] or " 'light mass' (under 4,000 lb)"[100]. For the Ariane 6 LV, the launch load lateral and axial accelerations are also partitioned by mass. These mass groupings (above 3,400 kg and between 2,000-3,400 kg [26]) are denoted as "light" and "standard" in the following table to create continuity within the data gathering convention of this trade study. These payload mass variations directly influence static launch load variables and are thus listed in their respective sections of the trade study table.

As seen in the G-force loadings of this data table, the positive magnitudes of loading denote compressive forces along with the axial or lateral orientation and the negative magnitudes of loading denote tensile forces along said LV orientations.

Max Launch Loads	Starship[101]	Falcon Heavy[100]	Delta IV Heavy[106]	New Glenn[29]	Ariane 6[26]	SLS Block 1B Cargo[86]
Lat Acceleration (g)	**+2 / -2**	**+2 / -2 (S), +3 / -3 (L)**	**+2 / -2 for MP >6577 kg**	**+2 / -2**	**+1.8 / -1.8 (S), +2 / -2 (L)**	**+3 / -3**
Axial Acceleration (g)	**+6 / -2**	**+6 / -2 (S), +8.5 / -4 (L)**	**+6 / -2 for MP >6577 kg**	**+6 / -2**	**+4.6 / -3.1 (S), +4.6/-3.1(L)**	**+4.1 /-1.0**
Acoustic Environment (dB)	**130 @ 100 Hz**	**121.5 @ 125 Hz**	**132.5 (CM), 132.5 (CC)**	**132 @ 125 to 200 Hz**	**136 @ 125 Hz**	**135.4 @ 50 Hz**
Lat Sinusoidal Vibration (g)	**Not Found**	**.5-.6 @ 85 to 100 Hz**	**.7 @ 5 to100 Hz**	**.8 @ 2 to 25 Hz**	**.8 @ 2 to 25 Hz**	**.26 @ 27 to 35 Hz**
Axial Sinusoidal Vibration (g)	**Not Found**	**.9 @ 85 to 100 Hz**	**1.0 @ 6.2 to 100 Hz**	**1.0 @ 2 to 50 Hz**	**1.0 @ 2 to 50 Hz**	**0.31 @ 31 to 60 Hz**

Table 45: Data-Driven LV Flight Environment Trade Study. S: Standard Payload Mass Configuration. L: Light Mass Configuration.

7.4.3 Trade Study Conclusions

After careful analytical speculation and inferences made with connection to LSM Trade Study done on payload-fairing compatibility, the Blue Origins New Glenn and SpaceX Falcon Heavy were chosen as viable candidates for later on external structural analyses and solutions. Trade Study essentially gave a foundation for the later buckling load and random vibration load stress analysis as allowable stress thresholds had been defined and agreed upon. Despite this being a project that focuses on the internal volumes components of the micro and partial gravity habitats, it is important to incorporate LSM solutions that promote the structural integrity of the habitat entities during its entire mission duration.

Figure 135: SpaceX Falcon Heavy Launching from NASA Cape Canaveral [55]

Figure 136: Blue Origins New Glenn Rocket Rendering [3]

Table 46 summarizes valuable launch load flight environment information of these two LV systems which was used extensively in later on external stiffening solutions. Further sections delve into how the conclusion of the Launch Load Trade Study was used to formulate external structural habitat components in order to decrease launch-induced buckling deflection and increase habitat survivability during all phases of its interplanetary mission.

	Falcon Heavy (Light)[100]	Falcon Heavy (Standard)[100]	New Glenn[29]
Max Lat Acceleration (g)	+3 / -3	+2 / -2	+2 / -2
Max Axial Acceleration (g)	+8.5 / -4	+6 / -2	+6 / -2
Max Acoustic Environment (dB)	121.5 @ 125 Hz	121.5 @ 125 Hz	132 @ 125 to 200 Hz
Max Lat Sinusoidal Vibration (g)	.5-.6 @ 85 to 100 Hz	.5-.6 @ 85 to 100 Hz	.8 @ 2 to 25 Hz
Max Axial Sinusoidal Vibration (g)	.9 @ 85 to 100 Hz	.9 @ 85 to 100 Hz	1.0 @ 2 to 50 Hz

Table 46: Maximum Launch Load Environments of LVs selected for Habitat Transportation

7.5 Primary Pressure Vessel Design (Eric Greenbaum)

The main pressure vessel structure of all habitat designs is a metallic, thin-walled pressure vessel that is rigidized by integrated external stiffeners. Although the surface airlock and micro-gravity airlock both incorporate inflatable structures in their designs, the rigid, metal pressure vessel was chosen for the main habitat as it was expected to safely resist the harsh loading conditions of launch better than the inflatable habitat variety. Throughout the lifetime of the habitats (both surface and micro-gravity versions) the most severe loading conditions experienced will be the acceleration and vibrations imposed on the structure due to launch.

In the aerospace industry, orthogrid and isogrid pocketing are two methods of stiffening features commonly found on launch vehicle staging and crew capsules. These stiffening methods were both investigated as possible stiffeners for the habitat pressure vessels. A trade study was performed to understand how each of these stiffening methods would perform for our specific application. This was accomplished by optimizing the geometry of orthogrid and isogrid stiffeners to reduce mass while still maintaining positive margins for all loading conditions and possible failure modes. The following sections of the report will detail the methods used in the stiffener trade study, and will outline the decision process for selecting the optimal stiffener method for use on the designed habitats.

7.6 Orthogrid External Stiffening Structure (Chirayu Gupta)

7.6.1 Orthogrid Background

Orthogrid, also known as Waffle-Grid due to its similarity in planar geometry to that of a Belgian Waffle, is a metal-based, external stiffening structure that has been commonly implemented on past aeronautic and astronautic projects. An orthogrid is essentially a layout of a set number of orthogonal horizontal ribs and vertical stringers that are machined into the hull structure that they are structurally supporting. The rib and stringer cross sectional geometries of the orthogrid is assumed to be that of a conventional I beam to simplify this system's structural analysis equations.The main purpose of the orthogrid is to increase the allowable stresses that the greater structure can bear during its intended mission. In the case of orthogonal stiffening systems being present on past LVs like the multi-stage Saturn V rocket and current spacecraft's like NASA's Orion, orthogrids are used to bolster said launch systems as they experience heavy buckling loads which are induced from axial launch accelerations.

Figure 137: Orthogrid Stiffening Structure On NASA Orion Spacecraft [79]

7.6.2 Orthogrid-Habitat Integration Rationale

For the Minimum Crew Cabin Studies project, the orthogrid system that will be present on the exterior surface of all 6 habitat configuration shells so that habitat internals and externals are not damaged due to structural buckling failure during or before Max Q LV launch regime. The orthogrid is in other words an astronautical solution to prevent loss of valuable mission assets as it's making its way to its intended destination.

7.6.3 Orthogrid Governing Mass/Stress Equations and Calculations

The goal of the calculations and analyses of the orthogrid system was to design and dimensionalize a set number of grids that could sustain a buckling stress load that was greater that the axial buckling load generated during launch and prior to the LV entering space. Following are the governing equations that were used to find buckling stresses, rib/stringer moment of inertias, and total orthogrid system mass value. [19].

$$\sigma_{\text{buckling}} = BKDF\left(\frac{c\pi^2 E}{L^*/\rho_{\text{gyration}}}\right) \geq \sigma_y \tag{3}$$

$$m = \rho_{Al}\left(n_{rib}A_{rib}W + bhL\right) \tag{4}$$

$$I = \frac{1}{12}bh^3 \tag{5}$$

$$\rho_{\text{gyration}} = \sqrt{\frac{I}{A}} \tag{6}$$

7.6.4 Equation and Constant Variable Clarifications

1. Buckling Knockdown Factor (BKDF) within Equation 3 was set to .65 as NASA claims this to be the accepted value for any axial compression exerted on a thin-walled orthotropic cylinder [10]. This BKDF value assumption aligns wells with the geometrical assumption of the cylindrical section of the greater habitat pressure vessel of this project.

2. Radius of Gyration (ρ_{gyration}) value found in the Equation 6 is based on the cross sectional area of the ribs and stringers beams which in turn is based on singular grid beam height (h) and base length (b) found in Equation 5.

3. Aluminum Alloy 7075-T6 [28] was used in this orthogrid structural analysis as it had the most beneficial material properties that promoted the marginal goals of the stiffening system. Selected aerospace-grade aluminum alloy's high ultimate strength, yield strengths, and relatively high Modulus of Elasticity made a reasonable alloy for the structural requirements of the orthogrid design and analysis process. More information on material selection can be found in Section 7.3.

4. Value of .5 (Fixed-Fixed) was chosen for the buckling boundary condition (c) within Equation 3 as ends of both the ribs and stringers are fixed flush to each other and the habitat pressure vessel.

5. Maximum Allowable Axial Acceleration for the New Glenn Rocket was set to 6 Gs (58.86 m/s^2) and for the Falcon Heavy Rocket was set to 8.5 Gs (83.39 m/s^2). G-force limit values were directly extrapolated from the data findings of the launch loads trade study.By using Newton's Second Law of Linear Motion, following maximum acceleration values were coupled with overall habitat mass values for each configuration to find allowable buckling loads felt doing spacecraft launch.

6. Width (W) of Equation 4 of total orthogrid system is being treated as the circumference of the cylindrical section of the habitat pressure vessel. Therefore W is dependent on the outer radius (R) of the habitat pressure vessel

7.6.5 Stress and Mass Calculation Results

Table 47 encapsulates all final results of the buckling load calculations for each habitable volume size configuration (20-40-80 m^3). Said table also indicates the buckling load margins of safety for each orthogrid design.

Habitat Configuration Size (m^3)	ρ_{grya} (m)	I_{rib} (m^4)	A_{rib} (m^2)	σ_{ortho} (Pa)	$F_{buckling}$ (N)	Buckling MOS
20	5.77E-03	1.33E-08	4.00E-04	1.51E+10	6.03E+06	3.28
40	5.77E-03	1.33E-08	4.00E-04	5.54E+09	2.22E+06	0.37
80	5.77E-03	1.33E-08	4.00E-04	9.16E+09	3.66E+06	1.82

Table 47: Multi-Volume Habitat Orthogrid Design Buckling Critical Loads and Stresses

Table 48 lists the allowable launch load buckling force quantities for each habitat mass-dependent configuration and respective LV.

F_AxialLaunchLoad (N) - Falcon Heavy - 20 m^3	9.59E+05
F_AxialLaunchLoad (N) - Falcon Heavy - 40 m^3	1.06E+06
F_AxialLaunchLoad (N) - New Glenn - 80 m^3	8.57E+05

Table 48: Multi-Volume and Respective LV Axial Launch Load

Table 49 includes habitat and orthogrid dimensions such as cylinder length (L), Width (W), Constant Rib Spacing (L*), number of ribs/stringers (n_{rib} and $n_{stringers}$), and shell diameter (d). All rib and stringers were prescribed a height and and base length of 20 mm to decrease moment of inertia, decrease radius of gyration, and therefore increase orthogrid buckling stress for a positive loading margin of safety.

Habitat/Orthogrid Dimensions	20 m^3	40 m^3	80 m^3
n_rib	20	20	30
n_stringers	143	143	130
L (m)	1.8498	5.0329	4.494
L* (m)	0.088	0.240	0.145
W (m)	12.57	12.57	16.49
d (m)	4	4	5.25

Table 49: Multi-Volume Habitat and Orthogrid Dimensions

Table 50 indicates mass breakdowns of each habitat configuration which used to find previously mentioned launch-induced buckling loads. Table 50 is a more conservative summarization of the more detailed mass breakdowns found in Tables 99, 100, and 101 of Sections 9.5 to 9.7. It has been seen by iterative analysis that adding more mass decreases the positive-valued Margins of Safeties of Table 47.

Mass Breakdowns	20 m^3	40 m^3	80 m^3
M_shell (kg) - Includes Internals and Airlock	11485.6	12716.4	14530.9
M_grid (kg)	579.81	1091.44	1212.82
M_total (kg)	12065.41	13807.84	15743.72

Table 50: Multi-Volume Orthogrid Integrated Total Mass Breakdown

7.6.6 CAD Models of Orthogrid Integration to Multi-Volume Habitat Shells

Following assortment of figures show CAD renderings of what designed orthogrid stiffening structures could look like once fabricated onto the pressure vessel shells of the planetary surface habitats.

Figure 138: 20 m^3 Orthogrid-Integrated Surface Habitat Pressure Vessel Isometric View

Figure 139: 40 m^3 Orthogrid-Integrated Surface Habitat Pressure Vessel Isometric View

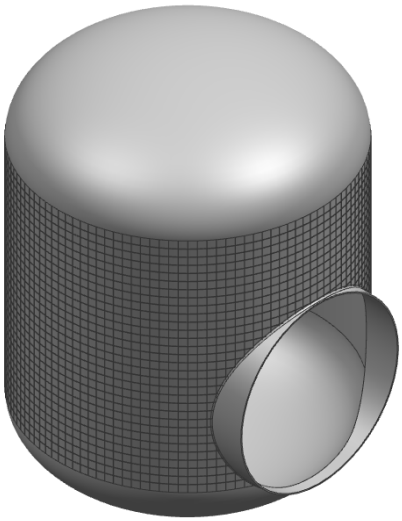

Figure 140: 80 m^3 Orthogrid-Integrated Surface Habitat Pressure Vessel Isometric View

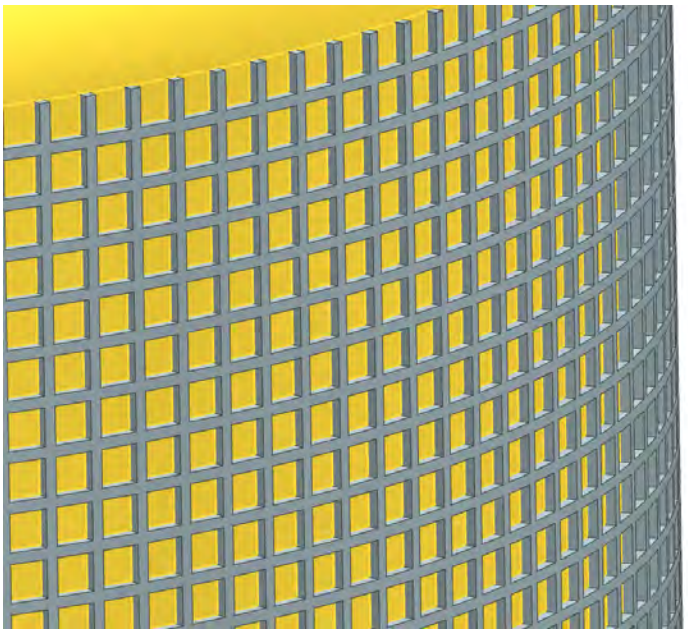

Figure 141: Rib And Stringer Connection to Pressure Vessel Close-Up View

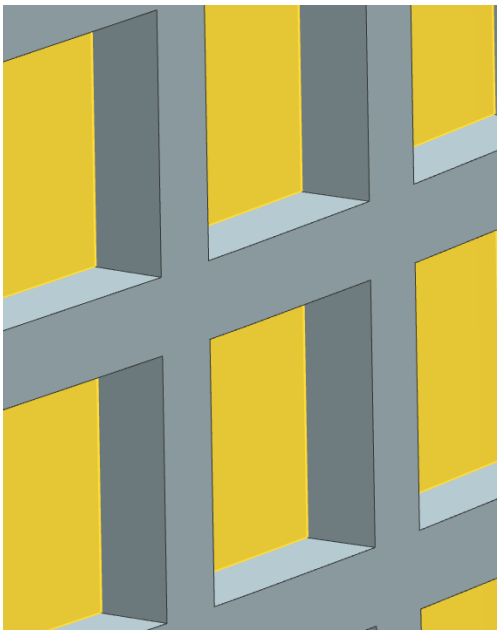

Figure 142: Rib And Stringer Orthogonal Connection Close-Up View

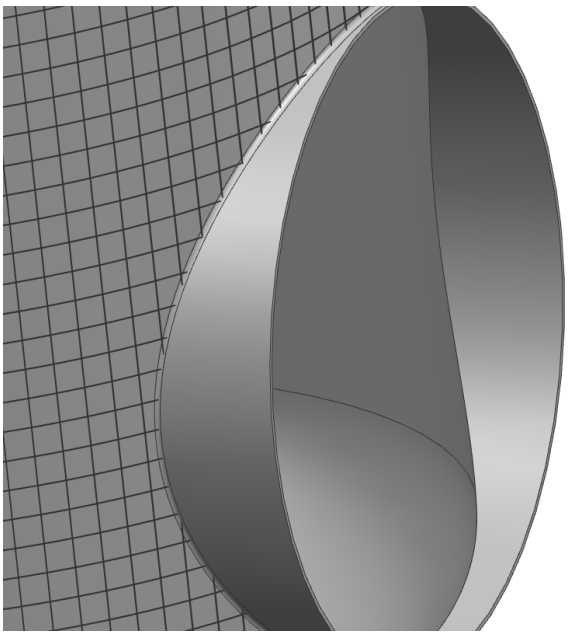

Figure 143: 80 m^3 Orthogrid Surface Airlock Region Cutout

7.6.7 Buckling Load Margin of Safety (MoS) Discussion

As seen in the right-most column of Table 47, all Buckling Loading Margins of Safety (MoS_{buck}) are positive indicating that orthogrid design can sustain more buckling force that is generated when the Falcon Heavy and New Glenn launch vehicle systems are being launched into their respective mission-directed parking/transfer orbits. Furthermore, the relatively low magnitudes of these Margin of Safeties shows that orthogrid design is reliable and would be feasible to be assembled onto the greater Habitat pressure vessel. The next section delves into an alternative approach of externally stiffening habitat pressure vessels by employing an isogrid design.

7.7 Isogrid External Stiffening Structure (Eric Greenbaum)

7.7.1 Isogrid Background

Originally developed in the early 1970s, isogrid is now widely used throughout the aerospace industry in a variety of aircraft, launch vehicles, crewed vehicles, and pressure vessels. The development of isogrid was primarily motivated by the need for lightweight and efficient integrated stiffening features for compression-carrying structures on aerospace vehicles [93]. As one of the primary load cases for the habitats is compressive force due to launch acceleration, isogrid is an ideal stiffening method to examine.

The lattice of equilateral triangles that make up isogrid structures present numerous structural benefits over the 0-degree, 90-degree, and 45-degree patterns that also fit in the machined stiffening features category. Due to the geometry of the ribs, the bulk properties of an isogrid plate replicate that of a solid, continuous plate of an isotropic material. Due to this predictability, isogrid does not exhibit any directions or orientations which are "weaker" than others, as the stiffness is equivalent in all directions [93]. Additionally, the equilateral triangle geometry is also more resistant to torsional loading than rectangular stiffeners, a disadvantage of orthogrid or orthogonal rib/stringer stiffening methods.

To assist with the design and analysis of isogrid pressure vessels for the pressure vessel stiffener trade study, the Isogrid Design Handbook (NASA CR-124075) [93] was consulted. This handbook details the geometric parameters that define isogrid stiffeners and the analysis methods that can be used for specific structural design applications. Four independent geometric parameters fully define the geometry of the iso-

grid pressure vessels: the thickness of the pressure vessel skin/membrane (t), the height of each equilateral triangle (h), the depth of the triangular pockets (d), and the width of each rib/stiffener (b). These four values are also used to define non-dimensional ratios which govern the rigidity and structural performance of the isogrid. These values can be seen in Figure 144 and Figure 145 which display close-up views of isogrid stiffener geometry, and the ratios are defined in Equations 7, 8, and 9.

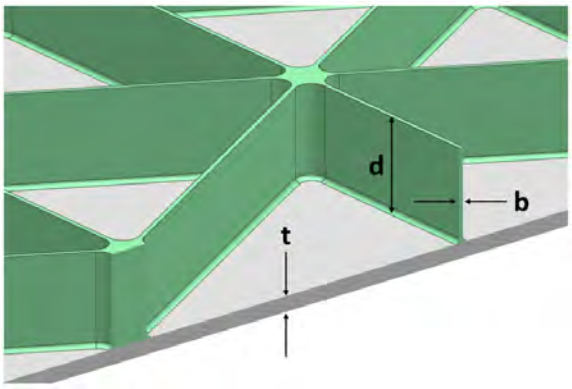

Figure 144: Geometric Parameters of Isogrid Stiffeners

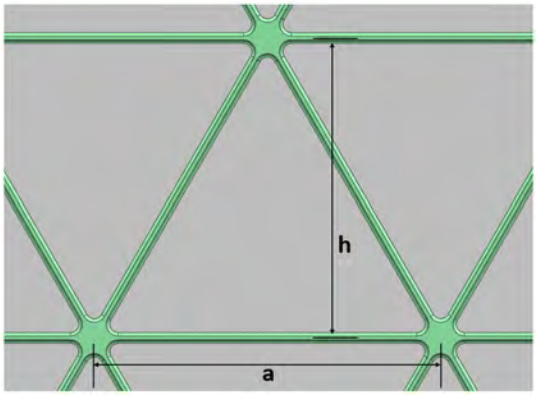

Figure 145: Equilateral Triangle Geometry of Isogrid

$$\delta = \frac{d}{t} \tag{7}$$

$$\alpha = \frac{bd}{th} \tag{8}$$

$$\beta = [3\alpha(1+\delta)^2 + (1+\alpha)(1+\alpha\delta^2)]^{\frac{1}{2}} \tag{9}$$

These design parameters determine the resistance of the isogrid to numerous loading conditions. They also can be used to define an equivalent stiffness and equivalent thickness for a solid, monocoque structure which is structurally equivalent to the given isogrid design. These equivalent parameters are defined in Equations 10 and 11. This follows from the isotropic nature of isogrid.

$$t^* = t\frac{\beta}{1+\alpha} \tag{10}$$

$$E^* = E_0\frac{(1+\alpha)^2}{\beta} \tag{11}$$

7.7.2 Mass Savings

Over the course of design efforts, the geometric design of the isogrid stiffeners was modified to account for additional loading conditions, minimize the mass of the pressure vessel, and increase the efficiency of the overall structure. The evolution of the isogrid stiffener geometry can be seen in Table 51. Subsequent sections will present the structural analysis that was used to validate the integrity of the pressure vessel throughout the design effort, as well as how the overall mass of the isogrid structure has changed as the stiffener geometry has changed.

Isogrid Geometry	**Original Design**	**Final Design**
t (mm)	10	10
h (mm)	500	250
d (mm)	20	60
b (mm)	10	3

Table 51: Isogrid Design Evolution

Using the equivalent thickness value outlined previously, the estimated mass savings accomplished by using isogrid stiffeners can be calculated. The mass of each habitat pressure vessel when constructed from isogrid was estimated by finding the mass of 1 m^2 of the designed isogrid geometry and integrating it around the full surface area of the pressure vessel. This value was then compared to the estimated mass of a pressure vessel of the same surface area with a monocoque skin that matched the equivalent thickness corresponding to the isogrid stiffener design. The estimated mass savings of isogrid stiffeners for each habitat size can be seen in Table 52.

Habitat Volume	**Monocoque Mass (kg)**	**Isogrid Structural Mass (kg)**	**Mass Savings**
20 m^3	5773	2333	59.6%
40 m^3	9756	3942	59.6%
80 m^3	13383	5389	59.6%

Table 52: Mass Savings Due To Isogrid Stiffeners

7.7.3 Buckling Analysis

During launch, habitats will be secured in a launch vehicle fairing, with their long axis parallel to the long axis of the launch vehicle. Attached at the base to the launch vehicle by a Payload Adapter and free at the opposite end, the habitats can be considered cantilevered. When also taking into account the airlock attached to the habitat at the top of the fairing, we can model the full assembly as a cantilevered beam cylinder with a tip mass. Due to large axial launch accelerations, the habitat must endure large compressive loads. The compressive force felt by the habitat is a function of the mass of the habitat and the axial acceleration that it experiences.

With any compressive force, a major failure mode that must be considered is buckling. Referring to the Isogrid Design Handbook [93] again, analysis methods for an isogrid cylinder in compression demonstrate three possible buckling failures that can occur: buckling due to general instability, buckling of the pressure vessel skin/membrane, and crippling of the ribs that make up the equilateral triangles. Using the stiffener geometry and corresponding non-dimensional ratios, the critical forces at which each of these buckling failure modes can be calculated. Equations 12 through 14 give the formulae which derive the critical compressive forces that would result in each corresponding failure mode. If the compressive load that the habitat experiences exceeds any of the critical forces, the rigidized pressure vessel would fail due to buckling of some form. After deriving the critical buckling loads for the isogrid geometry it was compared to the compressive force that each habitat would experience during launch, and the margins of safety for each design were calculated. Tables 53 through 55 demonstrate how the efficiency of the design has improved over the course of the design

cycle.

$$F_{cr_{GI}} = \frac{(0.65)(2\pi)}{3(1-\nu^2)} Et^2\beta \tag{12}$$

$$F_{cr_{SB}} = (10.2)(2\pi R)Et(1+\alpha)\frac{t^2}{h^2} \tag{13}$$

$$F_{cr_{RC}} = (0.616)(2\pi R)Et(1+\alpha)\frac{b^2}{d^2} \tag{14}$$

Failure Mode	**FOS**	**Original Design MOS**	**Final Design MOS**
General Instability	1.4	10.80	27.91
Skin Buckling	1.4	26.25	108.49
Rib Crippling	1.4	1027.42	9.33

Table 53: Buckling Margins of Safety for 20 m^3 Habitat

Failure Mode	**FOS**	**Original Design MOS**	**Final Design MOS**
General Instability	1.4	9.58	24.57
Skin Buckling	1.4	23.22	95.85
Rib Crippling	1.4	920.56	8.14

Table 54: Buckling Margins of Safety for 40 m^3 Habitat

Failure Mode	**FOS**	**Original Design MOS**	**Final Design MOS**
General Instability	1.4	8.67	22.16
Skin Buckling	1.4	28.31	114.16
Rib Crippling	1.4	1105.19	9.87

Table 55: Buckling Margins of Safety for 80 m^3 Habitat

The margins of safety for three possible buckling failures are given in the above tables. As observed, the rib crippling margins of safety all decreased greatly from the original to the final isogrid geometry. This corresponds to the depth of the pocket being increased and the width of the rib being decreased, following the the formula in Equation 14. Now, the ribs are more efficient by an order of magnitude. However, both the general instability failure and the skin buckling failure margins of safety increased from the initial isogrid design to the final isogrid design. By examining Equation 13, it can be observed that the skin buckling margin increased steeply because the height of the equilateral triangles was cut in half from the initial to the final design. The critical buckling force for skin buckling is proportional to the inverse square of the triangle height, so a decrease in the value of h increases the critical buckling force greatly. Although this change did reduced the efficiency of the isogrid, this decision to decrease the height of the triangles was executed after recommendations from faculty on the original design. Additionally, the general instability margin of safety increased due to this change in design geometry. Future analysis will demonstrate margins of safety which are more optimal, so the overall margin of the final isogrid design is much lower than is demonstrated in these tables.

7.7.4 Internal Pressure Analysis

Traditional thin-walled pressure vessel analysis was also conducted for the isogrid pressure vessel. The failure theory considered in this case was Von-Mises Yield criteria. The Von-Mises Stress Resultant was calculated for the plane stress state due to the internal pressure of the pressure vessel, and this was compared to the yield stress of Aluminum 7075-T6. Equations 15 and 16 display the hoop stress and axial stress of a thin walled pressure vessel, and Equation 17 gives the Von-Mises Stress Resultant that was calculated using the hoop and axial stress. Because the hoop stress and axial stress are principal stresses, there is no shear stress due to the internal pressure, and the Von-Mises Stress Resultant is based solely on the principal stresses. For conservative analysis the internal pressure used was 1 atm = 14.7 psi = 101.4 kPa and the external pressure was 0 atm = 0 psi = 0 kPa. Results of the analysis can be seen below in Table 56.

$$\sigma_h = \frac{pR}{t} \tag{15}$$

$$\sigma_a = \frac{pR}{2t} \tag{16}$$

$$\sigma_{VM} = \sqrt{\sigma_h^2 - \sigma_h \sigma_a + \sigma_a^2} \tag{17}$$

Habitat Volume	FOS	Original Design MOS	Final Design MOS
20 m^3	1.65	16.37	16.37
40 m^3	1.65	16.37	16.37
80 m^3	1.65	12.23	12.23

Table 56: Margins of Safety for Internal Pressure Loading

The margins of safety for pressure loading are quite large. This is because the stress of a thin-walled pressure vessel is only related to the thickness of the skin, not to the other design parameters of the isogrid. The skin thickness for each pressure vessel is 10 mm, which is a much greater thickness than is required for an internal pressure of 101.4 kPa. These margins show that the skin thickness is overdesigned when only considering the stress induced due to pressure. However, for additional loading conditions considered in future sections of this report, the thickness of the skin at 10 mm was crucial for maintaining positive margins. Additionally, this geometric parameter of the isogrid did not change between the original and final designs, which is why the margins of safety were identical for the original isogrid design and the final isogrid design.

7.7.5 Combined Loading Analysis

The previous two load sources were analyzed for both the original and final isogrid stiffener designs. However, for complete certainty of the structural integrity of the final isogrid pressure vessel structure, numerous additional loading conditions were also considered in a combined loading case. Once again, a cantilevered cylinder with a tip mass model was used to drive the structural analysis for the combined loading case. Figure 146 shows the diagram of this model which was used for the following analysis. All stresses that resulted from the separate loads were combined using superposition to ensure a conservative, worst-case analysis. The stresses that were considered include compressive stress due to axial acceleration during launch, bending stress due to lateral accelerations during launch, Von-Mises stress due to internal pressure, bending stress

due to random vibrations during launch, thermal stress due to temperature difference. This process was originally described in Lecture 17 (Structural Design and Analysis) [20] from ENAE 483.

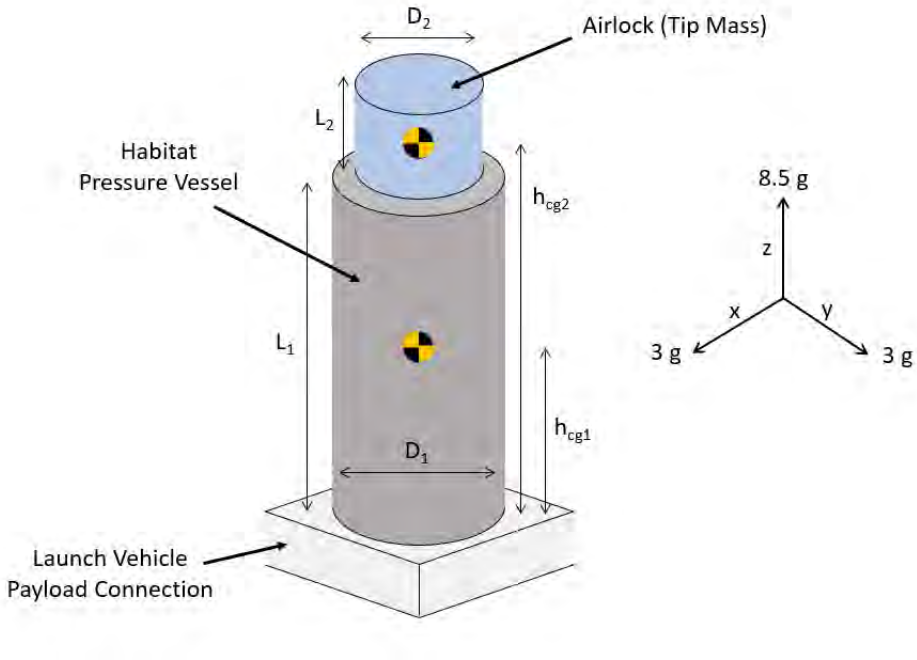

Figure 146: Physical Model for Combined Loading Analysis of Habitat and Airlock

To analyze the total stress developed due to launch accelerations, both axial and transverse accelerations were considered simultaneously. For axial compressive stress, the downward force from the tip mass accelerating was calculated and was averaged over the total cross sectional area of the pressure vessel skin. For the bending stress component, the moment was calculated using the combined transverse acceleration, the masses of the pressure vessel and the airlock, and the distances from the root of the cantilevered structure to the center of gravity of the pressure vessel and the airlock. For the maximum stress experienced during launch, the axial and bending stress components at the root of the pressure vessel were combined. Equations 18 through 22 outline the process which was just described.

$$\sigma_z = \frac{m_{airlock} * g_z}{A} \tag{18}$$

$$g_{transverse} = \sqrt{g_x^2 + g_y^2} \tag{19}$$

$$M = g_{transverse}(9.81)(m_{habitat}h_{cg_1} + m_{airlock}h_{cg_2}) \tag{20}$$

$$\sigma_{bending} = \frac{MR}{I} \tag{21}$$

$$\sigma_{LA} = \sigma_{bending} + \sigma_z = \frac{MR}{I} + \frac{m_{airlock} * g_z}{A} \tag{22}$$

To calculate the Von-Mises Stress which resulted from the internal pressure inside the pressure vessel, the same process that was described in Section 7.7.4 of this report was used. The hoop stress and axial stress for a thin-walled pressure vessel were calculated, and the Von-Mises Stress formula for a principal, plane stress state was recorded. Please refer to Section 7.7.4 for further clarification.

Next, the stress resulting from random vibration was incorporated into the combined loading case. Following the process outlined in Lecture 17 (Structural Design and Analysis) from ENAE483 [20], Miles' equation was utilized to accomplish this. Miles' equation, given in Equation 23, provides a quasi-static approximation of a lateral acceleration resulting from random vibration loading during launch. To use this process, the resonance frequency for the full structure, the damping ratio for the structure, and the Power Spectral Density (PSD) at the structure's resonance frequency were needed. First the resonance frequency for each habitat was calculated, using Equation 24. Next, using Table 57, the damping ratio for each habitat was approximated based on the resonance frequency of each structure. After these values were known for each habitat size, the PSD which corresponded to each resonance frequency was pulled from the Falcon Heavy Users Guide [100].

$$G_{RMS} = 3 * \sqrt{\frac{\pi f_n PSD}{4\zeta}} \tag{23}$$

$$f_n = \frac{1.732}{2\pi} \sqrt{\frac{EIg}{m_{airlock} g L_1^3 + 0.236 m_{hab} g L_1^3}} \tag{24}$$

f_n	ζ
$<$ 150 Hz	0.045
150 - 300 Hz	0.02
$>$ 300 Hz	0.005

Table 57: Structural Damping Ratio at Corresponding Natural Frequencies

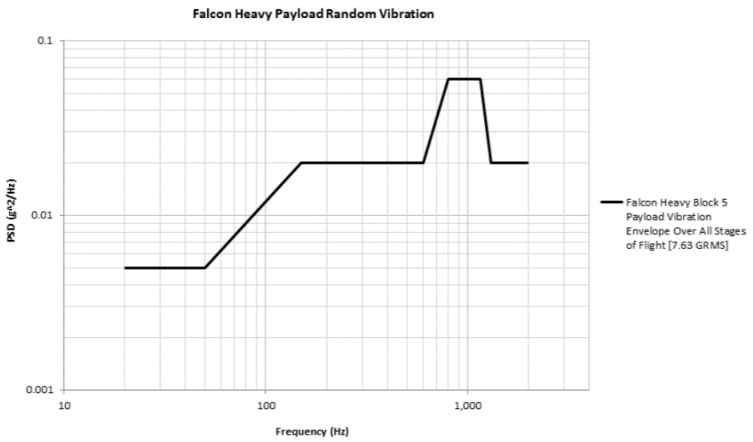

Figure 147: Predicted Random Vibration Envelope Within Falcon Heavy Fairing During Launch

By substituting these values into Equation 23, the corresponding "3-Sigma" lateral acceleration due to random vibration was known for each habitat. This "3-Sigma" G-RMS value is a conservative approximation for the quasi-static lateral acceleration due to random vibration loading, according to Robert Simmons from the NASA Goddard Spaceflight Center [97]. This lateral acceleration was used to calculate the bending moment at the root of each structure using Equation 20 again, but the transverse acceleration from launch was replaced with the approximate lateral acceleration due to random vibration. This bending moment then defined the maximum bending stress at the root of each habitat.

The final load case that was included in the combined loading analysis was stress that developed due to changes in the thermal environment. For conservative analysis, the change in temperature that the habitat experiences was considered to be -100 degrees Celsius, and it was assumed that any support structure that was connected to the habitat changed in length by half of the change in length that the habitat underwent. With these assumptions, Equations 25 and 26 were used to calculate the thermal stress endured by each habitat.

$$\epsilon_{thermal} = \alpha \Delta T \tag{25}$$

$$\sigma_{thermal} = E\epsilon_{thermal} * (0.5) \tag{26}$$

Using the principal of superposition, each of the limit stress values previously calculated for each habitat were summed, taking into account the specific factor of safety for each load case, to find the total design stress experienced by each habitat. These summations are demonstrated in Tables 58 through 60. Next, the combined design stress values were compared to the Ultimate Stress of Aluminum 7075-T6. The margins of safety for each habitat size under the outlined combined loading conditions are presented in Table 61.

Load Source	Limit Stress (Pa)	FOS	Design Stress (Pa)
Launch Acceleration	1.33E+07	1.4	1.86E+07
Internal Pressure	1.76E+07	1.65	2.90E+07
Random Vibration	1.90E+08	1.4	2.66E+08
Thermal	8.46E+07	1.4	1.18E+08
TOTAL			**4.32E+08**

Table 58: Combined Loading Design Stress for 20 m^3 Habitat

Load Source	Limit Stress (Pa)	FOS	Design Stress (Pa)
Launch Acceleration	2.32E+07	1.4	3.25E+07
Internal Pressure	1.76E+07	1.65	2.90E+07
Random Vibration	2.24E+08	1.4	3.14E+08
Thermal	8.46E+07	1.4	1.18E+08
TOTAL			**4.94E+08**

Table 59: Combined Loading Design Stress for 40 m^3 Habitat

Load Source	Limit Stress (Pa)	FOS	Design Stress (Pa)
Launch Acceleration	1.46E+07	1.4	2.04E+07
Internal Pressure	2.30E+07	1.65	3.80E+07
Random Vibration	1.70E+08	1.4	2.38E+08
Thermal	8.46E+07	1.4	1.18E+08
TOTAL			**4.15E+08**

Table 60: Combined Loading Design Stress for 80 m^3 Habitat

Habitat Size	Design Stress (Pa)	Ultimate Stress (Pa)	MOS
20 m^3	4.32E+08	5.72E+08	0.32
40 m^3	4.94E+08	5.72E+08	0.16
80 m^3	4.15E+08	5.72E+08	0.38

Table 61: Margins of Safety for Combined Loading Analysis

As demonstrated in Table 61, the isogrid pressure vessel is designed efficiently for the worst-case, conservative analysis method which considers a combined loading case. The margins of safety for this analysis method are positive and close to zero, indicating that the structure exceeds the requirements for redundancy without much additional material (additional mass). Although the other analysis methods demonstrated some large margins of safety, the overall margin of safety for each habitat is quite optimal, as shown in Table 61.

7.8 Airlock Design and Analysis (Zach Peters)

7.8.1 Microgravity and Surface Airlock Design Overview

The following sections will detail the designs for the microgravity and surface airlocks. There are two unique designs for these airlocks. One design is for each microgravity habitat, while the other is used on all of the surface habitats. Each airlock is shown with its respective habitat in the figure below along with renders of each airlock assembly.

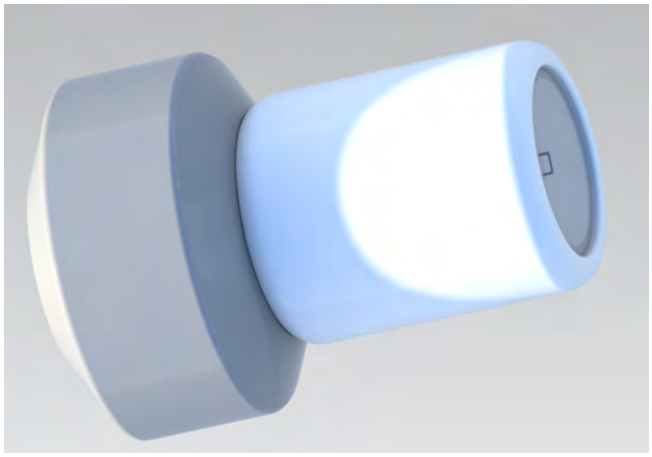

Figure 148: Microgravity Airlock

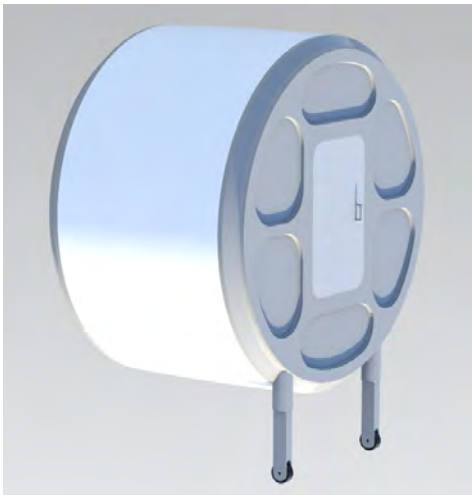

Figure 149: Surface Airlock

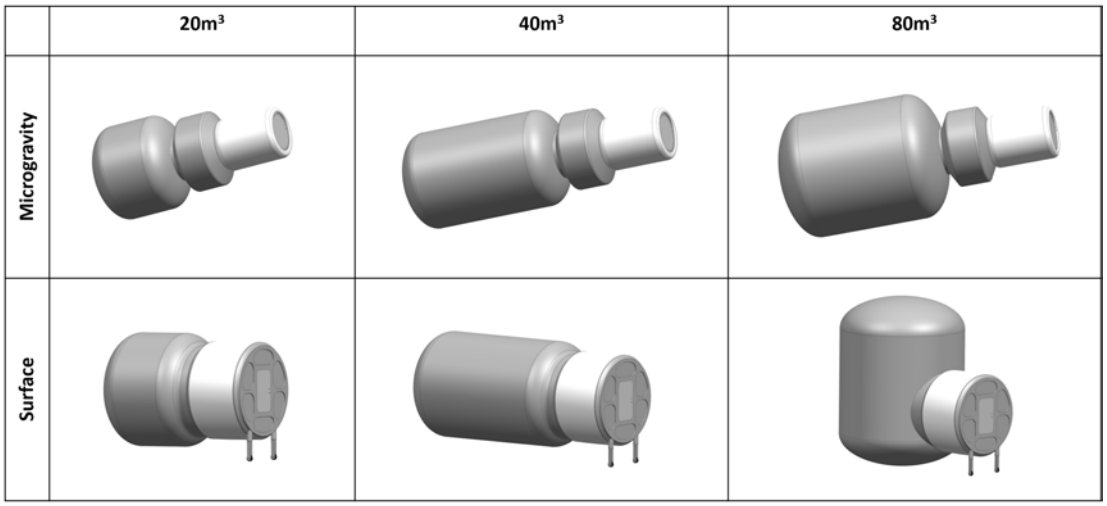

Figure 150: Habitat - Airlock Integration

7.8.2 Airlock Materials

Both the microgravity and surface airlock utilize inflatable and rigid components. All of the rigid components for each airlock are made from 7075 aluminum alloy. This design decision was made using the previously outlined structural materials trade study. The inflatable portions of the airlocks utilize multiple layers of materials. The design and order of these stacked layers was based on previous NASA inflatable structure designs [39].

The inner most layers of the inflatable airlock walls consist of redundant bladders. The material selection for the bladders was based on a few variables including operating temperature, tensile strength and oxygen transmission rate. The materials considered for the bladders included nylon 6, biaxially-oriented polyethylene, and polypropylene (PP). These materials and their properties are shown in the table below.

Bladder Material	Operating Temp	Tensile Strength	Oxygen Transmission Rate
Nylon 6	-40 to 160 °C	63.0 MPa	27.2 cc/m^2/day
Biaxially-oriented Polyethylene	-40 to 170 °C	190 MPa	90 cc/m^2/day
Polypropylene Film (PP)	-10 to 120 °C	32.4 MPa	375 cc/m^2/day

Table 62: Bladder Material Properties

Ultimately, nylon 6 was chosen as the bladder material, primarily for its low oxygen transmission rate, as well as its satisfactory operating temperatures and strength properties. Additionally, nylon has also been widely used in aerospace applications historically.

The next layer is the restraint layer. This is the layer that takes the pressure loads in the inflatable airlock. Therefore, it is important that the material selected have good strength properties, as well as the ability to be manipulated from the unpressurized state to the pressurized state within the thermal environment of space. The materials examined for this layer included Kevlar, Vectran, Zylon and Nomex. Their respective properties as they pertain to operating temperature and tensile strength are shown below.

Restraint Material	Operating Temp	Tensile Strength
Kevlar	-196 to 177 °C	3000 MPa
Vectran	-159 to 100 °C	1100 MPa
Zylon	Max: 650 °C	5800 MPa
Nomex	-55 to 260 °C	340 MPa

Table 63: Restraint Layer Material Properties

Here, Kevlar was chosen for its strength properties, satisfactory operating temperatures, and like nylon, its wide use in the aerospace industry. In this application, the layer of Kevlar fabric will likely be woven to provide strength in the axial and hoop directions of the pressure vessel. In subsequent sections, this is assumed to be the case when structural margins are calculated.

Following the Kevlar restraint layer are layers of MMOD shielding and thermal insulation. The material selection for these layers for both the microgravity and surface airlocks are discussed in the Power and Thermal section of this report.

7.8.3 Microgravity Airlock Design

The design for the microgravity airlock is largely based on NASA's Quest Joint Airlock on the International Space Station [67]. It is a dual chamber airlock consisting of two main pressurized volumes, the equipment lock and the crew lock. The full airlock assembly has a mass of approximately 2863 kg and a total volume of approximately 16.6 m^3. A dimensioned drawing of the full airlock assembly can be seen in the figure below.

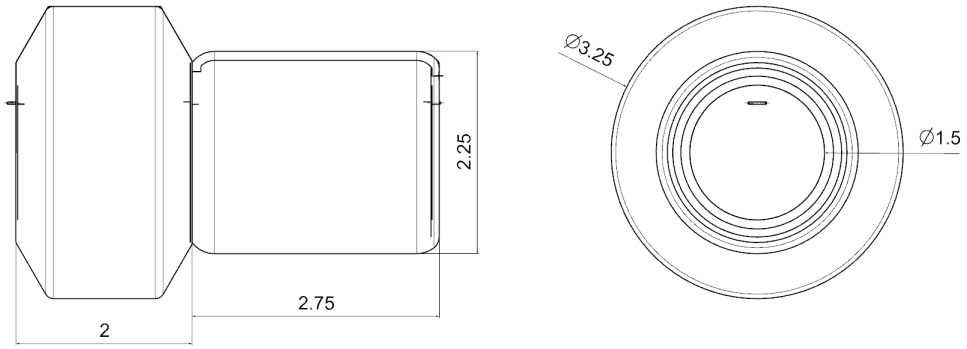

Figure 151: Dimensioned Drawing of Microgravity Airlock (meters)

The equipment lock is a rigid structure made from 7075 aluminum alloy. The equipment lock is mated directly to the endcap of each microgravity habitat. Travel in and out of the equipment lock is done via two identical hatches. One hatch separates the equipment lock and the main habitat volume, while the other separates the equipment lock and the crew lock. Each hatch is 1.5 m in diameter and 20 mm thick. Analysis to determine the thickness of the hatch will be outlined in following sections. The equipment lock is the portion of the airlock where the crew will don and doff their suits. Since the structure of this portion is rigid, equipment and suits can be easily mounted and stowed along the inner circumference of the equipment lock walls. The equipment lock has an internal volume of approximately 8.24 m^3.

The crew lock is an inflatable structure composed of the materials outlined in the previous section. It is mated directly to the outer face of the equipment lock and utilizes the same 1.5 m diameter hatch to allow astronauts to move between the two chambers, as well as an additional hatch separating the pressurized crew lock from vacuum. The crew lock chamber was designed to be inflatable to minimize the volume occupied within the fairing during launch.

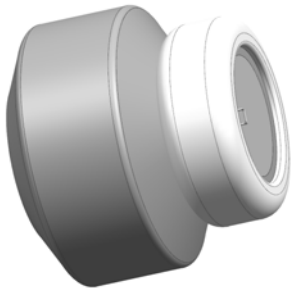

Figure 152: Crew Lock (Unpressurized)

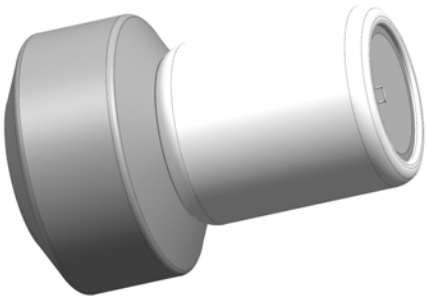

Figure 153: Crew Lock (Pressurized)

It is worth noting that while the hatches appear to be overhead relative to the orientation of the astronauts as they move from chamber to chamber, the relatively large diameter of both the equipment lock and the crew lock allow the astronauts to access these hatches in a manner such that they are oriented in front of them rather than above them. Internal handrails and foot restraints assist the astronauts in this process in the equipment lock, while straps placed along the inner wall of the crew lock function in the same way. The figure below illustrates the relative size of a 95^{th} percentile man within the crew lock, highlighting the ability for a person to orient themselves in line with the airlock hatch if they preferred to do so. Further details regarding the airlock volume requirements and crew procedures can be found in the airlock portion of the Crew Systems section of this report.

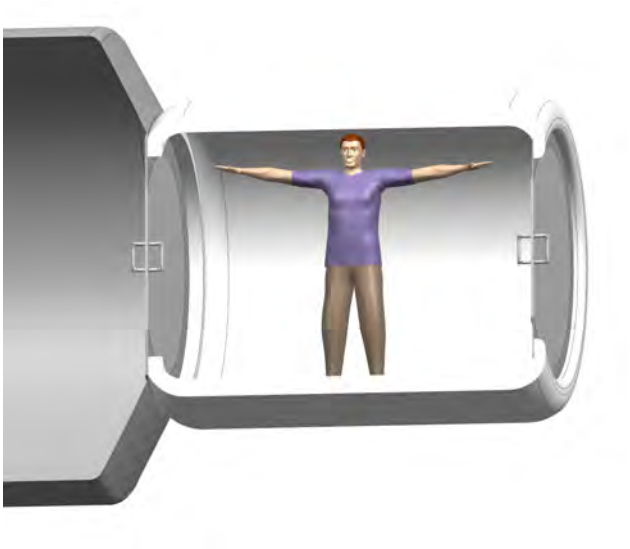

Figure 154: Astronaut Orientation within the Crew Lock

7.8.4 Microgravity Airlock Analysis

In order to determine certain aspects of the microgravity airlock design, such as wall and hatch thickness, structural margins of safety were calculated for various load cases. As in most pressure vessels, the main load case considered was hoop and axial stress due to internal pressure. Since the equipment lock and the crew lock are isolated in terms of their pressurized volumes, these load cases were examined individually for both chambers. The following equations were used to calculate the stresses in the hoop and axial directions in the walls of the equipment and crew lock.

$$\sigma_{hoop} = \frac{pr}{t} \tag{27}$$

$$\sigma_{axial} = \frac{pr}{2t} \tag{28}$$

The internal pressure, p, was conservatively taken to be 14.7 psi or 1 atm, as the internal atmospheric pressure of the habitat should not exceed this value. For the equipment lock, the shape of the pressure vessel was assumed to be a cylinder with a diameter of 3.25 m. This is the maximum diameter of the equipment lock and therefore maximizes r in the equations above, making this assumption conservative. The layer of Kevlar for the inflatable crew lock was assumed to be woven such that its tensile strength applied in both the hoop and axial directions of the pressure vessel. I was also assumed to be 1 mm thick. The material strength properties used in these margin calculations can be found in the table below.

Component	**Material**	**Yield Strength (MPa)**	**Ultimate Strength (MPa)**	**Young's Modulus (GPa)**
Equipment Lock	Al 7075	503	572	71.7
Crew Lock	Kevlar	898.5	3000	112

Table 64: Airlock Material Strength Properties [40]

In each calculation, a safety factor of 2 was used for the yield case. For the rigid equipment lock, a safety factor of 3 was used for the ultimate case, while a safety factor of 4 (which is a NASA standard for inflatable

structures) was used for the crew lock. For the equipment lock, it was found that a 2 mm wall thickness yielded satisfactory margins of safety. All of the calculated margins for the internal pressure load case are tabulated below.

Component	Hoop Stress (MPa)	FS (yield)	FS (ult)	MoS (yield)	MoS (ult)
Equipment Lock	82.32	2	3	2.05	1.32
Crew Lock	101.3	2	4	3.43	6.40

Table 65: Microgravity Airlock Hoop Stress Margins of Safety

Component	Axial Stress (MPa)	FS (yield)	FS (ult)	MoS (yield)	MoS (ult)
Equipment Lock	41.16	2	3	5.11	3.63
Crew Lock	50.66	2	4	7.87	13.80

Table 66: Microgravity Airlock Axial Stress Margins of Safety

Internal pressure loads were also examined when determining the thickness of the hatches. In this case, a simulation was run in Siemens NX. The airlock hatch and the panel that it interfaces with were meshed as separate bodies and a glue edge condition was applied between the two to simulate a securely sealed and locked hatch. A fixed constraint was then applied to the outer edge of the panel and a pressure load of 14.7 psi was applied across one side of the hatch and panel faces. The results of the simulation are shown below. The maximum stress was found to be approximately 133 MPa in elements along the outer portion of the panel, as well as stress concentrations near the hatch handle.

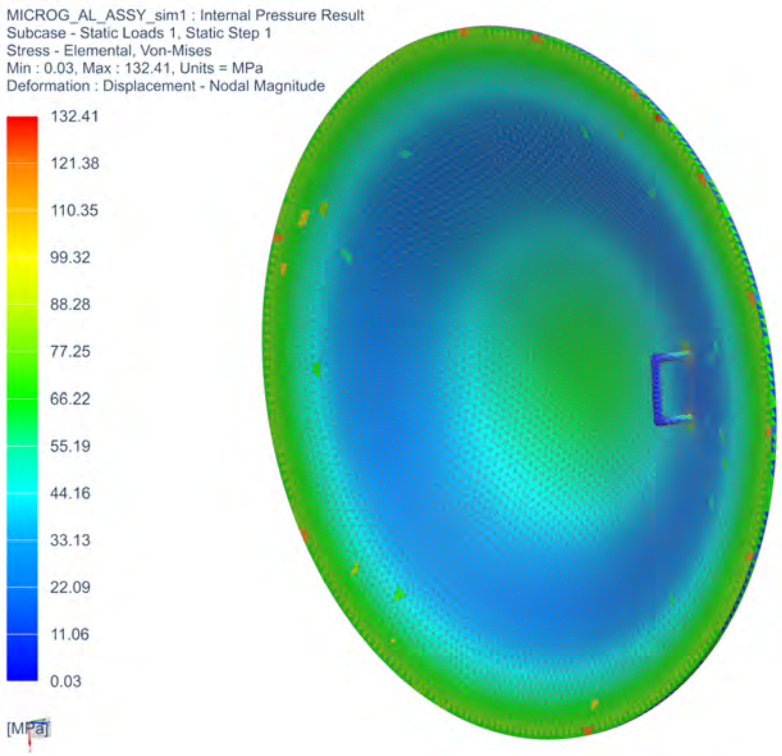

Figure 155: Microgravity Airlock Hatch Under Pressure Load

Through design iterations, it was determined that a hatch thickness of 20 mm resulted in appropriate

margins of safety. For these calculations, a safety factor of 2 was used for the yield case and a safety factor of 3 was used for the ultimate case. Again, the material properties used in both the model and the calculations were that of 7075 aluminum alloy. The margins are tabulated below.

Component	Von Mises Stress (MPa)	FS (yield)	FS (ult)	MoS (yield)	MoS (ult)
Hatch	133	2	3	0.89	0.43

Table 67: Microgravity Airlock Hatch Margins of Safety

7.8.5 Surface Airlock Design

The design for the surface habitat airlock is based on past NASA designs for a dual chamber hybrid inflatable suitlock (DCIS) [54]. This previous design featured two separate chambers with a center bulkhead that had locations for 2 suitports. The surface airlock design is also a suitport-airlock hybrid, but utilizes only one chamber. The design requirements and reasoning behind these decisions are outlined in greater detail in the airlock portion of the Crew Systems section. The surface airlock has an estimated mass of 4060 kg and an internal volume of 19.23 m^3. Notable dimensions, including the hatch size are given in the following drawing.

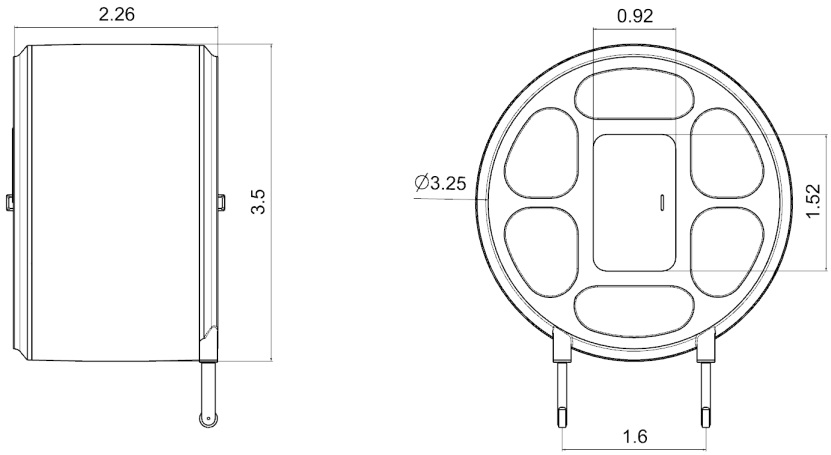

Figure 156: Dimensioned Drawing of Surface Airlock (meters)

The surface airlock design features two main panels and hatches. One panel separates the habitat from the airlock and contains the two suitports in addition to the hatch, while the other separates the airlock from the external atmosphere. All of the rigid components of the airlock, including these panels, are made of 7075 aluminum alloy. Similar to the crew lock in the microgravity airlock design, the surface airlock walls are inflatable and comprised of redundant nylon bladders, a Kevlar restraint layer, and outer shielding layers. The figures below show the two airlock panels as well as the internal components in their pressurized configuration.

Figure 157: Habitat-Airlock Panel

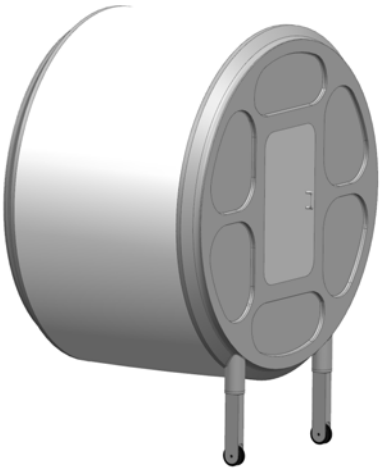

Figure 158: Airlock-Atmosphere Panel

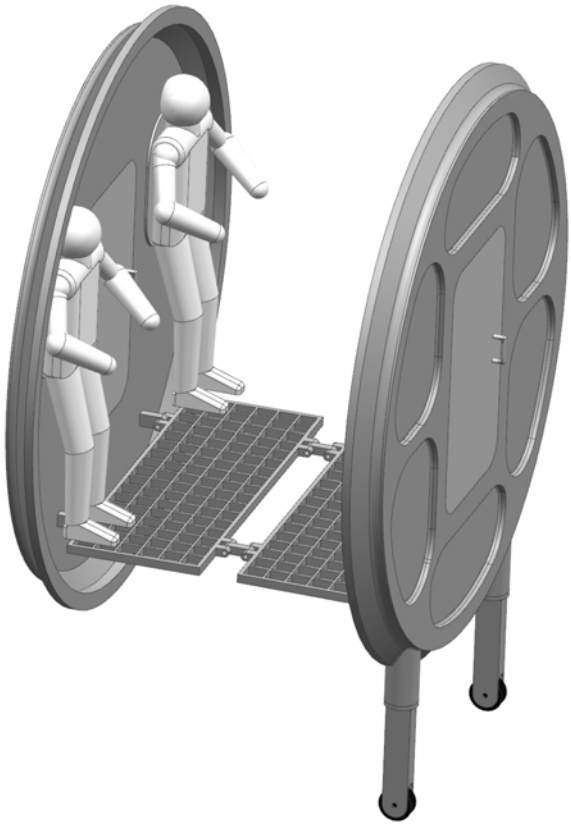

Figure 159: Surface Airlock Internals

When unpressurized, such as during launch, the airlock internals, like the orthogrid floor, collapse into a folded configuration. In this configuration, the spacesuits would be stored in the internal habitat volume. This design decision again stemmed from a need to make more efficient use of usable fairing volume. The next two figures show the surface airlock in its unpressurized configuration. While this design currently does not include steps or a ramp/ladder for astronauts to use when exiting the airlock, these could be added in

the form of a design similar to the collapsible floor. This way the structure could be stowed tightly against the outer panel of the airlock during launch and deployed once the airlock inflates.

Figure 160: Surface Airlock (Unpressurized)

Figure 161: Surface Airlock Collapsed Floor

One major consideration that must be made when designing inflatable structures for space habitats in a gravity field is their ability to withstand their own weight and hold their shape under the force of gravity when unpressurized. The previously referenced NASA dual chamber hybrid inflatable suitlock design proposed that this be achieved by adding additional inflatable structures such as internal rings and/or inflatable axially oriented struts. However, this design proposal did not quantify the effects that these additional structures had on the design in terms of mitigating deflection of components in the airlock assembly. The design for this surface airlock utilizes three types of structures to ensure that deflections are kept minimal when the airlock is deployed but the pressure is reduced. The first of these structures is the collapsible floor. In its extended configuration, the collapsible floor acts as a stiffening member of the overall airlock structure, providing support in the axial direction against the force of gravity acting perpendicularly. Additionally, nylon rings similar to those in the DCIS design are used to further stiffen the airlock and prevent primarily the top of the airlock walls from deflecting down into the internal airlock volume. These rings would accomplish this by remaining pressurized even when the airlock pressure has been equalized with the atmospheric pressure.

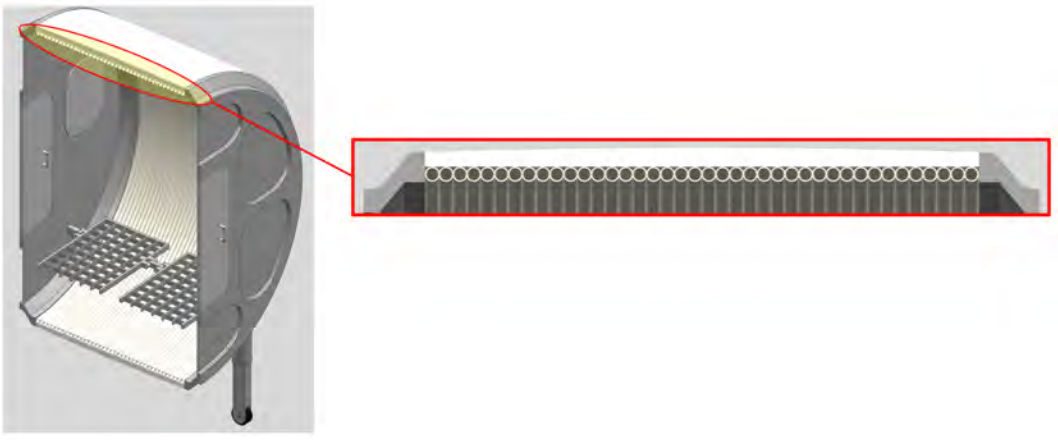

Figure 162: Pressurized Ring Support Structure

The final type of support structure is the airlock legs, which can be seen in Figure 159. These legs extend

down in a telescoping fashion from the outer airlock panel to a desired length before locking in place. At the bottom of each leg is a wheel such that the legs may extend before the airlock is pressurized and support the airlock during the process of the first initial pressurization. This aspect of the design was also utilized in NASA's DCIS airlock; however, some additional analysis was performed in order to quantify the impact that these legs had on the structure's ability to withstand deformations and deflections due to gravity. The two figures below show the maximum deflections seen under Mars gravity without the airlock walls and nylon ring structure present. The deflection in the model without the support legs is seen to be multiple orders of magnitude greater than the model with the legs included. In each simulation, the habitat-airlock panel was fixed in place and the force of gravity was applied to the entire model. In the case the legs, a fixed constraint was placed on the lower lug of each leg where the wheel shafts would be located.

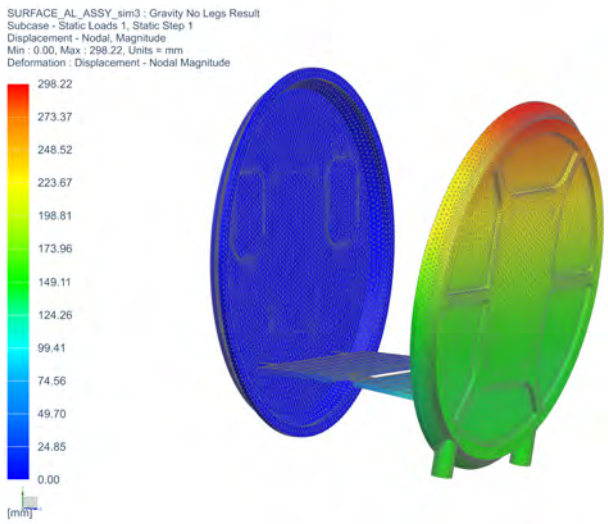

Figure 163: Airlock Deflection Due to Gravity (No Legs)

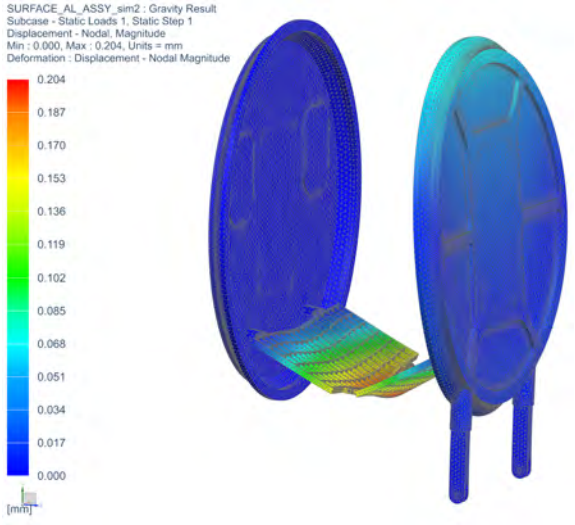

Figure 164: Airlock Deflection Due to Gravity (With Legs)

7.8.6 Surface Airlock Analysis

Similar to the analysis done on the crew lock chamber of the microgravity airlock, margins of safety were calculated for hoop and axial stresses due to the internal pressure of the airlock. The equations listed in the Microgravity Airlock Analysis section were used again along with a yield safety factor of 2 and an ultimate safety factor of 4, since the structure in question is inflatable. The Kevlar layer again was taken to be 1 mm thick and woven such that the tensile strength applied in both the axial and hoop directions. The resulting margins are tabulated below.

Component	Hoop Stress (MPa)	FS (yield)	FS (ult)	MoS (yield)	MoS (ult)
Airlock Inflatable Walls	167.2	2	4	1.69	3.49

Table 68: Surface Airlock Hoop Stress Margins of Safety

Component	Axial Stress (MPa)	FS (yield)	FS (ult)	MoS (yield)	MoS (ult)
Airlock Inflatable Walls	83.59	2	4	4.37	7.97

Table 69: Surface Airlock Axial Stress Margins of Safety

The thickness of the hatch and end panels of the surface airlock were also determined through analysis and design iterations. The models for both the hatch and panels were designed and meshed separately in Siemens NX. As was the case with the microgravity hatch, a glued condition was applied between the edges of the panels and the hatches themselves. For the panel with the suitports, the same process was done. A fixed constraint was applied to the outer circumferential face of the panel and 14.7 psi was applied over one face of the panel and the hatch. For the habitat-airlock panel, the pressure load was applied on the face internal to the habitat. For the airlock-atmosphere panel, the pressure was applied on the face internal to the airlock. The resulting von mises stresses in the elements of both models are shown below.

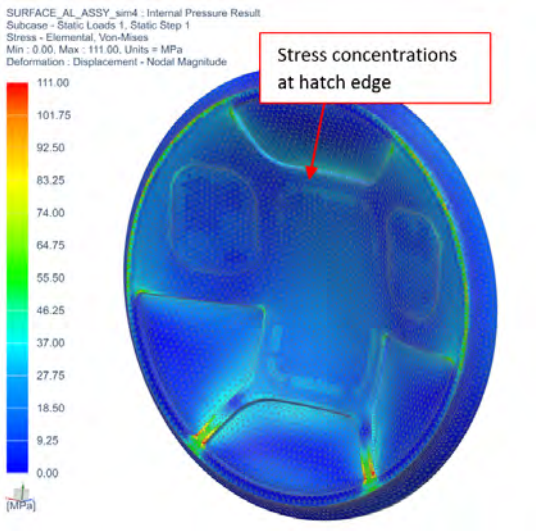

Figure 165: Habitat-Airlock Hatch and Panel Under Pressure Load

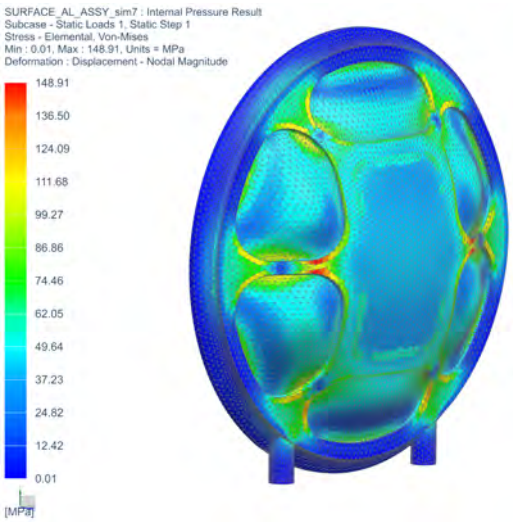

Figure 166: Airlock-Atmosphere Hatch and Panel Under Pressure Load

Through an iterative design process, material was removed from the panels until appropriate margins were achieved. The thickness of the hatches and maximum thickness of the panels was found to be 50 mm. The minimum thickness of the panels as a result of removing unnecessary material was found to be 10 mm. This is the remaining thickness of the pocketed areas of the panels above. The margins of safety for both cases are shown in the table below.

Component	Von Mises Stress (MPa)	FS (yield)	FS (ult)	MoS (yield)	MoS (ult)
Habitat-Airlock Hatch	111	2	3	1.27	0.72
Airlock-Atmosphere Hatch	149	2	3	0.69	0.28

Table 70: Surface Airlock Hatch and Panel Margins of Safety

The final analysis performed examined the stress in the collapsible floor due to the weight of the four crew members standing on top of it when fully deployed. For this analysis, each crew member was assumed to weigh 250 lbs. It was also assumed that they were all wearing their suits which added approximately an additional 280 lbs each [81]. This brings the total weight to 2120 lbs on Earth; however, Mars gravity was applied as a worst case nominal operating condition in comparison to possible use on a lunar habitat. This brings the weight to a total of 802 lbs. This force was distributed evenly over only half of the floor to represent a situation where all of the astronauts might be standing close together. Finally, an additional factor of 2 (separate from the later applied safety factors) was applied to the load to envelope a potential dynamic loading condition such as an impact from jumping or falling. The connections between each half of the floor were considered to be rigidly glued and the lugs on each end of the floor were held fixed. The

resulting von mises stresses and margins calculated can be seen below.

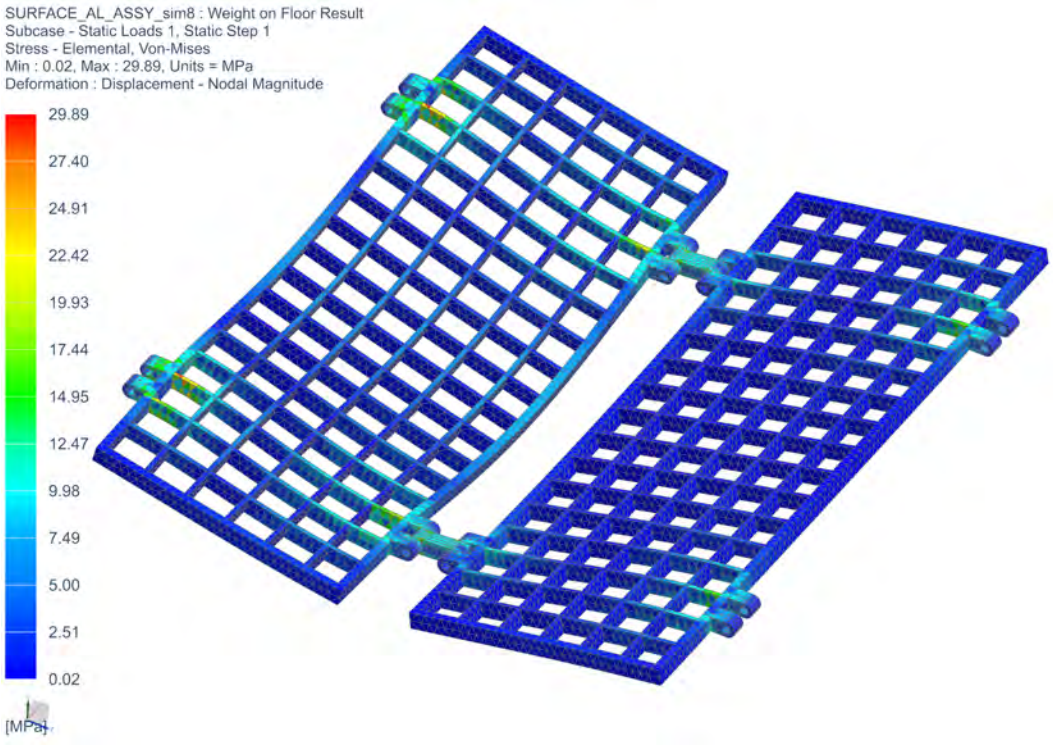

Figure 167: Surface Airlock Floor Under Distributed Weight

Component	Von Mises Stress (MPa)	FS (yield)	FS (ult)	MoS (yield)	MoS (ult)
Floor	30	2	3	7.38	5.36

Table 71: Surface Airlock Floor Margins of Safety

While these values for the margins of safety imply that material could be removed from the floor to save mass by means of either reducing the number of orthogrid members or decreasing the thickness, it is important to consider the implications for the resulting deflection of the airlock under gravity in a state in which its internal pressure is equalized with the atmospheric pressure of the moon or Mars. The floor acts as supporting structure stiffening the airlock in the axial direction. Reducing the floors stiffness properties by either of the two means described would also likely result in higher deflections in this case. Therefore, the margins of safety calculated were deemed acceptable.

7.9 Floor Design and Analysis (Matt Ostrow)

7.9.1 Design Goals

The floors of our habitats need to be:

- Lightweight
  - For launch vehicle performance and compatibility
- Stiff and strong

  - To support astronauts and heavy equipment

- Be an efficient use of volume
  - Overall project goal is finding minimum habitable volume

7.9.2 Design Overview

Considering the design constraints listed above, the floor structure was chosen to follow the concepts of airplane wing box. A wing box design utilizes the parallel axis theorem to its full potential by using outer face sheet plates connected via thin panel bulkheads and stringers, providing a high stiffness-to-weight and strength-to-weight ratio structure. A side-by-side comparison between an example real wing box structure and the vertical surface habitat's floor design is shown below:

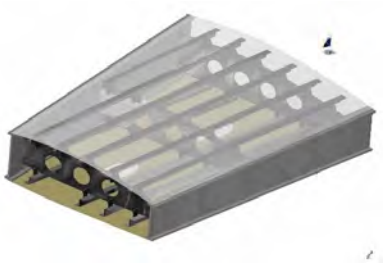

Figure 168: Real World Wingbox Structure [62]

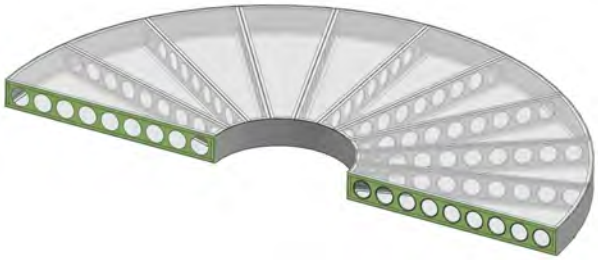

Figure 169: Floor Design - 80 m^3 Surface Habitat

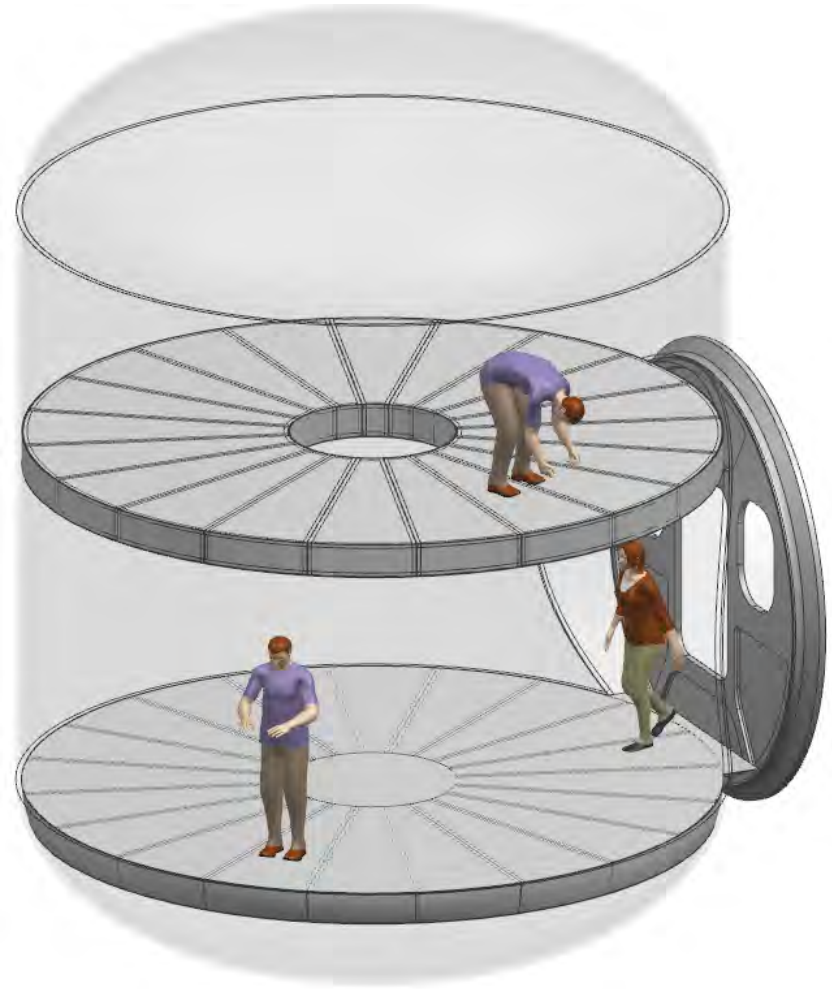

Figure 170: First & Second Floors - 80 m^3 Surface Habitat

All plates and shear bracket thicknesses are 3 mm. The radial stringers act as the webs for the built-up I-beam effect between the top and bottom outer plates of the floor. The stringer structure consists of a web plate with flanged circular lightening punchout features and angle brackets on the four corners to transfer shear between the outer plates through the stringer. Angle brackets were used in this iteration of the design due to stiffness concerns and to provide extra material near the top and bottom face plates, since this is where the highest stresses occur for the second floor of the 80 m^3 habitat. The circular lightening punchout features increase the natural frequency of the stringers by removing some mass and rigidizing the regions around the punchouts due to the angled flanges (localized parallel axis theorem). Although these cutouts act as stress concentrators, this is not a concern because the max stresses occur in the top and bottom plates due to induced bending stresses, following the formula:

$$\sigma = \frac{Mc}{I} \tag{29}$$

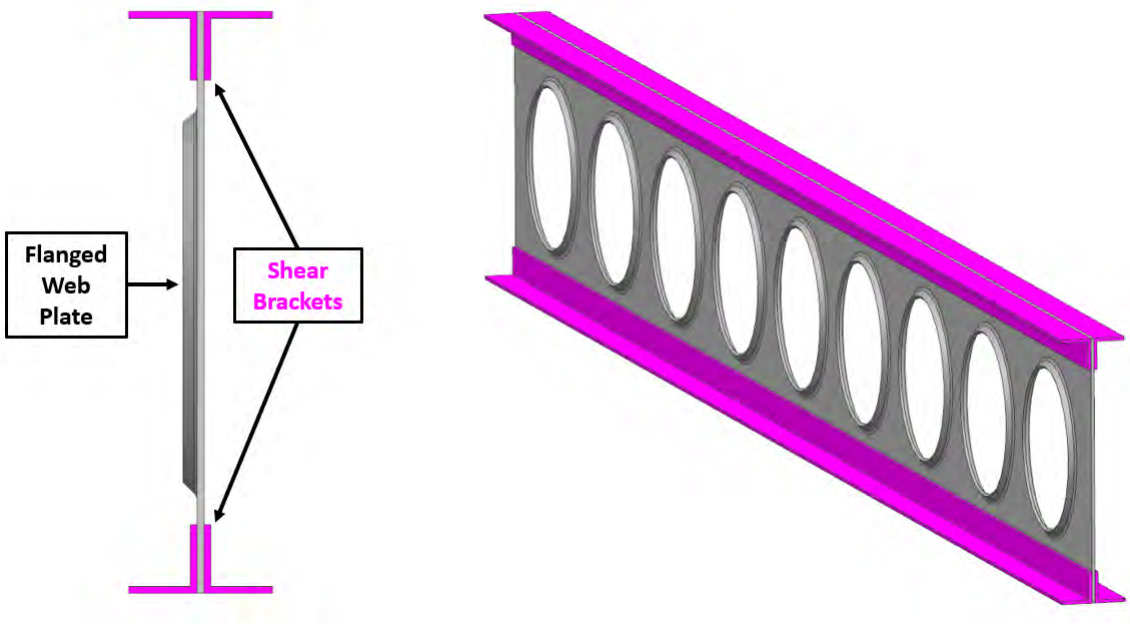

Figure 171: Stringer Structure Cross-section & ISO View (Angle brackets colored pink for clarity)

Another reason a wing box design was chosen is because the hollow inside of the structure can be utilized for other purposes, such as storage, mechanical, and electrical routing. Access panels can be installed in the top plate of any floor, as long as the access panel and any fasteners sit completely flush to prevent accidental tripping. The design of these access panels is not detailed in this report, as their design does not influence the project goal of finding minimum habitable volume. The overall thickness of the floors of the vertical 80 m^3 surface habitat were chosen to be 10 inches such that the largest sized CTB (Double) could fit within the floors. This allows the floor space to be used for more valuable utilities, such as crew berths and science lab stations. The floors in the horizontal habitats are taller than 10 inches, simply because their placement was optimized through the calculations detailed in section 7.1 and so their stringers/bulkheads simply extend to the internal diameter of the habitat shell.

The top and bottom outer face plates of the floors are aluminum honeycomb sandwich panels, with 1.5 mm thick top and bottom sandwich plates and a 13 mm thick aluminum 3003 honeycomb core, cell size 9 mm. [53] Sandwich panels were used for the outer face plates of the floors to prevent buckling due to normal stresses, and to minimize deflection under load. A floor should feel rigid when it is walked on and a rigid sandwich panel achieves this goal, as seen by the results in the analysis section. Stresses and buckling load factors are also detailed in the following analysis section (7.9.3).

Along with being used for storage space, the internal volume of the floors can be used for electrical and mechanical routing purposes. The lightening features in the stringers allow mechanical pipes and electrical wires to pass through unobstructed. Any plumbing or power routing can now be accomplished within the already-used volume the floors occupy. Utilizing the inside of the floor for storage space and routing is an efficient use of the volume that a wing box style structure occupies, and helps achieve the goal of finding minimum habitable volume.

Figure 172: CTB Storage & Routing Utilization of Floor Internal Volume

All components of the floor structure aside from the sandwich panels' honeycomb cores would be made of the same aluminum alloy as the habitat's outer shell, Al7075-T6, to ensure no thermal stresses are induced due to dissimilar coefficients of thermal expansion. Different alloys of aluminum do have slightly different coefficients of thermal expansion, but the difference is small enough to be negligible in the case of the floor plates. Large temperature gradients are also not expected to occur in the floors.

The horizontal habitat floors also utilize a wing box style construction, with a top aluminum honeycomb sandwich panel and supporting bulkheads underneath. The bulkheads also have flanged punchout lightening features, which help rigidize while reducing mass. The assembly for the 40 m^3 surface habitat is shown below alongside a closeup of the bulkhead design. The 20 m^3 surface habitat's floor assembly looks similar, just scaled down in length.

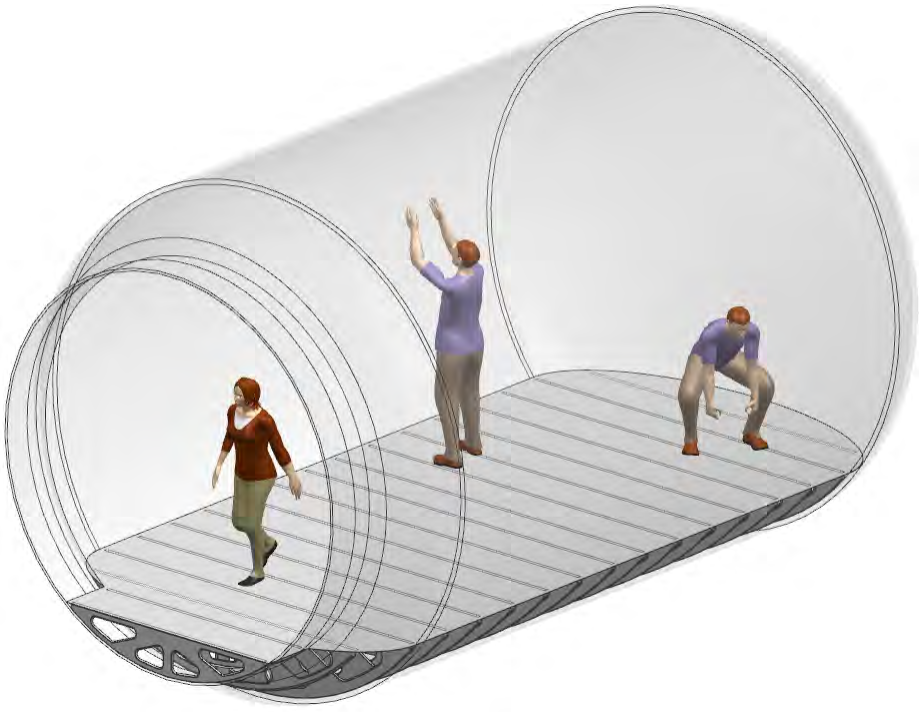

Figure 173: 40 m^3 Surface Habitat Floor Assembly (Habitat shell transparent for clarity)

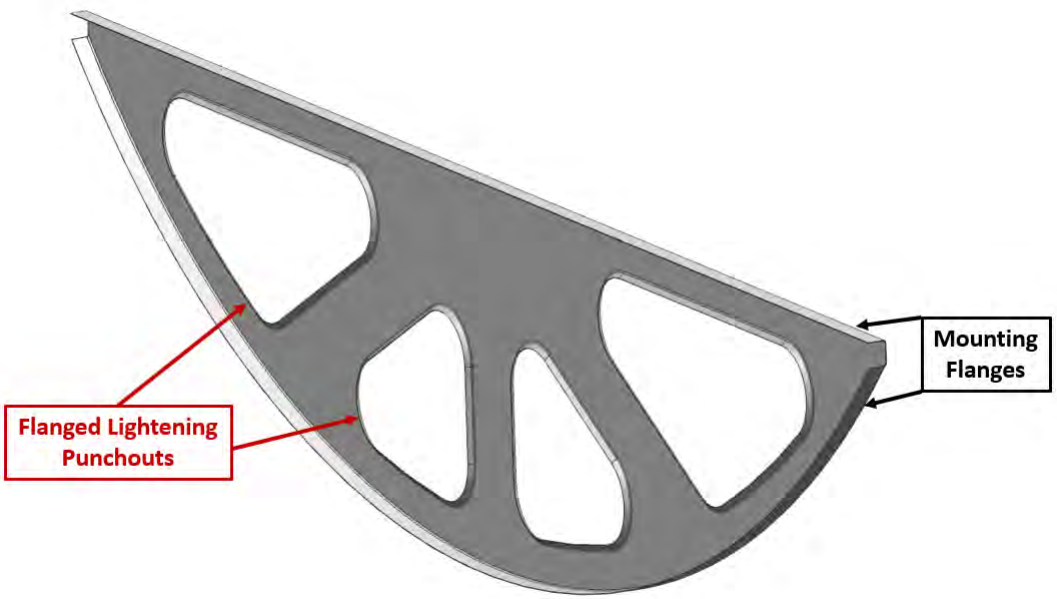

Figure 174: Bulkhead Design for Horizontal Surface Habitat Floors

The bulkhead design consists of a single 3 mm thick sheet of Aluminum 7075-T6 with mounting flanges bent from the same piece of aluminum, eliminating the need for additional angle brackets, as seen in the vertical habitat floor designs. This bent flange construction could be utilized in the vertical habitat floors and would need to be verified with a modified FEA model. The lightening punch-outs provide pass-throughs for mechanical and/or electrical routing.

The total of mass of the floor(s) for each habitat orientation and size are shown below in table 72 below:

Habitat Size + Application	Total Floor Mass (kg)
20 m^3 Micro-g	-
40 m^3 Micro-g	449.3
80 m^3 Micro-g	706.6
20 m^3 Surface	155.0
40 m^3 Surface	293.3
80 m^3 Surface	1403.9

Table 72: Floor Mass Table

7.9.3 Analysis

To quantify the loads imparted on the floor designs, the civil engineering standard ASCE 7-16 *Minimum Design Loads and Associated Criteria for Buildings and Other Structures* [27] was consulted. The standard defines two classification of loads: **dead load** and **live load**. Dead load in the case of the habitat floor would be the weight of the material under a 1g gravity load (pre-launch, assembled on Earth). The live load is quantified as a uniform constant magnitude pressure load based on what the occupancy or use of the area is. Table 4.3-1 of the ASCE 7-16 lists live loads for various use cases of the space, e.g. assembly areas, dining rooms, hospitals, etc. The live load values in this table are the minimum expected loads and can in reality exceed the values listed. To account for this, these values already have safety factors built in (i.e. are over estimates) and the floors are being designed with **safety factors** of 2 to yield and 3 to ultimate. Although the habitats are not exactly civil engineering designs, the live load values from this table provide an overly conservative estimate on the same order of magnitude as the real load. To remove some conservatism, the

live load value chosen will be multiplied by 0.9 to remove the redundancy factors built into in this civil engineering design standard, tailoring the design to be aerospace grade. The live load that will be used for the floor designs will be the value listed for Light Manufacturing, as this value should cover any heavy lab equipment and light tooling needed for repairs/maintenance of the habitat: 6.0 kPa $*$ 0.9 = **5.4 MPa**

Floor Load Summary Table	
Safety Factor, Yield	2
Safety Factor, Ultimate	3
Minimum Buckling Load Factor	1.5
Dead Load	1g gravity field
Live Load	5.4 kPa

Table 73: Floor Safety Factors and Load Definition

A minimum buckling load factor of 1.5 was chosen to ensure that even with conservative live loads, the structure will not fail in buckling. A buckling load factor greater than one means that the applied loads must be multiplied by that factor to cause the first buckling mode.

Due to the geometric complexity of these structures, it is difficult to perform representative hand calculations for stress and buckling analyses. FEM models were created for only the surface 80 m^3 2^{nd} floor (vertical) and the 40 m^3 surface habitat floor (horizontal). The 80 m^3 2^{nd} floor has a longer span and larger surface area than the 40 m^3 floor of the micro-g habitat under earth gravity, meaning the 80 m^3 second floor carries a larger load/is less stiff, which means this model's results envelope 40 m^3 micro-g floor. The second floor of the 80 m^3 features a central hole for the ladder to pass through, which means the analysis performed on the second floor of the 80 m^3 surface habitat envelope its first floor analysis, since the first floor does not have a central hole and is more stiff. Similarly, the 40 m^3 surface habitat floor's analysis envelopes the results that would have been found from a model of the 20 m^3 surface habitat floor since the surface area is larger, i.e. larger resultant load and the structures are similar, just scaled in size. A table to define how the analyses envelope one another is shown in table 74 below:

Index*	**Floor Design**	**Analysis Performed?**
A	80 m^3 Surface Habitat Second Floor (vertical)	FEA model developed
B	80 m^3 Surface Habitat First Floor (vertical)	*Enveloped by A*
C	40 m^3 Surface Habitat Floor (horizontal)	FEA model developed
D	20 m^3 Surface Habitat Floor (horizontal)	*Enveloped by C*
E	80 m^3 Micro-g Habitat Floor	*Enveloped by A, same design*
F	40 m^3 Micro-g Habitat Floor	*Enveloped by A*
G	20 m^3 Micro-g Habitat Floor	*No floor therefore no analysis*

Table 74: Floor Analysis Enveloping

All face sheet sandwich panels were modeled as 2D laminate meshes with the layup defined in NX Nastran. This allowed the FEA results to capture the rigidity of the top (and bottom for design A) face plates of the floor panels.

Instead of creating an FEA model of design A's entire assembly, a single "wedge" could instead be modeled due to symmetry of the structure. The same magnitude live load was applied, but the area was smaller, resulting in an appropriately scaled load for the scaled FEA model. 2D PSHELL elements were used for all plates and angle brackets, as these are all thin sheet metal parts. This speeds up analysis time while maintaining representative results. A 3D mesh for thin parts would require a very small element size to maintain the recommended 3-element-thru-thickness rule of thumb of FEA. Any mating parts (e.g. angle to stringer connection) were modeled through use of non-coincident mesh mating, which attaches the ad-

jacent nodes with RBE2 elements. The FEM setup for designs A and C are shown below in Figures 175 & 176:

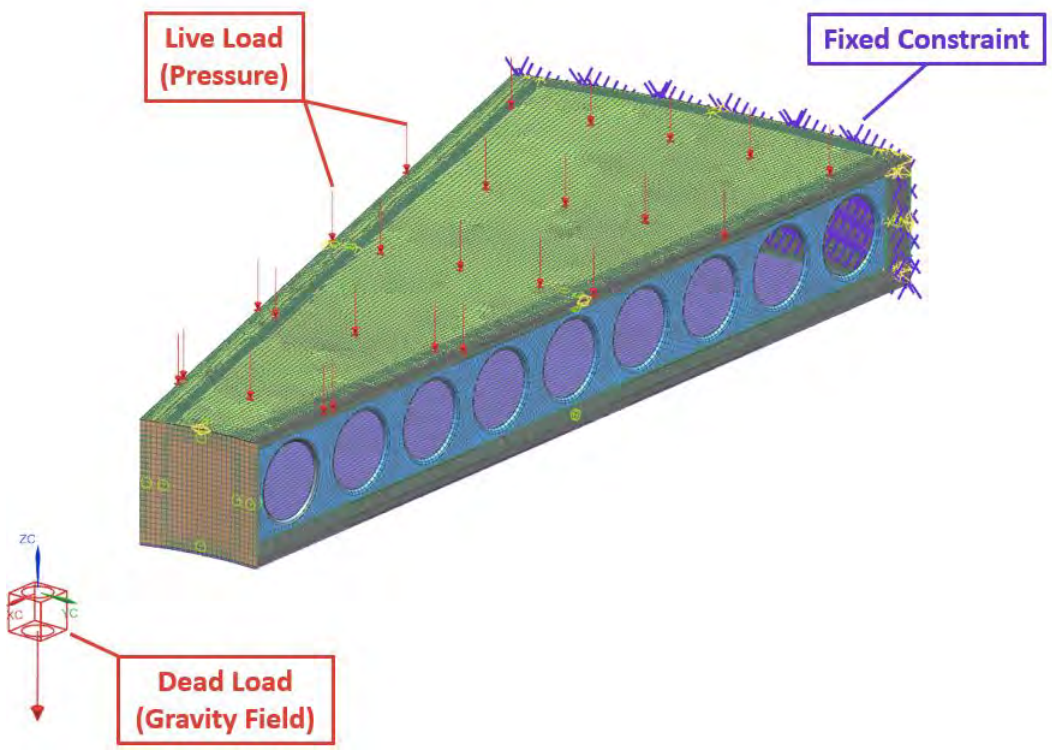

Figure 175: Design A - Wedge FEM Setup

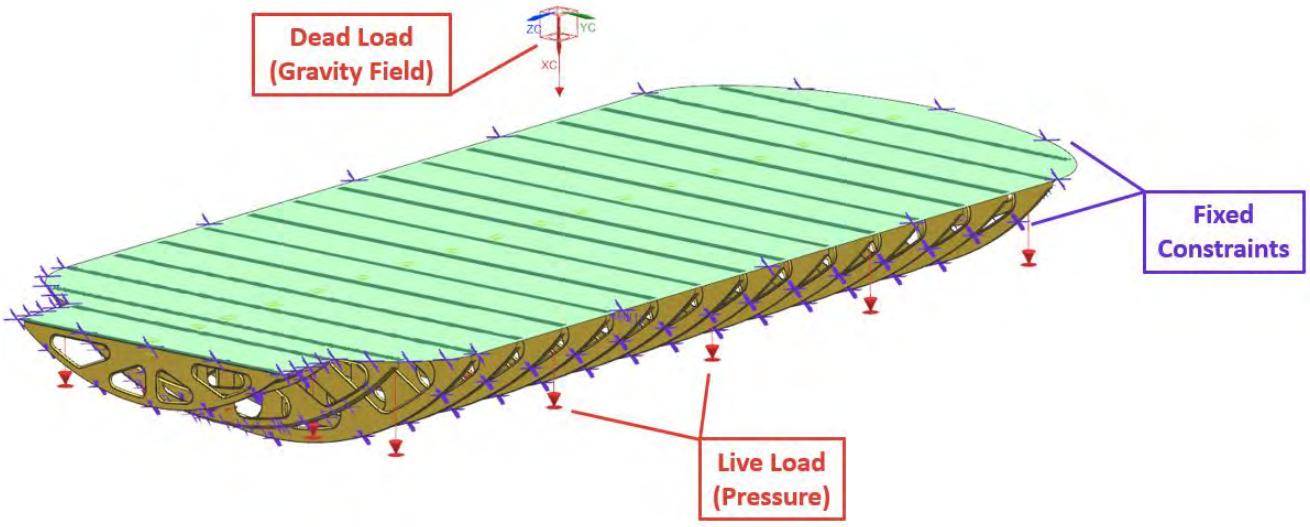

Figure 176: Design C - FEM Setup

Design A's FEM had fixed constraints applied to the outer diameter doubler plate which represents a cantilevered connection to the inner diameter wall of the habitat. A 1g gravity field was applied for the dead load (on Earth, highest dead load scenario) alongside the live load pressure applied across the top floor plate

surface to model weight of equipment and personnel.

Design B's FEM has fixed constraints applied along the outer edge of the floor plate to represent a welded connection to the inner diameter wall of the habitat. There were also fixed constraints along each of the bottom mounting flanges of the bulkheads to model a connection to the inner walls of habitat, which is assumed to be infinitely locally stiffer than the bulkhead flanges. In a higher fidelity model, these joints would be designed (e.g. bolted connection into threaded insert) and modeled with CBUSH elements, as previously described, and this fidelity is not required for this project for the same reasons described previously.

Non-coincident mesh mating allows for quicker FEM setup but does not correctly model the jointed connections. These simulations had the goal of viewing the overall performance of the structure though, so this modeling method is acceptable for these purposes. A more refined FEM could be made, modeling riveted or bolted connections with CBUSH elements and RBE2's from the fastener ends to washer contact areas. The CBUSH elements can then also report the forces through the fastener, which would allow the design engineer to know exactly which bolt will fail first and when. This level of fidelity is outside the scope of this project however, as bolt failure prediction does not help in finding the minimum habitable volume. These simulations verify that the overall designs of these floors are feasible structures for the application.

The FEA results provided max Von Mises Stress, Max deflection, and buckling load factors of each design. Using the safety factors from Table 73, margins of safety with respect to yield and ultimate stress could be calculated. An allowable deflection ratio of 1/1000 is defined, which defines the max deflection of each design to be $1/1000^{th}$ of its longest unsupported span length. The 105 Linear Buckling solver provides buckling load factors from the loads applied, and the first buckling mode load factors are reported. The first buckling mode load factor must be greater than the 1.5 value defined in Table 73.

In CDR, there were negative margins in regard to bending stress and deflection of design A. By increasing the number of radial stringers from 12 to 20, the effective size and area of the "wedge" model decreased, which causes lower stresses and deflections. The addition of sandwich panels on the top and bottom panels greatly reduced deflections and increased their critical buckling load. The tables below show the final design stress margins, buckling load factors, and deflection ratios for Design A, along with results for Design C (not reported in CDR):

Stress Margins	Floor Design	Von Mises Stress (MPa)	FS_y	FS_u	MoS (yield)	MoS (ult)
	A	175.96	2	3	0.4293	0.0836
	C	15.77	2	3	14.9480	11.0905

Deflection Analysis	Floor Design	Allowable Deflection Ratio; (Deflection/Span)	Largest Span (m)	Max Deflection (m)	Deflection Ratio
	A	0.001	1.99	0.00156	0.00078
	C	0.001	0.38879	0.000327	0.00084

Buckling Analysis	Floor Design	Allowable Buckling Load Factor	Lowest Buckling Load Factor
	A	1.5	15.8790
	C	1.5	4.0956

Material Constants	Floor Design	Material	Yield Strength (MPa)	Ult. Strength (MPa)
	All	Al 7075-T6	503	572

Figure 177: Floor Design - Margins & Post-Processing [28]

The simulation results used to compile tables in 177 are shown in Appendix A. As seen from these results, Design A's first failure mode is due to stress, while Design C's first failure mode seems to be buckling of the bulkheads, since they are in pure compression. In future design iterations, Design C could have it's number of bulkheads reduced to increase the average stress on each bulkhead, while adding stiffeners only where necessary to prevent buckling. This could potentially reduce overall mass of Design C. Design A's MoS w.r.t.ultimate stress is very low, so to cut mass in future iterations, the thickness of some of the secondary load paths can be reduced to cut into their large buckling load factor margin. Overall, this simulation results confirm that these are valid structure designs for these applications and would only need specific tweaking and scaling once a final habitat size is eventually chosen.

7.9.4 Floors for Micro-G Habitats

The floor design used for the 80 m^3 surface habitat was used for the 80 m^3 micro-g habitat and scaled down for the 40 m^3 micro-g habitat. The same floor design was used because although the micro-g habitat's floors will not be bearing any gravity loads once the habitat is in orbit, the habitat floors still need to support all internal equipment when the habitat is on the Earth's surface prior to launch. The micro-g variations of the floors would, however, be outfitted with handholds/footholds to assist astronauts maneuvering and anchoring when working around the habitat. Dividing the internal volume of 40m3 and 80m3 micro-g habitats also gives the habitable volume more wall space for mounting and provides a more natural feel, opposed to having one large open volume. These floors in their respective micro-g habitat assemblies can be seen in sections 9.3 & 9.4.

The 20 m^3 micro-g habitat does not have any separating "floors," as the height is too short for the floor to fit reasonably. The height of the inside of the 20 m^3 habitat is such that a separating floor would be too cramped for the astronauts to operate inside of.

7.10 Ladder Design and Analysis (Bob Nobles, Einar Terrill)

7.10.1 Ship-Ladder Staircase Analysis (Bob Nobles)

Figure 178: Ship-Ladder Staircase for 80 m^3 Habitat

The staircase in question was designed to be for the 80 m3 habitat, being it's the only vertically oriented habitat of the three considered. According to OSHA, any ship-ladder staircase must meet the following requirements [13]:

- Staircase must be able to hold a 1000 lb. point load.
- Angle from the horizontal must be between 50° and 70°.
- Risers must have a vertical height between 6.5" and 9.5".
- Treads must have a minimum depth of 5", and a width of 18".

The staircase was given an angle to the horizontal of 70° for volume considerations. In an FEM simulation, the treads were subjected to a 1000 lb load as shown below:

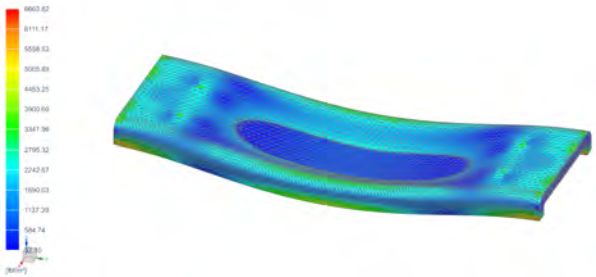

Figure 179: FEM for Stair Tread

The treads were made somewhat hollow to reduce the weight of the staircase. Before this the whole thing had a mass of roughly 43.5 kg. With the treads and handrails made hollow, the weight was reduced to something more reasonable. The mass and volume properties of the staircase are shown below:

```
Density              =    2710.995695081 kg/m³
Area                 =       7.109716265 m²
Volume               =       0.016033563 m³
Mass                 =      43.466919914 kg
```

Figure 180: Mass and Volume Properties of Ship-Ladder Staircase

Taking into account the volume underneath the staircase, the total volume taken up is actually 0.6469 (m^3).

The margins of safety for the FEM analysis were also calculated using excel (again using factors of safety of 2 for yield and 3 for ultimate):

	σ (psi)	FS	MoS
Ult	45000	3	1.251
Yield	40000	2	2.001

Figure 181: Margins of Safety for Ship-Ladder Staircase

7.11 Support Structures (Bob Nobles, Einar Terrill)

7.11.1 Support Structure for Vertical Habitat (Bob Nobles)

The support structure for a vertical habitat was inspired somewhat by the Europa Lander [12]. The structure will be made from beam components to form an equilateral triangular shape and loading as shown below. The load is based off the optimal dimensions for a 40 (m^3) habitat. It is multiplied by 10 to account for the additional weight of internal components as well as the main support truss. The structural member in the center is the same length as members AD and BD so it is pre-stressed.

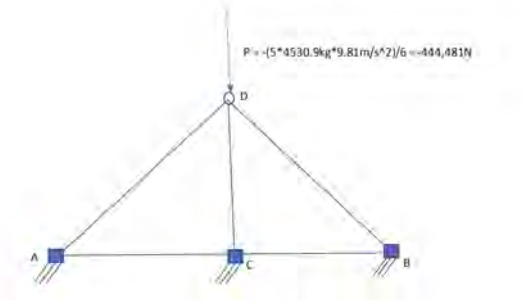

Figure 182: Foot Truss Free Body Diagram

There will be three 'feet' supporting the habitat. Each foot is made up of two units of the contraption shown above attached to mechanical legs via a ball joint. This will allow them to hold the habitat up on any surface (rough or flat). They will be organized in the manner shown below. Each step will hold 1/3 the

weight of the habitat, and each truss will hold half of that weight.

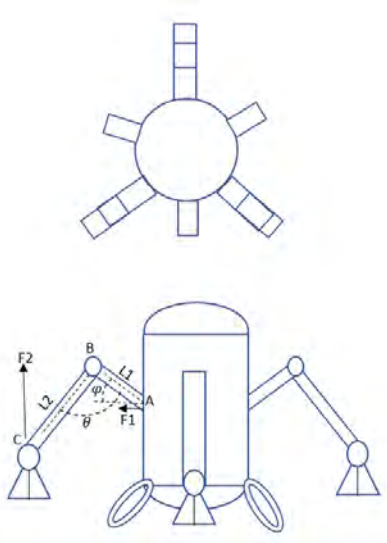

Figure 183: Truss Structure Layout

Taking the sum of moments about point B and setting them equal to zero:

$$\Sigma M_B = -F_1 * L_1 * sin(\theta)\hat{k} - F_2 * L_2 * cos(\theta - \phi) \tag{30}$$

If we let

$$\theta = 0, \tag{31}$$

then,

$$\frac{F_1}{F_2} = \frac{L_2}{L_1} \tag{32}$$

For the analysis, an FEM formulation for truss structures will be used to gain the stiffness matrices needed to calculate stresses and critical buckling loads. Each structural member will have an and elastic modulus E, and a moment of inertia I. For simplicity, they will each be one element long and have 4 degrees of freedom as shown below.

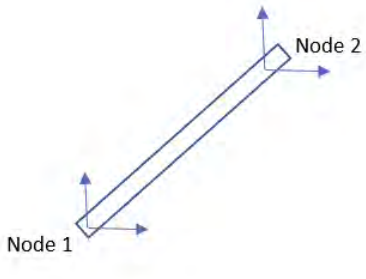

Figure 184: An element of the truss with 4 degrees of freedom

The free body diagram is shown below will forces and DoFs:

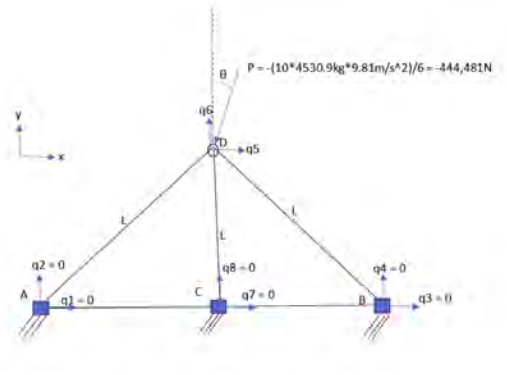

Figure 185: Free body Diagram of Truss Foot

There are 5 structural members, but only 3 can move.
Using MATLAB to calculate the strain ϵ
Let

$$\bar{\epsilon} = \epsilon * \frac{E * A}{L} \tag{33}$$

This allows for us to plot strain as a function of the force angle theta without knowing the materials or geometry of the structural members.

Plotting the strain as a function of theta from 0° to 45°:

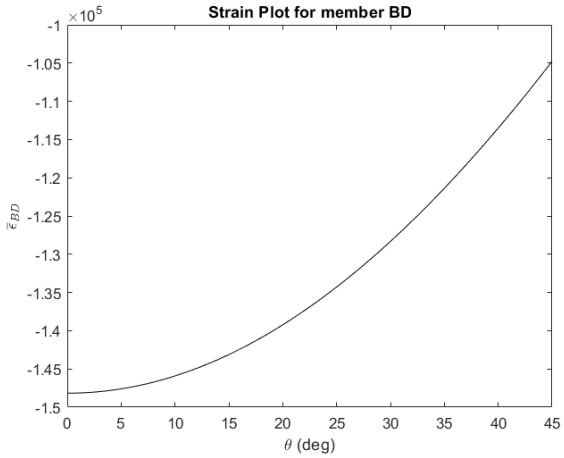

Figure 186: Strain of member BD

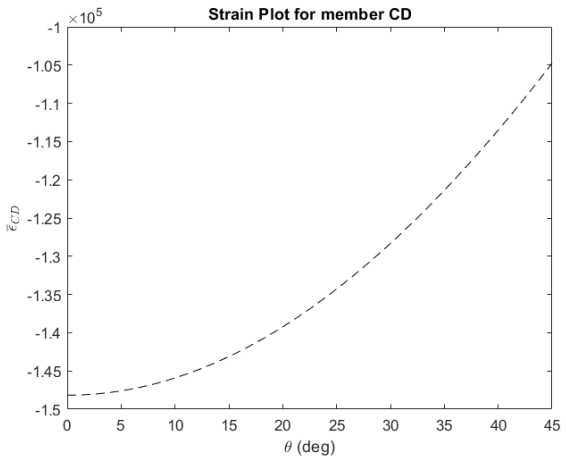

Figure 187: Strain of member CD

Stress can be calculated by just multiplying the result above by E.

Later, it was determined that the truss will be made from 2024 T6 Aluminum, in which:

E = 72.4 Gpa.

Also, the lengths of the members are 1m each. The cross-sectional area for each is .01 (m^3). Using these values, and solving the previous equation for ϵ The stress for members BD and CD can be plotted as shown below:

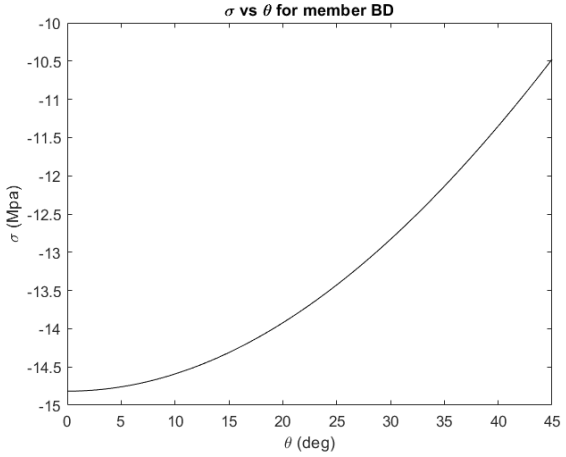

Figure 188: Stress in member BD

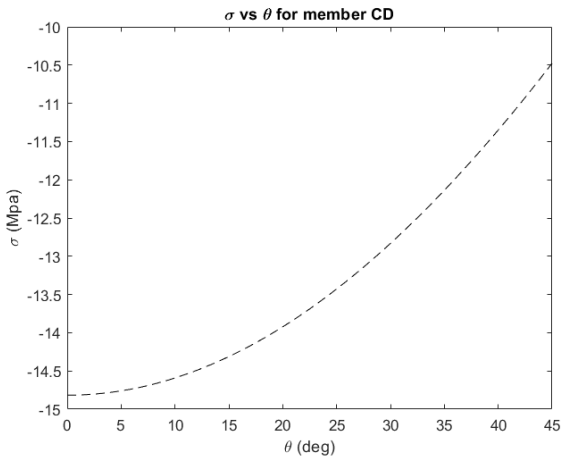

Figure 189: Stress in Member CD

From the plots above, the maximum stress seems to be around -14.8 Mpa. The yield strength of 2024 T6 Aluminum is 345 Mpa, and the ultimate strength is about 427 Mpa.
Using factors of safety of 2 (for yield) and 3 (for ultimate), the margins of safety can be calculated as follows:

$$MOS_y = \frac{\sigma_y}{\sigma_{allow} * FS} - 1 = \frac{345Mpa}{14.8Mpa * 2} - 1 = 10.66 \tag{34}$$

$$MOS_{ult} = \frac{\sigma_{ult}}{\sigma_{allow} * FS} - 1 = \frac{427Mpa}{14.8Mpa * 3} - 1 = 8.617 \tag{35}$$

The critical buckling load for the three beams can be calculated with the following equation (From [7]):

$$P_{cr} = 0.25 * (\pi^2) * E * I/L \tag{36}$$

For each member, the moment of inertia is load is:

$$I = \frac{b * (h^3)}{12} = \frac{0.1 * (0.1)^3}{12} = 8.333E - 6 \tag{37}$$

So, the critical bucking load is:

$$P_{cr} = 0.25 * (\pi^2) * (72.4E9Pa) * (8/333E - 6m^4)/1m = 1.489E5N \tag{38}$$

The habitat casing support structures are located just at the bottom of the habitat casing as shown below:

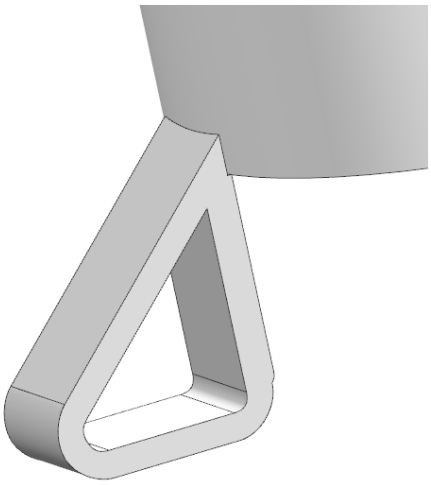

Figure 190: Casing Support Structure for Vertical Habitat

These structures would typically be welded to the habitat while getting additional support from a small shelf that the habitat would sit on. There would be three of these structures surrounding the habitat.

Below is an FEM plot of the casing support structure (which is also made from 2024 T6 Aluminum):

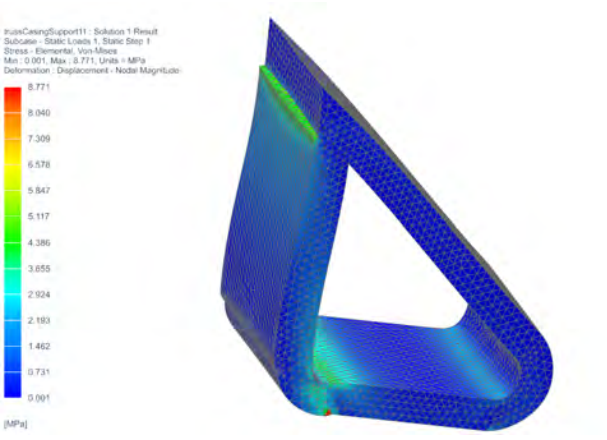

Figure 191: FEM for casing support structure

The maximum von mises stress is 8.771 Mpa. Using the same factors of safety as for the foot truss, the margins of safety can be calculated as followed:

$$MOS_y = \frac{\sigma_y}{\sigma_{allow} * FS} - 1 = \frac{345Mpa}{8.771Mpa * 2} - 1 = 18.67 \tag{39}$$

$$MOS_{ult} = \frac{\sigma_{ult}}{\sigma_{allow} * FS} - 1 = \frac{427Mpa}{18.67Mpa * 3} - 1 = 8.617 \tag{40}$$

Below are lists properties of both beams that make up the truss arms:

```
Weight data was calculated
Accuracy used        =       0.990000000

Density              =    2780.000000000 kg/m³
Area                 =      25.668112951 m²
Volume               =       0.128306221 m³
Mass                 =     356.691294029 kg

Center of Mass
Xcbar                =       2.054234119 m
Ycbar                =       0.000000140 m
Zcbar                =       0.513883403 m

First Moments
Mxc                  =     732.727425977 kg·m
Myc                  =       0.000049954 kg·m
Mzc                  =     183.297736146 kg·m

Moments of Inertia (Work)
Ixxw                 =     153.076334784 kg·m²
Iyyw                 =    2058.721792037 kg·m²
Izzw                 =    1925.949682538 kg·m²

Moments of Inertia (Centroidal)
Ixx                  =      58.882670294 kg·m²
Iyy                  =     459.334449524 kg·m²
Izz                  =     420.756004515 kg·m²
```

Figure 192: Truss Arm Beam 1 Properties

```
Weight data was calculated
Accuracy used        =       0.990000000

Density              =    2780.000000000 kg/m³
Area                 =      33.353637650 m²
Volume               =       0.166723232 m³
Mass                 =     463.490584089 kg

Center of Mass
Xcbar                =       2.500000046 m
Ycbar                =       0.000000000 m
Zcbar                =       0.500000000 m

First Moments
Mxc                  =    1158.726481761 kg·m
Myc                  =       0.000000000 kg·m
Mzc                  =     231.745292045 kg·m

Moments of Inertia (Work)
Ixxw                 =     192.725948814 kg·m²
Iyyw                 =    3973.789926033 kg·m²
Izzw                 =    3807.581632664 kg·m²

Moments of Inertia (Centroidal)
Ixx                  =      76.853302792 kg·m²
Iyy                  =     961.101021765 kg·m²
Izz                  =     910.765374417 kg·m²
```

Figure 193: Truss Arm Beam 2 Properties

Total Truss Structure Properties:

```
Weight data was calculated
Accuracy used        =       0.990000000

Density              =    2884.883314197 kg/m³
Area                 =     382.925408863 m²
Volume               =      11.506700201 m³
Mass                 =   33195.487410712 kg
```

Figure 194: Vertical Truss Structure Properties

7.11.2 Support Structure for Horizontal Habitats (Einar Terrill)

For the twenty and forty cubic meter pressurized volume habitats, a horizontal configuration was chosen contrary to the eighty cubic meter habitat. Utilizing inspiration from the storage methods breweries use to store barrels, a similar concept was implemented in creating the design for the smaller two planetary habitats. The twenty cubic meter habitats support structure is shown below(Material:2024-T6 Aluminum):

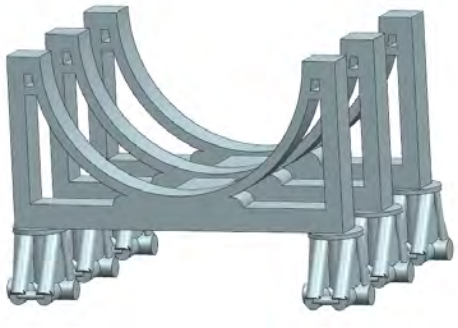

Figure 195: 20m^3 Horizontal support structure

The twenty cubic meter planetary habitat had to be able to endure the gravitational loading caused by 11063.947 kilograms of mass. Under Martian surface gravity, the load becomes:

$$11063.947kg * 3.71\frac{m}{s^2} = 4.105E4N \tag{41}$$

FEA was performed using NX1872 and a 41.05kN force was applied to each face of contact with six fixed points where the feet connect. The structure's stress distributions are shown below:

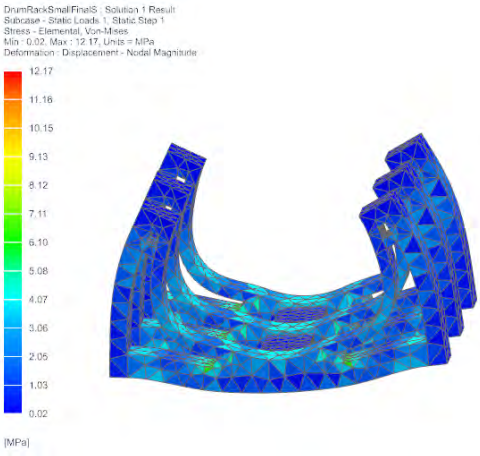

Figure 196: 20m^3 Horizontal support structure FEM

The maximum Von-Mises stress induced was 12.17MPa which when analyzed with the material properties of Aluminum 2024-T6: Yield Stress: 345MPa Ultimate Stress: 427MPa The Margins of Safety for both cases compute to:

$$MOS_y = \frac{\sigma_y}{\sigma_{allow} * FS} - 1 = \frac{345Mpa}{12.17Mpa * 2} - 1 = 13.17 \tag{42}$$

$$MOS_{ult} = \frac{\sigma_{ult}}{\sigma_{allow} * FS} - 1 = \frac{427MPa}{12.17MPa * 3} - 1 = 10.70 \tag{43}$$

The same process was done for the forty cubic meter planetary habitat shown below:

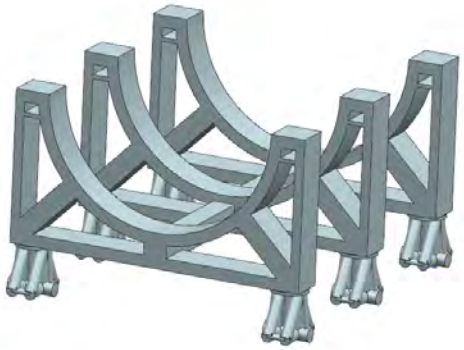

Figure 197: 40m^3 Horizontal support structure

The forty cubic meter planetary habitat had to be able to endure the gravitational loading caused by 12832.360 kilograms of mass. Under Martian surface gravity, the load becomes:

$$12832.360kg * 3.71\frac{m}{s^2} = 47.61kN \tag{44}$$

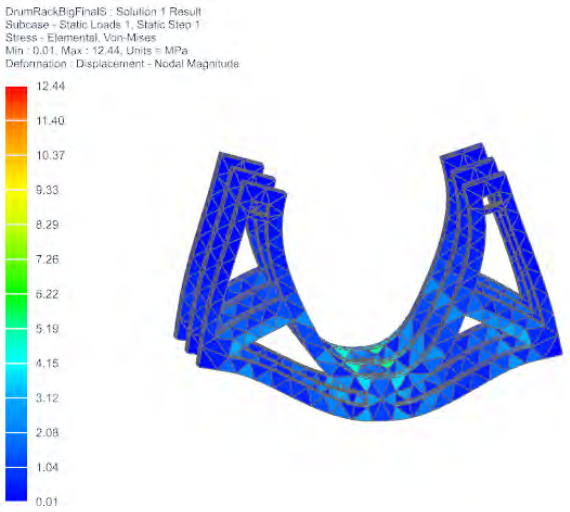

Figure 198: 40m^3 Horizontal support structure FEM

The maximum Von-Mises stress induced was 12.44MPa which when analyzed with the material properties of Aluminum 2024-T6:

$$MOS_y = \frac{\sigma_y}{\sigma_{allow} * FS} - 1 = \frac{345MPa}{12.44MPa * 2} - 1 = 12.87 \tag{45}$$

$$MOS_{ult} = \frac{\sigma_{ult}}{\sigma_{allow} * FS} - 1 = \frac{427MPa}{12.44MPa * 3} - 1 = 10.44 \tag{46}$$

Each of the horizontal support structures are held up by six truss structures each composed of six hollow cylindrical bars. Each contact with the ground is intended on bearing a sixth of the total load. These truss structures are composed of two sets of three bar trusses where each of the vertical members stands one meter long; each bar's cross section has inner and outer diameters of .230m and .250 m respectively. This nets an axial area-moment of inertia of:

$$I_{cyl} = \frac{\pi}{64} * (D_{out}^4 - D_{in}^4) = \frac{\pi}{64} * (.250m^4 - .23m^4) = 5.44E - 5m^4 \tag{47}$$

$$P_{cr} = \frac{\pi^2 * E * I}{4 * L} = \frac{\pi^2 * 7.24E9Pa * 5.44E - 5m^4}{4 * 1m} = 9.71E3kN \tag{48}$$

8 Power and Thermal

8.1 Habitat Thermal Insulation Design (Shelly Szanto)

8.1.1 Thermal Environment

The purpose of the insulation design for the habitat is to keep the habitat thermally insulated at different planetary and lunar regions, and maintain internal temperature of 22 C. The goal of the project is to focus on the internal volume of the habitat but thermal insulation is a principle part of habitat design, especially for a manned mission. The purpose this design trade study is to understand how many layers, and therefore volume, of a multi-layer insulation design will be required for different habitat volumes and for different locations.

The locations are summarized in the table below. I started with this research to get an accurate change in temperature from outside the wall to inside the wall. The polar and equator regions are two areas of interest for the trade study. The calculations that follow were done at the worst case scenario, using the delta T at the equator regions.

	T_{low} (C)	T_{high} (C)	T_{avg} (C)
Lunar Polar Regions [111]	-223	-123	-172
Martian Poles [4]	-127	-13	-70
Lunar Equator [111]	76	176	126
Martian Equator [4]	-88	7	-40.5
Micro-g Environment (LEO) [14]	-120	120	0

Table 75: The low, high, and average temperatures for each region.

8.1.2 Thermal Surface Finishes

The next part of the trade study was to understand what thermal surface finish would be applied to all visible surfaces on the outside wall layer of the habitat. Spacecraft are often painted to achieve high emittance and minimize the absorbed solar energy and infrared emission. Emissivity is the effectiveness of a material's ability to emit energy as thermal radiation. (This trade is under assumption that the surface radiating is an ideal black surface.) In terms of color of the paint finish, black is usually a conventional choice for painting spacecraft electronic boxes and their structure. White paint is typically used in the use of high emittance for radiator coatings and minimize solar absorbance. According to the figure below, a white paint finish would be optimal for the worst-case scenario of a habitat in the lunar equator region. Therefore, Aeroglaze® A276 White paint will be used as the outer surface finish.

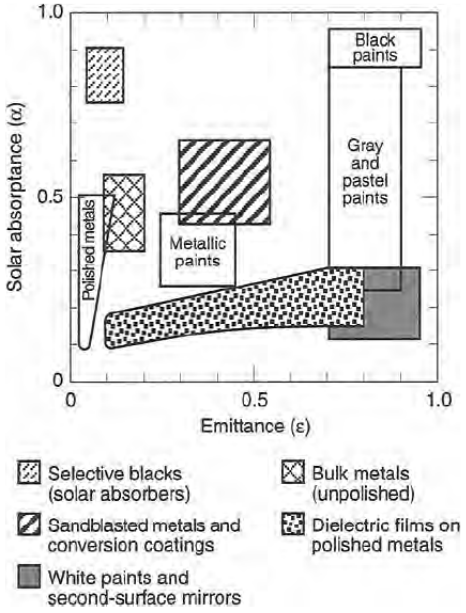

Figure 199: Surface properties by type of finish [38]

8.1.3 Multilayer Insulation Design

The purpose of multilayer insulation (MLI) is to use multiple layers of low-emittance films to prevent heat loss from the components and excessive heating from the environment. MLI blankets are very common in passive thermal control elements on spacecraft and assembled from thin mylar sheets with a vacuum-deposited finish on the side. The mylar sheets are aluminized on one side to act as a low-conductivity spacer. The purpose of this trade study is to design a thermal blanket with an enough layers to insulate the habitat in a worst-case thermal environment, understand what materials to use, and assess how the volume of the habitat impacts the insulation design. The effective emittance was calculated for all scenarios in terms of volume and temperature.

$$\varepsilon = \frac{Q}{A\sigma(T_H^4 - T_C^4)} \tag{49}$$

Where: Q ranged from 3.36 kW to peak power of 6.36 kW (used worst case at 6.35 kW), A is the surface area of the 3 different habitats 58 m^2, 98 m^2, and 135 m^2, σ is the Stefan-Boltzmann constant, T_{hot}, T_{hot} and T_{cold} are taken from thermal environment temperatures, and also treated with black body radiation assumption. All the emittance values calculated are stored in an excel file, however, because this study would focus on how the insulation impacts the volume, the worst case emittance based on temperature and peak power draw by volume are:

- $20m^3 : \varepsilon = 0.38$
- $40m^3 : \varepsilon = 0.22$
- $60m^3 : \varepsilon = 0.16$

These emittance values were then plugged into the "e-star" equation to determine the number of layers of mylar required from the following:

$$\varepsilon^* = \frac{1}{\frac{1}{\varepsilon_1} + \frac{1}{\varepsilon_2} - 1}\left(\frac{1}{N+1}\right) \tag{50}$$

It is concluded that the number of layers required are:

- $20m^3$: N = 10
- $40m^3$: N = 15
- $60m^3$: N = 20

Which is in accordance with the Thermal Control Handbook for the typical number of mylar layers [38].

8.1.4 MLI Schematic

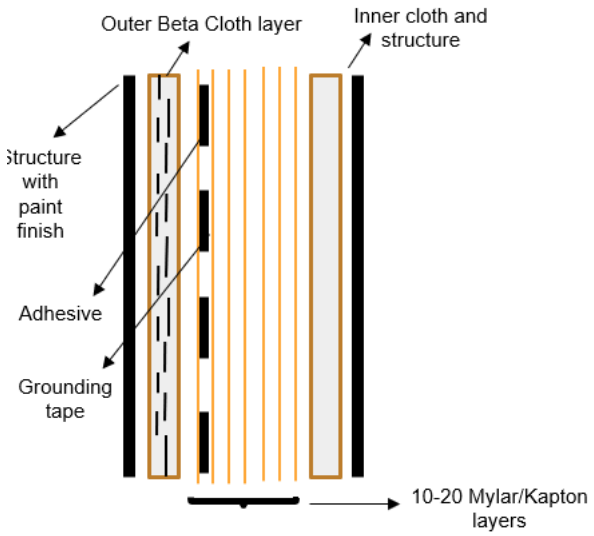

Figure 200: Schematic of insulating materials in MLI blanket

This schematic uses the most conservative of the effective emissivity which determined that 10-20 layers of Mylar/Kapton insulation must be used surrounding the entire habitat. The layers alternate between aluminized mylar and kapton with no spacers because effective emittance goes up by 19% when Dacron

spacers are replaced aluminized Kapton with no spacers [38]. Another important component of the blanket is outer layer selection. I chose to use Beta Cloth because it could be used as an essential layer for solar UV radiation and shielding for low impact MMOD if needed to be exposed. Otherwise the beta cloth layer will be used between the structure and the beginning of the mylar portion of the blanket. There are other components to the blanket such as grounding tape if used around electronics and adhesives which tend to have thermal losses.

Volume (m^3)	Number of Layers	Thickness (in.)
20	10	0.0055
40	15	0.00825
80	20	0.011

Table 76: Volume breakdown for each habitat size

This volume breakdown uses a mylar thickness of 0.00064 cm, kapton of 0.00076 cm, and beta cloth of 0.0035 cm [38]. These volumes and masses are summarized in the table of section 8.9.

In conclusion, the insulation only changes in volume and mass due to the surface area of the habitat increasing. Insulation obviously does not require any space internal to the habitat and will not affect the crew cabin size. However, it is important to understand the mass and volume of the habitat it still affected by the insulation and would have to be designed in manufactured with respect to the outside structure. As the crew size changes the peak power can vary, and as the seasons on the surface missions change the thermal environment with change, affecting the insulation. A MLI design takes into consideration all of these changing factors with having enough layers to take into account the changing external temperatures and internal peak power.

8.2 Active Thermal Control System (ACTS) (Hudson Paley)

8.2.1 Introduction

The solar heat permeating the habitat's insulation coupled with the thermal energy produced by the crew and electronics put both the crew and major electronic systems at risk of overheating; necessitating a system capable of adequate heat acquisition and transportation, heat transfer and heat rejection. The collection and transportation will be accomplished through an internal active thermal control system (IATCS), by which a fluid (gas or liquid) loop will collect a net positive thermal energy from the components, crew and solar radiation absorbed by the cabin air. For effective excess heat withdrawal, the heat flux from IATCS will be delivered to an external active thermal control system (EATCS), consisting of a fluid loop that will be delivered to an array of radiators to reject the excess away from the habitat.

The internal collection system will transfer the excess heat from the habitat to the external rejection system by means of heat exchangers. On each side of each heat exchanger, the respective IATCS and EATCS fluids are exposed to a certain surface area of a medium material, allowing for transfer through heat flux. As this surface area increases, so too will the amount of heat flux transferred from one fluid to the other. As the IATCS fluid exits the heat exchanger, the thermal energy and temperature will drop as long as the incoming EATCS fluid temperature is adequately dropped by the radiators. To that end, three acquisition systems for the IATCS were considered-air, heat pipes and pumped fluid loops.

8.2.2 Delivery Systems

One of the first systems considered was one where the internal cabin air acted as the heat acquisition and transportation system for the internal side of the heat exchanger. This option had been pursued by past capstone groups and was compelling due to the fact that it would drastically reduce the power and, subsequently, cost requirements for the IATCS. Besides the heat exchanger, the only other architecture needed for such a system would be a fan feeder system into the heat exchanger for effective heat transfer to the exterior

coolant. The fan assembly would consist of a fan array that would move the internal air past the metal channels of the heat exchanger. As the amount of heat rejection necessary for habitability increases, so too would the number of channels and the channels' internal surface areas necessary for effective transfer to the EATCS fluid loop. And as the habitats have increased thermal loadings put on them, the more difficult it will be for the air system to work effectively.

Heat pipes, which operate on the principle of capillary action, act independent of power systems. Assuming two heat pipes are connected by a heat exchanger, the first loop collects heat, which causes a liquid to vapor phase change, and delivers vaporized refrigerants to a heat exchanger [16]. Assuming the other heat pipe connected to the heat exchanger delivers cold enough secondary refrigerant, the first refrigerant will undergo a phase change back into liquid. Despite the zero-power costs of a heat pipe system, it does have some fundamental drawbacks, including expansion effects due to the two-phase system, which can cause significant stress and strain on the pipes themselves. Additionally, without active control, when certain temperature thresholds aren't met, the system becomes highly inefficient as the phase change doesn't occur.

Pumped loops act on a similar refrigerator cycle but are aided by controlled mass flow rates allowed through power inputs and refrigerant reservoirs. Both pumped loops and heat pipes could run along components-stringing together heat acquisition from most components on board. However, unlike the two-phase heat pipes, pumped loops can utilize single-phase liquids, which significantly reduce expansion effects. Furthermore, compared to an air system, a heat pump system would offer efficient heat redistribution between components (i.e.lab equipment excess heat to food prep stations). Unfortunately, the single-phase system would require high pressure, which comes with its own consequences for stress and strain in the walls of the pumped loops [15]. However, due to its high heat efficiency due to its utility and feedback control, we chose the pumped system.

Under the worst case thermal loading of the system, all of the internal heat from crew, components and solar radiation would need to be rejected from the system. In order to determine this total excess heat, we looked at the sum of peak loads on the system.

The peak thermal load from components and crew was 6356 W. However, to find the total we also needed the heat contribution from solar radiation absorption. The following was calculated for each habitat

$$A_{illuminated} = ldsin\beta + \frac{1}{4}\pi d^2 cos\beta [24] \tag{51}$$

$$Q_{solar} = A_{illuminated}\alpha I_s [24] \tag{52}$$

$$Q_{max,total} = Q_{max,crew/components} + Q_{max,solar} \tag{53}$$

Where α=absorbance of habitat, I_s=solar flux density reaching the habitat and $A_{illuminated}$=illuminated flat area of habitat. The solar flux density is 1370 $\frac{W}{m^2}$ and 595 $\frac{W}{m^2}$ for lunar and martian habitats, respectively. Assuming the absorbance of the habitat to be 0.14, we obtain the total heat produced in and absorbed by the habitat.

	Habitat $Q_{total}(W_{thermal})$			
	Mars		**Moon**	
Habitat Volume (m^3)	**Microgravity**	**Surface**	**Microgravity**	**Surface**
20	7437	8321	8855	10895
40	8498	9270	11300	13090
60	9357	10540	13290	16010

Table 77: Q_{total} for each habitat location

For the IACTS heat pump system, water was chosen as the working fluid due to its efficient thermal transport and non-toxicity in the event of leakage [15]. Analysis was performed on two different IATCS

systems that incorporated these heat pumps. Both were evaluated at maximum loading of the system (i.e. when all of the Q_{total} must be evacuated.

8.2.3 IATCS: Water Loop and Cold Plates

The first case was heat pump water loops in combination with cold plates. The cold plates would be placed adjacent to the major electronic systems and would vent their excess thermal energy to the heat pumps. The analysis of the system, necessitated some assumptions. Firstly, that the cold plates would be collecting the thermal energy from the air in addition to the components. Secondly, that the cold plates could be treated as a single unit and that their maximum allowable temperature is that of the component which necessitates the coolest conditions to operate efficiently (35 °C). This ensures that these components will never exceed their maximum allowable temperature. Thirdly, the maximum allowable temperature of the EATCS working fluid inputted to the heat exchanger is 18.33 °C, which is a NASA standard for their system in order to mitigate thermal expansion issues [15].

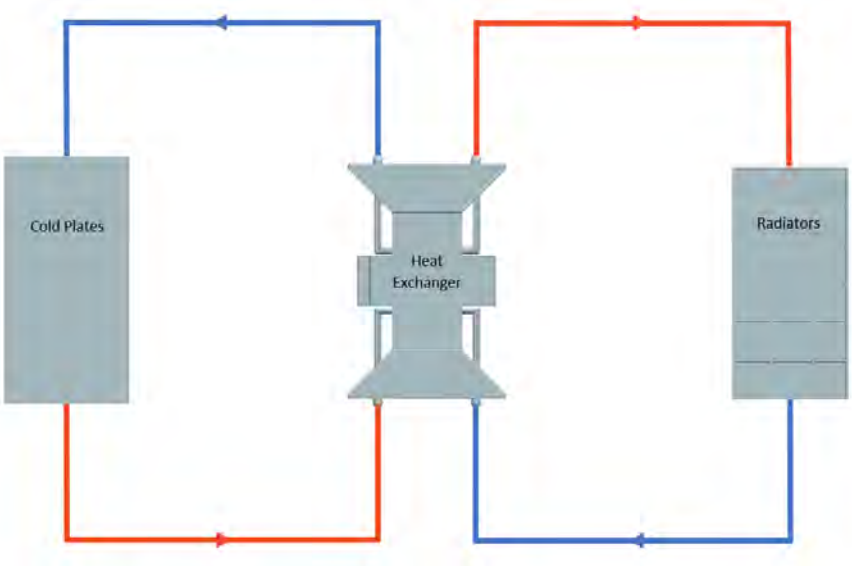

Figure 201: ATCS with Cold Plates

Directly calculating sizing and mass of the heat exchangers and cold plates is highly dependent on their internal surface area, which is difficult to estimate due to the number of assumptions necessary to make that leap. However, heat exchangers and cold plates mass and sizing are determined by mass flow rate and thermal resistance. Therefore, thermal resistance was analyzed.

8.2.4 Total Thermal Resistance Analysis

Thermal resistance (R) of a cold plate is given as,

$$R_{CP} = \frac{T_{S,CP} - T_{CP,outlet}}{Q_{total}} \tag{54}$$

Where $T_{CP,outlet}$ and $T_{CP,S}$ represent the outlet and maximum surface temperatures of the cold plate, respectively. While the the thermal capacitance (C) of a heat exchanger can be given by,

$$C_{HX} = \frac{Q_{total}}{T_{inlet} - T_{EATCS,input}} \tag{55}$$

Where, T_{inlet} for the heat exchanger is equal to T_{outlet} for the cold plate, and $T_{EATCS,input}$ is the temperature of the EATCS coolant entering the heat exchanger.

Since thermal resistance is the inverse of thermal capacitance, the above equations simplify

$$R_{system} = R_{CP} + R_{HX} = \frac{T_{S,CP} - T_{EATCS,input}}{Q_{total}} \tag{56}$$

	IATCS $R_{system}(\frac{K}{W})$			
	Mars		**Moon**	
Habitat Volume (m^3)	**Microgravity**	**Surface**	**Microgravity**	**Surface**
20	.00224	.00200	.00188	.00153
40	.00196	.00180	.00147	.00127
60	.00178	.00158	.00125	.00104

Table 78: Internal Active Thermal Control System: Total Thermal Resistivity

For the thermal control system to effectively handle the worst conditions, the sum of the thermal resistances of the bulk heat exchanger and cold plate must be less than or equal to these values in order to dissipate all of the excess heat effectively to the external system.

However, this system has some major problems. To effectively cool each component with cold plates, the budget for such a system would be inordinately high. And if the system began to fail due to lost contact with cold plate, it would be difficult to readily fix in a minimum sized habitat. Additionally, since the discrete mass and sizing of the cold plates and heat exchangers from this system cannot be found, it proves relatively meaningless within the confines of the minimum habitat design.

8.2.5 IATCS: Water Loop

The second IATCS analyzed was that of a water loop connecting to the heat exchanger. Due to water's high thermal conductivity, it would still be effective at withdrawing ample heat from the components and air as long as the water loop was strung along the components. Due to this system's similarity to that of the ISS's IATCS, we used the ISS's system as an analogue, which included its heat exchangers [15]. The potential lower cost compared to the cold plate design and its presence on the ISS lowered the risk associated with the system. Therefore, it was chosen as our final IATCS.

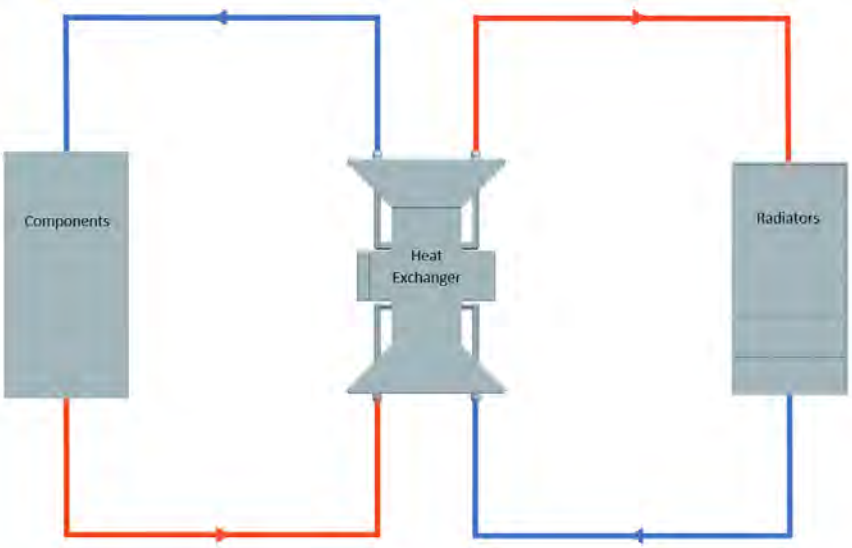

Figure 202: ATCS with Components

After calculating the average heat exchanger on board the ISS to be capable of 6385.6 W of heat removal, we developed a ratio between the capability of the ISS's heat exchanger and the heat necessary for removal under our worst case scenario, using table 77. We then used this to scale the mass and volume of the ISS's heat exchangers (41.28 kg and 0.06883 m^3, respectively)[15]. Since the lunar conditions provided higher values of necessary heat removal, they were used to calculate the following microgravity and surface habitat minimum requirements.

Heat Exchangers for Microgravity Habitat					
20 m^3 Habitat		**40 m^3 Habitat**		**80 m^3 Habitat**	
Volume (m^3)	**Mass (kg)**	**Volume (m^3)**	**Mass (kg)**	**Volume (m^3)**	**Mass (kg)**
0.09159	54.93	0.1142	68.50	0.1326	79.51

Table 79: Heat Exchanger Mass & Sizing for Micro-g Habs

Heat Exchangers for Surface Habitat					
20 m^3 Habitat		**40 m^3 Habitat**		**80 m^3 Habitat**	
Volume (m^3)	**Mass (kg)**	**Volume (m^3)**	**Mass (kg)**	**Volume (m^3)**	**Mass (kg)**
0.1104	66.24	0.1307	78.39	0.1577	94.59

Table 80: Heat Exchanger Mass & Sizing for Surface Habs

Conclusions Unsurprisingly, with the assumptions made, the mass and volume scale linearly with habitat size, which is mainly due to the linearly scaling of illuminated area from equation 51 with habitat volume. Overall, however, the mass and sizing of such a feature doesn't have much bearing on the minimum habitat design due to its inherently flexible placement in regards to the overall CAD mock-up. The only serious restriction on the heat exchanger placement is the fact that it must have both the inlet and outlet nozzles for the IATCS fluid within the confines of the habitat.

8.3 Radiators (Michael Baker)

8.3.1 Introduction (Michael Baker)

In our project we chose to investigate how volume impacts the crew performance in both a microgravity environment, and a surface environment. This makes the overall design process more difficult, as choosing one design which would fit both regimes is impossible. The microgravity environment has the benefit of having fewer structural constraints, as well as having a more favorable environment for radiative heat transfer. The surface habitats, on the other hand, have far more structural challenges to overcome and a less optimal environment for radiative heat transfer. Our analysis uses the steffan boltzmann radiative heat transfer equation to determine radiator size and working fluid for both operating regimes. For the microgravity environment a deployable radiator design was investigated, and for the surface environment both a static radiator design and a deployable design were analyzed. We were able to determine that for the microgravity environment a deployable radiator would be able to successfully cool all habitats investigated, and for the surface environment a static radiator design could cool all surface habitats.

8.3.2 Radiator Design Overview (Michael Baker)

There are various similarities across the different designs, namely the radiator materials and coatings. For both the microgravity and surface habitats, the radiator surface and radiator heat pipes are made out of Aluminum 5052 and filled with an aluminum honeycomb core composed of the same alloy. The honeycomb core assumed to be bounded by two aluminum plates with a thickness of .794 millimeters to increase rigidity, and to ensure that the radiating surface was uniform. This type of aluminum was chosen due to its low reactivity, low corrosion, high thermal conductivity, and high strength [71]. We chose to use an aluminum honeycomb core as it offers excellent strength for its weight, and has a high stiffness which was important to the design of the microgravity radiators. All of the radiator designs considered have the same overall thickness of .0254 meters, which was chosen primarily to limit the total mass and material used. Finally all of the radiator designs are coated in LP-10A ($ZrSiO_4/K_2SiO_4$), which was developed by the Lockheed Missile and Space Company. LP-10A was chosen over other surface paints and finishes for its very low absorbance and very high emissivity [99].

8.3.3 Microgravity Radiators (Michael Baker)

To ensure we were capturing every possible working environment that could be experienced in a short to medium duration mission we investigated three main microgravity regimes that would influence the thermal performance of the habitat. The three microgravity regimes are in orbit around the moon, in orbit around mars, and in free space. Heat energy entering the habitat will come from both internal and external sources, and will depend on the internal components, crew size, and the location of the habitat. The power required to run the electrical components and the crew metabolic heating both add to the thermal energy in the cabin, and are assumed to be constant for a given configuration. The operating regime controls the amount of solar energy that is absorbed by the habitat in the form of heat due to solar insolation. The heat that can be radiated away will similarly change based on the operating regime, specifically with the body that is being orbited due to the black body radiation from the planet surface. Looking at those three locations and operating principles we devised six different cases that were used to guide the analysis.

Case one is that all radiator surfaces radiate to deep space on both sides where $T_{env} = 4\ (K)$. This can be seen both in orbit around a body, and in transit orbits between to bodies. Case two is that one side of the radiators radiate to free space and the other side is illuminated by the sun. Case three is that one side of the radiators radiate to free space and the other side radiates to the surface of the moon where $T_{Moon} = 279\ (K)$. Case four is when one side of the radiators radiate to the surface of the moon and the other side is illuminated by the sun. Case five and six are similar to cases three and four, but replacing the Moon with Mars. Case five is one side of the radiators radiates to Mars with a temperature of $T_{Mars} = 226\ (K)$ and the other side radiates to deep space. Finally, case six is when one side of the radiators radiate to Mars and

the other side is illuminated by the sun. Our target design was the design that would be able to operate in all six cases, while maintaining a reasonable overall mass.

Working Fluid Selection For the analysis of this system we assumed that the radiators would be run at a constant temperature and that the temperature would be the maximum temperature possible from the working fluid before it begins to boil. The process of selecting a working fluid for the system was iterative and was dependent on the necessary radiator temperature. Initially the working fluid was ammonia, due to its high conductivity and successful use in the ISS Environmental Active Thermal Control System [30]. We found, however, that using ammonia did not allow for a high enough radiator temperature due to its relatively low boiling point. The next working fluid we investigated was methanol. Methanol has a higher boiling point, giving better performance, but due to its reactivity with aluminum we decided to eliminate it as an option [38]. Ultimately, we chose Freon-11 due to the fact that it has similar thermodynamic properties to methanol, but does not react as much with aluminum [38].

	Ammonia [38]	Methanol [38]	Freon 11 [38]
Boiling point (K)	239.82	337.95	297.15
Freezing point (K)	195.42	175.25	162.15

Table 81: Boiling and freezing points of microgravity working fluid choices

Analysis Methods Heat transfer from the radiators was solved using the non-ideal Stefan-Boltzmann radiative heat transfer equation. The general form of this equation for any of the cases we investigated can be expressed as

$$Q_{int} + Q_{solar} = \epsilon\sigma A_{rad}(T_{rad}^4 - T_{env}^4)$$

Where Q_{int} is the internal power from the crew, Q_{solar} is the heating introduced by the solar insolation, and $\epsilon\sigma(T_{rad}^4 - T_{env}^4)$ represents the heat energy radiated by the radiator surfaces. For each case defined above the radiative heat transfer equation can be expressed, and reformulated to give an equation for the overall surface area of the radiators.

Case one is expressed in the standard form as

$$I_s\alpha A_{cs} + Q_{int} = \epsilon\sigma A_{rad}(T_{rad}^4 - {T_{env}}^4) \tag{57}$$

Where A_{cs} is the cross sectional area of the habitat that is being illuminated by the sun, and $Q_{solar} = I_s\alpha A_{cs}$. This equation can be rearranged to give a value for A_{rad} as

$$A_{rad} = \frac{I_s\alpha A_{cs} + Q_{int}}{\epsilon\sigma({T_{rad}}^4 - {T_{env}}^4)} \tag{58}$$

Case two can similarly be expressed in the same standard form as

$$I_s\alpha A_{cs} + \frac{I_s\alpha_{rad}A_{rad}}{2} + Q_{int} = \epsilon\sigma A_{rad}(T_{rad}^4 - {T_{env}}^4) \tag{59}$$

where α_{rad} is the radiator absorptivity. This equation was rearranged to give A_{cs} as

$$A_{rad} = \frac{I_s\alpha A_{cs} + Q_{int}}{\epsilon\sigma({T_{rad}}^4 - {T_{env}}^4) - \frac{I_s\alpha_{rad}}{2}} \tag{60}$$

Cases three and four, as well as cases five and six, share the same form. The distinguishing factor between the cases is the values that are used for the environment temperature and for the solar insulation constant. For cases three and four the standard form is expressed as

$$I_s\alpha A_{cs} + Q_{int} = \epsilon\sigma\frac{A_{rad}}{2}(T_{rad}^4 - {T_{env}}^4) + \epsilon\sigma\frac{A_{rad}}{2}(T_{rad}^4 - {T_{planet}}^4) \tag{61}$$

which can be rearranged to give the form

$$A_{rad} = \frac{I_s \alpha A_{cs} + Q_{int}}{\frac{\epsilon\sigma}{2}({T_{rad}}^4 - {T_{env}}^4) + \frac{\epsilon\sigma}{2}({T_{rad}}^4 - {T_{planet}}^4)} \tag{62}$$

Finally cases four and six are similar to cases three and five, only now there is an additional term in the Q_{in} portion of the equation due to the solar insolation on the radiator face. Cases four and six can be expressed in the standard form as

$$I_s \alpha A_{cs} + I_s \alpha_{rad} \frac{A_{rad}}{2} + Q_{int} = \epsilon\sigma \frac{A_{rad}}{2}(T_{rad}^4 - {T_{env}}^4) + \epsilon\sigma \frac{A_{rad}}{2}(T_{rad}^4 - {T_{planet}}^4) \tag{63}$$

and after similar rearrangement is expressed as

$$A_{rad} = \frac{I_s \alpha A_{cs} + Q_{int}}{\frac{\epsilon\sigma}{2}({T_{rad}}^4 - {T_{env}}^4) + \frac{\epsilon\sigma}{2}({T_{rad}}^4 - {T_{planet}}^4) - \frac{I_s \alpha_{rad}}{2}} \tag{64}$$

The amount of heat energy that is introduced to the system depends only on the cross-sectional area of the surface that the sun is illuminating. Generally this would depend on the orientation of the spacecraft with respect to the surface of the sun, but for this analysis a 'worst case orientation' is assumed to give a conservative estimate. Finally, each of the equations above is solved for all of the different volumes we are investigating using the values presented in table 82.

Variable	$Q_{int}(W)$	α_{rad}	ϵ	$T_{rad}(K)$	$I_{s,Moon}(W/m^2)$	$I_{s,Mars}(W/m^2)$	$A_{cs,20}$ (m^2)	$A_{cs,40}$ (m^2)	$A_{cs,80}$ (m^2)	$T_{moon}(K)$	$T_{mars}(K)$
Value	6356	.12	.9	296	1370	595	13.0	25.7	36.1	279	226

Table 82: Variables and their respective values for microgravity calculations

Results From the given analysis the required radiator areas to sufficiently cool the habitat is determined for each case and volume. Generally, we can also predict which case would be the most challenging to cool by looking at the area required to reject all excess heat from the habitat. From table 83, we can see that case 4, where the spacecraft is in orbit around the moon with sunlight striking the radiators, is the most challenging to cool. For these habitat designs we chose the system that could successfully cool the most challenging environment, with all additional heat rejection capacity acting as overhead. This choice corresponds to a minimum radiator surface area of 85.1 meters squared, which corresponds to an 80 meters cubed habitat in a sun lit orbit around the moon. This design choice allows for one radiator design that can be used for all near term missions.

Case 1	A_{rad} (m^2)	Case 4	A_{rad} (m^2)
H_{20}	22.6	H_{20}	56.7
H_{40}	28.9	H_{40}	72.3
H_{80}	33.9	H_{80}	85.1
Case 2	A_{rad} (m^2)	Case 5	A_{rad} (m^2)
H_{20}	28.6	H_{20}	22.9
H_{40}	36.6	H_{40}	26.2
H_{80}	43.0	H_{80}	28.8
Case 3	A_{rad} (m^2)	Case 6	A_{rad} (m^2)
H_{20}	37.3	H_{20}	25.7
H_{40}	47.7	H_{40}	29.4
H_{80}	56.0	H_{80}	32.4

Table 83: Radiator size for microgravity habitats

Design The microgravity design regime does not pose many immediate difficulties structurally. Most if not all of the loads imparted on the system would come at launch and these loads can be minimized by using a deployable design. For this reason, and to decrease the overall launch envelope of the vehicle, we chose to use a deployable radiator design using a scissor mechanism. Initial designs had only one large deployable radiator that would have a total surface area of 85.1 m^2, however, this was abandoned due to the fact that having a large amount of mass extended from the center of the habitat would make attitude control far more difficult than if it were equally spaced around the system. The design which followed as a result of that decision was an array of four deployable radiators, each with 6 panels with dimensions of 1.25 by 1.42 m^2 and a total surface area of 85.2 m^2. Internally, in addition to the previously stated radiator design components, we assumed an equal spacing of 8 heat pipes that would run the length of the deployed radiator system and return to the habitat.

Overall, this design has an estimated mass of 709 kilograms for the radiators, and closer to 1400 kilograms for the radiators and their structure. The structural mass estimate came from finding the volume of the structural components in the CAD assemblies, and comparing that mass to the current Thermal Radiator Rotary Joint used on the ISS. The CAD itself is not very high fidelity, so we assumed a reduction in overall volume of the mounting mechanism by one quarter of the volume depicted in the CAD model. Ultimately we found that the mass of one mounting mechanism to be around 168 kilograms compared to 420.5 kg for the ISS TRRJ [30]. Our system is far less complicated than the system employed on the ISS, so a reduction in overall system mass was expected. Finally the mass of the scissor arms was found in a similar way, and it amounted to 23 kilograms for the entire system. Ultimately, the overall system mass meets the reasonable mass estimate we were attempting to achieve.

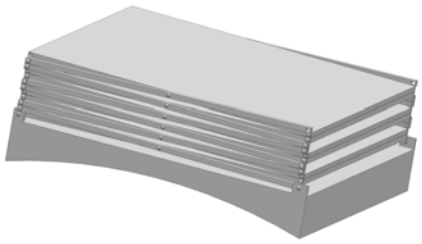

Figure 203: Microgravity radiator in the stowed configuration

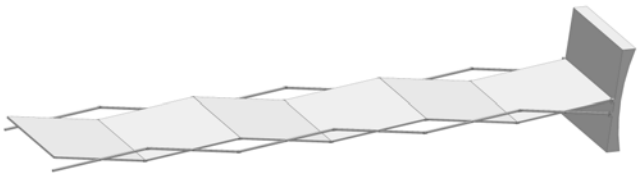

Figure 204: Microgravity radiator in the deployed configuration

Conclusions As it relates to the target of minimizing functional crew volume, this analysis shows that, for any near term mission NASA would undertake, all volumes in the range of 20 to 80 cubic meters can be successfully cooled using a deployable radiator with Freon-11 as the working fluid. Through a similar analysis, one could find an effective radiator system to best fit any near term mission. This design allows for simple adjustment where the number of radiator panels can be changed to fit the requirements of the mission, while leaving the remainder of the design constant.

The results of our microgravity radiator required area analysis can give further insight into the cost of a mission by giving a means to estimate the mass for all volumes and scenarios we analyzed without rigorously designing the system. Table 84 gives estimates of the mass of the radiators calculated by multiplying a reference radiator density by the radiator volume for the different cases and habitat volumes. The reference radiator density was found by dividing the total radiator mass we calculated above by the overall radiator

volume and has a value of $\rho_{rad} = 655$. This is useful information to consider because it can offer a clear look into the required mass of the radiators, which can then be used to make more informed decisions about the allocation of mass in the remainder of the habitat. This mass estimate analysis does not include the mass of the system that would be deploying these radiators, but generally speaking that system would scale with the mass of the radiators, thus decreasing as the radiator mass decreases.

Case 1	Mass (kg)	Case 4	Mass (kg)
H_{20}	188	H_{20}	472
H_{40}	240	H_{40}	602
H_{80}	282	H_{80}	708
Case 2	Mass (kg)	Case 5	Mass (kg)
H_{20}	238	H_{20}	191
H_{40}	304	H_{40}	218
H_{80}	358	H_{80}	240
Case 3	Mass (kg)	Case 6	Mass (kg)
H_{20}	311	H_{20}	214
H_{40}	397	H_{40}	245
H_{80}	466	H_{80}	269

Table 84: Radiator masses for all investigated microgravity habitats and volumes

8.3.4 Surface Habitats (Michael Baker)

Surface environments differ from microgravity environments in the structural challenges that come from moving to an environment where structural components are under constant load. A more structurally sound design must be developed that takes advantage of the spacecraft structure to withstand these new loads. Two main designs were analyzed to determine the most efficient radiator system for the surface habitats. Both designs have the radiators mounted to the external surface of the habitat. Design one would be static, and design two would be able to deploy to face upwards away from the surface of the planet. Overall, design one is a more simple approach that would minimize mass added to the system by minimizing necessary structure. It suffers, however, from losses in efficiency due to the fact that some portions of the radiators would be radiating to the surface of the planet. Design two overcomes these losses in efficiency by maneuvering the radiator surfaces to always radiate to deep space, but this added performance comes with additional structure and in turn adds more mass to the system.

Analysis was done for both designs and it was determined that design one was the preferred system. Since we could not perform a full thermodynamic loop analysis, we were unable to prove that the deployable radiator of design two would be more efficient than design one. Due to the fact that design two would always add mass and structure to the system, if we could not prove better efficiency, the design will be less feasible. We chose to focus on the static radiators of design one that mount to the surface of the habitat because we can design the surface area of the habitat with more certainty.

Design Unlike the microgravity habitat, there is not one design that can be developed for both orientations that would successfully cool all surface habitats. There instead needs to be two separate designs that conform to the geometric differences in the vertical and horizontal habitat orientations. In both the vertical and horizontal case a similar approach was used. Each habitat would be equipped with radiators that are mounted to its surface. The radiators fall into two general forms: dome radiators and panel radiators. For each case the radiator that was facing directly away from the surface of the planet was called the critical radiator because it radiates entirely to deep space, and subsequently radiates the most thermal energy. For all other radiators, they were assumed to radiate half to deep space, and half to the surface temperature of the planet due to black body radiation effects at the planet's surface [24]. In all cases this was an overestimate due to the fact that nothing acts as a perfect black body, but the assumptions were conservative and would

give additional overhead to our analysis. A similar design approach has been investigated before in projects like NASA ECLIPSE, but those designs did not investigate how volume, orientation, and the planet on which the habitat is stationed affects radiator size and working fluid temperature [37].

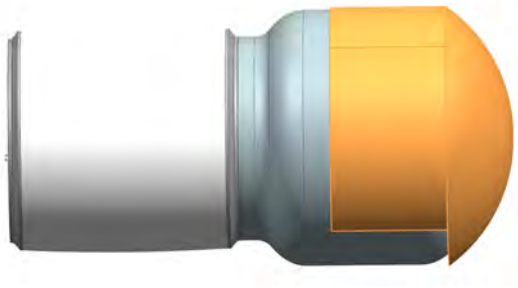

Figure 205: 20 meters cubed horizontal habitat with horizontal radiators

Figure 206: 80 meters cubed vertical habitat with vertical radiators

In the vertical habitat there are six panel radiators that have a width of one sixth of the circumference. The seventh radiator is a dome radiator, acting as the critical radiator of the system. To integrate with the full system CAD one of the six panel radiators needed to be shrunk slightly to account for the height of the airlock. The change was small, however, so the impact on the overall analysis would be minimal. In the horizontal habitat there are three panel radiators, one of which is the critical radiator. Each panel radiator has a length equal to the length of the straight portion of the habitat, and a width equal to one quarter of the circumference. Additionally, there is one dome radiator that will be attached to the side of the habitat not being used for the airlock.

	$20m^2$	$40m^2$	$80m^2$
A_{dome}	15.7	15.7	27.1
A_{Vpanel}	1.94	5.27	6.18
A_{Hpanel}	5.81	15.8	18.5

Table 85: Surface radiator panel areas

The similarities between the vertical and horizontal habitats allow for a very similar analysis process, beginning with calculating solar flux. For both orientations, the cross-sectional area of the habitat which experiences solar insolation can be approximated by a function with respect to the solar angle incident on the habitat. This is given for the vertical habitat by

$$A_{cs} = (2Rh + \pi R^2)sin(\theta) + \pi R^2 cos(\theta) \tag{65}$$

and for the horizontal habitat by

$$A_{cs} = (2Rh + \pi R^2)cos(\theta) + \pi R^2 sin(\theta) \tag{66}$$

These equations allow us to find the maximum solar flux for both configurations by finding the maximum cross-sectional area and multiplying that value by the solar insolation constant at each planet surface. The values of the maximum cross-sectional area are the same for both orientations but the solar angle at which the maximum occurs will be different for both cases. The maximum solar flux for all three habitat volumes being analyzed was calculated and tabulated in 86.

	H_{20}	H_{40}	H_{80}
$A_{cs}(m^2)$	23.6	35	50.2
$Q_{solar,Moon}(W)$	3890	5750	8270
$Q_{solar,Mars}(W)$	1680	2500	3580

Table 86: Cross sectional area and solar heating values for all habitat volumes

To simplify our analysis we assumed the worst case scenario where the solar insolation was at a maximum for all external temperatures, and all locations. This is not strictly the case due to the fact that the temperature and solar insolation vary with latitude, but a conservative estimate allows for additional design flexibility.

Mass Estimates Unlike in the microgravity case, the radiator volume is restricted by the external surface area of the habitat, so a mass estimate can be found as soon as the dimensions of the habitat are known. To find the radiator mass we assumed a similar radiator panel design to the design chosen for the microgravity radiators. We found the total density of the radiator panels by comparing the ratio of overall radiator panel mass to the overall radiator panel volume found previously in the microgravity mass estimation. By performing this calculation, we found an reference radiator density $\rho_{rad} = 655$ that was used to find the mass of the surface radiators.

	H_{20}	H_{40}	H_{80}
Vertical radiator volume (m^3)	1.02	1.52	2.18
Horizontal radiator volume (m^3	1.32	2.08	2.92
Mass (vertical) (kg)	665	997	1430
Mass (horizontal) (kg)	867	1370	1920

Table 87: Mass estimates for given radiator volumes and orientations.

Analysis The analysis used to quantify the radiator temperatures begins with the same fundamental equation as the previous analysis done on the microgravity radiators. The general radiative heat transfer equilibrium can be given as

$$Q_{int} + Q_{solar} = \epsilon\sigma A_{rad}(T_{rad}^4 - T_{env}^4) \tag{67}$$

that can then be solved for, in this case, the temperature of the radiators as a function of the environment temperature and the number of working radiators. To simplify calculations we decided to take the temperature of space to be zero for all surface radiator calculations. To account for the variation in the radiator area, the A_{rad} portion of this expression must be appropriately represented by the number of active panels. In both the vertical and horizontal cases additional variables n_{crit}, n_{panel}, and n_{dome} can be introduced to represent whether or not the critical radiator is operating, the number of active panel radiators, and the number of active dome radiators, respectively. In the case of the vertical orientation, A_{rad} can be given as

$$A_{rad} = n_{crit}A_{dome} + n_{panel}A_{panel} \tag{68}$$

Leading to the general thermodynamic expression to be given as

$$I_s\alpha A_{cs} + Q_{int} = \epsilon\sigma(n_{crit}A_{dome} + n_{panel}A_{panel})(T_{rad}^4 - {T_{env}}^4) \tag{69}$$

Carrying through the subsequent algebra the final equation for radiator temperature can be given as

$$T_{rad,V} = \left[\frac{1}{n_{crit}A_{dome} + n_{panel}A_{panel}}\left(\frac{Q_{int} + Q_{solar}}{\epsilon\sigma} + \frac{n_{panel}A_{panel}T_{planet}^4}{2}\right)\right]^{\frac{1}{4}} \tag{70}$$

Similarly for the horizontal orientation the radiator area can be expressed as,

$$A_{rad} = n_{crit}A_{panel} + n_{panel}A_{panel} + n_{dome}A_{dome} \tag{71}$$

that can be reformed to give an expression for the radiator temperature

$$T_{rad,H} = \left[\frac{1}{n_{dome}A_{dome} + n_{crit}A_{panel} + n_{panel}A_{panel}}\left(\frac{Q_{int} + Q_{solar}}{\epsilon\sigma} + T_{planet}^4\left(\frac{n_{dome}A_{dome}}{2} + \frac{n_{panel}A_{panel}}{2}\right)\right)\right]^{\frac{1}{4}} \tag{72}$$

Solving the above expressions for the different environment temperatures and numbers of radiators gives a comprehensive look at the radiator temperatures necessary to adequately cool the habitats in those specific scenarios.

Variable	$Q_{int}(W)$	α_{rad}	ϵ	$T_{max,lunar}(K)$	$T_{min,lunar}$	$T_{max,Mars}(K)$	$T_{min,Mars}(K)$
Value	6356	.12	.9	449.2	50.2	280.2	146.2

Table 88: Variables and their respective values for surface radiator calculations

Working Fluid Selection Similar to the microgravity habitat, the working fluid was selected to match the performance characteristics that were determined by the surface habitat radiator temperature analysis. Initially, the working fluid we investigated was a 60 percent mix by volume of Ethylene Glycol and water. This mix gave us reasonable boiling point and freezing point temperatures that worked well for all of our habitat volumes and external temperatures [104]. We discovered, however, that once our analysis was expanded to include the loss of the critical radiator the temperature of the working fluid was well above the boiling point of 60 percent Ethylene Glycol and water. We chose to change the working fluid to pure Ethylene Glycol because it would allow us to operate with a relatively high degree of redundancy in both nominal operation, and in the case of a critical radiator failure due to its higher boiling point [104].

	T_{boil} (K) [104]	T_{freeze} (K) [104]
60 percent Ethylene Glycol and Water	384.25	220.35
Ethylene Glycol	470.15	260.35

Table 89: Boiling and freezing points of different percentage mixtures of Ethylene Glycol and Water

Volume (m^3)	Orientation	$T_{rad,max}(K)$	$T_{rad,min}(K)$	Radiator Layout
20	Horizontal	431	431	Top
		394	311	Top, 1 dome
		407	363	Top, 1 side
		398	328	Top, 2 sides
		391	293	Top, 1 side, 1 dome
		389	279	Top, 2 sides, 1 dome
40	Horizontal	350	350	Top
		365	295	Top, 1 dome
		365	294	Top, 1 side
		369	266	Top, 2 sides
		369	266	Top, 1 side, 1 dome
		371	248	Top, 2 sides, 1 dome
80	Vertical	334	305	Top, 1 panel
		342	292	Top, 2 panel
		347	282	Top, 3 panel
		351	273	Top, 4 panel
		354	265	Top, 5 panel
		357	259	Top, 6 panel

Table 90: Radiator maximum and minimum operating temperatures on the surface of the Moon

Volume (m^3)	Orientation	$T_{rad,max}(K)$	$T_{rad,min}(K)$	Radiator Layout
20	Horizontal	406	406	Top
		313	294	Top, 1 dome
		351	342	Top, 1 side
		325	310	Top, 2 sides
		301	278	Top, 1 side, 1 dome
		292	265	Top, 2 sides, 1 dome
40	Horizontal	324	324	Top
		290	274	Top, 1 dome
		290	274	Top, 1 side
		275	248	Top, 2 sides
		275	249	Top, 1 side, 1 dome
		267	232	Top, 2 sides, 1 dome
80	Vertical	283	277	Top, 1 panel
		277	266	Top, 2 panel
		273	257	Top, 3 panel
		269	249	Top, 4 panel
		266	243	Top, 5 panel
		263	237	Top, 6 panel

Table 91: Radiator maximum and minimum operating temperatures on the surface of Mars

Analysis Results We can see that, when using Ethylene Glycol as the working fluid, we would be able to adequately cool the system with only the critical radiator and one panel radiator for the vertical orientation, and only the critical radiator for the horizontal orientation habitats. This allows for a significant amount of operational overhead, where as many as five of the panel radiators can fail in the vertical 80 meters cubed habitat and as many as two panel radiators, or the dome, can fail in the horizontal habitats.

Volume (m^3)	Orientation	$T_{rad,max}(K)$	$T_{rad,min}(K)$	Radiator Layout
20	Horizontal	427	336	1 dome
		484	431	1 side
		440	363	2 sides
		415	311	1 side, 1 dome
		408	293	2 sides, 1 dome
40	Horizontal	434	351	1 dome
		434	350	1 side
		409	294	2 sides
		409	295	1 side, 1 dome
		399	266	2 sides, 1 dome
80	Vertical	508	464	1 panel
		457	390	2 panel
		435	353	3 panel
		423	328	4 panel
		415	310	5 panel
		409	297	6 panel

Table 92: Radiator temperatures if critical radiator is lost on the surface of the Moon

Volume (m^3)	Orientation	$T_{rad,max}(K)$	$T_{rad,min}(K)$	Radiator Layout
20	Horizontal	417	316	1 dome
		467	406	1 side
		429	293	2 sides
		408	293	1 side, 1 dome
		402	276	2 sides, 1 dome
40	Horizontal	421	324	1 dome
		421	324	1 side
		401	272	2 sides
		401	272	1 side, 1 dome
		394	246	2 sides, 1 dome
80	Vertical	477	421	1 panel
		436	354	2 panel
		419	320	3 panel
		410	298	4 panel
		404	282	5 panel
		400	269	6 panel

Table 93: Radiator temperatures if critical radiator is lost on the surface of Mars

An additional challenge comes when the failure of the critical radiator is considered in both cases. For the vertical habitat, there would need to be a minimum of two panel radiators operational to make up for the lost performance from the critical radiator. Similarly, for the 20 m^3 horizontal habitat if the critical radiator was to fail it would need to be replaced by the dome radiator, by both of the panel radiators, or by one panel and one dome radiator. In the case of a critical radiator loss in the 40 m^3 habitat the habitat can function with at least the dome radiator, or one panel radiator running.

Finally, some upper bounds are placed on performance of the system when all radiators are operational on the surface of Mars. If the habitat is located in an area where the temperature is at, or near, the minimum surface temperature, such as at the poles, having too many radiators operational runs the risk of freezing the working fluid. For both the 40 and 80 meters cubed habitats, if too many radiators are run at once then the temperature of the working fluid in the radiators would fall below the freezing point of the working fluid. To avoid freezing of the fluid, the horizontal habitat would only be able to run with the critical radiator, the critical and the dome radiators, or the critical and one panel radiators. For the 80 meters cubed habitat, the maximum number of radiators that can be run simultaneously is the critical radiator and three panel radiators. In all cases these restrictions are lifted when the habitat is positioned in a location where the temperature is at or near the max temperature on Mars, such as on the equator.

Conclusions The surface radiator temperature analysis shows us that all habitat volumes in the range considered could be designed in such a way that they are successfully cooled when Ethylene Glycol is used as the working fluid. The final designs we chose offered the greatest amount of operational overhead, but the analysis performed could be used to find the corresponding radiator size for any mission should mass requirements or other mission guidelines constrict radiator size.

This analysis can also be used to investigate overall system optimization by performing mass estimates for the different combinations of radiators whose performance we quantified in our analysis. Performing this mass estimate allows us to trade off between operational overhead, and overall system mass when not all radiators are necessary to provide nominal performance. For example, the analysis showed that, given a failure in the critical radiator for the vertical habitat, there would need to be two radiators to allow for nominal performance. If we decide that only one excess panel radiator is enough from an investigation of

radiator panel reliability, we can reduce the overall radiator count from one dome radiator and six panel radiators to one dome radiator and three panel radiators. This would mean a reduction in mass from 1430 kilograms to 939 kilograms from Table 94. This would adjacently impact habitability by offering additional mass for additional components for the crew.

Volume (m^3)	Radiator Layout	Volume (m^3)	Mass (kg)
20	Top	.31	202
	Top, 1 dome	.71	463
	Top, 1 side	.62	404
	Top, 2 sides	.92	605
	Top, 1 side, 1 dome	1.01	655
	Top, 2 sides, 1 dome	1.32	867
40	Top	.56	368
	Top, 1 dome	.96	629
	Top, 1 side	1.12	736
	Top, 2 sides	1.68	1100
	Top, 1 side, 1 dome	1.52	997
	Top, 2 sides, 1 dome	2.08	1370
80	Top, 1 panel	.94	613
	Top, 2 panel	1.18	776
	Top, 3 panel	1.43	939
	Top, 4 panel	1.68	1100
	Top, 5 panel	1.93	1270
	Top, 6 panel	2.18	1430

Table 94: Mass and Volume for each combination of radiators investigated

8.4 Power Generation (Ramin Rafizadeh)

The overall goal of generating power for the proposed habitat is to maximize efficiency, safety, reliability, and radiation harness while minimizing mass, volume, thermal requirements, and cost. The complete electrical power system of our habitat will take comprise of a power source, energy source, power regulators and controllers, and a power distribution system. The thee most important components to sizing an electrical power system comprises of demand for average and peak electrical power, orbital inclination, and mission life. The preliminary steps required to properly size a power generating system are as follows:

1. Identify requirements
2. Select and size power source
3. Select and size energy source
4. Identify power regulation, control, and distribution
5. Estimate the mass, avg, peak power requirements

Photovoltaic Cell are connected in series to form a string, as the number of cells in a string determines the voltage. A Solar Array is made up of one or more strings in parallel. This is an automatic candidate for power generation if less than 15 kW of power is required. Photovoltaic sources are not an attractive power source for interplanetary missions to the outer planets because solar radiation decreases with the square of the distance. They are also a poor power source for a mission lasting longer than 10 years because of the natural degradation of the solar array. It is required to size a solar array to meet power requirements at end of life (EOL) due to the inherent degradation of solar arrays. Best suitable cells with respect to cost, performance, high efficiency and radiation resistance are gallium-arsenide (GaAs), with thousands of proven

reliable performance with on-orbit data. In the US, these cells are produced by Emcore and Spectrolab.

The following steps were performed to determine the appropriate solar array size for the system. First, it is required to determine requirements and constraints for the power subsystem, which include the average power required during daylight and eclipse, habitat altitude and eclipse duration, and the design lifetime. The amount of power that must be produced by the solar arrays, P_{sa}, needs to be determined. Next, we must select the type of solar cell and estimate power output, Po, with the sun normal to the surface of the cells. Additionally, one must determine the beginning of life (BOL) and end of life (EOL) power production capacity, P_{BOL} and P_{EOL}, per unit area of the array. Next, we must estimate the solar array area, A_{sa}, required to produce the necessary power, P_{sa}, based on P_{EOL}. Finally, we can estimate the mass of the solar array.

A solar array illumination intensity typically depends on orbital parameters such as the Sun incident angles, eclipse periods, solar distance, and concentration of solar energy. Tracking and pointing mechanisms on the solar array often adjust to these influences. To estimate the solar array area we first need to determine how much power the solar array must provide during the daylight to power the spacecraft for the entire orbit, P_{sa}, estimated from Equation 73:

$$P_{sa} = \frac{\frac{P_e T_e}{X_e} + \frac{P_d T_d}{X_d}}{T_d} \tag{73}$$

For our system, Xe = 0.65 and Xd = 0.85. Pe and Pd are the spacecraft power requirements during eclipse and daylight, and Te and Td are the lengths of the period of orbits. $P_e = P_d = 5.96kW$. $T_e = T_d$= 29 days 12 hours 44 min = 42524 min. Thus, $P_{sa} = 17.38kW$. GaAs has a performance degradation of 2.75% per yr, Si: 3.75% per yr, and Tripple Junction 0.5% per yr. Si has a lower cost but not suitable for radiation exposure. GaAs has an efficiency of 21.8% with a solar constant of 1368 W/m^2 at the top of the earth's atmosphere. Thus, the ideal performance output per unit area, Po, is 298 W/m^2.

An analysis was done on the different types of solar cells and their respective power outputs. Si: $P_o = 0.148 * 1368W/m^2 = 202W/m^2$. GaAs: $P_o = 0.185 * 1368W/m^2 = 253W/m^2$. Multi-junction: $P_o = 0.28 * 1368W/m^2 = 383W/m^2$. This information can be used to determine the solar array area and mass by applying Equation 74:

$$A_{sa} = \frac{P_{sa}}{P_{EOL}} \tag{74}$$

From the above analysis $P_{sa} = 17383W$ and $P_{EOL} = 293W/m^2$, resulting in $A_{sa} = 59.3m^2$. Assuming GaAs (MJ) has a mass of $2.8kg/m^2$, the overall solar array will have a mass of 166kg.

We will consider and identify losses inherent to panel assembly due to components such as diodes, interconnect cabling, transmission losses. Some of these thermal losses need to be considered in our analysis. The temperature of a typical flat solar panel receiving normal incident radiation ranges from about 67 C in LEO to 53 C in GEO. The reference temp for silicon solar cells is about 28 C, with performance falling off 0.5% per degree C above 28 C.

Solar array mounting configurations are either planar or concentrator, and each type can be body mounted or panel mounted. Most solar applications take advantage of the planar array method where solar cells are mounted to a hard surface. With respect to thermal design, the hardware mounting the panel to the spacecraft body is typically a composite panel with either insulated aluminum or carbon facesheets. Concentrator solar arrays increase the output of the entire array by using mirrors or lenses to focus more solar energy on a smaller portion of the array. This method is known for adding significant complexity to a system. With respect to a thermal standpoint, this design can easily approach the material thermal limits, thus it is important to take this into consideration. Panel mounted solar arrays are typically used in the application of 3 axes stabilized spacecraft. This method would nominally track the ideal angle for maximum illumination. Some drawbacks about this method entail the less effective sun incident angle and increased array temperature which would result in lower efficiency in orbit.

Further analysis was done on array sizing considering degradation. At the beginning of life, the arrays power per unit area is

$$P_{BOL} = P_o I_d cos(\theta) \tag{75}$$

Where P0 is the ideal solar cell output performance, and Id is the inherent degradation followed by the solar incident angle. Lifetime degradation can be estimated using the Equation 76

$$L_d = (1 - D)^L \tag{76}$$

where D is the degradation per year for a specific solar array, and L is the lifetime in years. The arrays performance at the end of the life is estimated with Equation 77

$$P_{EOL} = P_{BOL} L_d \tag{77}$$

Estimating a mission lifetime of 25 years, $P_{EOL} = P_{BOL} * 0.66$.

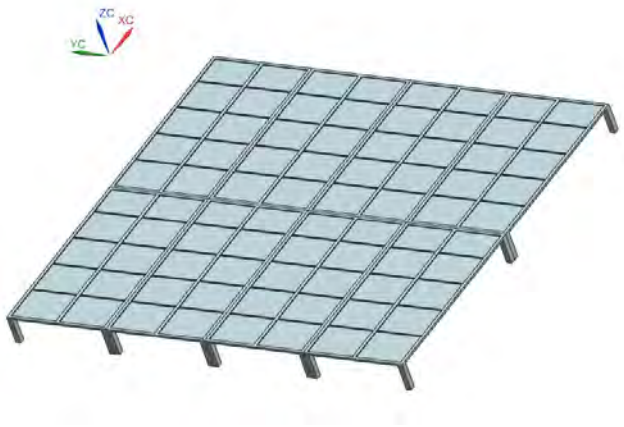

Figure 207: CAD of required solar array

8.5 Energy Storage (Ramin Rafizadeh)

There are two types of batteries used in spacecraft, due to the nature of the long-duration mission the x-hab team proposes, this document will discuss secondary (rechargeable) batteries only. Secondary batteries are capable of many thousands of charge/discharge cycles. A battery consists of individual cells internally connected in series, the number of cells determines the voltage of the battery. The total energy stored in the batteries can be measured with ampere-hour capacity or watt-hour capacity, the later of the two simply takes ampere-hours times operating voltage. Some simple examples of primary batteries are Li-SOCI2, LiSO2, and LiMnO. Some examples of secondary batteries include Li-Ion, Mi/MH, Ni/H2, Ni/Cd, and Pb/PbO.

As stated before, secondary battery cells are capable of converting chemical energy to electrical energy and vice versa, thousands of times. Some important characteristics needed to analyze batteries further is the depth of discharge (DOD) and state of charge (SOC). Simply put, the DOD is the percentage of the total battery used during a discharge cycle. The SOC is the total amount of remaining battery capacity at any time.

During the 1980s the most common type of battery used in a space environment was Nickel-Cadmium (Ni-Cd). This common battery was replaced by Nickel-Hydrogen (Ni-H2) during the 1990s. Ni-H2 batteries are all encapsulated in a pressure vessel to mitigate the inherent internal pressure of the hydrogen supply. Lithium-ion (Li-Ion) battery technology provides advantages with respect to volume and energy density. Additionally, this type of battery has a higher recharge efficiency, requiring less complex and less thermally costly controllers. Another advantage of Li-Ion batteries is their very low (on the order of 5%) self-discharge

rate. Li-Ion systems provide a 65% volume advantage and 50% mass advantage in comparison to older energy storage systems described above. One major drawback to Li-Ion systems is their tighter thermal control requirements which range between 10-25 C.

In order to effectively size an energy storage system, we must follow the following steps. We must first determine the energy storage requirements, which depend on a multitude of different factors such as mission length, eclipse length and frequency, depth of discharge, duty cycle, and bus voltage and current. Additionally, we must select the type of secondary battery most suitable for the application, in this case Li-Ion. Finally, we must determine the required battery capacity, taking into consideration the total number of batteries and the transmission efficiency between the battery and the load.

The ideal battery capacity is the average eclipse load, P_e, times the eclipse duration, T_e. There are a few transient terms that need to be considered including but not limited to the battery to load transmission efficiency, n, number of batteries, N, and the depth of discharge, DOD, constraints. The total capacity of the energy storage system can be estimated from Equation 78:

$$C = \frac{P_e T_e}{(DOD)Nn} \tag{78}$$

Where $P_e = 2956W$, $T_e = 42526min$, $n = 0.9$, and $DOD = 0.4$. Therefore, the total capacity of the system is required to a minimum of $C = 155.186kW(4310Ah$ with 36 V bus). Given that Li-Ion batteries have a mass density of approximately 125 W/kg, a total subsystem mass of 1242 kg can be estimated.

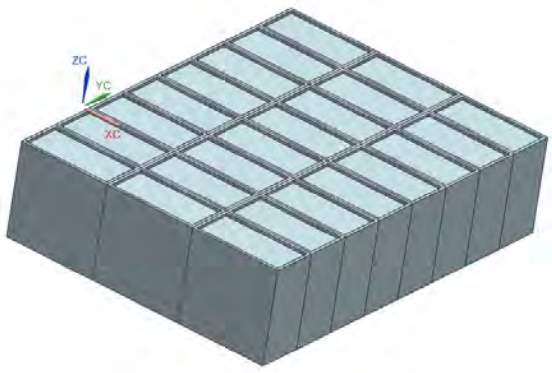

Figure 208: CAD of required battery array

8.6 Power and Thermal Conclusion

9 Systems Integration

9.1 Overview (Blaire Weinberg)

The majority of the systems work was done towards the end of the semester, and was tasked with integrating all of the CAD work done by all the other teams into fully functioning mockups of habitats. This involved getting updated CAD from others, deciding what would fit where, and making decisions on what would have to go in space constrained situations.

The following sections outline what each of the individual habitats look like, the components in them, and total volume and mass estimates. Any conclusions and recommendations that come out of there are

described in both §9.8 and §10.

The following sections contain color coded images of the interior of each habitat. The color code is described in Table

Color	Designation
Life Support	Brown
Hygiene and Food	Purple
Fire Suppresion	Pink
Science	Yellow
Crew Berthing	Teal
Storage	Red
Exercise Equipment	Green
Water	Blue

Table 95: Color Code for Interior Habitat

9.2 20m^3 Microgravity Habitat (Blaire Weinberg)

A short, one word summary of the smallest microgravity habitat would be: cramped. There is very little space for additional equipment, or walking around space at all in this habitat. For this specific habitat, we were unable to fit the MSG, and instead opted for using that space for the two exercise machines, CEVIS and the treadmill.

The outside of the habitat can be seen in Figure 209. There are four radiators, where currently two are stowed (top and bottom) and two are deployed (sides). This would not be how they are used operationally, but more to show that they have two states. Additionally, there are heat exchangers on the back side of the habitat.

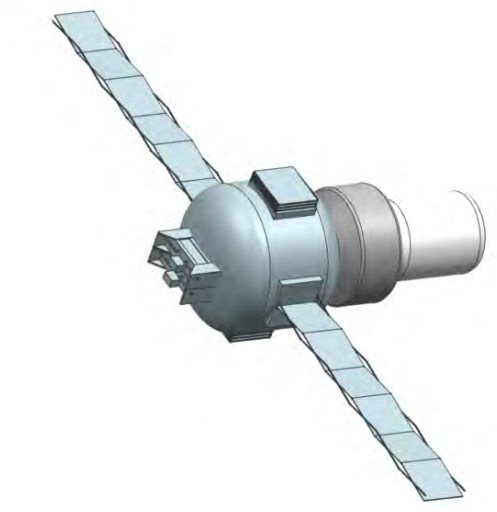

Figure 209: Exterior of the 20m^3 Microgravity Habitat

The interior of the habitat can be seen in Figure 210, where there is very little additional space for large components, such as the MSG. A fully detailed mass and volume breakdown of each individual component can be found in Table 96. Interior components in the habitat are likewise colored in this table to show precisely what is included where.

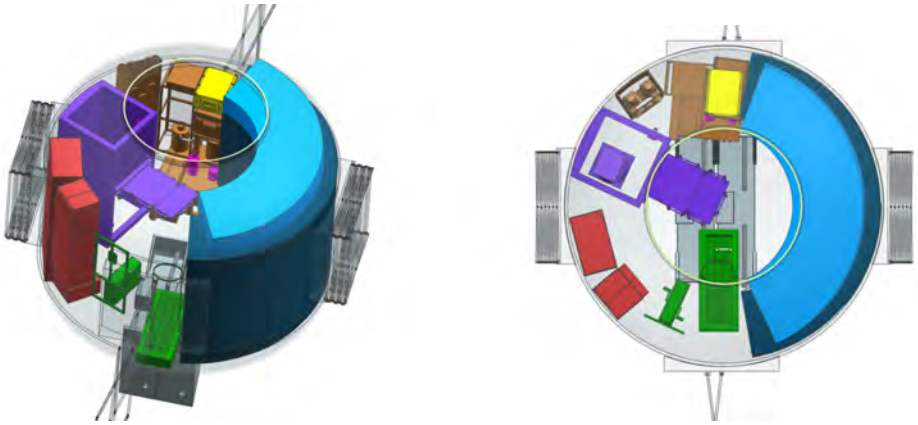

Figure 210: Interior of the 20m^3 Microgravity Habitat

Component	Component Volume (m^3)	Mass (kg)
Main Pressure Vessel	N/A	1500
Thermal Insulation	N/A	11
Solar Array	N/A	170
Battery	N/A	1200
Airlock	17	2900
Suitports	N/A	150
Radiators	1	1400
Heat Exchangers	0.09	55
Fire Detector	0.003	1.5
Fire Extinguisher	0.021	10
Dining Table	0.034	75
Shower/Bathroom	1.8	602
Toilet	0.15	50
4BMS	0.44	320
EVA Prep	0.165	48
Urine Processing	0.62	100
Condensate Processing	0.7	120
Potable Water	1.0	1030
Berths	8.2	1300
Logistics rack	0.025	45
CTB Storage Rack	1.1	400
3d Printer	0.071	45
Treadmill (TVIS-like)	0.32	200
Cycle (CEVIS)	0.080	82
Totals	**15.7**	**11,700**

Table 96: Volume and Mass Breakdown for 20m^3 Microgravity Habitat

The total component volume for this habitat design is 15.7 m^3. This includes all internal components. The airlock is not counted in this tally. Based on this component volume we determined that the total free volume is 4.3 m^3. Free volume is the amount of space not occupied by equipment. This value can be misleading as it does not include the space within the berths or other components, which is usable but dedicated. In this case, the free volume is slightly exaggerated because it does not include the glove box.

In order to include everything and make it a little less cramped, we would recommend having fewer than four crew members, or to shrink the crew berths somewhat so that less space is taken up by the berths.

There is a tight squeeze between the shower unit and the 4BMS, which may make it somewhat difficult for servicing any of the life support equipment. Additionally, the 3D printer is rather high up on the life support systems rack, so it may be difficult without having to utilize weightlessness to get to. All of the other systems were meant to be as realistic in placement for height as they could be relative to a floor design to keep astronauts as comfortable as possible.

9.3 40m^3 Microgravity Habitat (Blaire Weinberg)

The 40 microgravity habitat is probably the most adequately sized habitat that we designed, at least relative to the four crew that we were working with. For this habitat, there was a two-story design with bed and hygiene on the lower floor, and all of the science, life support, exercise equipment, and storage on the bottom.

The outside of the habitat can be seen in Figure 211. There are four radiators, where currently two are stowed (top and bottom) and two are deployed (sides). This would not be how they are used operationally, but more to show that they have two states. Additionally, there are heat exchangers on the back side of the habitat.

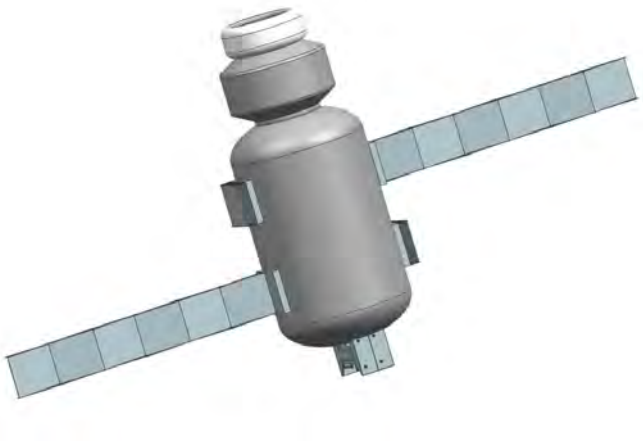

Figure 211: Exterior of the 40m^3 Microgravity Habitat

The interior of the habitat can be seen in Figure 212, where there is some additional room for components that we hadn't yet thought of, probably a good deal more storage. A fully detailed mass and volume breakdown of each individual component can be found in Table 97. Interior components in the habitat are likewise colored in this table to show precisely what is included where.

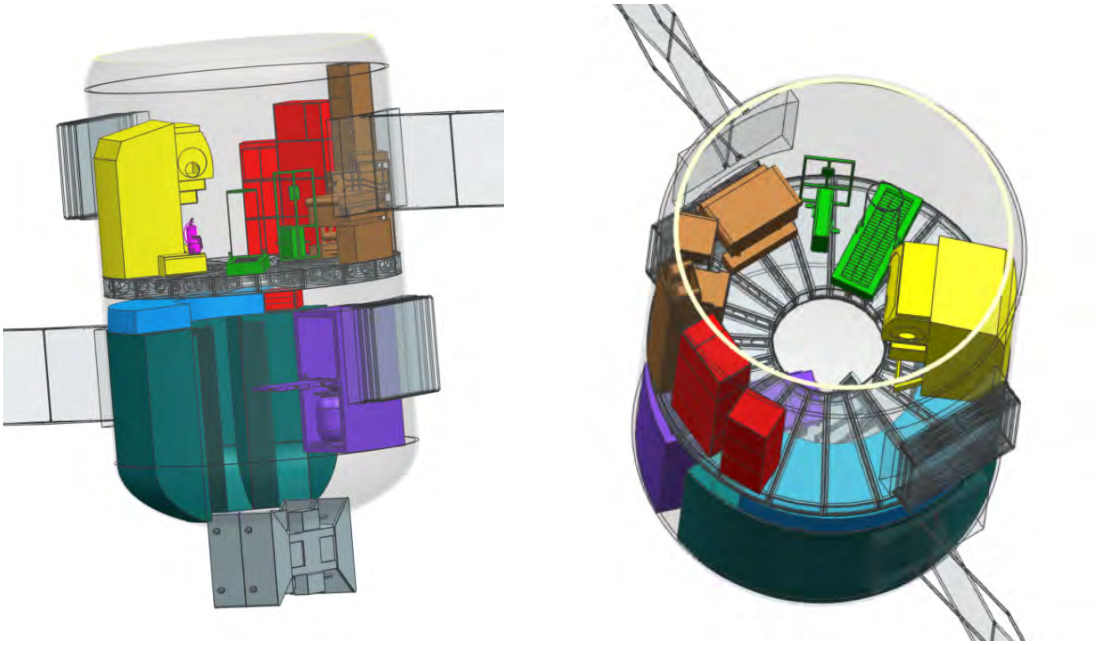

Figure 212: Interior of the 40m^3 Microgravity Habitat

Component	Component Volume (m^3)	Mass (kg)
Main Pressure Vessel	N/A	2700
Thermal Insulation	N/A	29
Solar Array	N/A	170
Battery	N/A	1200
Airlock	17	2900
Suitports	N/A	150
Radiators	1.1	1400
Heat Exchangers	0.11	69
Fire Detector	0.003	1.5
Fire Extinguisher	0.021	10
Dining Table	0.034	75
Shower/Bathroom	1.8	602
Toilet	0.15	50
4BMS	0.44	320
EVA Prep	0.165	48
Urine Processing	0.62	100
Condensate Processing	0.7	120
Potable Water	1.0	1030
Berths	8.2	1300
Logistics rack	0.025	45
CTB Storage Rack	1.1	400
3d Printer	0.071	45
Glovebox	1.81	400
Treadmill (TVIS-like)	0.32	200
Cycle (CEVIS)	0.080	82
Totals	**17.5**	**13,400**

Table 97: Volume and Mass Breakdown for 40m^3 Microgravity Habitat

The total component volume for this habitat design is 17.5 m^3. This includes all internal components. The airlock is not counted in this tally. Based on this component volume we determined that the total free volume is 22.5 m^3. Free volume is the amount of space not occupied by equipment. This value can be misleading as it does not include the space within the berths or other components, which is usable but dedicated.

There is ample additional space in this habitat for a good deal more equipment than what we have right now, yet it isn't cramped or too open. The lower floor with the crew berths can probably include some storage for food and clothing, especially in the case of a solar particle event where they need to shelter in place. The theory with isolating the life support equipment, science, and exercise equipment on the top shelf was to somewhat separate loud, noisy machinery from where the crew were sleeping. There is still some additional space for storage or equipment that could be added.

9.4 80m^3 Microgravity Habitat (Blaire Weinberg)

The 80 microgravity habitat is the most spacious design that we had, with lots of empty room. For this habitat, there was a two-story design with bed and hygiene on the lower floor, and all of the science, life support, exercise equipment, and storage on the bottom.

The outside of the habitat can be seen in Figure 213. There are four radiators, where currently two are stowed (top and bottom) and two are deployed (sides). This would not be how they are used operationally, but more to show that they have two states. Additionally, there are heat exchangers on the back side of the habitat.

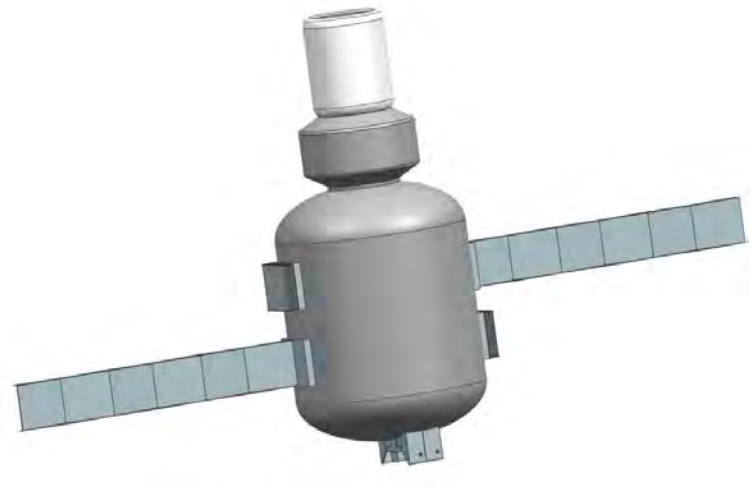

Figure 213: Exterior of the 80m^3 Microgravity Habitat

The interior of the habitat can be seen in Figure 214, where there is some additional room for components that we hadn't yet thought of, probably a good deal more storage. A fully detailed mass and volume breakdown of each individual component can be found in Table 98. Interior components in the habitat are likewise colored in this table to show precisely what is included where.

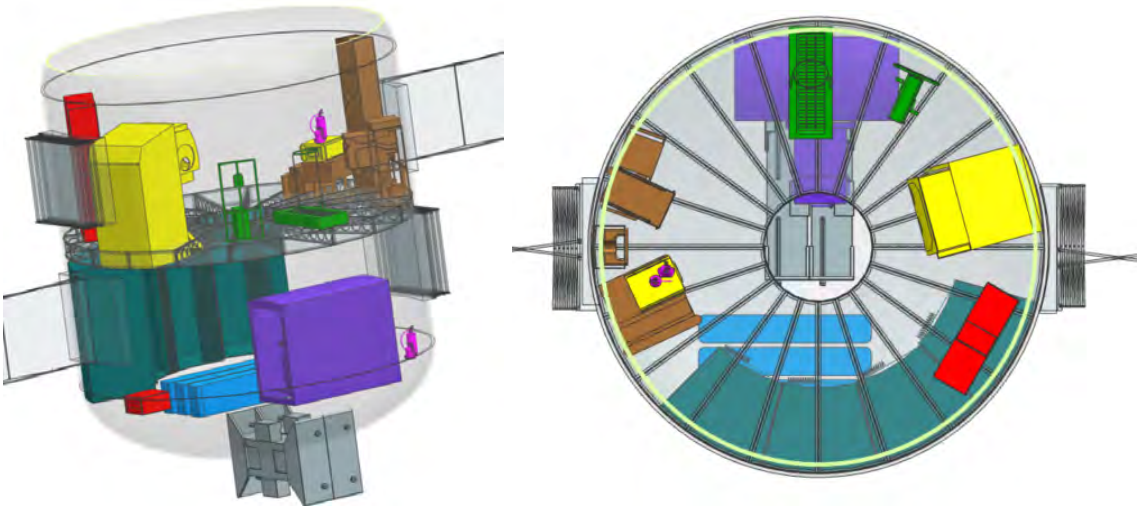

Figure 214: Interior of the 80m^3 Microgravity Habitat

Component	Component Volume (m^3)	Mass (kg)
Main Pressure Vessel	N/A	4500
Thermal Insulation	N/A	53
Solar Array	N/A	170
Battery	N/A	1200
Airlock	17	2900
Suitports	N/A	150
Radiators	1.1	1400
Heat Exchangers	0.13	80
Fire Detector	0.003	1.5
Fire Extinguisher	0.021	10
Dining Table	0.034	75
Shower/Bathroom	1.8	602
Toilet	0.15	50
4BMS	0.44	320
EVA Prep	0.165	48
Urine Processing	0.62	100
Condensate Processing	0.7	120
Potable Water	1.0	1030
Berths	8.2	1300
Logistics rack	0.025	45
CTB Storage Rack	1.1	400
3d Printer	0.071	45
Glovebox	1.81	400
Treadmill (TVIS-like)	0.32	200
Cycle (CEVIS)	0.080	82
Totals	**17.9**	**15,300**

Table 98: Volume and Mass Breakdown for 80m^3 Microgravity Habitat

The total component volume for this habitat design is 17.9 m^3. This includes all internal components. The airlock is not counted in this tally. Based on this component volume we determined that the total free volume is 62.1 m^3. Free volume is the amount of space not occupied by equipment. This value can be mis-

leading as it does not include the space within the berths or other components, which is usable but dedicated.

There is ample additional space in this habitat for a good deal more equipment than what we have right now, though there is still a lot of empty space even with that. The lower floor with the crew berths can probably include some storage for food and clothing, especially in the case of a solar particle event where they need to shelter in place. The theory with isolating the life support equipment, science, and exercise equipment on the top shelf was to somewhat separate loud, noisy machinery from where the crew were sleeping. There is still some additional space for storage or equipment that could be added. With the same equipment fitting nicely into the $40m^3$ habitat, you would need to find a lot of additional equipment to have this start to become cramped.

9.5 $20m^3$ Surface Habitat (Blaire Weinberg)

The $20m^3$ surface habitat, while cramped, is somewhat less packed than the equivalent microgravity habitat. Raised bunks help with that, allowing for narrow hallways split across the hygiene area.

The outside of the habitat can be seen in Figure 215. The radiator wraps around the backend of the habitat, like a curved camera lens. This would have cutouts for the heat exchangers and the geolab. Additionally, there are heat exchangers on the back side of the habitat.

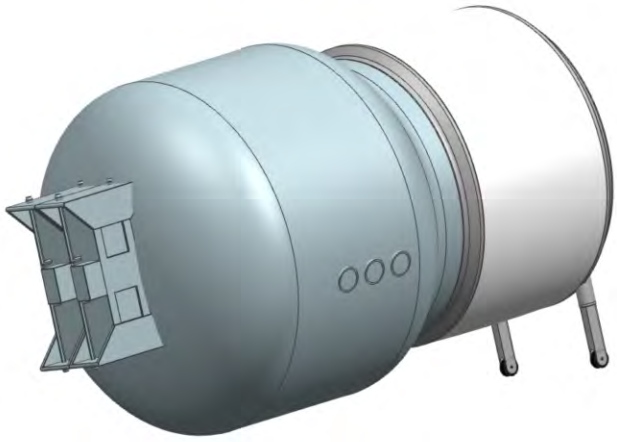

Figure 215: Exterior of the $20m^3$ Surface Habitat

The interior of the habitat can be seen in Figure 216, where there is Not really much additional space for components. A fully detailed mass and volume breakdown of each individual component can be found in Table 99. Interior components in the habitat are likewise colored in this table to show precisely what is included where.

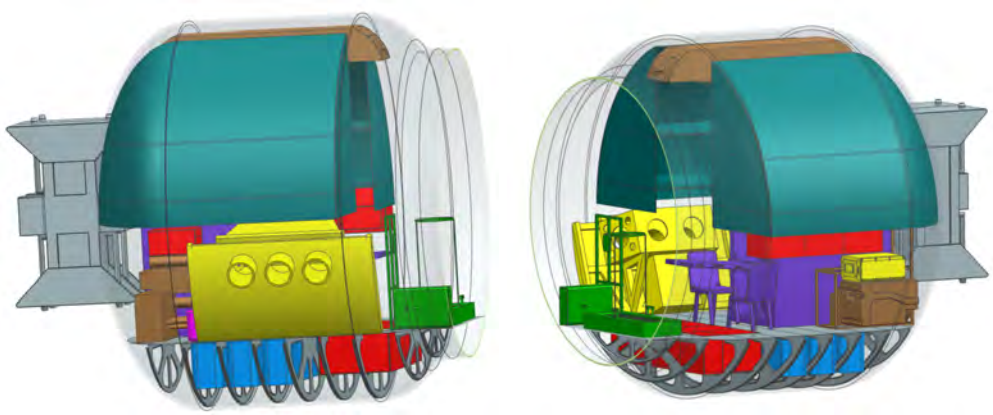

Figure 216: Interior of the 20m^3 Surface Habitat

Component	Component Volume (m^3)	Mass (kg)
Main Pressure Vessel	N/A	1500
Thermal Insulation	N/A	11.4
Solar Array	N/A	170
Battery	N/A	1200
Airlock	19.2	4060
Suitports	N/A	150
Radiators	1.3	870
Heat Exchangers	0.11	66.2
Fire Detector	0.004	3
Fire Extinguisher	0.021	10
Dining Table	0.034	75
Seating	0.04	27
Shower/Bathroom	2.8	804
Toilet	0.15	50
4BMS	0.44	320
EVA Prep	0.165	48
Urine Processing	0.61	100
Condensate Processing	0.66	115
Potable Water	0.91	910
Berths	7.8	670
Logistics rack	0.025	45
CTB Storage Rack	1.1	400
3d Printer	0.071	45
Geolab	1.8	400
Treadmill (TVIS-like)	0.32	200
Cycle (CEVIS)	0.080	82
Totals	**18.4**	**12,300**

Table 99: Volume and Mass Breakdown for 20m^3 Surface Habitat

The total component volume for this habitat design is 18.4 m^3. This includes all internal components. The airlock is not counted in this tally. Based on this component volume we determined that the total free volume is 1.58 m^3. Free volume is the amount of space not occupied by equipment. This value can be misleading as it does not include the space within the bunks or other components, which is usable but dedicated.

Additional space in this habitat is rather limited. As it is, the exercise equipment is parked up next to the airlock, so it would have to be stowed elsewhere during pre and post EVA preparations. The geolab is also tilted slightly to allow it to fit reasonably. This may pose some issues for how the astronauts would interact with it. From our estimation, it looks like it may be high enough to allow someone kneeling better access to it, in which case the tilt may play as an advantage. The 4BMS is located on the ceiling, which may be a potential servicing issue if there aren't any naturally tall crew members. There is also enough space for at least a couple seats, though there is a crew of four planned for this habitat. Similar to the microgravity habitat, it may make more sense to have fewer crew members in a habitat this small due to how much of the habitat is consumed with the crew berths.

9.6 40m^3 Surface Habitat (Tuvia Rappaport)

The 40m^3 surface habitat is an adequate size for the mission objectives. It is more cramped than the comparable volume 40m^3 micro-gravity habitat because it is not able to use the vertical space as effectively. This habitat is effectively the 20m^3 habitat stretched out. This extra stretch provides enough space for all of the equipment as well as areas for dedicated equipment. Unused areas for storage space is plentiful. The floors are an optimal location for storage, and in the current configuration it is only used for the potable water storage, leaving plenty of space for CTB storage. The raised beds provide enough space for a comfortable seated workstation below. This space was also sufficient for the storage requirements for the 30 day mission.

The outside of the habitat can be seen in Figure 217. The radiator wraps around the top of the habitat, like a blanket. Additionally, there are heat exchangers on the back side of the habitat.

Figure 217: Exterior of the 40m^3 Surface Habitat

The interior of the habitat can be seen in Figure 218, there is plenty of space for additional components. A detailed mass and volume breakdown of each individual component can be found in Table 100. Interior components in the habitat are likewise colored in this table to show precisely what is included where.

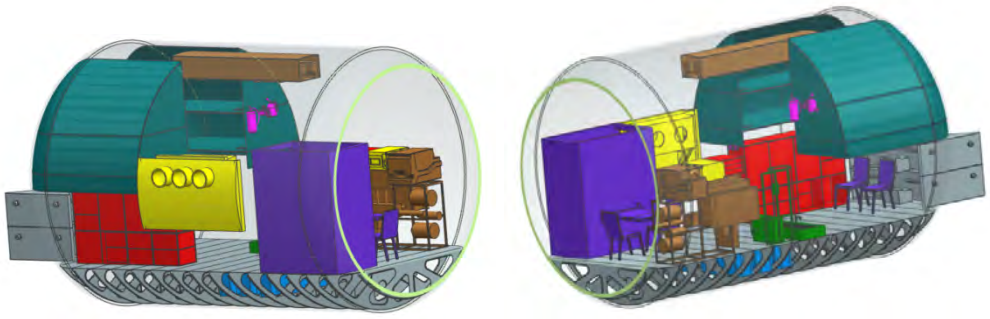

Figure 218: Interior of the 40m^3 Surface Habitat

Component	Component Volume (m^3)	Mass (kg)
Main Pressure Vessel	N/A	2720
Thermal Insulation	N/A	29
Solar Array	N/A	170
Battery	N/A	1240
Airlock	19.2	4060
Suitports	N/A	148
Radiators	2.1	1365
Heat Exchangers	0.13	78.4
Fire Detector	0.004	3
Fire Extinguisher	0.021	10
Dining Table	0.034	75
Seating	0.08	54
Shower/Bathroom	2.8	804
Toilet	0.15	50
4BMS	0.44	320
EVA Prep	0.165	48
Urine Processing	0.61	100
Condensate Processing	0.66	115
Potable Water	0.91	910
Berths	7.8	670
Logistics rack	0.025	45
CTB Storage Rack	1.1	400
3d Printer	0.071	45
Geolab	1.8	400
Treadmill (TVIS-like)	0.32	200
Cycle (CEVIS)	0.080	82
Totals	**19.2**	**14,000**

Table 100: Volume and Mass Breakdown for $40m^3$ Surface Habitat

The total component volume for this habitat design is 19.2 m^3. This includes all internal components. The airlock is not counted in this tally. Based on this component volume we determined that the total free volume is 20.8 m^3. Free volume is the amount of space not occupied by equipment. This value can be misleading as it does not include the space within the bunks or other components, which is usable but dedicated.

This habitat is likely close the optimal size for this mission profile. The existing equipment can all be used simultaneously without too much interference between the crew. The optimal habitat size is likely slightly smaller than this design. By exclusively relying on the floor for storage, shifting the bunks slightly higher and incorporating more multi purpose areas (e.g. beds that fold up). This habitat could easily support much more complex science objectives that require more equipment and storage.

9.7 $80m^3$ Surface Habitat (Blaire Weinberg)

The $80m^3$ surface habitat is the most spacious design that we had, with lots of empty room. For this habitat, there was a two-story design with bed and hygiene on the upper floor, and all of the science, life support, exercise equipment, and storage on the top. This is swapped from the microgravity habitat, in part to the fact that the life support – namely the EVA prep tools – could be close to the airlock.

The outside of the habitat can be seen in Figure 219. The radiator wraps around the backend of the habitat, like a curved camera lens. This would have cutouts for the heat exchangers, which are located on the back side of the habitat.

Figure 219: Exterior of the 80m^3 Surface Habitat

The interior of the habitat can be seen in Figure 220, where there is ample space for additional storage and equipment. A fully detailed mass and volume breakdown of each individual component can be found in Table 101. Interior components in the habitat are likewise colored in this table to show precisely what is included where.

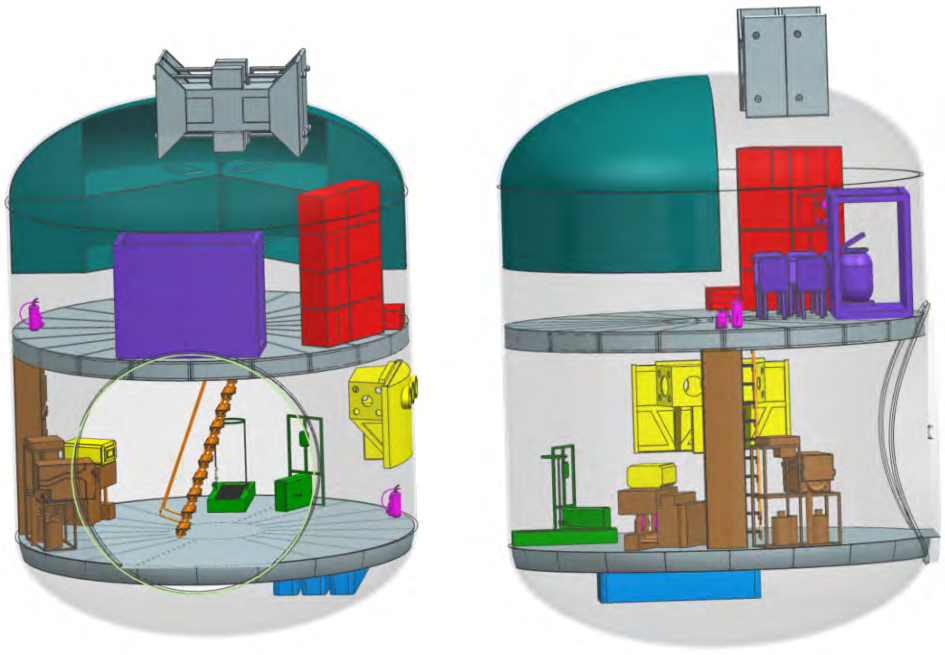

Figure 220: Interior of the 80m^3 Surface Habitat

Component	Component Volume (m^3)	Mass (kg)
Main Pressure Vessel	N/A	4531
Thermal Insulation	N/A	52.9
Solar Array	N/A	170
Battery	N/A	1242
Airlock	19.2	4060
Suitports	N/A	148
Radiators	2.08	1370
Heat Exchangers	0.16	95
Fire Detector	0.004	3
Fire Extinguisher	0.021	10
Dining Table	0.034	75
Seating	0.08	54
Shower/Bathroom	2.8	804
Toilet	0.15	50
4BMS	0.44	320
EVA Prep	0.165	48
Urine Processing	0.61	100
Condensate Processing	0.66	115
Potable Water	0.91	910
Berths	12.4	1500
Logistics rack	0.025	45
CTB Storage Rack	1.1	400
3d Printer	0.071	45
Geolab	1.8	400
Treadmill (TVIS-like)	0.32	200
Cycle (CEVIS)	0.080	82
Ladder	0.65	44
Totals	**23.9**	**16,800**

Table 101: Volume and Mass Breakdown for $80m^3$ Surface Habitat

The total component volume for this habitat design is 23.9 m^3. This includes all internal components. The airlock is not counted in this tally. Based on this component volume we determined that the total free volume is 56.1 m^3. Free volume is the amount of space not occupied by equipment. This value can be misleading as it does not include the space within the bunks or other components, which is usable but dedicated.

There is ample additional space in this habitat for a good deal more equipment than what we have right now, though there is still a lot of empty space even with that. The upper floor with the crew berths can probably include some storage for food and clothing, especially in the case of a solar particle event where they need to shelter in place. The theory with isolating the life support equipment, science, and exercise equipment on the lower shelf was to somewhat separate loud, noisy machinery from where the crew were sleeping. There is still some additional space for storage or equipment that could be added. With the same equipment fitting nicely into the $40m^3$ habitat, you would need to find a lot of additional equipment to have this start to become cramped.

9.8 Net Impact on Habitable Volume (Blaire Weinberg, Tuvia Rappaport)

The mission requirements described in §5 drive the minimum viable volume for a habitat. Based on our analysis, the $20\,m^3$ surface habitat and the $40\,m^3$ microgravity habitat are capable of satisfying these requirements. Since the $20\,m^3$ microgravity habitat does not have any science equipment outside of the 3D printer, it would not meet all of the requirements.

While those designs are sufficient for the mission requirements, to ensure quality of life, both microgravity and surface missions should use at least a $40\,m^3$ habitat. However as we are designing only for a 30 day mission, there may be some things that can be learned from Gemini 7 and their two week flight that may say otherwise. The primary difference between our mission design and Gemini 7 is the science objectives necessitate more equipment and work areas.

Habitat Type (m^3)	**Used Volume (m^3)**	**Free Volume (m^3)**	**Total Mass (kg)**	**Total Floor Space (ft^2)**	**Free Floor Space (ft^2)**
$20m^3$ Surface	18.4	1.58	12300	141	39
$20m^3$ MicroG	15.7	4.3	11700	110	37
$40m^3$ Surface	19.2	20.8	14000	217	145
$40m^3$ MicroG	17.5	22.5	13400	282	135
$80m^3$ Surface	23.9	56.1	16800	472	370
$80m^3$ MicroG	17.9	62.1	15300	440	312

Table 102: Summary of Habitat Mass and Volume Estimates

The free floor space was calculated by looking at the habitat from a top view and removing the areas covered by components. Because the components remain relatively constant across habitat sizes, the smaller habitats have a majority occupied, but this is quickly reversed for larger habitats. For the $20\,m^3$ habitats this leaves less than 40 square feet of space (units were changed to provide a better intuition). This is slightly smaller than a king sized bed. The larger habitats provide substantially more space, but even these are still relatively small. If the $40\,m^3$ habitats were bedrooms, it would be the size of a master bedroom (a bedroom large enough for a king sized bed). These area estimates intentionally do not include the usable areas within the crew berths and other usable components.

This conclusion assumes that our design has incorporated every component needed for a successful mission, and we definitely did not. However, by utilizing more reconfigurable components in the habitats (e.g. beds that function as tables) more space can be freed up even in the smallest designs. With that being said, the $40\,m^3$ for both microgravity and surface should incorporate enough extra space to work with additional components.

10 Conclusion

The second half of this report detailed trade studies conducted in mission planning, crew systems, loads and structures, power and thermal, and systems integration. In this section, we will summarize the impact of each subsystem on habitable volume and provide guidelines to future researchers for minimizing required habitable volumes.

10.1 Mission Planning and Analysis (Brady Sack)

The mission itself is driven by its science objectives, which trade studies demonstrated to have a significant impact on the habitat volume. However, since science is not critical to crew survival, habitat volume can be safely reduced by removing science equipment. One might argue that is a viable option for short duration missions meant only to prove technologies and collect samples without in-situ research conducted; however, the Human Exploration of Mars Science Analysis Group(HEM-SAG) predicts a well-equipped laboratory will significantly reduce the mass of sample material that must be returned. Thus, while removing science equipment may reduce volume, it might actually increase mass on return.

10.2 Crew Systems

Clearly, mission duration, location, and crew size all have impacts on crew systems requirements. Thus, for these analyses we assumed that all of these factors would remain constant (30 days/short-term, 4 crew). Important takeaways include:

- The sanitation station's volume requirement is independent of both crew size habitat volume
- The preferred airlock configuration is highly mission dependent:
  - Microgravity habitats, which do not require dust mitigation, benefit from venting the cabin airlock to minimize volume
  - Surface habitats, which require dust mitigation, require a suitport or rear-entry airlock

10.3 Loads and Structures

Airlocks not positioned on the endcap of a cylindrical habitat create wall interference and greatly detract from habitable volume. They are also more difficult to package in the launch vehicle.Additionally, larger diameter airlocks work better with horizontal habitats if the habitats are small.

A wing box style floor structure is both an efficient use of mass and volume, which helps achieve the goal of minimizing habitat volume.

10.4 Power and Thermal (Brady Sack, Michael Baker)

Trade studies revealed that radiator analysis can be tailored to any volume to give required dimensions, performance, and location. Overall there was not a minimum volume value which couldn't be sufficiently cooled given the design choices made. The majority of the equipment related to power and thermal can be located outside of the habitat and thus has no immediate impact on the habitable volume. The heat exchanger is the only component that needs to contact the inside of the habitat. To save volume, the heat exchanger pipes can be built into components that already extrude into the habitat, such as the floor structure.

Radiator sizing analysis also gives insight into system mass and how it varies with the habitat volume. In both the surface and microgravity environments the overall radiator mass decreases as volume decreases due to the decrease in heat energy imparted onto the system by solar insolation. This pertains to the research guidelines of this project because any additional mass that is saved could be used to store additional items that would be beneficial to the mission, and directly reflects in a lower production cost for the radiators.

10.5 Systems Integration (Tuvia Rappaport)

Based on equipment requirements driven by the science objectives, we were unable to fit the necessary equipment in the $20\,m^3$ micro-gravity habitat. Redesigning some of the internal components to be more efficient may make this habitat viable, but once additional equipment is included it may remain non-viable. Based on this for the mission outlined, a $20\,m^3$ micro-gravity habitat is marginal and slightly larger habitats should be considered.

The analysis of the free volume across the habitat sizes shows that baseline required components for the system to not grow significantly with the increase in volume. This places the baseline required volume of just components around $18\,m^3$. From here it should be sufficient to design enough free space in to the system, likely around $20\,m^3$.

For the surface habitats we managed to integrate all of the required components into the $20\,m^3$ surface habitat. The main reason this one was possible whereas the micro-g one was not was the size of sleeping bunks. On the surface we could design the sleep areas like bunks and rely on gravity. For micro-g we opted for larger berths to provide personal space and the ability to move around within. Larger surface

habitats should be considered for human factors concerns. For example in the $20\,m^3$ surface habitat without re-purposing bunks there is barely enough space for a single workstation area.

Based on this for both surface and micro-gravity missions we can conclude that the minimum viable habitat volume is around the $20\,m^3$, moving above or below depending on the mission requirements.

10.6 Next Steps

The students regret not having the chance to conduct the experiments described in the first half of the report due to facilities closures from the COVID-19 pandemic. Clearly, the obvious next steps are to complete the manufacturing of the rack designs and begin conducting tests. These tests would provide future researchers with valuable data regarding the required volume for a variety of essential habitat tasks and the effect of gravity on those workspace envelopes. In lieu of in-person testing, future researchers could consider conducting virtual reality spatial testing, in which they could use virtual reality tools, such as the Oculus Rift or Vive, to virtually explore the habitats outlined in this report. While this would not be as effective as actual habitat tests in the NBRF, it would provide an idea of what it would be like to live in of these habitats.

A Floor Design FEA Results

A.1 Floor Design A - FEA Results

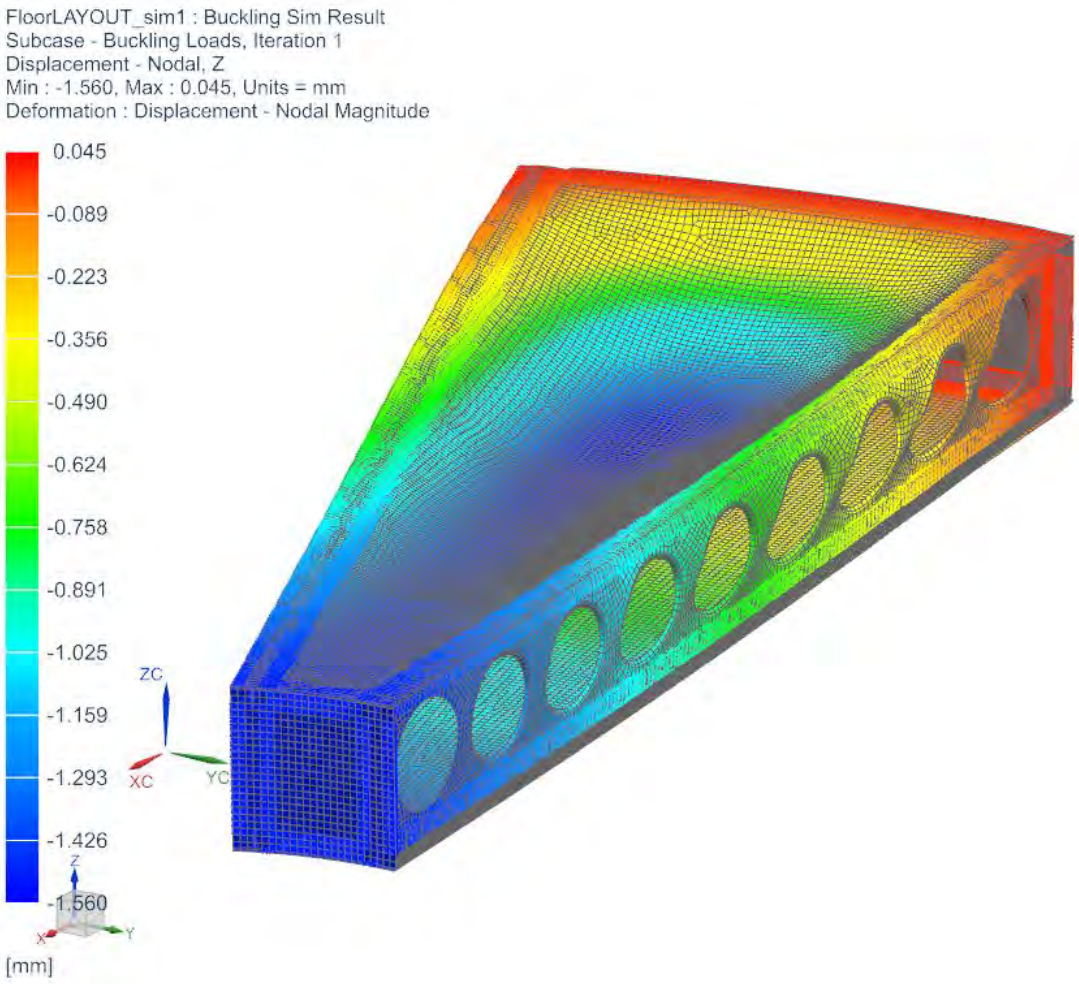

Figure 221: Floor Design A - Deflection Results

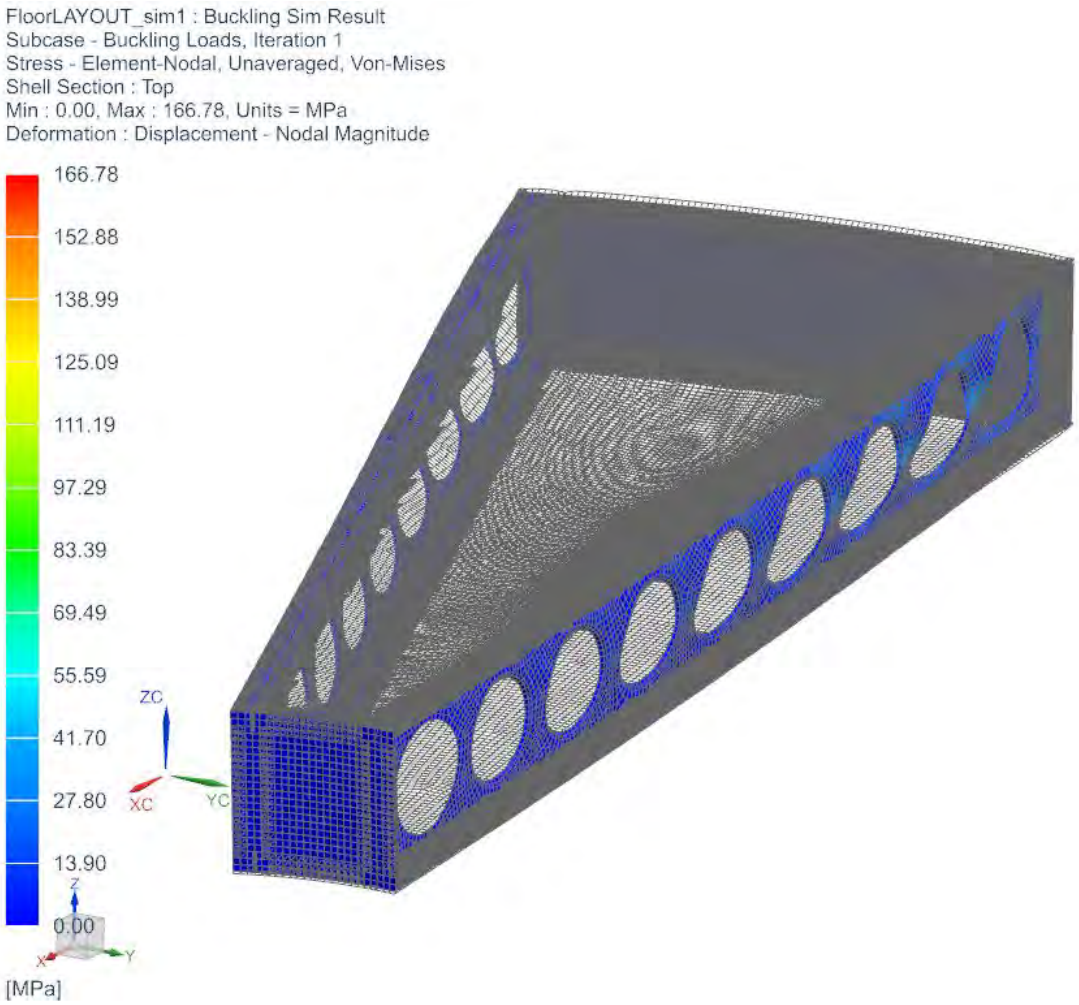

Figure 222: Floor Design A - Von-Mises Stresses (not including outer plates)

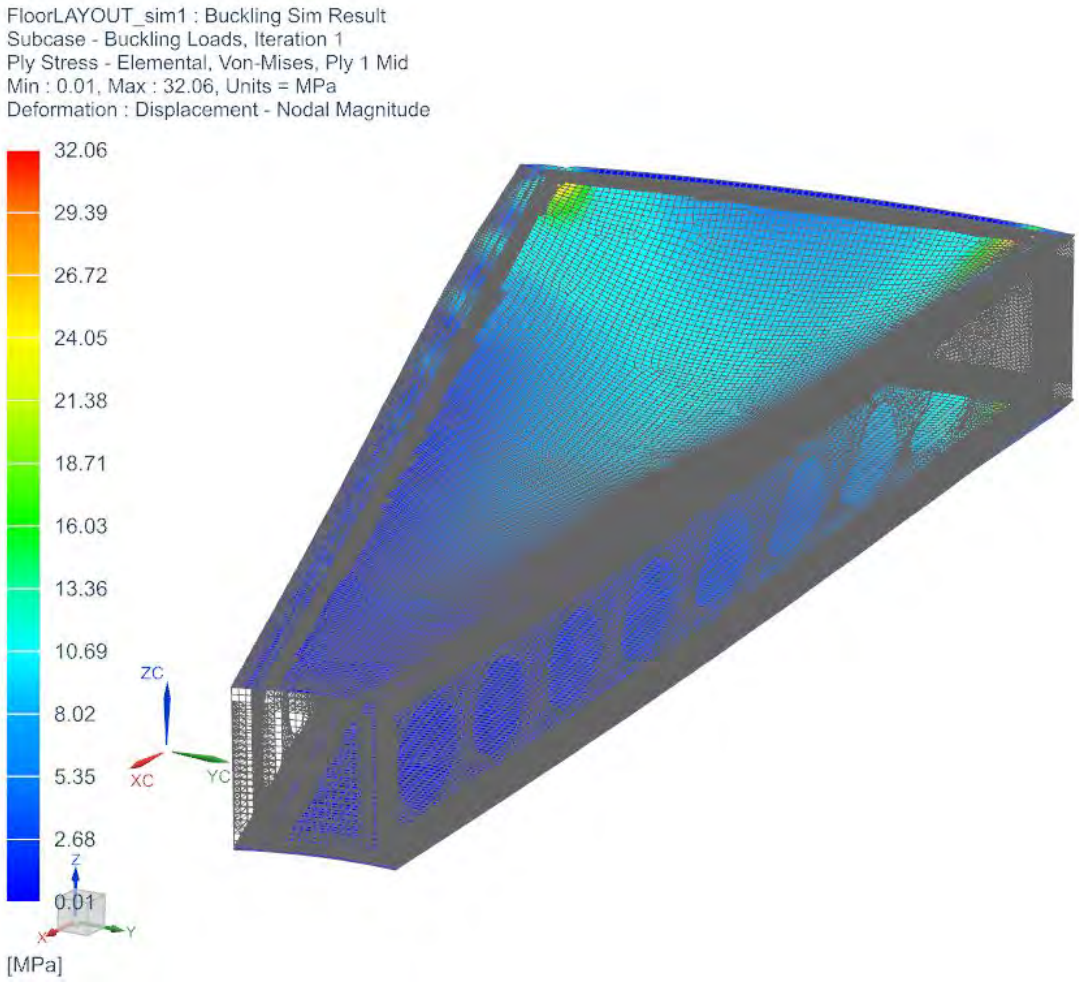

Figure 223: Floor Design A - Ply 1 Von-Mises Stresses (Outermost plates of honeycomb panels)

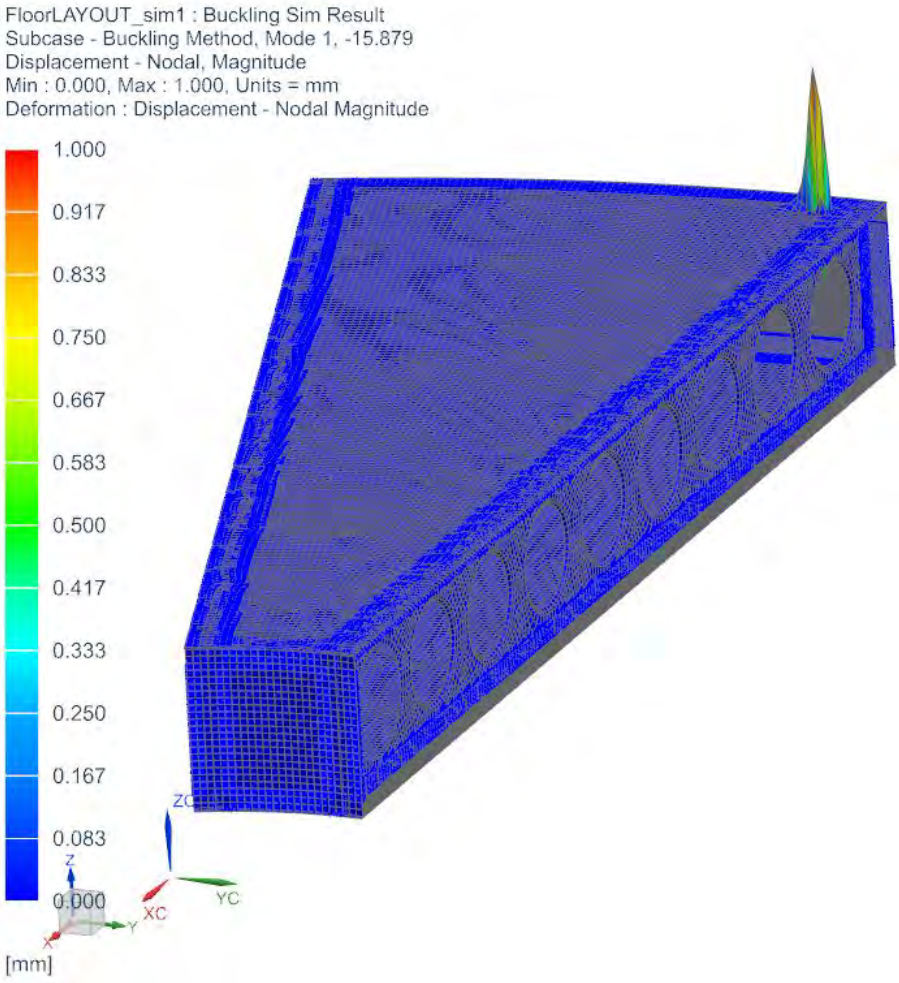

Figure 224: Floor Design A - First Buckling Mode - 15.879

A.2 Floor Design C - FEA Results

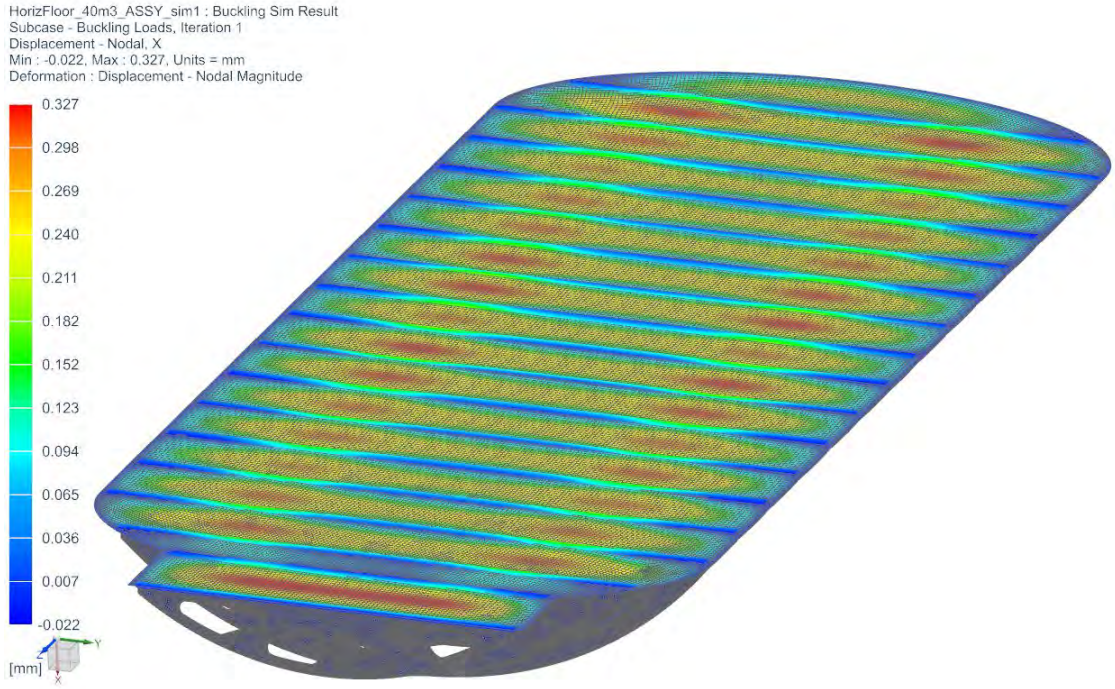

Figure 225: Floor Design C - Deflection Results

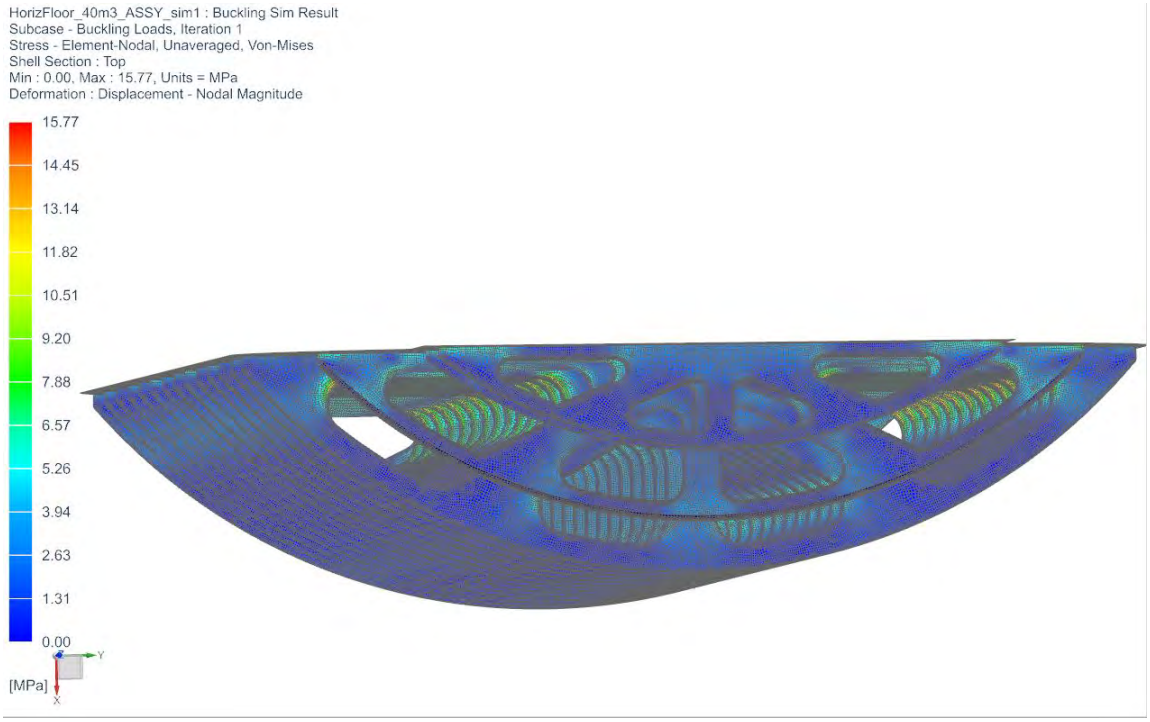

Figure 226: Floor Design C - Von-Mises Stresses (not including top floor plate)

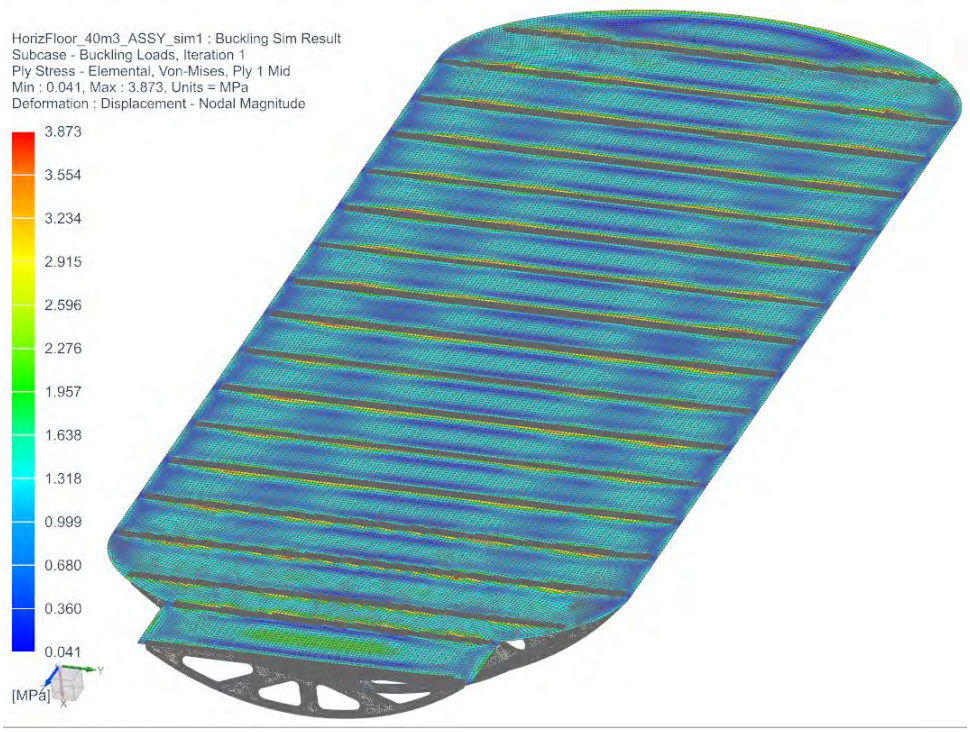

Figure 227: Floor Design C - Ply 1 Von-Mises Stresses (Top plate of honeycomb panel)

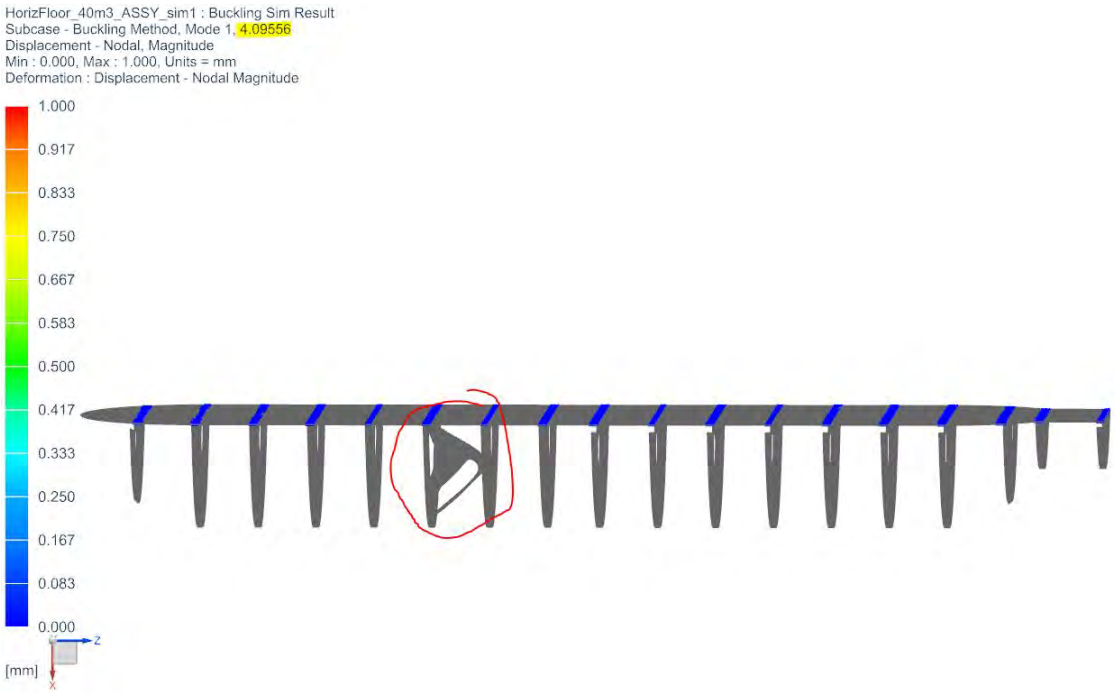

Figure 228: Floor Design C - First Buckling Mode - 4.09

B Matlab Scripts

B.1 Truss Analysis

```
1  %Bob Nobles
2  %ENAE484
3
4
5
6
7
8
9
10
11
12
13
14
15
16
17
18
19
20
21
22
23
24
25
26
       connectivity);
27
28
29
30
31
32
33
34     _
35
36
37
38
39
40
41
42
43
44                 _
45
46
47
48
49
```

References

[1] Fire extinguisher, skylab. Smithsonian National Air and Space Museum, 2000. https://airandspace.si.edu/collection-objects/fire-extinguisher-skylab/nasm_A19772551000.

[2] Advanced Life Support Requirements Document. Engineering Directorate CTSD-ADV-245C, National Aeronautics and Space Administration, Lyndon B. Johnson Space Center, Houston, Texas, 77058, 2 2003. http://www.marsjournal.org/contents/2006/0005/files/Lange2003.pdf.

[3] Blue Origin — New Glenn. online, 2007-2019. https://www.blueorigin.com/new-glenn/.

[4] Temperature measurements taken by phoenix spacecraft, September 2008.

[5] Mars design reference architecture 5.0 addendum. Technical report, NASA, 2009. https://www.nasa.gov/pdf/373667main_NASA-SP-2009-566-ADD.pdf.

[6] CHeCS (Crew Health Care Systems): International Space Station (ISS) Medical Hardware Catalog. Version 10.0. Technical Report JSC-CN-24908, National Aeronautics and Space Administration, NASA Johnson Space Center; Houston, TX, United States, 3 2011. https://ntrs.nasa.gov/archive/nasa/casi.ntrs.nasa.gov/20110022379.pdf.

[7] Euler's column formula. https://www.google.com/amp/s/www.engineeringtoolbox.com/amp/euler-column-formula-d_1813.html, 2012.

[8] Fire extinguishers. National City Corporation, 2013. http://www.nationalcitycorporation.sg/fire-extinguishers.html.

[9] NASA Space Flight Human-System Standard Volume 1, Revision A: Crew Health. Technical Standard NASA-STD-3001, Volume 1, National Aeronautics and Space Administration, 7 2015. https://www.nasa.gov/sites/default/files/atoms/files/nasa-std-3001-vol-1a-chg1.pdf.

[10] Buckling Knockdown Factors for Composite Cylinders. Technical report, National Aeronautics and Space Administration, 2016. https://ntrs.nasa.gov/archive/nasa/casi.ntrs.nasa.gov/19690013955.pdf.

[11] Would Current International Space Station (ISS) Recycling Life Support Systems Save Mass on a Mars Transit? Conference Paper ARC-E-DAA-TN43289, National Aeronautics and Space Administration, NASA Ames Research Center, Moffett Field, CA, United States, 7 2017. https://ntrs.nasa.gov/archive/nasa/casi.ntrs.nasa.gov/20170007268.pdf.

[12] Mission to europa: Europa lander. jpl.nasa.gov: https://www.jpl.nasa.gov/missions/europa-lander/, 2019.

[13] Shipladders. https://www.archtoolbox.com/materials-systems/vertical-circulation/shipladders.html, 2019.

[14] Staying Cool on the ISS, April 2020. https://science.nasa.gov/science-news/science-at-nasa/2001/ast21mar_1.

[15] National Aeronautics and Space Administration. Active Thermal Control System Overview. online, 2001. https://www.nasa.gov/pdf/473486main_iss_atcs_overview.pdf.

[16] National Aeronautics and Space Administration. Capillary Two-Phase Thermal Devices for Space Applications. online, 2016. https://ntrs.nasa.gov/archive/nasa/casi.ntrs.nasa.gov/20160004212.pdf.

[17] National Aeronautics and Space Administration. About the Kibo Laboratory. online, 2017. https://www.nasa.gov/mission_pages/station/structure/elements/kibo.html.

[18] National Aeronautics and Space Administration. Exploration Extravehicular Mobility Unit Outer Rendering Configuration Control Computer-Aided Design Model User's Guide. online, 2019. https://ntrs.nasa.gov/archive/nasa/casi.ntrs.nasa.gov/20190030871.pdf.

[19] D. L. Akin. ENAE 483/788D LECTURE #17-21 (STRUCTURAL DESIGN AND ANALYSIS. Technical report, University of Maryland, 2019. https://spacecraft.ssl.umd.edu/academics/483F19/483F19L1720and21.probs.pdf.

[20] David Akin. Structural Design and Analysis, 11 2019. Lecture 17.

[21] David L. Akin. EANE697 Air Revitalization. Technical report, University of Maryland, 2018.

[22] David L. Akin. ENAE483 Habitability. Technical report, University of Maryland, 2019.

[23] David L. Akin. ENAE483 Space Life Support Systems. Technical report, University of Maryland, 2019.

[24] David L. Akin. Thermal Analysis and Design Lecture #24 ENAE483. Online, 2019. https://spacecraft.ssl.umd.edu/academics/483F19/483F19L24.thermal/483F19L24.thermal.pdf.

[25] NASA Ames. Nasa task load index, August 2019. https://humansystems.arc.nasa.gov/groups/TLX/.

[26] ARIANESPACE. *ARIANE 6 USER'S MANUAL*, March 2018. https://www.arianespace.com/wp-content/uploads/2018/04/Mua-6_Issue-1_Revision-0_March-2018.pdf.

[27] ASCE. *ASCE 716 Design Loads and Associated Criteria for Buildings and Other Structures*. ASCE, 2017. https://www.academia.edu/39324420/7-16_Minimum_Design_Loads_and_Associated_Criteria_for_Buildings_and_Other_Structures.

[28] ASM Aerospace Specification Metals, Inc. Aluminum 7075-T6; 7075-T651. online. http://asm.matweb.com/search/SpecificMaterial.asp?bassnum=MA7075T6.

[29] Blue Origin, LLC. *NEW GLENN PAYLOAD USER'S GUIDE*, c edition, October 2018. https://yellowdragonblogdotcom.files.wordpress.com/2019/01/new_glenn_payload_users_guide_rev_c.pdf.

[30] Boeing. *Active Thermal Control System (ACTS) Overview*.

[31] M. J. Calaway C. A. Evans and M. S. Bell. Geolab – a habitat-based geoscience laboratory for human exploration missions. Technical report, National Aeronautics and Space Administration, Astromaterials Acquisition and Curation Office, Mail Code KT, NASA Johnson Space Center, 2101 NASA Pkway, Houston TX 77058, 2012. https://ntrs.nasa.gov/archive/nasa/casi.ntrs.nasa.gov/20120015450.pdf.

[32] S. Canright. Fire prevention in space. National Aeronautics and Space Administration, 8 2004. https://www.nasa.gov/audience/foreducators/k-4/features/F_Fire_Prevention_in_Space.html.

[33] Javier Benlloch-Marco Carolina Caballero-Arce, Adolfo Vigil-de Insausti. Lighting of space habitats: Influence of color temperature on a crew's physical and mental health. Technical report, Universitat Politècnica de València, Valencia,46022, Spain, July 2012. AIAA.

[34] Dennis Walsh Subir Roychoudhury Morgan B. Abney Jay L. Perry Christian Junaedi, Kyle Hawley. Compact and Lightweight Sabatier Reactor for Carbon Dioxide Reduction. Technical report, Precision Combustion, Inc., NASA George C. Marshall Space Flight Center, Precision Combustion, Inc., North Haven, CT, 06473, July 2011. AIAA.

[35] David Coan. Research and Technology Studies (RATS) 2012: Mission Day 1, 2012. National Aeronautics and Space Administration. https://blogs.nasa.gov/analogsfieldtesting/author/rlind/.

[36] V. E. Byrne D. P. Smith and C. Hudy. Human factors assessment of international space station (iss) medical equipment packs. *Proceedings of the Human Factors and Ergonomics Society Annual Meeting*, 49(1):1–4, 9 2005. https://journals.sagepub.com/doi/pdf/10.1177/154193120504900102?casa_token=Fr8o2CWx0fYAAAAA:V0Ejxq-YjDG5SAab7a8lwWGLsbpnqxgviLCSyQhym5B88abfRwyEAbyxfTG6Bm64qLufgGttARKwUg.

[37] Omar Medina David L. Akin, Massimiliano Di Capua and Adam Mirvis. Minimal Functional Habitat Final Review Presentation. Technical report, Natioal Aeronautics and Space Administration, 2009.

[38] Martin Donabedian and DG Gilmore. *Spacecraft Thermal Control Handbook*. Aerospace Press, 2003.

[39] Eric Vitug Drew Hope. Lightweight materials and structures, 2020. https://gameon.nasa.gov/archived-projects2/lightweightmaterialsandstructures/.

[40] DuPont. *Kevlar Aramid Fiber Technical Guide*. DuPont, 2017. https://www.r-g.de/w/images/b/bd/Kevlar_Technical_Guide.pdf.

[41] ESA. THE MOMA INSTRUMENT AND ITS MODULES. website, October 2010. https://exploration.esa.int/web/mars/-/47875-the-moma-instrument-and-its-modules.

[42] Goesmann et al. The Mars Organic Molecule Analyzer (MOMA) Instrument: Characterization of Organic Material in Martian Sediments. *Astrobiology*, 17(6/7), 2017.

[43] Gomez-Elvira et al. Rems: The environmental sensor suite for the mars science laboratory rover. Technical report, NASA, July 2012.

[44] Zeitlin et al. Calibration and characterization of the radiation assessment detector (rad) on curiosity. Technical report, NASA, November 2016.

[45] European Space Agency. *Microgravity Science Glovebox*, 2 edition. http://wsn.spaceflight.esa.int/docs/Factsheets/14%20MSG%20HR.pdf.

[46] R. Friedman. Fire safety in extraterrestrial environments. Technical Report NASA/TM-1998-207417, National Aeronautics and Space Administration, Lewis Research Center, Cleveland, Ohio, United States, 5 1998. https://ntrs.nasa.gov/archive/nasa/casi.ntrs.nasa.gov/19980209743.pdf.

[47] R. Friedman and D. L. Dietrich. Fire suppression in human-crew spacecraft. Conference Paper NASA Technical Memorandum 104334, National Aeronautics and Space Administration, Lewis Research Center, Cleveland, Ohio, United States, 5 1991. https://ntrs.nasa.gov/archive/nasa/casi.ntrs.nasa.gov/19910011869.pdf.

[48] R. Friedman and D. L. Urban. Progress in fire detection and suppression technology for future space missions. Technical Report NASA/TM-2000-210337, National Aeronautics and Space Administration, NASA Glenn Research Center, Cleveland, Ohio, United States, 44135, 9 2000. https://ntrs.nasa.gov/archive/nasa/casi.ntrs.nasa.gov/20000120278.pdf.

[49] J. Brooker G. A. Ruff and D. L. Urban. Fire safety technology development for exploration spacecraft and habitats. Conference Paper AIAA 2010-6240, National Aeronautics and Space Administration, NASA Glenn Research Center, Cleveland, Ohio, United States, 44135, 7 2010. https://arc-aiaa-org.proxy-um.researchport.umd.edu/doi/10.2514/6.2010-6240.

[50] Mars Architecture Steering Group. Humans Exploration of Mars Design Reference Architecture 5.0. Technical report, NASA, 7115 Hanover, MD 21076, 2009.

[51] GSSI. Compact GPR System for Utility Locating. website, February. https://www.geophysical.com/products/utilityscan.

[52] Makuch Heinz. Thiophenes on Mars: Biotic or Abiotic Origin? *Astrobiology*, 20(4), Janurary 2020.

[53] HONYLITE. *Aluminum Honeycomb Cores*. HONYLITE. http://www.honylite.com/honeycomb-cores/aluminumhoneycombcores/.

[54] Kriss; Guirgis Peggy; Boyle Robert Howe, A. Scott; Kennedy. A dual-chamber hybrid inflatable suitlock (dcis) for planetary surfaces or deep space. Technical report, NASA JPL, 2011. https://trs.jpl.nasa.gov/handle/2014/43909.

[55] Elizabeth Howell. Facts About SpaceX's Falcon Heavy Rocket. online, February 2018. https://www.space.com/39779-falcon-heavy-facts.html.

[56] ION. ION Geophones. website. http://www.iongeo.com/virtuals/ResourceArchives/content/documents/Resource%20C

[57] J. Norcross, et al. Effects of the 8 psia / 32% O2 Atmosphere on the Human in the Spaceflight Environment. Technical report, National Aeronautics and Space Administration, 2013. NASA/TM2013-217377.

[58] J. Norcross, et al. Risk of Hypobaric Hypoxia from the Exploration Atmosphere. Technical report, National Aeronautics and Space Administration, 2015.

[59] L. P. Jordan. *Microgravity Science Glovebox (MSG).* National Aeronautics and Space Administration, 2013. http://www.spacestationresearch.com/wp-content/uploads/MSG_flyer.pdf.

[60] B. Keeter. ISS On-Orbit Status Report, 2020. National Aeronautics and Space Administration. https://blogs.nasa.gov/stationreport/.

[61] Y. Kim and M. Choi. Synergistic Integration of Ion-Exchange and Catalytic Reduction for Complete Decomposition of Perchlorate in Waste Water. *Environmental Science & Technology*, 48:7503–7510, 6 2014. https://doi.org/10.1021/es501003m.

[62] Koyovis. How are aircraft wings protected against flutter - aerodynamic oscillations that can break bridges?, 11 2017. https://aviation.stackexchange.com/questions/45137/howareaircraftwings-protectedagainstflutteraerodynamicoscillationsthat.

[63] N. Samsonov L. Bobe and L. Gavrilov. Regenerative water supply for an interplanetary space station: The experience gained on the space stations "salut", "mir", iss and development prospects. *Acta Astronautica*, 61:8–15, 8 2007. https://doi.org/10.1016/j.actaastro.2007.01.003.

[64] C. A. Evans M. J. Calaway and M. S. Bell. Geolab 2010 hardware in nasa's pressurized excursion module. Technical report, Jacobs Technology (ESCG), National Aeronautics and Space Administration, NASA Johnson Space Center, Astromaterials Acquisition and Curation Division, Houston, TX 77058, 2010. https://ntrs.nasa.gov/archive/nasa/casi.ntrs.nasa.gov/20100003462.pdf.

[65] Made In Space, Inc. *Additive Manufacturing Facility (AMF) User Guide*, 4 2016. https://madeinspace.us/wp-content/uploads/2019/07/AMFuserguide-1.pdf.

[66] Malvern. Portable & handheld VNIR analyzers for mineral exploration and ore analysis. website. https://www.malvernpanalytical.com/en/products/product-range/asd-range/terraspec-range.

[67] Brian Dunbar Mark Garcia. Joint quest airlock overview, 2019. https://www.nasa.gov/mission_pages/station/structure/elements/jointquestairlock.

[68] C. E. Martin and R. C. DaLee. Spacecraft fire detection and suppression (fds) systems: An overview and recommendations for future flights. *SAE Transactions*, 102:1079–1093, 1993. https://www.jstor.org/stable/44740058?seq=1.

[69] Natalie Mary. EVA Office Extravehicular Activity (EVA) Airlocks and Alternative Ingress/Egress Methods Document. Technical report, National Aeronautics and Space Administration, 2018. EVA-EXP-0031.

[70] Christopher M Matty. Overview of Carbon Dioxide Control Issues During International Space Station/Space Shuttle Joint Docked Operations. Technical report, NASA Lyndon B. Johnson Space Center, NASA Lyndon B. Johnson Space Center, Houston, Texas, 77058, 2010. AIAA.

[71] MatWeb. Aluminum 5052-. online. http://www.matweb.com/search/datasheet_print.aspx?matguid=96d768abc51e4157

[72] MATWEB. Aluminum 8090-T8771 and 8090-T651. http://www.matweb.com/search/datasheet.aspx?matguid=da67441 Material Properties.

[73] ASM MATWEB. Aluminum 2024-T6. http://asm.matweb.com/search/SpecificMaterial.asp?bassnum=MA2024T6. Material Properties.

[74] ASM MATWEB. Aluminum 2219-T62. http://asm.matweb.com/search/SpecificMaterial.asp?bassnum=MA2219T62. Material Properties.

[75] ASM MATWEB. Aluminum 6061-T6; 6061-T651. http://asm.matweb.com/search/SpecificMaterial.asp?bassnum=MA6 Material Properties.

[76] ASM MATWEB. Aluminum 7075-T6; 7075-T651. http://asm.matweb.com/search/SpecificMaterial.asp?bassnum=MA7 Material Properties.

[77] Grace Douglas Maya Cooper and Michele Perchonok. Developing the NASA Food System for Long-Duration Missions. Technical report, Journal of Food and Science, 2011 Nov.

[78] Ellen S. Baker Michael R. Barratt and Sam L. Pool, editors. *Principles of Clinical Medicine for Space Flight*. Springer, 2nd edition, 2019.

[79] Talia Landman Mike Killian. NASA Shows Off Orion EM-1 Structure at KSC for Inaugural SLS Lunar Flight Test. https://www.americaspace.com/2016/02/03/nasa-shows-off-orion-em-1-structure-at-ksc-for-inaugural-sls-lunar-flight-test/, February 2016.

[80] L. Bobe N. Samsonov and V. Novikov. Systems for Water Reclamation from Humidity Condensate and Urine for Space Station. *SAE Transactions*, 103:1500–1507, 1994. https://www.jstor.org/stable/44614974.

[81] NASA. Facts about spacesuits and spacewalking. https://www.nasa.gov/audience/foreducators/spacesuits/facts/index.

[82] NASA. Science Objectives. https://mars.nasa.gov/msl/mission/science/objectives/.

[83] NASA Exploration Atmospheres Working Group. Recommendations for Exploration Spacecraft Internal Atmospheres: The Final Report of the NASA Exploration Atmospheres Working Group. Technical report, National Aeronautics and Space Administration, 2010. NASA/TP-2010-216134.

[84] National Aeronautics and Space Administration. The Lunar Electric Rover in 3D. Website, 2009.

[85] National Aeronautics and Space Administration. *HUMAN INTEGRATION DESIGN HANDBOOK*, volume 1 of *1*. NASA, Washington, DC 20546-0001, 2 edition, June 2014.

[86] National Aeronautics and Space Administration. *SPACE LAUNCH SYSTEM (SLS) MISSION PLANNER'S GUIDE*, a edition, December 2018. https://ntrs.nasa.gov/archive/nasa/casi.ntrs.nasa.gov/20170005323.pdf.

[87] Sudo Null IT News. Where Do Water and Oxygen Come From on The ISS?, 2019. https://sudonull.com/post/20543-Where-do-water-and-oxygen-come-from-on-the-ISS.

[88] Olympus. Olympus Tough TG-6 Digital Camera. website, February. https://www.bhphotovideo.com/c/product/1477205-REG/olympus_v104210ru000_tough_tg_6_digital_camera.html.

[89] Tim Peake. https://www.flickr.com/photos/timpeake/sets/72157634315750824/with/9129763971/.

[90] Diament Pletser. Subsurface water detection on Mars by astronauts using a seismic refraction method: Tests during a manned Mars mission simulation. *Acta Astronautica*, 64(4):457–466, February 2009.

[91] F. H. Schubert R. D. Marshall and J. N. Carlson. Electrochemical Carbon Dioxide Concentrator: Math Model Final Report. Technical report, Life-Systems Inc., Cleveland, Ohio, August, 1973.

[92] R. R. Woods R. D. Marshall and F. H. Schubert. Zinc Depolarized Electrochemical CO2 Concentration. Technical report, Life-Systems Inc. for Ames Research Center NASA, Cleveland, Ohio, October, 1975.

[93] O. Harwood R. Meyer and J. Orlando. Isogrid Design Handbook. Technical Report NASA-CR-124075, National Aeronautics and Space Administration & McDonnell Douglas Aerospace Company, 5301 Bolsa Avenue, Huntington Beach, CA 92647, 2 1973. https://femci.gsfc.nasa.gov/isogrid/NASA-CR-124075_Isogrid_Design.pdf.

[94] Kristine Rainey. Water production in space: Thirsting for a solution. October 2015.

[95] Sauke and Becker. Stable isotope laser spectrometer for exploration of Mars. *Planetary Space Science*, 46(6/7):805–812, June 1997.

[96] Brian Shiro. Seismic Success at MDRS. website, February 2010. http://www.astronautforhire.com/2010/02/seismic-success-at-mdrs.html.

[97] Ryan Simmons. Miles' Equation. https://femci.gsfc.nasa.gov/random/MilesEqn.html, 5 2001. Basics of Miles' Equation.

[98] Tony C. Slaba. Optimal shielding thickness for galactic cosmic ray environments. Technical report, NASA Langley Research Center, 2016.

[99] F. J. Smith and J. G. Grammer. Emissivity Coatings for Low-Temperature Space Radiators. Technical report, National Aeronautics and Space Administration, December 1965.

[100] Space Exploration Technologies Corp. (SpaceX). *FALCON USER'S GUIDE*, January 2019. https://www.spacex.com/sites/spacex/files/falcon_users_guide_10_2019.pdf.

[101] Space Exploration Technologies Corp. (SpaceX). *STARSHIP USERS GUIDE*, 1.0 edition, March 2020. https://www.spacex.com/sites/spacex/files/starship_users_guide_v1.pdf.

[102] R. Spivey and G. Flores. An overview of the microgravity science glovebox (msg) facility. National Aeronautics and Space Administration, June 2009. https://www.nasa.gov/pdf/360397main_P07_0955_Teledyne_msg.pdf.

[103] Michael Swickrath Molly S. Anderson Henry Rotter Su Curley, Imelda Stambaugh. Deep Space Habitat ECLSS Design Concept. Technical proposal, NASA, Houston, TX, 77058, July 2012. AIAA.

[104] Engineering Toolbox. Ethyline Glycol Heat Transfer Fluid. online, 2003. https://www.engineeringtoolbox.com/ethylene-glycol-d_146.html.

[105] Todd H. Treichel. Reliability Analysis of Light Emitting Diode Technologies for Cabin Lighting in Manned Space Flight Applications. Technical report, Orbital Technologies Corporation, Orbital Technologies Corporation, Madison, Wisconsin 53717, July 2013. AIAA.

[106] United Launch Alliance. *Delta IV Launch Services User's Guide*, June 2013. https://www.ulalaunch.com/docs/default-source/rockets/delta-iv-user's-guide.pdf.

[107] unknown. Space food, March 2020. http://tomatosphere.letstalkscience.ca/Resources/library/ArticleId/4752/space-food.aspx.

[108] D. L. Urban et al. Spacecraft fire detection: Smoke properties and transport in low-gravity. Conference Paper 20080012612, National Aeronautics and Space Administration, NASA Glenn Research Center, Cleveland, Ohio, United States, 44135, 1 2007. https://ntrs.nasa.gov/archive/nasa/casi.ntrs.nasa.gov/20080012612.pdf.

[109] UTC Aerospace Systems. Sabatier. UTC Website.

[110] E. Orndoff V. Byrne and D. Poritz. Advanced Exploration Systems (AES) Logistics Reduction and Repurposing Project: Advanced Clothing Ground Study Final Report. Technical Report CTSD-ADV-1088, National Aeronautics and Space Administration, NASA Johnson Space Center; Houston, TX, United States, 11 2013. https://ntrs.nasa.gov/search.jsp?R=20160010481.

[111] J-P Williams, DA Paige, BT Greenhagen, and E Sefton-Nash. The global surface temperatures of the moon as measured by the diviner lunar radiometer experiment. *Icarus*, 283:300–325, 2017.